

**Development of nano-encapsulation systems for the food antifungal natamycin  
Formulation, characterization and post-processing**

Bouaoud, Clotilde

**DOI**

[10.4233/uuid:bdea8caa-28fa-40e5-822b-fe7a23c6dfb3](https://doi.org/10.4233/uuid:bdea8caa-28fa-40e5-822b-fe7a23c6dfb3)

**Publication date**

2016

**Document Version**

Final published version

**Citation (APA)**

Bouaoud, C. (2016). *Development of nano-encapsulation systems for the food antifungal natamycin: Formulation, characterization and post-processing*. [Dissertation (TU Delft), Delft University of Technology]. <https://doi.org/10.4233/uuid:bdea8caa-28fa-40e5-822b-fe7a23c6dfb3>

**Important note**

To cite this publication, please use the final published version (if applicable).  
Please check the document version above.

**Copyright**

Other than for strictly personal use, it is not permitted to download, forward or distribute the text or part of it, without the consent of the author(s) and/or copyright holder(s), unless the work is under an open content license such as Creative Commons.

**Takedown policy**

Please contact us and provide details if you believe this document breaches copyrights.  
We will remove access to the work immediately and investigate your claim.

**Development of nano-encapsulation  
systems for the food antifungal  
natamycin**

*Formulation, characterization  
and post-processing*

Clotilde BOUAOUD



# **Development of nano-encapsulation systems for the food antifungal natamycin**

*Formulation, characterization  
and post-processing*

## **Proefschrift**

ter verkrijging van de graad van doctor  
aan de Technische Universiteit Delft,  
op gezag van de Rector Magnificus Prof. ir. K.C.A.M. Luyben,  
voorzitter van het College voor Promoties,  
in het openbaar te verdedigen op  
donderdag 27 oktober 2016 om 15.00 uur

door

**Clotilde BOUAOUD**

Diplôme d'ingénieur, Ecole Nationale Supérieure de Chimie de Paris, France  
Master of Science "Chimie et Ingénierie de la Formulation", Ecole Nationale Supérieure  
de Chimie de Lille, France

geboren te Maubeuge, Frankrijk.



This dissertation has been approved by the

Promotor: Prof. dr. A. Schmidt-Ott

Copromotors: Dr.ir. G. M.H.Meesters / Dr.hab. E. Mendes

#### Composition of the doctoral committee

Rector Magnificus

Prof.dr. A. Schmidt-Ott

Dr.ir. G.M.H. Meesters

Dr.hab. E. Mendes

chairperson

Technische Universiteit Delft, promotor

Technische Universiteit Delft, copromotor

Technische Universiteit Delft, copromotor

Independent members

Prof.dr.ir. R. Tuinier

Prof. G. N.M. Ferreira

Prof.dr. S. J. Picken

Dr. A. Sein

Prof.dr. E.J.R. Sudhölter

Technische Universiteit Eindhoven

University of Algarve, Portugal

Technische Universiteit Delft

DSM Food Specialties

Technische Universiteit Delft, reservelid

Substantial support in the preparation of this doctoral thesis has been received from H.E.A. De Braal (Senior Scientist, DSM Food Specialties) and Dr. J.G.J.L. Lebouille (Senior Applied Development/Technical Support Specialist Coatings, DSM Biomedical).

The research described in this thesis was performed at the Downstream Processing Department of the DSM Biotechnology Center (DSM Food Specialties, Delft) and the Chemical Engineering Department of the Faculty of Applied Sciences of the TU Delft. This research was co-funded by the European Union (Marie Curie Actions 7<sup>th</sup> Framework, Initial Training Network PowTech, grant agreement n°264722) and DSM Food Specialties B.V.



ISBN: 978-94-6186-507-6

Copyright © 2016 by Clotilde BOUAOUD

All rights reserved. Save exceptions stated by the law, no part of this thesis may be reproduced, stored in a retrieval system of any nature, or transmitted in any form or by any means, electronic, mechanical, photocopying, recording or otherwise, included a complete or partial transcription, without the prior written permission of the author. The author encourages the communication of scientific contents and explicitly exempts the use for scientific, non-commercial purposes, provided the proper citation of the source. Parts of the thesis are published in patents and scientific journals and copyright is subject to different terms and conditions.

*“We dance for laughter*

*We dance for tears*

*We dance for madness*

*We dance for fears*

*We dance for hopes*

*We dance for screams*

*We are the dancers*

*We create the dreams”*

Albert Einstein



# Table of contents

|  |           |
|--|-----------|
| List of abbreviations and symbols.....   | xi        |
| Summary.....   | xiii      |
| Samenvatting.....  | xvii      |
| <b>Chapter 1 – General introduction</b>  | <b>1</b>  |
| 1.1 Food spoilage, a worldwide challenge.....                                  | 2         |
| 1.2 Natamycin, usage and properties.....                                       | 3         |
| 1.3 Nano-encapsulation, a valuable option for natamycin.....                   | 6         |
| 1.4 Liposomes.....   | 8         |
| 1.5 Biodegradable polymeric nanospheres.....                                   | 11        |
| 1.6 Post-processing of nano-carriers, a prerequisite for industrial use.....   | 14        |
| 1.6.1 Purification and concentration.....                                      | 14        |
| 1.6.2 Preparation of dried products.....                                       | 16        |
| 1.7 Aims and scope of the thesis.....  | 18        |
| References.....  | 19        |
| <b>Part I – Development and characterization of nano-encapsulation systems</b> | <b>27</b> |
| <b>Chapter 2 – Natamycin-loaded biodegradable polymeric nanospheres</b>        | <b>29</b> |
| 2.1 Introduction.....  | 30        |
| 2.2 Materials and methods.....   | 33        |
| 2.3 Formulation of unloaded polymeric nanospheres.....                         | 37        |
| 2.3.1 Solvent and polymer selection.....                                       | 37        |
| 2.3.2 Influence of polymer concentration and composition.....                  | 38        |
| 2.3.3 Influence of solvent/non-solvent ratio.....                              | 39        |
| 2.3.4 Influence of stirring rate.....  | 40        |
| 2.3.5 Selected formulations.....   | 40        |
| 2.4 Incorporation of natamycin in the nanospheres.....                         | 41        |
| 2.4.1 Effect on size and polydispersity.....                                   | 41        |
| 2.4.2 Encapsulation and loading efficiencies.....                              | 44        |
| 2.4.3 Zeta-potential.....  | 45        |
| 2.4.4 Morphology.....  | 46        |
| 2.4.5 Physical state of natamycin.....   | 46        |
| 2.5 Performance tests.....   | 50        |
| 2.5.1 <i>In vitro</i> release kinetics.....                                    | 50        |
| 2.5.2 Antifungal activity against <i>Saccharomyces cerevisiae</i> .....        | 52        |
| 2.6 Stability tests.....   | 53        |
| 2.7 Conclusions.....   | 54        |
| References.....  | 55        |
| <b>Chapter 3 – Liposomal formulations of natamycin</b>                         | <b>59</b> |
| 3.1 Introduction.....  | 60        |
| 3.2 Materials and methods.....   | 64        |
| 3.3 Formulation of sterol-free soybean liposomes.....                          | 67        |
| 3.3.1 Preparation of unloaded liposomal formulations.....                      | 67        |

|   |    |
|---|----|
| 3.3.2 Incorporation of natamycin in sterol-free liposomes.....        | 68 |
| 3.3.3 Morphology of the liposomes.....                                | 72 |
| 3.3.4 Stability of sterol-free liposomal formulations.....            | 73 |
| 3.4 Sterol-enriched liposomal formulations.....                       | 74 |
| 3.4.1 Effect on size and encapsulation efficiency.....                | 74 |
| 3.4.2 Stability of sterol-enriched liposomal formulations.....        | 76 |
| 3.5 Performance tests.....  | 76 |
| 3.5.1 <i>In vitro</i> release kinetics.....                           | 76 |
| 3.5.2 Antifungal performance of sterol-enriched loaded liposomes..... | 81 |
| 3.6 Conclusions.....  | 82 |
| References.....   | 83 |

## **Part II – Post-processing of nano-encapsulation systems** **87**

### **Chapter 4 – Purification and concentration of nano-suspensions by tangential flow filtration** **89**

|  |     |
|--|-----|
| 4.1 Introduction.....  | 90  |
| 4.2 Basic principles of Tangential Flow Filtration.....              | 94  |
| 4.3 Materials and methods.....                                       | 98  |
| 4.4 Tangential Flow Filtration applied to PLGA nanospheres.....      | 103 |
| 4.4.1 Concentration of PLGA nanospheres.....                         | 103 |
| 4.4.1.1 Fouling and flux decline.....                                | 103 |
| 4.4.1.2 Removal and stability of natamycin.....                      | 106 |
| 4.4.2 Diafiltration of PLGA nanospheres.....                         | 108 |
| 4.4.3 Conclusions for PLGA nano-suspensions.....                     | 111 |
| 4.5 Tangential Flow Filtration applied to liposomal suspensions..... | 112 |
| 4.5.1 Concentration of liposomes.....                                | 112 |
| 4.5.1.1 Influence of TMP and MWCO.....                               | 112 |
| 4.5.1.2 Influence of sterol incorporation.....                       | 116 |
| 4.5.2 Diafiltration of liposomes.....                                | 120 |
| 4.5.3 Conclusions for liposomal suspensions.....                     | 122 |
| 4.6 Conclusions.....   | 123 |
| 4.7 Nomenclature.....  | 125 |
| 4.8 Appendices.....  | 125 |
| 4.8.1 Appendix A: Mass balance for concentration step.....           | 126 |
| 4.8.2 Appendix B: Mass balance for diafiltration step.....           | 126 |
| References.....  | 127 |

### **Chapter 5 – Lyophilization of polymeric and liposomal nano-suspensions** **131**

|  |     |
|--|-----|
| 5.1 Introduction.....  | 132 |
| 5.2 Materials and methods.....   | 135 |
| 5.3 Lyophilization of PLGA nanospheres.....  | 139 |
| 5.3.1 Addition of cryoprotectants and freeze-thawing.....                                  | 140 |
| 5.3.2 Lyophilization and stability of the nano-carriers upon storage.....                  | 142 |
| 5.3.3 Thermal analysis of lyophilized PLGA cakes.....                                      | 146 |
| 5.3.4 Natamycin stability upon storage.....  | 150 |
| 5.3.5 Conclusions for PLGA nanospheres.....  | 153 |
| 5.4 Lyophilization of liposomal suspensions.....   | 154 |
| 5.4.1 Lyophilization of sterol-free liposomes.....   | 154 |
| 5.4.2 Lyophilization of sterol-enriched liposomes.....                                     | 158 |
| 5.4.3 Thermal analysis of liposomal lyophilized cakes.....                                 | 162 |
| 5.4.4 Natamycin stability in sterol-free and sterol-enriched lyophilized formulations..... | 163 |
| 5.4.5 Conclusions for liposomal suspensions.....   | 166 |

|  |            |
|--|------------|
| 5.5 Conclusions.....                               | 167        |
| References.....                                    | 168        |
| <b>Chapter 6 – General conclusions and outlook</b> | <b>175</b> |
| 6.1 Conclusions and future work Part I.....        | 177        |
| 6.2 Conclusions and future work Part II.....       | 182        |
| Acknowledgements.....                              | 187        |
| Curriculum Vitae.....                              | 191        |
| List of publications.....                          | 192        |



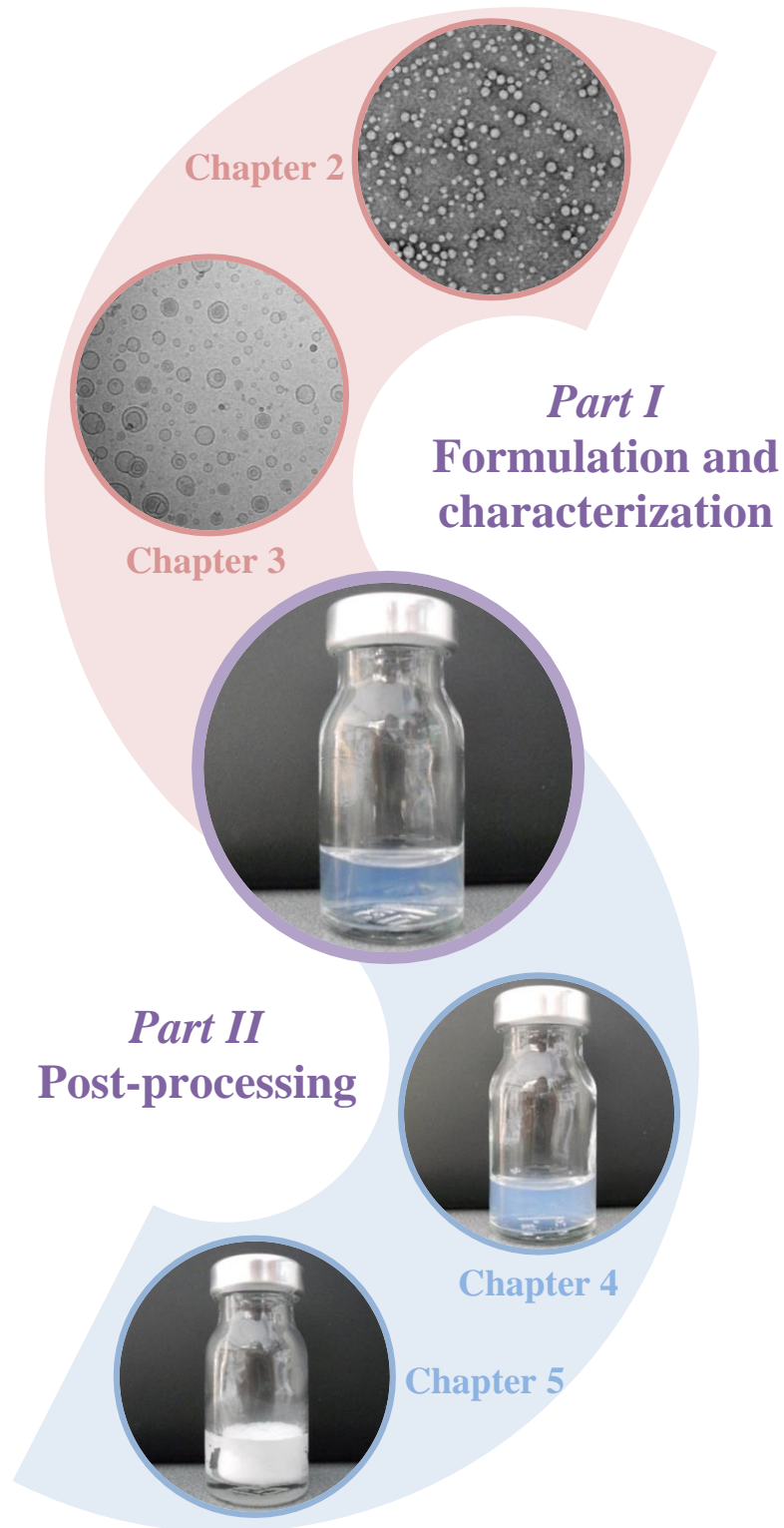
# *List of abbreviations and symbols*

|                 |  |
|-----------------|--|
| Ac              | Acetone  |
| AmB             | Amphotericin B   |
| BPF             | Bilayered Phospholipid Fragments   |
| CHOL            | Cholesterol  |
| CHOL/L          | Cholesterol-to-lipid ratio   |
| Cryo-TEM        | Cryogenic Transmission Electron Microscopy                                   |
| CF              | Concentration factor   |
| d               | Mean hydrodynamic diameter   |
| DLS             | Dynamic Light Scattering   |
| DSC             | Differential Scanning Calorimetry  |
| EE              | Encapsulation efficiency   |
| ERG             | Ergosterol   |
| ERG/L           | Ergosterol-to-lipid ratio  |
| FT-IR           | Fourier Transform Infrared   |
| HPLC            | High Performance Liquid Chromatography                                       |
| L:G             | Lactide-to-glycolide ratio in PLGA polymer                                   |
| LE              | Loading efficiency   |
| MeOH            | Methanol   |
| MIC             | Minimum inhibitory concentration   |
| MQ water        | MilliQ water   |
| MWCO            | Molecular weight cut-off   |
| N/L             | Natamycin-to-lipid ratio   |
| NPs             | Nanoparticles  |
| PdI             | Polydispersity index   |
| ppm             | Parts per million ( $\mu\text{g}/\text{mL}$ )                                |
| PA              | Phosphatidic acid  |
| PC              | Phosphatidylcholine  |
| $\epsilon$ -PCL | Polycaprolactone   |
| PE              | Phosphatidylethanolamine   |
| PGA             | Poly(glycolic acid)  |
| PLA             | Poly(lactic acid)  |
| PLGA            | Poly(lactic-co-glycolic acid)  |
| PVA             | Polyvinylalcohol   |
| RT              | Room temperature   |
| SD              | Standard deviation   |
| SEM             | Scanning Electron Microscopy   |
| S/L             | Sterol-to-lipid ratio  |
| S/NS            | Solvent/non-solvent ratio  |
| $T_c$           | Collapse temperature   |
| TEM             | Transmission Electron Microscopy   |
| TFF             | Tangential Flow Filtration   |
| $T_g$           | Glass transition temperature   |
| $T_g^*$         | Glass transition temperature of the maximally freeze-concentrated suspension |
| $T_m$           | Gel-to-liquid crystalline phase transition temperature                       |
| TMP             | Transmembrane pressure   |
| UV              | Ultraviolet  |
| XRD             | X-ray Diffraction  |
| $\zeta$         | Zeta-potential   |





# Summary



Food spoilage has become in the last decades one of the biggest challenges faced by the food industry. Contamination by micro-organisms resulting in products unacceptable for human consumption is listed as one of the major causes of food spoilage and can be at a large extent prevented by preservation methods among which application of antimicrobial compounds is quite popular. In the past years, a growing demand of customers for more natural antimicrobials and reduced processing treatments, coupled with high research costs and numerous regulatory hurdles set by health authorities while considering development of new preservative molecules, has led the food antimicrobial suppliers to preferentially focus on the reformulation and improvement of already approved ingredients, aiming at maximizing their antimicrobial efficiency and adapting their functionality to new food applications. Natamycin, a naturally-occurring preservative produced by DSM Food Specialties, is one of the most widely used antifungal molecules for the protection of food surfaces. This compound presents several appealing properties linked to its natural origin, long history of safe use, efficiency at low concentrations and limited impact on organoleptic properties of food products. Current existing formulations based on crystalline natamycin particles face however several challenges to provide appropriate antimicrobial activity. Low aqueous solubility which limits significantly the availability of natamycin in dissolved state, necessary for antifungal activity and diffusion towards the sites of action, is the first hurdle encountered. High sensitivity and undesired degradation of the preservative while exposed to environmental conditions such as extreme pHs, UV light or oxidation, is also a significant issue. Finally, current formulations offer limited specificity, tunability and possibilities of controlled release.

In this PhD thesis, incorporation of natamycin within nano-encapsulation systems was explored to evaluate if these new formulations could bring effective answers to the issues of availability, early-stage degradation and limited tunability identified for the native crystalline preservative. A product development approach was implemented with **Part I** focusing on the development and characterization of nano-carriers presenting suitable properties for the encapsulation, delivery and protection of the preservative, while **Part II** describes further treatment of the obtained nano-suspensions and transformation into purified, concentrated or dried products that could possibly be commercialized.

In **Part I**, nano-encapsulation systems based on biodegradable polymeric nanospheres (**Chapter 2**) and liposomes (**Chapter 3**) were evaluated as model nano-carriers for natamycin and compared in terms of relative benefits and limitations for the encapsulation, delivery, antifungal performance towards the model yeast *Saccharomyces cerevisiae* and stability of the preservative upon storage. Polymeric nanospheres and liposomes were respectively prepared by nanoprecipitation and solvent injection. Both methods are compatible with the restricted solubility properties of natamycin and are based on the preparation and single-step injection of an organic phase – containing the preservative, the carrier material (in our case poly-lactide-co-glycolide PLGA and soybean lecithins) and a solvent fully miscible with water – into an aqueous phase.

Nanoprecipitation of low molecular weight PLGA dissolved in an acetone/methanol 2:1 mixture allowed reproducible formation of nano-sized spherical particles (60-120 nm) with a narrow polydispersity (0.15-0.2). Formation of an electrostatic complex with PLGA and presence of natamycin in a non-crystalline state were evidenced. Encapsulation levels were however limited (maximum 1.4% of loading efficiency), with a large amount of preservative remaining in the aqueous phase or adsorbed at the surface of the particles. Although this translated interestingly into higher availability, fast release kinetics rates and enhanced antifungal activity over the first two days of application, the preservative stability upon storage could not be ensured successfully.

Nano-liposomal suspensions prepared from deoiled food-grade soybean lecithins dissolved in methanol were the second option studied and led to the formation of small unilamellar vesicles (< 130 nm) with less controlled polydispersities (0.21-0.26) than PLGA nanospheres. Encapsulation of natamycin was however possible at much larger extents with a particular affinity highlighted for charged phospholipid heads. Addition of sterols (cholesterol, ergosterol) in the lipid mixture was found essential for the maximization of the entrapment levels (up to 5.6-5.8% loading efficiency) and for the reduction of chemical instability of the preservative via specific complexation and improvements of the mechanical stability of the membrane, avoiding extensive leakage of natamycin towards the external medium. By modulating the membrane permeability, incorporation of sterols allowed additionally fine-tuning of the release rates and durations of the antifungal activity.

In relationship with the challenges identified for crystalline natamycin, **Part I** gave the proof of principle that nano-encapsulation can bring an answer to the desired higher availability of preservative molecules for enhanced antifungal activity. Possible tunability

and controlled release were also highlighted for liposomes. However, nano-encapsulation systems did not bring an effective answer to the chemical instability of the preservative, with losses of natamycin remaining at levels too high to be acceptable for customers even for the best liposomal formulations prepared.

In *Part II*, possibly scalable post-treatments were applied to both PLGA nanospheres and liposomes with the aim of simultaneously developing commercially suitable formulations and tackling remaining stability issues. Tangential Flow Filtration (TFF) was applied in *Chapter 4* to obtain either concentrated suspensions or suspensions purified from non-encapsulated preservative and unassociated carrier material. In *Chapter 5*, lyophilization was investigated as an approach to transform liquid suspensions into redispersible dry powders, easier to store, transport and handle by customers. Focus was put on the evaluation and comparison of both techniques in terms of conservation of the nanoparticle integrity and original size characteristics, undesired premature release of the encapsulated preservative and benefits for the physical stability of the nanoparticles and chemical stability of natamycin upon storage.

TFF implemented at lab scale with polysulfone hollow fibers membrane was found acceptable for the preparation of concentrated PLGA nano-suspensions, leading to a beneficial increase in solid content and reduced losses of natamycin upon storage. Membrane fouling and long processing times remained however non-negligible and could become a hurdle at larger scale. Benefits of concentration and purification processes were not evidenced in the case of liposomal suspensions due to premature leakage of natamycin and low resistance of the lipid bilayers – even when sterol-enriched – to mechanical stresses occurring during the process, leading upon storage to higher losses of preservative than in the original suspension.

Preparation of dry powders by lyophilization in presence of protective excipients turned out more valuable than TFF for the physical and chemical stability of both natamycin and nano-carriers. Particularly, incorporation of trehalose in the nano-suspension allowed formation of easily redispersible amorphous cakes with conservation of PLGA nanospheres and liposomes size characteristics not only after lyophilization but also upon storage. Shelf-life of natamycin in the dried products was undoubtedly enhanced compared to corresponding aqueous suspensions and concentrates obtained by TFF, making lyophilization a very promising technique to consider for development of commercial formulations of the nano-suspensions.

# *Samenvatting*



In de laatste decennia is voedselvergiftiging een van de grootste uitdagingen geworden voor de voedingsmiddelenindustrie. Microbiële groei wordt genoemd als een van de belangrijkste oorzaken van voedselbederf. Besmetting door micro-organismen kan grotendeels worden voorkomen door beschermingsmethoden, waaronder het gebruik van antimicrobiële verbindingen een populaire methode is. In de afgelopen jaren werd er een groeiende vraag van klanten naar meer natuurlijke conserveringsmiddelen of verminderd gebruik van deze middelen waargenomen. De ontwikkeling van nieuwe antimicrobiële moleculen wordt echter bemoeilijkt door hoge onderzoekskosten en talrijke wettelijke obstakels gesteld door de gezondheidsautoriteiten. Daarom hebben leveranciers de voorkeur gegeven aan herformulering en verbetering van al goedgekeurde ingrediënten, met focus op het maximaliseren van hun antimicrobiële efficiëntie en aanpassing van hun functionaliteit voor specifieke levensmiddelen toepassingen. Natamycine, een conserveermiddel geproduceerd door DSM Food Specialties, is een van de meest gebruikte antischimmelmiddelen in voedsel beschermlaag. Dit molecuul heeft een aantal gunstige eigenschappen, zoals een natuurlijke oorsprong, lange geschiedenis van veilige menselijke consumptie, efficiëntie bij lage concentraties en geen merkbare invloed op de organoleptische eigenschappen van voedingsmiddelen. Huidige natamycine formuleringen zijn er alleen op basis van kristallijne deeltjes, wat verschillende uitdagingen geeft in de toepassing. De eerste hindernis is de slechte oplosbaarheid in water, wat de beschikbaarheid van moleculaire natamycine, noodzakelijk voor de antischimmelactiviteit, aanzienlijk begrenst. Een ander belangrijk probleem is de hoge gevoeligheid en ongewenste degradatie van het conserveermiddel bij blootstelling aan omgevingsomstandigheden, zoals extreme pHs, UV licht of oxidatie. Tenslotte is het niet mogelijk om specificiteit, maatwerk en gecontroleerde afgifte te bieden met de huidige formuleringen.

Het onderzoek beschreven in dit proefschrift heeft betrekking op de incorporatie van natamycine in nano-encapsulatie systemen om te evalueren of deze nieuwe formuleringen doeltreffende oplossingen kunnen bieden voor de problemen die geïdentificeerd zijn voor kristallijne natamycine, waaronder beschikbaarheid, vroegtijdige degradatie en beperkte mogelijkheden voor maatwerk. *Deel I* van dit proefschrift is gericht op de ontwikkeling en karakterisering van twee nanocarriers met geschikte eigenschappen voor het inkapselen, afgifte en bescherming van het conserveermiddel. *Deel II* beschrijft de nabewerking van de geproduceerde nanosuspensies en hun transformatie naar gezuiverde, geconcentreerde of gedroogde producten die geschikt zijn voor commercialisering.

In *Deel I*, zijn nanosferen gemaakt van biodegradeerbare polymeren (*Hoofdstuk 2*) en liposomen (*Hoofdstuk 3*) geëvalueerd als potentiële nanocarriers voor natamycine. Beide systemen werden vergeleken op hun relatieve voordelen en beperkingen wat betreft inkapseling, afgifte, antifungale activiteit tegen het modelgist *Saccharomyces cerevisiae* en stabiliteit na opslag. Polymere nanodeeltjes en liposomen werden respectievelijk bereid door nanoprecipitatie en “oplosmiddel injectie”. Beide methoden zijn compatibel met de slechte oplosbaarheid van natamycine en bestaan in de bereiding en snelle injectie in een waterige fase van een organische fase, wat bestaat uit het antischimmelmiddel, het materiaal voor de nanocarriers (in ons geval poly(lactide-co-glycolide) PLGA en sojalecithine) en een oplosmiddel dat volledig mengbaar is met water.

PLGA met een laag molecuulgewicht werd geselecteerd en opgelost in een mengsel aceton /methanol 2:1 v/v om de nanoprecipitatie uit te voeren. Sferische nanodeeltjes met smalle polydispersiteiten werden met goede reproduceerbaarheid verkregen. De vorming van een elektrostatisch complex met PLGA en de aanwezigheid van natamycine in een niet-kristallijne toestand werden aangetoond. Inkapseling werd echter beperkt en een groot deel van natamycine bleef in de waterige fase of werd geadsorbeerd op het oppervlak van de deeltjes. Dit resulteerde in opvallende hogere beschikbaarheid van moleculaire natamycine, snelle afgifte en verbeterde antifungale activiteit tijdens de eerste twee dagen. Helaas kon er niet voldoende stabiliteit worden bereikt tijdens opslag.

Nanoliposomale suspensies gemaakt uit ontoliede food-grade sojalecithine, opgelost in methanol, werden als tweede mogelijkheid onderzocht. Door oplosmiddel injectie werden kleine unilamellaire vesicles geproduceerd, echter met minder gecontroleerde polydispersiteiten en reproduceerbaarheid dan de PLGA nanosferen. Inkapseling van natamycine was echter mogelijk op een hoger niveau en werd vergemakkelijkt door de aanwezigheid van geladen fosfolipiden. Het toevoegen van sterolen (cholesterol, ergosterol) in het lipiden mengsel werd essentieel bevonden voor het bereiken van maximale efficiëntie van de inkapseling en voldoende chemische instabiliteit, via specifieke complexvorming van natamycine met de sterolen en verbetering van de mechanische stabiliteit van het lipiden membraan. Door incorporatie van sterolen werden ook modulatie van de membraanpermeabiliteit en het afstellen van de afgiftesnelheden en antifungale activiteit mogelijk gemaakt.

Met betrekking tot uitdagingen van het kristallijne conserveermiddel gaf *Deel I* het bewijs dat nano-inkapseling een oplossing kan bieden voor de gewenste hogere beschikbaarheid van moleculaire natamycine voor verbeterde antischimmelactiviteit.



Interessante opties voor product-specifieke afstemming en gecontroleerde afgifte werden ook voor liposomen aangetoond. Beide nano-systemen boden helaas geen doeltreffende oplossing voor de stabiliteit, zelfs bij de meest optimale liposomale formuleringen.

In *Deel II* werden potentiële opschaalbare nabewerkingsmethoden op PLGA nanosferen en liposomen toegepast om tegelijk commerciële formuleringen te ontwikkelen en de stabiliteitsproblemen verder aan te pakken. In *Hoofdstuk 4* werd Tangentiële flowfiltratie (TFF) bestudeerd met als doel om suspensies te zuiveren van losse natamycine of polymeren en fosfolipiden, en om geconcentreerde suspensies te verkrijgen. In *Hoofdstuk 5* werden vloeibare suspensies bij lyofilisatie in herdispergeerbare droge poeders getransformeerd. Het doel was hier de evaluatie en vergelijking van beide technieken met betrekking tot de instandhouding van de integriteit en de grootte van de nanodeeltjes, tot ongewenste vroegtijdige afgifte van de inkapselde natamycine en tot voordelen voor de fysische stabiliteit van de nanodeeltjes en de chemische stabiliteit van het antischimmelmiddel.

TFF werd met holle vezel polysulfon membranen op laboratoriumschaal geprobeerd en werd voor de bereiding van geconcentreerde PLGA nanosuspensies aanvaardbaar gevonden door een verhoging van deeltjesconcentratie en een verminderde degradatie van natamycine. Membraanvervuiling en lange doorlooptijden bleven echter niet verwaarloosbaar en zou een hindernis op industriële schaal worden. Voordelen van concentratie en zuivering werden niet voor liposomale suspensies aangetoond ten gevolge van de slechte weerstand van lipide bilagen – zelfs indien verrijkt met sterolen – tegen mechanische belastingen tijdens het TFF proces en de vroegtijdige lekkage van natamycine, die tot hogere degradatie dan in de originele suspensie na opslag leidde.

De productie van droge poeders door lyofilisatie in aanwezigheid van beschermende hulpstoffen leek waardevoller dan TFF voor de fysische en chemische stabiliteit van natamycine en nanodeeltjes. Vooral, de incorporatie van de suiker trehalose in de nanosuspensies maakte de vorming van gemakkelijk herdispergeerbare amorfe poeders mogelijk, waarin de instandhouding van de eigenschappen van zowel PLGA nanosferen en liposomen niet alleen net na het vriesdrogen maar ook na opslag wordt bereikt. The houdbaarheid van natamycine in de gedroogde producten werd ook aanmerkelijk verbeterd in vergelijking met waterige of geconcentreerde suspensies, waardoor lyofilisatie een veelbelovende techniek voor de ontwikkeling van commerciële formuleringen uit nanosuspensies lijkt.





# *Chapter 1*

## *General introduction*

*The opposite for courage is not cowardice, it is conformity.*

*Even a dead fish can go with the flow.*

Jim Hightower

## 1.1. Food spoilage, a worldwide challenge

Food spoilage has in the last decades become an enormous problem throughout the world with a significant amount of raw materials, food, feed and agricultural products thrown away every day by food companies, retailers or consumers. Precise numbers are difficult to obtain but rough estimations of the FAO indicate that approximately one-third of the food produced for human consumption is wasted globally each year [1]. Economic losses and environmental impact related to this spoilage are of course considerable with not only a waste of resources like raw materials, water, fertilizers and energy but also the emission of greenhouse gases during production, transport and waste treatment. An ethical aspect is also present with food losses creating a lack of security and higher price volatility that quite often impacts populations in the developing countries. Facing the limited resources available on the planet and the growing world population, reduction of food spoilage throughout the whole supply chain has become one of the biggest challenges faced by the food industry [2-5].

Spoilage occurs when food products become unacceptable for human consumption, either due to modifications in sensorial characteristics such as texture, taste, smell or appearance that are rejected by the consumers, or due to the formation of pathogens or toxins harmful for humans [5]. Environmental factors such as temperature, humidity, oxygen and light can trigger several reaction mechanisms leading to food degradation and changes in organoleptic properties. The major cause of food spoilage remains however the contamination by micro-organisms such as bacteria (*Pseudomonas*, *Salmonella*, *Escherichia Coli*) and fungi (yeasts (*Saccharomyces*, *Candida*) or molds (*Penicillium*, *Aspergillus*)). Microbial contamination appears as a constant risk along the whole supply chain and is estimated to cause about a quarter of the world's food supply loss [2]. This represents for instance an economic loss of one billion per year in the USA and ten millions in Australia. In countries with tropical climates, fungal spoilage alone is responsible for an estimated 5-10% of total food losses.

Food spoilage is preventable to a large degree by a number of preservation methods that can reduce, slow down or eradicate the risk of microbial contamination and extend the product shelf-life. Preservation techniques used in the food industry [4-5] can be classified in two categories (physical and chemical protection) and are nowadays quite often used in combination to set-up multiple barriers against micro-organisms. Physical preservation relates to the application of measures such as heat treatment (sterilization,

pasteurization), refrigeration (cooling, freezing), dehydration (drying) and irradiation, mainly aiming at suppressing essential microbial growth conditions. Chemical methods are characterized by the addition of preservative molecules [6-8] acting either on environment (pH stabilizer, antioxidant), in the same purpose than physical methods, or on the micro-organisms themselves via killing or inhibition action (antimicrobial compounds). Traditional preservatives englobe simple acid compounds and their salts (benzoate, acetate, nitrate, sorbate, propionate), parabens, sulfites, as well as more complex naturally-occurring compounds such as lactoferrin, peptides (lysozyme, nisin) and natamycin. More recently, antimicrobial compounds have been developed from natural sources including for instance essential oils and spices [9-10].

Recent trends on the market indicate a growing demand and preference of customers for reduced processing treatments of food products as well as limited use of chemical compounds [9-10]. Shifting towards new natural antimicrobials is one possibility explored by food manufacturers but is not favored by high research costs and regulatory hurdles set by health authorities that make the approval procedure very tedious. Improving the functionality of already approved ingredients, mainly by working on their reformulation, is nowadays the preferred approach of food preservative suppliers to maximize antimicrobial efficiency and reduce the quantities involved in food protection treatments. The need for enhanced functionality and efficiency of the preservative molecule natamycin supplied by DSM Food Specialties is addressed in this PhD thesis.

## 1.2. Natamycin, usage and properties

Natamycin (Figure 1.1) [11], also known as pimaricin, is a naturally-occurring polyene antifungal compound, discovered in 1955 in a soil sample from the province of Natal, South Africa, and introduced to the market in 1967. Produced by fermentation of the bacteria *Streptomyces natalensis*, natamycin is commercialized by DSM Food Specialties under the Delvocid<sup>®</sup> family brand and is approved worldwide as food preservative by food safety authorities [6-7], without adverse effects on human health reported. Main applications of this antimicrobial compound in the past decades focused on the long-term protection of food surfaces of cheese and fermented meat (sausages for instance), by applying coatings containing natamycin crystalline particles that dissolve slowly to provide the antifungal activity. More recently, applications by direct

incorporation of natamycin in food products such as yoghurts, beverages, wines or baked goods have emerged in some countries.

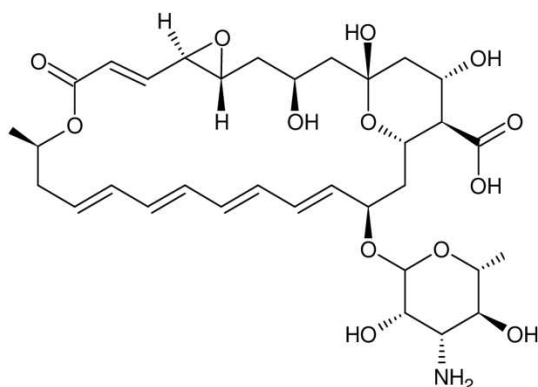


**Figure 1.1: Chemical structure of natamycin**

Natamycin provides antimicrobial action selectively towards fungi without activity against bacteria, preventing interference with food processing. Compared to other food preservatives, natamycin possesses a broad activity spectrum and is efficient at low doses with minimum concentration necessary to inhibit microbial growth (MIC) below 3-10 ppm for most known food microbes [12-14]. Natamycin presents the added advantage of not triggering development of resistance mechanisms by fungi as could be the case for other antibiotics compounds. Finally, when incorporated or applied on food products, natamycin has not been reported to affect the food quality or organoleptic properties.

The mechanism of action of the polyene has been recently explained by the diffusion and strong binding of natamycin molecules to the ergosterol present in biological membranes [15]. Ergosterol is a building block of yeast and molds membranes, responsible mainly for intracellular nutrient transport, protein function and vacuole fusion. The complex natamycin-ergosterol limits the mobility of the latter in the membrane and prevents it to play its active role in the survival of the fungi. Absence of ergosterol in the membrane of bacteria explains the absence of antibacterial activity of natamycin.

Regarding its chemical properties, natamycin displays the classical structure observed for other polyene macrolide antifungals [13-14] such as the well-known amphotericin B (AmB) and nystatin. These compounds are characterized by the presence of a macrocyclic ring closed by lactonization, with one side containing conjugated tetraene double bonds while the opposite side features various oxygen functions. An additional sugar moiety, called mycosamine, is also present and linked to the ring by a glycosidic bond. The presence of a carboxylic group on the ring and an amino group on the sugar

moiety confers an amphoteric character to natamycin with an isoelectric point around pH 6.5 ( $pK_a$  4-4.5,  $pK_b$  8.6) [11]. Natamycin also presents an amphiphilic aspect explained by a very polar end (carboxylic group and mycosamine) and a macrocyclic ring in which the two sides themselves have different properties (rigidity and hydrophobicity for the tetraene structure, flexibility and hydrophilicity for the opposite side). Though it has been proven that natamycin does not form self-association structures in water [16], in opposite to polyene antibiotics with larger molecular weight such as amphotericin and nystatin, this feature leads however to an intermediate behaviour and rigid conformation that must be considered in formulations. Particularly, this limits considerably the solubilization of natamycin in water or solvents (Table 1.1). Highest solubilization levels have been reported for polar solvents among which methanol, dimethylsulfoxide, glycerol and propylene glycol [11,13]. The presence of hydroxyl and zwitterionic groups makes natamycin insoluble or very sparingly soluble in any other solvents like higher alcohols, ethers, esters, aromatic or aliphatic hydrocarbons or ketones. Solubility in water is very poor (20-50 ppm), mainly due to the tetraene structure, and can be enhanced by dissolution in acidic or alkaline solutions with natamycin still being active against fungi on the pH range 4-9. Natamycin suspensions with pH in the range 5-9 are stable for several years while stored in the dark, almost as stable as the native powder (trihydrate crystalline form). However, stability can be tremendously reduced by the use of extreme pH (hydrolysis of the glycosidic link, saponification of the lactone), exposure to heat, oxidation or UV light (fast cleaving of the tetraene bonds) and presence of heavy metals (catalysts for the cleaving). All mechanisms quite often happen simultaneously and deactivate natamycin rapidly, creating non-toxic but unfortunately non antifungal decomposition products [11,13].

**Table 1.1: Solubility of natamycin in various solvents, adapted from [11]**

| Solvent                            | Solubility (mg/mL) |
|------------------------------------|--------------------|
| Water                              | 0.020-0.050        |
| Methanol                           | 3.3                |
| Ethanol                            | 0.04               |
| Acetone                            | < 0.01             |
| Ethylacetate                       | < 0.01             |
| Glycerol                           | 15                 |
| Propylene glycol / ethylene glycol | > 20               |
| Dimethylsulfoxide                  | 1.5                |
| Glacial acetic acid                | 250                |



### **1.3. Nano-encapsulation, a valuable option for natamycin**

Thanks to its natural origin, long history of safe use, efficiency at low concentrations and limited modification of food products, natamycin remains particularly appealing for food preservation but could undoubtedly benefit from further enhancement of functionality and efficiency.

Main challenges faced while using natamycin are related to the solubility and stability properties mentioned previously. The poor aqueous solubility of natamycin indeed not only limits its availability in molecular state for antimicrobial activity but also its diffusion rate to the site for antifungal action. This is particularly relevant for food coating applications where limited diffusion rate can result in heterogeneous protection of the surface and difficulty to maintain on the long-term a concentration superior to the MIC required against micro-organisms. On the other hand, stability issues, particularly exposure to extreme pH and oxidation phenomena common for food products, result in a premature decrease in the antimicrobial activity. In both cases, higher quantities of preservative have to be incorporated in the formulation to compensate the loss and ensure protection during the desired period. Another important aspect is the limited specificity and tunability of current natamycin formulations, based mainly on the dissolution of crystalline particles that offer little possibilities of targeted action or controlled/triggered release rate.

Answers to availability and degradation issues as well as tunability could all be provided by performing encapsulation of natamycin into nano-carriers.

Technologies to encapsulate molecules of interest inside nano-carriers have emerged in the last decades making use of the specific physicochemical properties of nanoparticles, namely their large surface-to volume ratio that results in high reactivity and confers to them properties substantially different from microparticles. Pharmaceutical and medical applications are predominant in the literature [17-18], acknowledging many advantages of nano-encapsulated drugs over the native drug, such as prolonged life-time and stability, improved solubility, release at a sustained and controlled rate, delivery to targeted tissues or cells, reduced toxicity of the drug or enhanced bioavailability. Nano-encapsulation is also under development in the food industry though products on the market are still limited [19-23]. Main applications so far relate to functional ingredients such as vitamins, antioxidants, coloring or flavoring agents, antimicrobials, enzymes, etc... Stated benefits

of nano-encapsulation are in these cases higher availability of food bioactive component ingredients, selective delivery to specific location in the food product (for instance, lipid domains), reduction of incompatibility with other food components and stability improvements, avoiding unnecessary overdosing of the compound of interest.

A wide range of nano-carriers including mainly lipid-based nano-systems (nano-emulsions, solid lipid nanoparticles, microemulsions, liposomes) or biodegradable polymer-based nano-carriers (polymeric nanospheres, polymeric micelles, nanocapsules, polyelectrolytes complexes) has been investigated for food or drug nanodelivery with their own specific advantages and disadvantages for encapsulation, protection, and release of functional ingredients, as well as for production costs, regulatory status, biodegradability and biocompatibility [19,22].

The main hurdle to take into account in the case of natamycin is its specific structure and solubility properties. Most encapsulation systems are indeed described for either hydrophilic or lipophilic compounds but limited knowledge has been established for small amphoteric and amphiphilic molecules. It is however legitimate to assume that, based on its chemical structure, natamycin will interact preferentially with carrier material having the ability to create electrostatic/hydrogen bonding or presenting a polar/amphiphilic character. A limited number of attempts have been reported so far with such nano-carriers for the encapsulation of natamycin and were all focused on application for ocular antifungal treatment. Bhatta et al. [24] described for instance the inclusion of natamycin in charged chitosan/lecithins mucoadhesive nanoparticles, characterized by high levels of encapsulation and a slow release pattern that demonstrated a clear benefit for prolonged ocular delivery. Similar increase of performance, improvement of bioavailability and prolonged release were observed by Phan et al. [25] while encapsulating the preservative in polar poly(*D,L*-lactide)-dextran copolymer micelles and incorporating them in contact lenses. These preliminary results confirm that interesting properties can be generated via the encapsulation of natamycin inside nano-carriers.

While looking broader at the encapsulation of antimicrobial compounds in nanoparticulate systems [26-28], either for pharmaceutical or food purposes, for polyene antimicrobials or other antibiotics with a chemical structure similar to natamycin, liposomes and biodegradable polymeric nanospheres emerge as the two most promising formulations that could be evaluated.

## 1.4. Liposomes

Liposomes are commonly defined as closed spherical-shaped vesicles consisting of an internal aqueous core surrounded by one or more lipid bilayers, in a structure very similar to biological membranes (Figure 1.2) [29-30]. The lipid bilayer contains polar amphiphilic molecules such as phospholipids [31-32], extracted from natural oils (sunflower lecithin, soya lecithin) or egg yolk. Phospholipids possess a hydrophobic double fatty acid tail, with variable composition and length related to their original source, as well as a hydrophilic head, made of a phosphate group connected to a small molecule, conferring a charge or neutral/zwitterionic aspect to the molecule. The classical phospholipids structure is illustrated in Figure 1.3a. Sterols are also commonly added to the lipid mixture and known to modify the fluidity and stability of the bilayer (Figure 1.3b) [33-34].

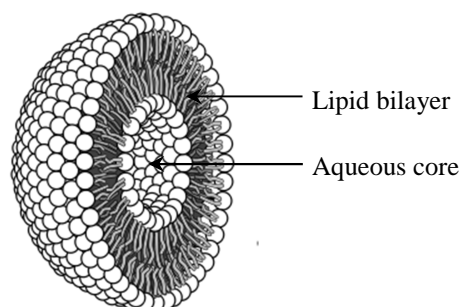


**Figure 1.2: Structure of liposome assemblies**

Formation of liposomes is based on the non-spontaneous assembly of phospholipids related to unfavorable interactions occurring between these amphiphilic molecules and water [35-36]. Under the right conditions, hydrophobic tails are forced to face each other creating the bilayer, while polar heads are oriented towards the external inner or outer aqueous medium. Depending on the manufacturing process, liposomes can range from tens of nanometers to a few micrometers and show a variety of structures such as unilamellar (single bilayer), multilamellar (multiple bilayer membranes arranged in a concentric structure) or multivesicular (when liposomes contains other random-sized vesicles [29]). Nano-liposomes are known as small unilamellar vesicles (SUVs) with diameters ranging from 20-100 nm. These nano-sized liposomes can be obtained by two main techniques [29-30,37]. The first type involves two steps: the formation of large or multilamellar vesicles with further post-treatment either by sonication or extrusion through filters of well-defined pore size [37-38]. A simple one-step method called solvent

injection [29,39-40] is also available and involves the dissolution of the phospholipids in a solvent miscible in water in all proportions. The injection of this lipid solution in an aqueous phase and the rapid diffusion of the solvent trigger the sudden desolvation of phospholipids and their assembly into bilayers.

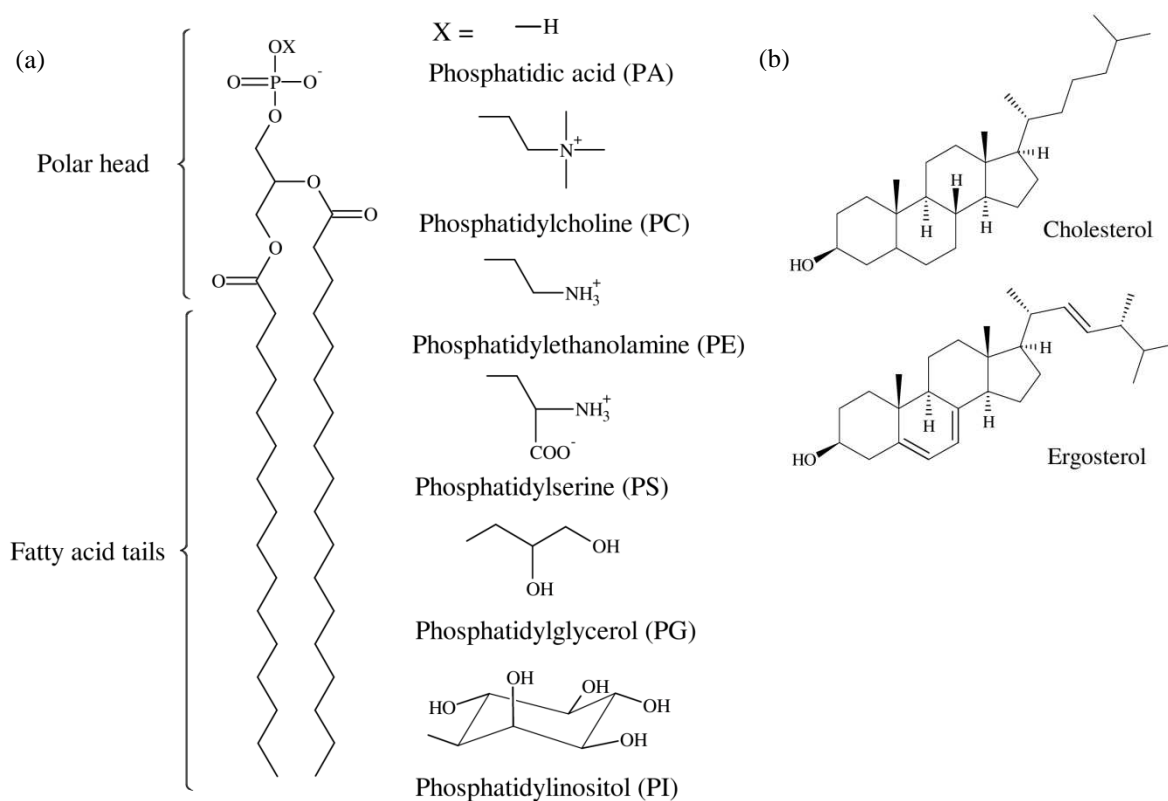


**Figure 1.3: Phospholipids composition (a) and sterols structure (b)**

Liposomes are highly attractive for pharmaceutical or food applications [41-43] owing to their natural origin, biodegradability, biocompatibility and inherent non-toxicity. Liposomes are moreover recognized as universal carriers that can entrap a wide variety of water-soluble, lipid-soluble or amphiphilic materials. Hydrophilic molecules are generally encapsulated within the aqueous core, protected from changes in the external aqueous phase or from interaction for other components. Lipophilic molecules are on the other hand entrapped in the core of the bilayer, while amphiphiles preferentially position themselves between the phospholipids molecules close to the water interface. Eventually, highly versatile physicochemical properties can be obtained from the liposomes by playing for instance with the phospholipid composition, the addition of additives such as sterols, the size or the number of bilayers, etc... enabling the development of fine-tuned

formulations to achieve the desired encapsulation and delivery properties. Main limitations of liposomal formulations [29,44] are in some cases the poor mechanical integrity of the bilayer and low resistance to shear occurring during pumping or mixing that limits the possibility of post-treatment and might trigger early release while use in the final application. Physical instability (fusion, rearrangement) or chemical instability (hydrolysis, oxidation) [45] and rapid leakage of encapsulated compound outside of the vesicles is also a frequent issue encountered. Both problems can be solved or reduced by choosing appropriate bilayer composition or by modifying the surface of the liposomes for instance by deposition of an oppositely-charged polymer [46-47], providing a coating layer that can stabilize the formulation and control the release.

Advantages of liposomal formulations have been clearly established in the field of antibiotics [26-27, 48] and recognized as optimum formulation to decrease toxicity, improve bioavailability and shelf-life, as well as enhance activity against targeted cells to overcome for instance microbial resistance or to reduce dosages employed.

Liposomes have been in particular extensively studied and characterized for polyene antimycotics [28], among which amphotericin B is the most famous example [49-51] as well as the first liposomal formulation ever approved by the Food and Drug Administration (FDA). Commercialized under the name AmBisome<sup>®</sup> (Vestar Inc.), this product consists of SUVs, made of hydrogenated soybean PC, cholesterol and distearoylPC, that presents a diameter of about 80 nm and a very rigid bilayer, in which up to 10% mol of amphotericin B is incorporated. Compared to the native antibiotic and its conventional formulation (Fungizone<sup>®</sup>, mixed micelles with sodium deoxycholate), the liposomal formulation demonstrated similar antifungal activity but significantly reduced toxicity, allowing higher doses to be used with attenuated side-effects and reduction of the frequency of injections. Further studies performed with *Candida* yeasts showed a greater specificity of action towards fungal infections, with liposomes absorbing and merging with fungi membrane thanks to their resemblance to natural bilayer of the microbes and delivering locally the amphotericin B. Success of new liposomal formulations of amphotericin B stimulated also the interest for parent compounds such as nystatin. Liposomal nystatin, based on multilamellar vesicles, (Nyotran<sup>®</sup>, Aronex Pharmaceuticals, dimyristoylPC and dimyristoylPG in a 7:3 ratio), is in late phase III clinical trials for topical antifungal treatment [52]. In vitro tests demonstrated, as for

amphotericin B, a similar activity compared to the native nystatin but a more targeted delivery. Liposomal entrapment has also proven to be beneficial for other macrolide antibacterials, with for instance in the case of clarithromycin a 30-fold increase of concentration reachable via incorporation in multilamellar 100 nm-liposomes compared to the aqueous solubility of this compound [53].

In the field of food antimicrobials, liposomal formulations are mainly described for antimicrobial peptides (nisin, lysozyme) [54], essentially aiming at preventing early stage degradation or undesirable interactions with other food components. Benech et al. [55] demonstrated that nisin can be encapsulated within hydrogenated PC liposomes and used for protection against microbial growth during cheese ripening. Liposomes enabled at the same time higher resistance of nisin to heat treatment happening during the manufacturing process and sustained activity of nisin against the bacteria *Listeria innocua* over a period of 6 months. Further microscopic studies performed by Colas et al. [56] proved that interaction between nisin-loaded nano-liposomes and the bacteria happened by membrane fusion, enabling a close contact and delivery of the preservative. For cheese manufacturing, it was also shown that liposomes and microbes end up in similar lipid phases during the food processing allowing close contact and thus enhanced activity. Besides, Zou and al. [57] demonstrated that the incorporation of nisin in hydrogenated PC-cholesterol nano-liposomes enhanced the antimicrobial activity against *Listeria monocytogenes* and *Staphylococcus aureus* micro-organisms compared to free nisin, with reduced MIC and prolonged release and inhibition of antimicrobial growth. Encapsulation of nisin and lysozyme was also achieved in PC/PG/cholesterol nano-liposomes and showed enhanced antimicrobial activity and growth inhibition against *Listeria monocytogenes*. This improved activity was confirmed while incorporating the liposomal formulations in milk [58].

## 1.5. Biodegradable polymeric nanospheres

Nanospheres can be defined as matrix-type colloidal particles, i.e. spherical particles, whose entire mass is solid, characterized by a size usually ranging between several tenths to a few hundreds nanometers. The compound of interest can be dissolved, entrapped, chemically bound or adsorbed at the surface via interactions with the polymer forming the nanoparticles [59-61].

Polymeric nanospheres can be obtained from synthetic or natural preformed polymers by one-step or two-steps solvation/desolvation processes [59, 62-63]. One-step techniques, namely nanoprecipitation [64-66] or dialysis [62, 67-68], involve the solubilization of the polymer and compound to encapsulate in a solvent fully miscible with water. The sudden diffusion of the solvent while this organic phase is put in contact with an aqueous phase triggers the precipitation of the macromolecules and their assembly in nanospheres. Two-step techniques [62,69] consist in an emulsification phase, in which the polymer and compound are dissolved in droplets of a solvent immiscible in water, followed by a step of solvent removal (evaporation, sudden dilution, salting-out) that trigger the precipitation of the polymer.

The most commonly used biodegradable polymers belong to the family of hydrophobic polyesters [70-71] (Figure 1.4) such as poly-lactic acid (PLA), poly-glycolic acid (PGA), poly(*D,L*-lactic-co-glycolic) acid (PLGA) and  $\epsilon$ -polycaprolactone ( $\epsilon$ -PCL). Particular features of these polymers are their commercial availability with versatile molecular weights and compositions, their good biocompatibility and minimal toxicity, the wide range of degradation behaviors thus tunable release rates that they offer and their approval by the FDA. Their hydrophobic polar structure added to the presence of hydroxyl and carboxylic groups enables encapsulation of lipophilic molecules as well as hydrophilic ones, though at a lower extent.

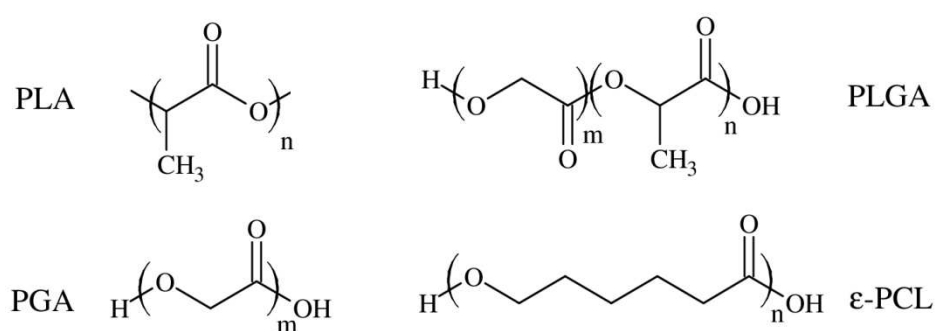


Figure 1.4: Chemical structure of classical biodegradable polyesters

Due to their solid matrix structure, polymeric nanospheres are mechanically stable and can be processed without disruption or incorporated in application without collapsing. They are however likely to aggregate. The surface of the nanoparticles can be treated by surfactants or polymer deposition to limit aggregation and improve stability of the formulations. This also gives a possibility for functionalization or tunable controlled release of the compound encapsulated.

Numerous authors already implemented the use of polymeric nanospheres for entrapments of antimicrobials and antibiotics compounds, demonstrating improved delivery and efficacy [60-61,72].

Van de Ven et al. [73] investigated the incorporation of amphotericin B in PLGA 50:50 polymeric nanospheres and reported encapsulation levels of up to 60% allowing drug dose reduction and limited side-effects of the polyene. Compared to the liposomal commercial form AmBisome, 10-fold higher *in vitro* antifungal activities against *Candida albicans* and *Aspergillus fumigatus* were highlighted. The authors also indicated that, used *in vivo*, polymeric nanospheres interacted better with the targeted organisms and were taken up at a higher degree, enabling local prolonged delivery and superior efficacy. Italia et al. [74] gave evidence that these nanoparticles are suitable for oral delivery applications and displayed lower toxicity levels for human, sustained release and superior bioavailability related probably to the protection of amphotericin B from enzymatic and chemical degradation. On the other hand, Espuelas et al. [75] attempted to incorporate AmB in  $\epsilon$ -PCL nanospheres but low affinity for the polymer and self-aggregation properties of AmB limited its incorporation to a simple adsorption at the surface of the nanoparticles. Successful PLGA formulations are described for the encapsulation of other macrolide antibacterials such as clarithromycin [76] and azithromycin [77] with 8-fold lower MICs observed *in vitro* against respectively *Staphylococcus aureus* and *Salmonella typhi*. The hypothesis made by the authors to explain this higher efficacy relates to a change of crystallinity of the drugs while incorporated in the nanoparticles and the formation of an amorphous state that enables higher levels of bioavailability. Esmaili et al. [78] showed successful encapsulation of rifampicin in PLGA nanoparticles and a considerable increase in *in vitro* antibacterial activity, related to better penetration of the nanoparticles in the bacteria cell as previously experienced for amphotericin B.

Regarding the encapsulation of food antimicrobials, polymeric nanospheres have been explored mainly for essential oils and antimicrobial peptides [79]. Gomes et al. [80] optimized for instance the encapsulation of two natural essential oils, eugenol and cinnamaldehyde, within PLGA nanoparticles. High levels of encapsulation (> 92%) were achieved and led to sustained release coupled with enhanced efficacy against *Salmonella* and *Listeria*. Incorporation of nisin in PLA nanoparticles was studied by Salmaso et al. [81]. Nanospheres in the range 200-400 nm were successfully obtained and showed sustained release of the antimicrobial peptide, with variation under different salts and pH



conditions. Antibacterial activity in vitro against the bacteria *Lactobacillus delbrueckii* showed a sustained release of nisin in its active form over 45 days.

## **1.6. Post-processing of nano-carriers, a prerequisite for industrial use**

While development of nano-encapsulation systems is well described and characterized for a large variety of molecules, limited research integrates simultaneously the preparation of the nanoparticles and post-treatments necessary for their use in real applications. Such post-preparation treatments include for instance the purification from large aggregates, non-encapsulated materials or residual solvents involved in the formulation process in order to comply with regulatory requirements. Another relevant aspect is the concentration of nano-suspensions that are obtained in certain cases at low solid content, hampering their use in commercial applications and leading to high costs of transport and storage. Finally, storage as a suspension or concentrate might be detrimental for the long-term shelf-life of the nano-carriers or the compound of interest with a risk of chemical degradation or physical instability of the suspensions (aggregation, fusion, sedimentation). Transforming nano-suspensions into redispersible dry powders is a convenient way to increase shelf-life of the product as well as easiness of handling for customers and reduced costs of storage and transport. Whatever post-treatment needs to be applied, it is essential that the technique employed allows a conservation of nanoparticle integrity and limits premature release of the encapsulated molecule. In the case of dried forms, it is also necessary to ensure an appropriate redispersibility of the powder into native nanoparticles with similar physicochemical properties and release behavior.

### **1.6.1. Purification and concentration**

Various techniques have been proposed in the literature [59,82] to tackle simultaneously purification and concentration issues: evaporation under reduced pressure, dialysis, ultracentrifugation and filtration.

Evaporation under reduced pressure is an easy and efficient way to remove volatile organic solvents involved in the preparation methods of both polymeric nanospheres and liposomes. Water can also be removed by this process at some extent but it becomes an expensive and tedious process while considering scaling-up [82-83].

Dialysis is a relatively common technique implemented for purification [82, 84-85]. By equilibration of the nano-suspension towards fresh aqueous mediums and choice of an appropriate molecular weight cut-off of the dialysis membrane, residual solvent and non-encapsulated compound can be efficiently removed. Concentration can also be performed via dialysis by applying osmotic stress in the counter-dialysis medium. This technique, implemented for instance for polymeric nanospheres by Vauthier et al. [82], enables a control of the final concentration of particles in the nano-suspension and can also be scaled-up. Dialysis is particularly relevant when sensitive molecules or fragile nano-carriers are considered as it does not involve applying forces altering the nanoparticles or form aggregates. This method requires however large volumes of counter-dialysis medium as well as long purification times to ensure efficient removal. Coupled to the existence of a concentration gradient during the process, these long periods of time quite often trigger premature release of the active compound which is detrimental to the encapsulation.

Ultracentrifugation is the classical method performed at lab scale for both purification and concentration of polymeric nanospheres [86]. High speeds involved in the centrifugation enable nanoparticles to sediment into a pellet. Alternate cycles of pellet resuspension in fresh medium and ultracentrifugation are a convenient method to flush away solvent and non-encapsulated materials. Purified pellet can then eventually be resuspended in the desired quantity of aqueous medium to obtain the desired concentration for further use. The main limitation of this method is the formation of aggregates and/or compact pellets due to the strong interactions occurring between nanoparticles. In this latter case, redispersion is very difficult, preventing at the same time efficient washing steps during purification and reconstitution of the native nano-suspension properties. Additional steps of vortexing or ultrasonication are usually implemented but can be detrimental for the physical and chemical stability of the nanospheres as well as for the compound of interest. Ultracentrifugation is also reported for liposomes [87-88] treatment but is barely applicable for SUVs owing to their small size and low density. Fragility of the vesicles also needs to be taken into account while applying strong centrifugation forces, as disruption, fusion or rearrangement of the liposomes could be engendered and could trigger leakage of the encapsulated molecule.

Tangential Flow Filtration (TFF), also known as cross-flow filtration, is the most recently studied technique and so far the most promising approach to purify and concentrate nanoparticles without significant modification of their properties or detrimental loss of loaded compound [89-91]. This technique involves the filtration with a feed flow tangential to the membrane instead of a perpendicular flow used in classical filtration, limiting the formation of cake and blocking of the membrane by constant flush away of absorbed particles. Besides the concentration of nano-suspensions, TFF can also be combined with one or more additional steps of diafiltration, i.e. a filtration where the aqueous phase is progressively replaced by a fresh aqueous medium, allowing for instance reduction of residual solvent to acceptable levels. In both cases, infrastructures and processes to use TFF at large scale already exist and require fast treatment times compared for instance to dialysis, making the perspective of scale-up realistic. While establishing the optimal process parameters for the filtration, attention has however to be paid to the possible loss of nanoparticles by adsorption on the membrane that can still happen and decrease the process efficiency dramatically if a cake is formed [92-93]. If appropriate parameters are chosen, it has been proven that TFF does not alter either the size of the particles or the encapsulation efficiency of the nano-carriers [90]. Same considerations apply to liposomes filtration [94] with the additional fragility of the structure to take into account to avoid unwanted extrusion process of the liposomes through the membrane pores and significant loss of lipid materials through the discarded filtrate.

### **1.6.2. Preparation of dried products**

Transforming nanoparticles into redispersible dried powders has been addressed mainly by two approaches used commonly in the food or pharmaceutical industry: spray-drying and freeze-drying.

Spray-drying enables the formation of micron-sized carriers containing the nanoparticles dispersed in an inert matrix, protecting the nano-carriers upon storage and enabling short redispersion time. The process consists in adding to the nano-suspensions a drying auxiliary chosen among hydrophilic materials (sugars (mannitol, lactose), starches, dextrans, chitosan, maltodextrins, etc...). This liquid phase is then atomized in micro-droplets and dried in hot air to form the microparticles. Spray-drying is a rapid and low-

cost process available at larger scale and offers additionally the possibility to further modify the properties of the microparticles to produce powders with the desired behaviour. Spray-drying has been reported successfully for polymeric particles [95-98] with a clear influence of process parameters (temperatures, atomizing rate, nozzle characteristics, etc...) and compatibility between the drying auxiliary and the nano-carrier material. Spray-drying has also been described at a lesser extent for liposomes, essentially for pulmonary delivery purposes [99-101], but success was limited to lipophilic entrapped-compounds while important leakage of hydrophilic compounds was observed during the process.

Lyophilization, also known as freeze-drying, is the second option available to remove water from the nano-suspensions. This well-established method consists in three steps: 1) freezing of the nano-suspensions, 2) primary drying (ice sublimation) and 3) secondary drying (removal of unfrozen water). Though this technique involves relatively mild conditions, various stresses can be induced during these three steps. Formation of ice crystals can for instance exert mechanical stress on the particles which can be critical if they are deformable or fragile like liposomes [102]. Progressive concentration of the nanoparticles during the process of water removal can also lead to the formation of aggregates. Lyoprotective or cryoprotective agents such as sugars (glucose, lactose, sucrose, trehalose) or polyalcohols (mannitol, glycerol, polyvinylalcohol, etc...) are commonly incorporated to prevent the formation of ice crystals, to improve the resistance of the nanoparticles by forming a protective layer at their surface, to limit the leakage of the encapsulated compound and to help the redispersion of the powder. A substantial number of parameters were shown to impact the final morphology and redispersion properties of the freeze-dried powder, among which process parameters (freezing temperature, rate of water removal during drying steps, etc...) and concentration of protectant involved in the formulation. Lyophilization has been reported successfully for both polymeric nanospheres [103-104] and liposomes [105] with applications for both hydrophilic and lipophilic entrapped compounds.

## 1.7. Aims and scope of the thesis

Liposomes and polymeric nanospheres could be an elegant approach to tackle the challenges faced by current formulations of natamycin and have demonstrated clear benefits for other polyene antibiotics or food antimicrobials. Both nano-carriers present properties expected to ensure efficient encapsulation of the antifungal such as polarity, amphiphilicity and possibility to create electrostatic/hydrogen bonding. Methods such as solvent injection for liposomes and nanoprecipitation for polymeric nanospheres, involving solvents fully miscible with water in which natamycin could be dissolved at acceptable levels, are possible options to nano-encapsulate the preservative. **Part I** of this thesis presents the proof of principle of the possibility to encapsulate the antifungal within these types of nano-carriers and assesses benefits and limitations for encapsulation, delivery and performance in antimicrobial protection.

**Chapter 2** focuses on the optimization process of biodegradable polymeric nanoparticles obtained from polyesters by the nanoprecipitation method. **Chapter 3** focuses on the development of SUV liposomal formulations of natamycin based on food-grade soybean lecithins by the solvent injection method and highlights the advantages of incorporating sterols in the bilayer. Both chapters include a description of the preparation method selected, a systematic screening of formulation parameters for the preparation of unloaded nano-carriers and finally the effect of natamycin incorporation on the process and physicochemical characteristics of the nanoparticles (size, polydispersity, surface charge, morphology, thermal and crystalline properties). Affinity of natamycin for the nano-carriers, encapsulation/loading efficiency, stability, *in vitro* release performances under various conditions and antimicrobial tests against the model yeast *Saccharomyces cerevisiae* are also reported.

The development of commercially suitable formulations by post-treatment of the nanosuspensions is addressed in **Part II** of this thesis. More particularly, attention is focused on Tangential Flow Filtration and lyophilization, which appear to be the most convenient and reliable approaches for the concentration and drying of both types of nano-carriers in the presence of natamycin.

**Chapter 4** reports investigations related to the purification and concentration of nano-suspensions using the TFF method. Various process parameters (filtration pressure, membrane properties) and their effect on the final properties of the nano-suspensions

(evolution of size characteristics, losses of natamycin or carrier material during the process, encapsulation efficiency, morphology and stability upon storage in terms of size and natamycin content) are evaluated in a comparative way for both types of nano-carriers.

**Chapter 5** focuses on the transformation of liposomes and polymeric nanospheres into powders as an alternative for concentrated suspensions, in presence of various types and concentrations of protective excipients. Effectiveness of each protectant is assessed during the different steps of the lyophilization process to establish conditions and compositions maintaining the integrity of the nanoparticles and allowing obtention of easily redispersible powders able to protect efficiently both natamycin and nano-carriers towards degradation over time.

Finally, **Chapter 6** summarizes advantages and limitations of each nano-formulations as well as their potential for development of concentrated or dried formulations, followed by recommendations for further exploration of these nano-systems.

## References

- [1] J.Gustavsson, C.Cederberg, U.Sonesson, R. van Otterdijk, A.Meybeck, Global food losses and food waste - Extent, causes and prevention, *FAO*, Rome, **2011**
- [2] J.I.Pitt, A.D.Hocking, Fungi and Food Spoilage, *Springer Science & Business Media*, **2009**
- [3] M.Ellin Doyle, Microbial food spoilage – Losses and Control Strategies. A brief review of the literature, *Food Research Institute Briefings - University of Wisconsin*, **2007**
- [4] G.W.Gould, Preservation: past, present and future, *British Medical Bulletin*, **2000**, 56, 84-96
- [5] M.S.Raman, Handbook of Food Preservation, 2<sup>nd</sup> edition, CRC Press, Taylor& Francis group, **2007**
- [6] N.J.Russell, G.W.Gould, Food Preservatives - 2<sup>nd</sup> edition, Chapter 9: Natamycin, Springer Science & Business Media, **2003**
- [7] E.Lück, M.Jager, Antimicrobial Food Additives: Characteristics, Uses, Effects, Volume 2, Chapter 28 –Natamycin, Springer Science & Business Media, **1997**
- [8] P.M.Davidson, J.N.Sofos, A.L.Branen, Antimicrobials in Food, Third Edition, CRC Press, **2005**
- [9] F.J.Señorans, E.Ibáñez, A.Cifuentes, New Trends in Food Processing, *Critical Reviews in Food Science and Nutrition*, **2003**, 43 (5), 507-526
- [10] R.Bhat, A.K.Alias, G.Paliyath, Progress in Food Preservation, John Wiley & Sons, **2012**

- [11] H. Brik, Natamycin, *Analytical Profiles Drug Substances*, Academic Press Inc. (London), **1981**, *10*, 513-561
- [12] J.B. Klis, L.D. Witter, Z.J. Ordal, The effect of several antifungal antibiotics on the growth of common food spoilage fungi, *Food Technology*, **1959**, *13*, 124-128
- [13] A.H. Thomas, Analysis and assay of polyene antifungal antibiotics. A review, *The Analyst*, **1976**, *101*, 321-340
- [14] J.M.T. Hamilton-Miller, Chemistry and Biology of the Polyene Macrolide Antibiotics, *Bacteriological Reviews*, **1973**, *37(2)*, 166-196
- [15] Y.M. te Welscher, H.H. ten Napel, M. Masià Balagué, C.M. Souza, H. Riezman, B. de Kruijff, E. Breukink, Natamycin blocks fungal growth by binding specifically to ergosterol without permeabilizing the membrane, *J. Biol. Chem.*, **2008**, *283(10)*, 6393-6401
- [16] J.L.Koontz, J.E.Marcy, Formation of natamycin:cyclodextrin inclusion complexes and their characterization, *J.Agric.Food Chem.*, **2003**, *51*, 7106-7110
- [17] D.Thassu, M.Deleers, Y.V.Pathak, *Nanoparticulate Drug Delivery Systems*, CRC Press, **2007**
- [18] A.Z. Wilczewska, K.Niemirowicz, K.H.Markiewicz, H.Car, Nanoparticles as drug delivery systems –Review, *Pharmacological Reports*, **2012**, *64*, 1020-1037
- [19] J.Weiss, P.Takhistov, D.J. McClements, Functional materials in food nanotechnology, *Journal of Food Science*, **2006**, *71*, R107-R116
- [20] Q.Chaudhry, M.Scotter, J.Blackburn, B.Ross, A.Boxall, L.Castle, R.Aitken, R.Watkins, Applications and implications of nanotechnologies for the food sector, *Food Additives and Contaminants*, **2008**, *25(3)*, 241-258
- [21] M.A.Augustin, Y.Hemar, Nano- and micro-structured assemblies for encapsulation of food ingredients, *Chem.Soc.Rev.*, **2009**, *38*, 902-912
- [22] B.S.Sekhon, Food nanotechnology – an overview, *Nanotechnology, Science and Applications*, **2010**, *3*, 1-15
- [23] P.N.Ezhilarasi, P.Karthik, N.Chhanwal, C.Anandharamakrishnan, Nanoencapsulation techniques for food bioactive components: a review, *Food Bioprocess.Technol.*, **2013**, *6*, 628-647
- [24] R.S.Bhatta, H.Chandasana, Y.S.Chhonker, C.Rathi, D.Kumar, K.Mitra, P.K.Shukla, Mucoadhesive nanoparticles for prolonged ocular delivery of natamycin: *In vitro* and pharmacokinetics studies, *International Journal of Pharmaceutics*, **2012**, *432*, 105-112
- [25] C.M. Phan, L. Subbaraman, S. Liu, F. Gu, L. Jones, *In vitro* uptake and release of natamycin Dex-b-PLA nanoparticles from model contact lens materials, *J. Biomater. Sci. Polym. Ed.*, **2013**
- [26] J.Weiss, S.Gaysinsky, M.Davidson, J.McClements, *Global Issues in Food Science and Technology - Chapter 24: Nanostructured encapsulation systems: Food antimicrobials*, Academic Press, **2009**, 425-479
- [27] L.Zhang, D.Pornpattananangkul, C.-M.J.Hu, C.-M.Huang, Development of nanoparticles for antimicrobial drug delivery, *Current Medicinal Chemistry*, **2010**, *17*, 585-594

- [28] A.W. Ng, K.M. Wasan, G. Lopez-Berestein, Development of liposomal polyene antibiotics: an historical perspective, *J. Pharm. Pharmaceut. Sci.*, **2003**, 6(1), 67-83
- [29] A.Laouini, C.Jaafar-Maalej, I.Limayem-Blouza, S.sfar, C.Charcosset, H.Fessi, Preparation, characterization and applications of liposomes: state of the art, *Journal of Colloid Science and Biotechnology*, **2012**, 1, 147-168
- [30] A. Akbarzadeh, R. Rezaei-Sadabady, S. Davaran, S.W. Joo, N. Zarghami, Y.Hanifehpour, M.Samiei, M.Kouhi, K.Nejati-Koshki, Liposome: classification, preparation and applications, *Nanoscale Research Letters*, **2013**, 8 (102)
- [31] D.J.Hanahan, A guide to phospholipid chemistry, Oxford University Press, **1997**
- [32] G.Cevc, Phospholipids Handbook, CRC Press, **1993**
- [33] M.Eeman, M.Deleu, From biological membranes to biomimetic model membranes, *Biotechnol.Agron.Soc.Enviro.*, **2010**, 14(4), 719-736
- [34] T.Róg, M.Pasenkiewicz-Gierula, I.Vattulainen, M.Karttunen, Ordering effects of cholesterol and its analogues, *Biochimica et Biophysica Acta*, **2009**, 1788, 97-121
- [35] D.Lasic, The mechanism of vesicle formation, *Biochem. J.*, **1988**, 256, 1-11
- [36] M.Antonietti, S.Förster, Vesicles and liposomes: a self-assembly principle beyond lipids, *Advanced Materials*, **2003**, 15, 1323-1333
- [37] A.Wagner, K.Vorauer-Uhl, Liposome technology for industrial purposes, *Journal of Drug Delivery*, **2011**
- [38] Y.P.Patil, S.Jadhav, Novel methods for liposome preparation, *Chemistry and Physics of Lipids*, **2014**, 177, 8-18
- [39] S.Batzri, E.D.Korn, Single bilayer liposomes prepared without sonication, *Biochimica et Biophysica Acta*, **1973**, 298, 1015-1019
- [40] C. Jaafar-Maalej, R.Diab, V.Andrieu, A.Elaissari, H. Fessi, Ethanol injection method for hydrophilic and lipophilic drug-loaded liposome preparation, *Journal of Liposome Research*, **2010**, 20, 228-243
- [41] M.Fathi, M.R.Mozafari, M.Mohebbi, Nanoencapsulation of food ingredients using lipid based delivery systems, *Trends in Food Science & Technology*, **2012**, 23, 13-27
- [42] M.R.Mozafari, C.Johnson, S.Hatziantoniou, C.Demetzos, Nanoliposomes and their applications in food nanotechnology, *Journal of Liposome Research*, **2008**, 18, 309-327
- [43] M.R.Mozafari, K.Khorasvi-Daradni, G.G.Borazan, J.Cui, A.PArdakht, S.Yurdugul, Encapsulation of food ingredients using nanoliposome technology, *International Journal of Food Properties*, **2008**, 11(4), 833-844
- [44] A.Sharma, U.S.Sharma, Liposomes in drug delivery: progress and limitations, *Int.J.Pharm.*, **1997**, 154, 123-140
- [45] M.Grit, D.J.A.Crommelin, Chemical stability of liposomes: implications for their physical stability, *Chemistry and Physics of Lipids*, **1993**, 64, 3-18
- [46] C.Laye, D.J.McClements, J.Weiss, Formation of biopolymer-coated liposomes by electrostatic deposition of chitosan, *Journal of Food Science*, **2008**, 73(5), N7-N15
- [47] K.Kawakami, Y.Nishihara, K.Hirano, Effect of hydrophilic polymers on physical stability of liposome dispersions, *J.Phys.Chem.B*, **2001**, 105, 2374-2385
- [48] Z.Drulis-Kawa, A.Dorotkiewicz-Jach, Liposomes as delivery systems as antibiotics, *International Journal of Pharmaceutics*, **2010**, 387, 187-198



- [49] I.M.Hann, H.G.Prentice, Lipid-based amphotericin B: a review of the last 10 years of use, *International Journal of Antimicrobial Agents*, **2001**, *17*, 161-169
- [50] G. Barratt, S. Bretagne, Optimizing effect of amphotericin B through nanomodification, *International Journal of Nanomedicine*, **2007**, *2(3)*, 301-313
- [51] B.Dupont, Overview of the lipid formulations of amphotericin B, *Journal of Antimicrobial Chemotherapy*, **2002**, *49(S1)*, 31-36
- [52] R.T.Mehta, R.L.Hopfer, L.A.Gunner, R.L.Juliano, G.Lopez-Berestein, Formulation, toxicity, and antifungal activity in vitro of liposome-encapsulated nystatin for systematic fungal infections, *Antimicrob. Agents Chemother.*, **1987**, *31*, 1897-1900
- [53] X.Liu, B.Zhang, B.Tian, X.Tang, N.Qi, H.He, H.Li, X.Jin, Clarithromycin-loaded liposomes offering high drug loading and less irritation, *International Journal of Pharmaceutics*, **2013**, *44*, 318-327
- [54] P.da Silva Malheiros, D.J.Daroit, A.Brandelli, Food applications of liposome-encapsulated antimicrobial peptides, *Trends in Food Science and Technology*, **2010**, *21*, 284-292
- [55] R.O.Benech, E.E.Kheadr, R.Laridi, C.Lacroix, I.Fliss, Inhibition of *Listeria innocua* in cheddar cheese by addition of nisin Z in liposomes or by in situ production in mixed culture, *Appl. Environ. Microbiology*, **2002**, *68(8)*, 3683-3690
- [56] J.C.Colas, W.L.Shi, V.S.N.M.Rao, M.R.Mozafari, H.Singh, Microscopical investigations of nisin-loaded nanoliposomes prepared by the Mozafari method and their bacterial targeting, *Micron*, **2007**, *38*, 841-847
- [57] Y.Zou, H.-Y. Lee, Y.-C. Sep, J. Ahn, Enhanced antimicrobial activity of nisin-loaded liposomal nanoparticles against foodborne pathogens, *Journal of Food Science*, **2012**, *77(3)*, M165-M170
- [58] L.M.Were, B.D.Bruce, P.M.Davidson, J.Weiss, Encapsulation of nisin and lysozyme in liposomes enhances efficacy against *Listeria monocytogenes*, *J.Food Protect.*, **2004**, *67(5)*, 922-927
- [59] C.Vauthier, K.Bouchemal, Methods for the preparation and manufacture of polymeric nanoparticles, *Pharmaceutical Research*, **2009**, *26 (5)*, 1025-1058
- [60] K.S.Soppimath, T.M.Aminabhavi, A.R.Kulkarni, W.E.Rudzinski, Biodegradable polymeric nanoparticles as drug delivery devices, *Controlled Release*, **2001**, *70*, 1-20
- [61] A.Kumari, S.K.Yadav, S.C.Yadav, Biodegradable polymeric nanoparticles based drug delivery systems, *Colloids and Surfaces B: Biointerfaces*, **2010**, *75*, 1-18
- [62] C.P.Reis, R.J.Neufeld, A.J.Ribeiro, F.Veiga, Nanoencapsulation I. Methods for preparation of drug-loaded polymeric nanoparticles, *Nanomedicine: Nanotechnology, Biology, and Medicine*, **2006**, *2*, 8-21
- [63] J.P.Rao, K.E.Geckeler, Polymer nanoparticles: preparation techniques and size-control parameters, *Progress in Polymer Science*, **2011**, *36*, 887-913
- [64] S.Schubert, J.T.Delaney Jr, U.S.Schubert, Nanoprecipitation and nanoformulation of polymers: from history to powerful possibilities beyond poly(lactic acid), *Soft Matter*, **2011**, *7*, 1581-1588

- [65] M.Chorny, I.Fishbein, H.D.Danenber, G.Golomb, Lipophilic drug loaded nanospheres prepared by nanoprecipitation: effect of formulation variables on size, drug recovery and release kinetics, *Journal of Controlled Release*, **2002**, 83, 389-400
- [66] H.Fessi, F.Puisieux, J.-P.Devissaguet, N.Ammoury, S.Benita, Nanocapsule formation by interfacial polymer deposition following solvent displacement, *Int. J. Pharm.*, **1989**, 55, R1-R4
- [67] Y.-I. Jeong, C.-S.Cho, S.-H.Kim, K.-S.Ko, S.-I.Kim, Y.-H.Shim, J.-W.Nah, Preparation of poly(DL-lactide-co-glycolide) nanoparticles without surfactant, *Journal of Applied Polymer Science*, **2001**, 80, 2228-2236
- [68] M.Liu, Z.Zhou, X.Wang, J.Xu, K.Yang, Q.Cui, X.Chen, M.Cao, J.Weng, Q.Zhang, Formation of poly(L,D-lactide) spheres with controlled size by direct dialysis, *Polymer*, **2007**, 48, 5767-5779
- [69] N.Anton, J.P.Benoit, P.Saulnier, Design and production of nanoparticles formulated from nano-emulsion templates - A review, *Journal of Controlled Release*, **2008**, 128, 185-199
- [70] Y.Ikada, H.Tsuji, Biodegradable polyesters for medical and ecological applications, *Macromol. Rapid Commun.*, **2000**, 21, 117-132
- [71] I.Vroman, L.Tighzert, Biodegradable Polymers, *Materials*, **2009**, 2, 307-344
- [72] S.Abdollahi, F.Lotfipour, PLGA and PLA-based polymeric nanoparticles for antimicrobial drug delivery, *Biomedecine International*, **2012**, 3, 1-11
- [73] H.Van de Ven, C. Paulussen, P.B. Feijens, A.Matheeussen, P.Rombaut, P. Kayaert, G. Van den Mooter, W. Weyenberg, P. Cos, L. Maes, A. Ludwig, PLGA nanoparticles and nanosuspensions with amphotericin B: Potent *in vitro* and *in vivo* alternatives to Fungizone and AmBisome, *Journal of Controlled Release*, **2012**, 161, 795-803
- [74] J.L.Italia, M.M.Yahya, D.Singh, M.N.V. Ravi Kumar, Biodegradable nanoparticles improve oral bioavailability of Amphotericin B and show nephrotoxicity compared to intravenous Fungizone®, *Pharmaceutical Research*, **2009**, 26(6), 1324-1331
- [75] M.S. Espuelas, P. Legrand, J.M. Irache, C. Gamazo, A.M. Orecchioni, J.-Ph. Devissaguet, P.Ygartua, Poly( $\epsilon$ -caprolacton) nanospheres as an alternative way to reduce amphotericin B toxicity, *International Journal of Pharmaceutics*, **1997**, 158, 19-27
- [76] G.Mohammadi, A.Nokhodchi, M.Barzegar-Jalali, F.Lotfipour, K.Adibkia, N.Ehyaeei, H.Valizadeh, Physicochemical and anti-bacterial performance characterization of clarithromycin nanoparticles as colloidal drug delivery system, *Colloids and Surfaces B: Biointerfaces*, **2011**, 88, 39-44
- [77] G.Mohammadi, A.Nokhodchi, M.Barzegar-Jalali, F.Lotfipour, K.Adibkia, M. Milani, A.Azhdarzadeh, F.Kiafar, A.Nokhodchi, Development of azithromycin-PLGA nanoparticles: Physicochemical characterization and antibacterial effect against *Salmonella typhi*, *Colloids and Surfaces B: Biointerfaces*, **2010**, 80, 34-39
- [78] F.Esmaeili, M. Hosseini-Nasr, M.Rad-Malekshahi, N.Samadi, F.Atyabi, R.Dinarvand, Preparation and antibacterial activity evaluation of rifampicin-loaded poly lactide-co-glycolide nanoparticles, *Nanomedicine*, **2007**, 3(2), 161-167

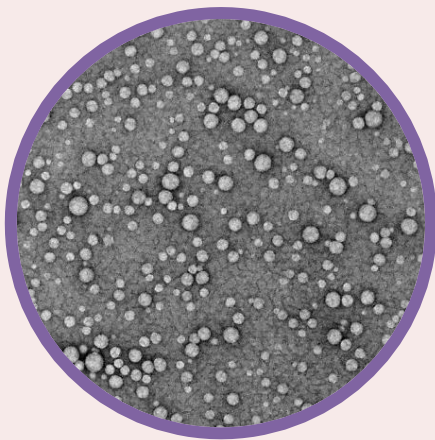
- [79] A. Blanco-Padilla, K.M. Soto, M. Hernández Iturriaga, S. Mendoza, Food Antimicrobials Nanocarriers, *The Scientific World Journal*, **2014**, vol.2014, article ID 837215
- [80] C.Gomes, R.G.Moreira, E.Castell-Perez, Poly (DL-lactide-co-glycolide) (PLGA) nanoparticles with entrapped trans-cinamaldehyde and eugenol for antimicrobial delivery applications, *Journal of Food Science*, **2011**, 76(2), N16-N24
- [81] S.Salmaso, N.Elvasore, A.Bertucco, A.Late, P.Caliceti, Nisin-loaded poly-L-lactide nano-particles produced by CO<sub>2</sub> anti-solvent precipitation for sustained antimicrobial activity, *International Journal of Pharmaceutics*, **2004**, 287, 163-173
- [82] C.Vauthier, B.Cabane, D.Labarre, How to concentrate nanoparticles and avoid aggregation?, *Eur.J.Pharm.Biopharm.*, **2008**, 69, 466-475
- [83] Patent US2009/0294357, Method for concentrating nanosuspensions
- [84] E.Leo, C.Contado, F.Bortolotti, B.Pavan, A.Scatturin, G.Tosi, S.Manfredini, A.Angusti, A.Dalpiaz, Nanoparticle formulation may affect the stabilization of an antiischemic prodrug, *Pharmaceutical Nanotechnology*, **2006**, 307, 103-113
- [85] H.-Y.Kwon, J.-Y.Lee, S.-W.Choi, Y.Jang, J.-H.Kim, Preparation of PLGA nanoparticles containing estrogen by emulsification-diffusion method, *Colloids Surf.A Physicochem.Eng.Asp.*, **2007**,182,123-130
- [86] T.Govender, S.Stolnik, M.C.Garnett, L.Illum, S.S.Davis, PLGA nanoparticles prepared by nanoprecipitation: drug loading and release studies of a water soluble drug, *J.Control.Release*, **1999**, 57, 171-185
- [87] V.Torchilin, V.Weissig, *Liposomes: A Practical Approach*, OUP Oxford, **2003**
- [88] D.Tortorella, N.D.Ulbrandt, E.London, Simple centrifugation method for efficient pelleting of both small and large unilamellar vesicles that allows convenient measurement of protein binding, *Biochemistry*, **1993**, 32, 9181-9188
- [89] G.Dalwadi, H.E.A.Benson, Y.Chen, Comparison of diafiltration and tangential flow filtration for purification of nanoparticle suspensions, *Pharmaceutical Research*, **2005**,22, 2152-2162
- [90] I.Limayen, C.Charcosset, H.Fessi, Purification of nanoparticle suspensions by a concentration/diafiltration process, *Separation and Purification Technology*, **2004**, 38, 1-9
- [91] S.Hirsjarvi, L.Peltonen, J.Hirvonen, Effect of sugars, surfactant and tangential flow filtration on the freeze-drying of poly(lactic acid) nanoparticles, *AAPS PharmaSciTech*, **2009**, 10, 488-493
- [92] S.Kim, M.Marion, B.-H.Jeong, E.M.V.Hoek, Crossflow membrane filtration of interacting nanoparticle suspensions, *Journal of Membrane Science*, **2006**, 284, 361-372
- [93] G. Belfort, R.H. Davis, A.L. Zydney, The behavior of suspensions and macromolecular solutions in cross-flow microfiltration, *Journal of Membrane Science*, **1994**, 96, 1-58
- [94] K.-J. Hwang, Y.-C.Chang, The use of cross-flow microfiltration in purification of liposomes, *Separation and Purification Technology*, **2004**, 39, 2557-2576
- [95] A.Grenha, B.Seijo, C.Remunan-Lopez, Microencapsulated chitosan nanoparticles for lung protein delivery, *European Journal of Pharmaceutical Sciences*, **2005**, 25, 427-437

- [96] A.Grenha, B.Seijo, C.Serra, C.Remunan-Lopez, Chitosan nanoparticle-loaded mannitol microspheres: structure and surface characterization, *Biomacromolecules*, **2007**, 8, 2072-2079
- [97] M.V.Chaubal, C.Popescu, Conversion of nanosuspensions into dry powders by spray-drying: a case study, *Pharmaceutical Research*, **2008**, 25, 2302-2308
- [98] J.O.-H.Sham, Y.Zhang, W.H.Finlay, W.H.Roa, R.Lobenber, Formulation and characterization of spray-dried powders containing nanoparticles for aerosol delivery to the lung, *Int.J.Pharm.*, **2004**, 269, 457-467
- [99] P.Golbach, H.Brochart, A.Stamm, Spray-drying of liposomes for a pulmonary administration.I.Chemical stability of phospholipids, *Drug Dev. Ind. Pharm.*, **1993**, 19, 2611-2622
- [100] P.Golbach, H.Brochart, A.Stamm, Spray-drying of liposomes for a pulmonary administration.II.Retention of encapsulated materials, *Drug Dev. Ind. Pharm.*, **1993**, 19, 2623-2636
- [101] A.Misra, K.Jinturkar, D.Patel, J.Lalani, M.Chougule, Recent advances in liposomal dry powder formulations: preparation and evaluation, *Expert Opin. Drug Deliv.*, **2009**, 6(1), 71-89
- [102] P.Wessman, K.Edwards, D.Mahlin, Structural effects caused by spray- and freeze-drying of liposomes and bilayer disks, *Journal of Pharmaceutical Sciences*, **2010**, 99(4), 2032-2048
- [103] W.Abdelwahed, G.Degobert, S.Stainmesse, H.Fessi, Freeze-drying of nanoparticles: Formulation, process and storage considerations, *Advanced Drug Delivery Reviews*, **2006**, 58, 1688-1713
- [104] S.De Chasteigner, H.Fessi, G.Cavé, J.P.Devissaguet, F.Puisieux, Freeze-drying of itraconazole-loaded nanosphere suspensions: a feasibility study, *Drug Dev.Res.*, **1996**, 38, 116-124
- [105] C.Chen, D.Han, C.Cai, X.Tang, An overview of liposome lyophilization and its future potential, *Journal of Controlled Release*, **2010**, 142, 299-311

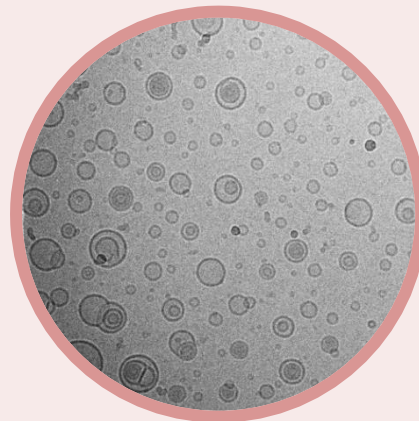


# *Part I*

## *Development and characterization of nano-encapsulation systems for natamycin*



**Chapter 2**  
*Biodegradable polymeric  
nanospheres*



**Chapter 3**  
*Liposomes*

*Do the difficult things while they are easy and do the great things while they are small.  
A journey of a thousand miles must begin with a single step.*

Lao Tzu



# Chapter 2

## *Natamycin-loaded biodegradable polymeric nanospheres prepared by nanoprecipitation*

---

Biodegradable poly(lactide-co-glycolide) (PLGA) nanospheres are prepared by the nanoprecipitation technique and evaluated as potential nano-delivery system for natamycin. Preservative-loaded PLGA nanoparticles are successfully obtained using a solvent phase containing low molecular weight PLGA (L:G 75:25 ratio), acetone/methanol 2:1 v/v mixture and natamycin. Injection of this organic phase in water at 4% v/v leads to nanoparticles (60-120 nm) with a narrow size distribution and a smooth spherical morphology. Active participation of natamycin to the nanoprecipitation process by complexation with PLGA is indicated by mean diameters reduced by 10-30 nm. Limited encapsulation is evidenced with a maximum of 1.4% loading efficiency, in accordance with the intermediate hydrophilic-hydrophobic behavior of natamycin, while zeta-potential variations confirm partial adsorption at the surface of the nanoparticles. Physical state analyses highlight the presence of natamycin in an amorphous or molecularly-dispersed state within the polymeric matrix and possible preservative-PLGA electrostatic interactions. Limited levels of entrapment and presence of non-crystalline natamycin translate into higher availability of free preservative molecules, reflected in faster release rates compared to crystalline native natamycin (80% released over the first 48h compared to 29%) and enhanced antifungal performance against *Saccharomyces cerevisiae* on the same period of time. This higher availability is however resulting in a relative fast degradation of the preservative upon storage that remains to be addressed.

---

Part of this chapter has been patented (WO/2015/044465 Submicron natamycin particles) and submitted as: C. Bouaoud, S. Xu, E. Mendes, J.G.J.L. Lebouille, H.E.A. De Braal, G.M.H. Meesters, Development of biodegradable polymeric nanoparticles for encapsulation, delivery and improved antifungal performance of natamycin, *Journal of Applied Polymer Science*, **2016**, 133, 43736.



## 2.1. Introduction

Biodegradable polymeric nanospheres have been extensively described and characterized for encapsulation and delivery applications in the pharmaceutical field in the past decades [1-2]. Nanospheres can be defined as matrix-type colloidal particles, i.e. spherical particles whose entire mass is solid, characterized by a size usually ranging between several tenths of nanometers to a few hundreds. The active ingredient can be dissolved, entrapped, chemically bound or adsorbed at the surface via interactions with the polymer forming the nanospheres.

Formation of nanospheres from preformed polymers is the preferred approach in many cases to prevent the presence of residual monomers or toxicity risks coming from in-situ polymerization. Hydrophobic polyesters such as poly(*D,L*-lactic-co-glycolic)acid (PLGA) are among the most commonly used biodegradable polymers [3-4] owing to their good biocompatibility and minimal toxicity as well as their commercial availability. PLGA polymers in particular are available with versatile molecular weights and lactide-to-glycolide L:G ratios, enabling preparation of nanoparticles with tuned sizes, hydrophobicity, crystallinity, release behavior and degradation rates (a couple of months to several years [3]).

Various methods of producing polymeric nanospheres from preformed polymers such as PLGA have been reported in the literature [5-7]. Due to the incompatibility of natamycin with water-insoluble solvents and its solubilization, at acceptable levels for encapsulation, in polar solvents miscible with water in all proportions (e.g. methanol), the nanoprecipitation technique, also known as solvent displacement, was selected for the preparation of natamycin-loaded nanoparticles. This method [8-9] consists in the preparation of a water-miscible organic solution (“solvent phase”) containing the polymer and the active ingredient, followed by the injection of this solvent phase into an aqueous solution (“non-solvent phase”) as illustrated in Figure 2.1. The sudden solvent diffusion upon injection in the aqueous phase triggers the assembly of the macromolecules into nanospheres. Formation of nanospheres via the solvent displacement process is controversially explained by two different mechanisms:

- ✓ Mechanical forces based on significant interfacial turbulences occurring during solvent diffusion (Gibbs-Marangoni effect [10-11]), resulting in continuous break-up of organic solvent droplets until formation of submicron droplets where the polymer eventually precipitates.

- ✓ Formation of polymeric nuclei (Ouzo effect), due to supersaturation [12] occurring locally upon solvent diffusion, followed by growth and aggregation over time.

All formulation parameters possibly influencing to some extent the solvent diffusion, interfacial turbulences and rates of nucleation/growth processes (to name a few, polymer composition and concentration, solvent composition, solvent/non-solvent S/NS ratio, stirring rate, aqueous phase composition, etc...) are known to have an effect on the formation of nanospheres [13]. Common agreement is that low concentration of polymer and low S/NS ratio make the nucleation-growth process more likely to happen, while at higher concentration and S/NS ratio, the Gibbs-Marangoni effect is the preferred explanation. In a general way, both factors need to remain under a certain limit (“Ouzo” region) [14] to allow efficient formation of nanoparticles while avoiding formation of large aggregates of polymer.

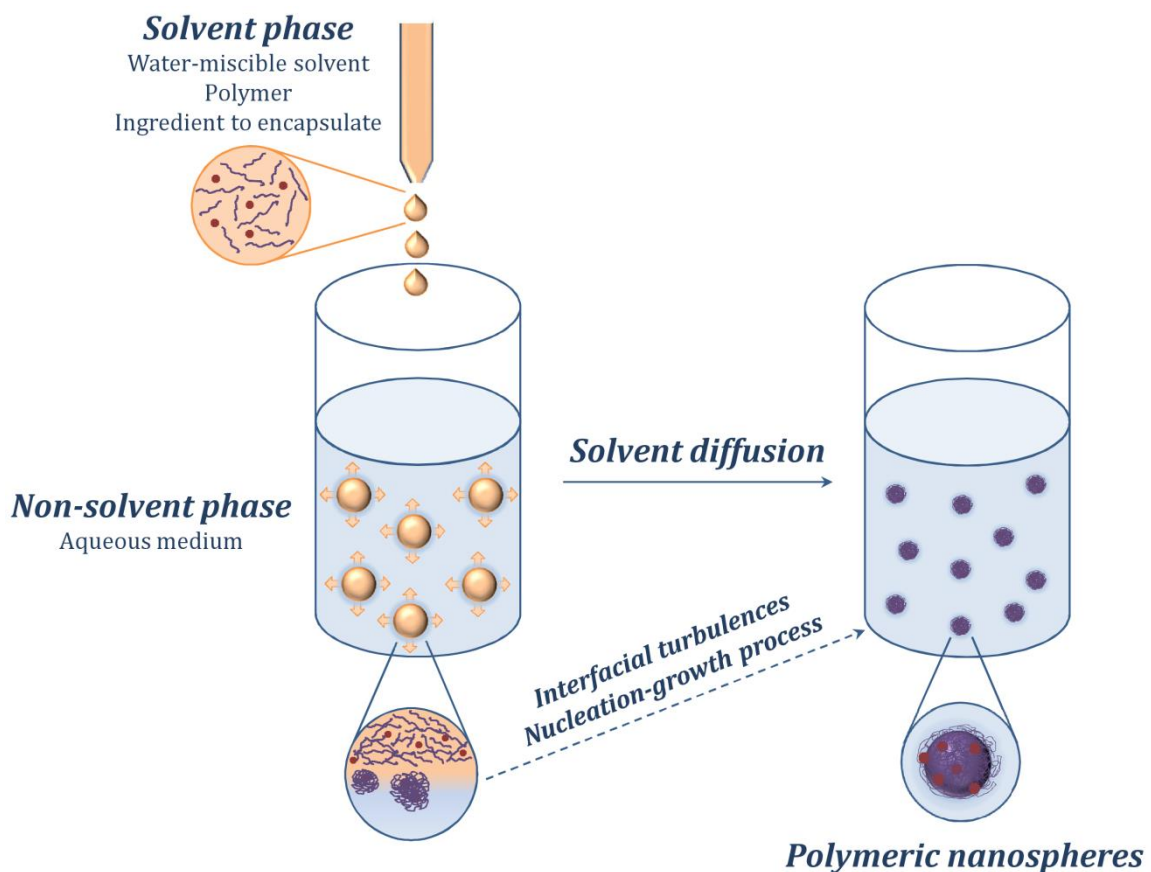


Figure 2.1: Schematic representation of the formation of polymeric nanospheres by nanoprecipitation

While considering the encapsulation and delivery of natamycin, the nanoprecipitation method presents the major advantage of allowing the production of nanospheres in a controlled way [5] and of generating narrow unimodal distribution, which is an important feature to ensure homogeneity and reproducible behavior for instance while incorporating natamycin-loaded nanoparticles in food coatings. Other interesting features are the easiness and potential scalability of this one-step procedure and the opportunity to prepare nanoparticles without the necessity to use surfactants or stabilizers. However, it has to be mentioned that nanoprecipitation is known to result in limited encapsulation levels while working with rather hydrophilic compounds [15-16], which could also be the case for molecules with intermediate behavior such as natamycin.

The primary objective of this chapter is to assess if natamycin can be efficiently encapsulated in polymeric nanospheres prepared by the nanoprecipitation method and if these formulations bring an improvement to the delivery and antifungal performance of the molecule.

First part of this chapter focuses on the preparation of unloaded polymeric PLGA nanospheres in a solvent mixture appropriate for further incorporation of natamycin. Influence of several factors such as polymer composition (molecular weight, L:G ratio), concentration in the solvent phase, S/NS ratio and stirring rate are investigated. Selection of most promising formulations, i.e. nanospheres with low polydispersity, small sizes and limited formation of aggregates during the process, is described.

In a second step, incorporation of natamycin is performed and effects on physicochemical properties of the nanoparticles studied to confirm incorporation of natamycin and evaluate optimum conditions to ensure maximal loading of the nanoparticles and high encapsulation efficiency. Further investigations were performed on the physical state and crystallinity character of natamycin in the nanoparticles. Finally, stability tests and performance tests, namely release kinetics out of the nanoparticles and antifungal activity against the model yeast *Saccharomyces cerevisiae* were carried out.

## 2.2. Materials and methods

### 2.2.1. Materials

Natamycin (90.6% purity, trihydrate crystalline form, MW 665.7 g/mol) was kindly supplied by DSM Food Specialties (Delft, The Netherlands). Poly(*D,L*-lactic-co-glycolic acid) polymers Resomer<sup>®</sup> RG752H (L:G ratio 75:25, MW 4-15 kDa) and Resomer<sup>®</sup> RG502H (L:G ratio 50:50, MW 7-17 kDa) were purchased from Sigma-Aldrich. Methanol EMSURE<sup>®</sup> ACS and dried acetone Seccosolv<sup>®</sup> were purchased from Merck and used for the preparation of the nanoparticles. Potassium dihydrogen phosphate, methanol and acetonitrile Lichrosolv<sup>®</sup> were obtained from Merck and used for HPLC analyses. High quality water purified in a Milli-Q system was used in all experiments.

### 2.2.2. Preparation of polymeric nanospheres

PLGA nanoparticles were prepared by the nanoprecipitation technique. Briefly, the PLGA polymer was dissolved at room temperature in dried acetone at the desired concentration while natamycin was dissolved in methanol (0.5-2.5 mg/mL). Both solutions were mixed at a ratio acetone/methanol 2:1 v/v. After homogenization, 0.4 mL of this organic phase was injected by one-shot addition under moderate magnetic stirring into 10 mL of MilliQ water. The resulting nanosuspension was kept under slow stirring overnight for complete evaporation of organic solvent. For some analyses, suspensions were freeze-dried for 48 hours using a commercial lyophilizer (Advantage 2.0 Bench Top Model XL, VirTis Advantage, SP Scientific, USA) and lyophilized nanopowders were stored at 4 °C until further use.

### 2.2.3. Physicochemical characterization

#### 2.2.3.1 Particle size and zeta-potential

The mean particle diameter and polydispersity index (PDI) of the nanospheres were determined by Dynamic Light Scattering (DLS) (Zetasizer Nano ZS, Malvern Instruments Ltd., UK). Three consecutive measurements were performed on each nanosuspension at 25 °C at a scattering angle of 173 °, after an equilibration time of 180 seconds. The electrical charge of the nanoparticles (zeta-potential  $\zeta$ ), was assessed on undiluted nanosuspensions with the same equipment. Zeta-potential was obtained by three consecutive measurements of 200 sub-runs at 25 °C after an equilibration time of 180 seconds. All

measurements were performed in triplicate and results are presented as mean  $\pm$  standard deviation (SD).

### 2.2.3.2 Morphology

Morphology of PLGA nanoparticles was investigated using transmission electron microscopy (TEM) (Tecnai G<sup>2</sup>, FEI, Hillsboro, USA) with an acceleration voltage of 200 kV. Prior to examination, samples were submitted to negative staining by mixing 20  $\mu$ L of solvent-free nanosuspension with 20  $\mu$ L of a 2% w/v neutralized phosphotungstic acid solution. 10  $\mu$ L of the mixture were placed on a Formvar-coated grid (Copper with Formvar 0.5%, 200 mesh) and allow to adsorb for 90 s. After blotting off excess solution, the grid was left to dry at room temperature overnight before analysis.

### 2.2.3.3 Encapsulation (EE) and loading (LE) efficiencies

Content of natamycin in the nanospheres was determined by reverse-phase high-performance liquid chromatography (HPLC). A high pressure liquid chromatograph Ultimate 3000 Dionex equipped with a variable wavelength detector was used. Separation was achieved by injecting 20  $\mu$ L of sample on a reverse phase column Licrospher<sup>®</sup> RP18 (Merck, 125 nm x 4 mm, pore size 100 Å) with a mobile phase consisting of 35:65 v/v acetonitrile: potassium dihydrogenphosphate buffer (pH 3.05) at a flow rate of 1.0 mL/min. Natamycin was detected by UV at 303 nm and quantified using a calibration curve designed over the range 0.05-50 ppm ( $R^2 = 0.9996$ ). All HPLC samples were analyzed in triplicate. Total amount of natamycin was obtained by dilution of an aliquot of the nano-suspension in acetonitrile/methanol 50/50 v/v. Amount of free natamycin in solution was obtained by subjecting the nano-suspensions to ultracentrifugation (Beckman Coulter L8-70M, rotor 50, 50000 rpm, 1h, 10 °C). An aliquot of the supernatant was withdrawn and diluted with the same mixture acetonitrile/methanol. EE and LE were calculated according to Equations (1) and (2). Determination of EE and LE was performed on three samples for each composition. Results are presented as mean  $\pm$  standard deviation.

$$EE (\%) = \frac{\text{Total amount of natamycin} - \text{Amount of natamycin in the supernatant}}{\text{Total amount of natamycin}} * 100 \quad (\text{Eq. 1})$$

$$LE (\%) = \frac{\text{Total amount of natamycin} - \text{Amount of natamycin in the supernatant}}{\text{Amount of nanospheres}} * 100 \quad (\text{Eq. 2})$$

#### 2.2.3.4 Differential scanning calorimetry (DSC)

Thermograms of natamycin, PLGA, unloaded and loaded lyophilized nanoparticles as well as corresponding physical mixtures PLGA-natamycin were recorded on a differential scanning calorimeter DSC7 (Software Pyris Series, Perkin-Elmer, USA). Accurately weighed samples (2-10 mg) were analyzed at a scan rate of 10 °C/min covering the temperature range 25-270 °C.

#### 2.2.3.5 X-Ray diffraction (XRD)

Crystalline properties of natamycin, PLGA, unloaded and loaded lyophilized nanoparticles as well as corresponding physical mixtures PLGA-natamycin were determined by X-ray powder diffraction (XRD). XRD patterns were recorded on a Brüker D8 Discover diffractometer using a Co K $\alpha$  radiation ( $\lambda = 1.788 \text{ \AA}$ ). Data were collected over an angular range comprised between 5 and 50° (2 $\theta$ ) with a step size of 0.02° (0.5 second per step).

#### 2.2.3.6 Fourier-transform infrared spectroscopy (FT-IR)

FT-IR spectra of natamycin, PLGA, physical mixture, unloaded and loaded lyophilized nanoparticles were recorded on a spectrophotometer Brüker Tensor 27 (Brüker Corporation, Billerica, USA) equipped with an attenuated total reflectance module (ATR). Spectra were collected on the range 400-4000 cm<sup>-1</sup> (64 scans per spectrum) with a resolution of 4 cm<sup>-1</sup>.

### 2.2.4. Performance tests

#### 2.2.4.1 *In vitro* release kinetics

*In vitro* release studies were carried out using the dialysis bag technique [17] for the prepared nanoparticles, pure natamycin and PLGA as well as the physical mixture. Powders or lyophilized nanopowders were suspended in MilliQ water to reach an initial natamycin concentration of 100 ppm. 1 mL of these suspensions was placed in a dialysis bag (Float-A-Lyzer® G2, Biotech Grade Cellulose Ester, MWCO 8-10 kDa, Spectrumlabs, USA) and incubated in 35 mL of MilliQ water at 25 °C under moderate stirring. Total volume was collected at predetermined intervals and replaced with equal volume of fresh release medium to maintain sink conditions. Amount of natamycin in the aliquots were assayed by the HPLC, as described in 2.2.3.3. The cumulative percentage of natamycin released was calculated for triplicates and plotted versus time.

To further characterize the rate and mechanism of release of natamycin out of the liposomes, the release data were fitted to classical mathematical models [18] including first-order kinetics (Eq.3), Higuchi kinetics (Eq.4) and Korsmeyer-Peppas model (Eq.5).

$$M_t/M_\infty = 1 - e^{-kt} \quad (\text{Eq. 3})$$

$$M_t/M_\infty = k \cdot t^{1/2} \quad (\text{Eq. 4})$$

$$M_t/M_\infty = k \cdot t^n \quad (\text{Eq. 5})$$

Where  $M_t/M_\infty$  represents the cumulative fraction of natamycin released at the time  $t$  over the total amount released,  $k$  is the release rate constant and  $n$  is the diffusion exponent indicative of the mechanism of release. Fittings were obtained by plotting respectively log (100-%released) vs time (first-order) and %released vs square root of time (Higuchi). The initial 60% of preservative released were fitted in the Korsmeyer-Peppas model by plotting of log (%released) vs log (time) and the value of “ $n$ ” determined from the slope. For swellable nanocarriers [19-20],  $n = 0.43$  represents a release mechanism based only on Fickian diffusion while  $n = 0.85$  corresponds to a case-II transport based on relaxation/swelling of the nano-carriers. Intermediate values indicate an anomalous transport and combination of both diffusion and relaxation phenomenon.

#### 2.2.4.2 *In vitro* antifungal activity

Antifungal activity of natamycin-loaded nanoparticles, physical mixtures and pure natamycin against *Saccharomyces cerevisiae* (ATCC 9763) was assessed by agar disk diffusion assay. Briefly, a layer of nutrient OGYE agar inoculated with *Saccharomyces cerevisiae* was allowed to solidify in a Petri dish. Sterile blank disks were placed in a stainless steel cylinder and impregnated with 50  $\mu\text{L}$  of nano-suspension (nanopowders resuspended in 1 mL MilliQ water with an equivalent concentration of natamycin of 100 ppm). A similar procedure was applied to standard solutions of natamycin to establish a calibration curve on the range 30-300 ppm. The disks impregnated with standards or nano-suspensions were placed on the solidified agar layer and Petri dishes were kept at 4  $^\circ\text{C}$  overnight to allow the diffusion of natamycin. After removal of the disks, plates were incubated at 30  $^\circ\text{C}$  for 24 h. The diameter of the zone of inhibition was measured and compared to a calibration curve established with the standard samples to determine the quantity of natamycin released. Disks impregnated with the nanosuspensions were transferred to a fresh Petri dish and the procedure was repeated over 5 days to follow the release of natamycin. Results are presented as cumulative activity ( $\mu\text{g}$  of natamycin

released per day/ total  $\mu\text{g}$  of natamycin released over 5 days) calculated from triplicate measurements.

### **2.2.5. Stability tests**

Stability tests were performed over 1, 2, 5 and 10 weeks for nano-suspensions or natamycin dispersions stored at 4 °C, room temperature ( $23 \pm 2$  °C) or room temperature coupled with light exposure. Evolution of the samples was followed by size analysis as described in 2.2.3.1 and determination of natamycin content evolution by the HPLC method described in 2.2.3.3.

## **2.3. Formulation of unloaded polymeric nanospheres**

### **2.3.1. Solvent and polymer selection**

PLGA nanospheres are classically prepared by nanoprecipitation using acetone as a solvent for the polymer [13]. As natamycin is not soluble in acetone, a binary mixture acetone/methanol was selected to ensure satisfying solubilization of both PLGA and natamycin in the organic phase. A preliminary study performed with various ratios acetone/methanol showed that addition of methanol results in desolvation of the polymer from the solvent phase. To ensure simultaneously solubilization of the polymer and incorporation of a content of natamycin in the formulation acceptable for antimicrobial applications, a ratio acetone/methanol 2:1 v/v was found to be the best option.

The selected solvent mixture limits however significantly the variety of PLGA polymers suitable for the nanoprecipitation process, with considerable desolvation observed for polymers with high molecular weight ( $> 24$  kDa). An option to overcome the effect of high MW would be to reduce the concentration of PLGA in acetone, which would further reduce the quantity of nanospheres formed. As the nanoprecipitation method inherently requires already diluted solvent phase, this would lead to an extremely low solid content suspension and limit the encapsulation of natamycin. For this study, it was thus decided to work with two low molecular weight PLGA commercially available: Resomer<sup>®</sup> RG752H (L:G ratio 75:25, MW 4-15 kDa) and Resomer<sup>®</sup> RG502H (L:G ratio 50:50, MW 7-17 kDa).



### 2.3.2. Influence of polymer concentration and composition

The two selected polymers were dissolved in the mixture acetone/methanol 2:1 v/v at concentrations ranging from 5 to 25 mg/mL. Organic phases (0.4 mL) were injected in 10 mL of MilliQ water with a stirring rate of 500 rpm. Weakly opalescent suspensions were obtained with a bluish-reddish aspect related to the Tyndall effect commonly encountered for nanosuspensions. For both polymers, large aggregates of polymers were formed together with nanospheres for concentrations superior to 10 mg/mL.

Figure 2.2 presents the mean diameters and polydispersity indexes obtained by nanoprecipitation of PLGA 75:25 and PLGA 50:50 at different concentrations. The nanoparticle sizes were found to be directly dependent on the polymer concentration, with a significant increase in size while using larger amounts of polymer accompanied by visual formation of aggregates. This phenomena can be explained by two facts [13,21]: (1) a larger number of polymer chains by unit volume of solvent, meaning more polymer chains available to create the nuclei and so larger final size of the nanoparticles; (2) higher viscosity of the solvent phase, causing a higher mass transfer resistance to the solvent diffusion and thus formation of larger particles or even aggregates if the solvent diffusion is significantly hindered.

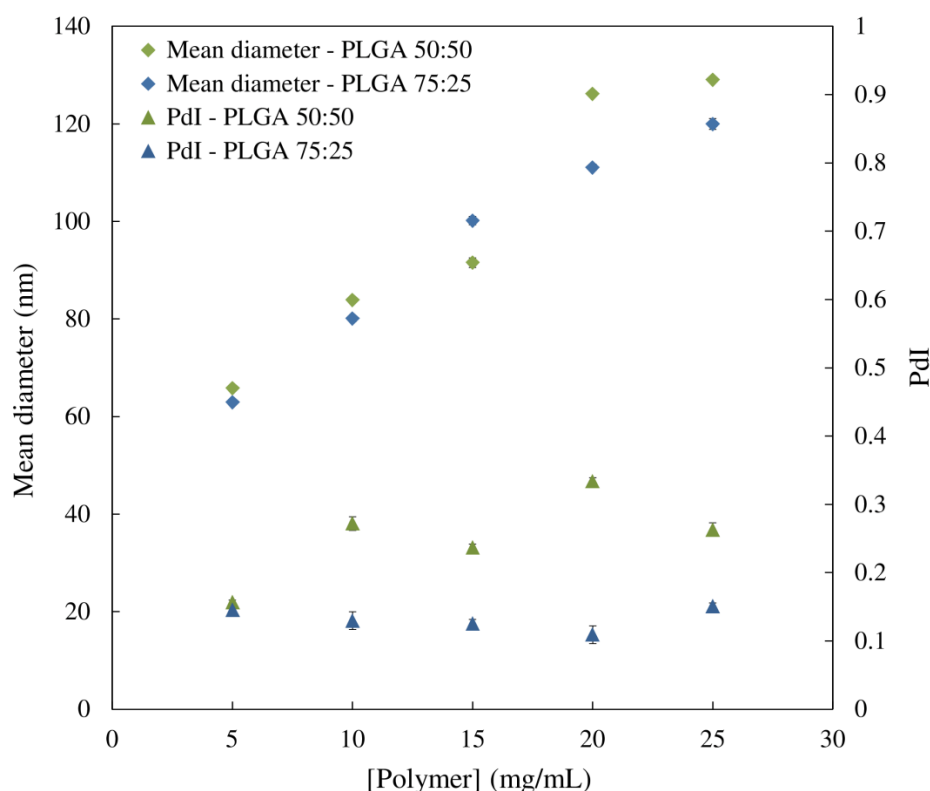


**Figure 2.2: Influence of polymer composition and concentration on the size and polydispersity of PLGA nanospheres**

While comparing both polymers, slightly higher sizes were observed for the L:G ratio 50:50 which might come from the slight difference in molecular weight (7-17 kDa compared to 4-15 kDa). Polydispersity is however distinctly lower for the L:G ratio 75:25 (0.1-0.2), which is likely to be related to the presence of a higher number of lactide monomer units, naturally more hydrophobic than the glycolide unit. Higher hydrophilicity in the case of PLGA 50:50 reduces the tendency of the polymer to aggregate upon contact with water and could lead to less homogeneous nanoprecipitation [11,13]. To meet our criteria of small sizes, homogeneous distribution and limited aggregates formation, PLGA 75:25 was kept for further formulations.

### 2.3.3. Influence of S/NS ratio

Nanospheres were prepared using extreme concentrations of PLGA 75:25 (5 mg/mL and 25 mg/mL) by injection, under 500 rpm stirring, of variable volumes of organic phase in 10 mL MilliQ water to obtain S/NS ratio ranging from 1 to 10% v/v. Figure 2.3 represents the diameter and PdI of the obtained nano-suspensions.

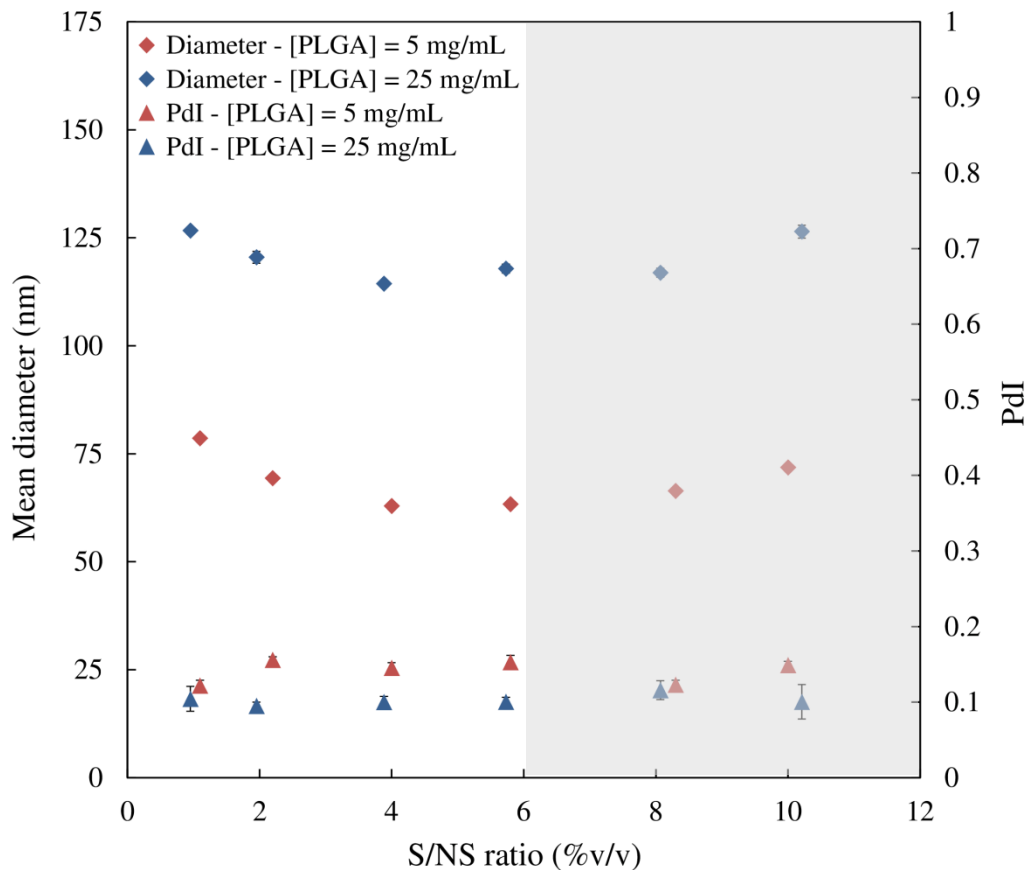


**Figure 2.3: Influence of S/NS ratio on the size and polydispersity of PLGA 75:25 nanospheres (grey area: significant formation of aggregates observed)**

Effect of the S/NS ratio was found to be independent of the concentration of polymer involved in the formulation. In both cases, polydispersities remained low while a minimum diameter was observed around 5-6% v/v. Predominant and significant formation of aggregates was however visible in the sample at and above this S/NS ratio. As mentioned earlier, a dilute state needs to exist to allow efficient formation of nanospheres by the nanoprecipitation process [14]. The S/NS ratio 6% v/v seems to be the boundary for the system PLGA 75:25/acetone/methanol/water. On the range 1-6% v/v, the increase in size can be explained by a very fast diffusion of the solvent and nearly immediate precipitation of the polymer. To obtain simultaneously acceptable sizes and polydispersities as well as acceptable solid content in the formulation with limited loss via aggregation, the ratio 4% v/v was found optimum.

#### **2.3.4. Influence of stirring rate**

Nanospheres were prepared using extreme concentrations of PLGA 75:25 (5 mg/mL and 25 mg/mL) by injection of 0.4 mL of organic phase in 10 mL MilliQ water under magnetic stirring rate ranging from 100 to 1100 rpm.

As displayed in Figure 2.4, low-intermediate stirring rates up to 700 rpm have limited effect on the size and polydispersity of the nanosuspensions as well as on the visual aggregates formed, independently from the polymer concentration involved. Higher stirring rates enhance the solvent diffusion as well as micro-mixing and turbulences in the suspension, leading to faster but less controlled precipitation [13]. Moderate stirring rate (500 rpm) was kept for further experiments to simultaneously enable good mixing and diffusion of the solvent while avoiding the increase in size previously mentioned.

#### **2.3.5. Selected formulations**

Unloaded PLGA nanospheres meeting the requirements of small diameters, low polydispersity and limited formation of aggregates have been successfully obtained from PLGA 75:25 (MW 4-15 kDa) using the acetone/methanol 2:1 v/v mixture. Sizes and polydispersities were found to be mainly related to the concentration of polymer involved. Optimum S/NS ratio and stirring speed were respectively set at 4%v/v and 500 rpm. 10 mg/mL and 25 mg/mL PLGA concentrations were kept for further study of incorporation of natamycin.

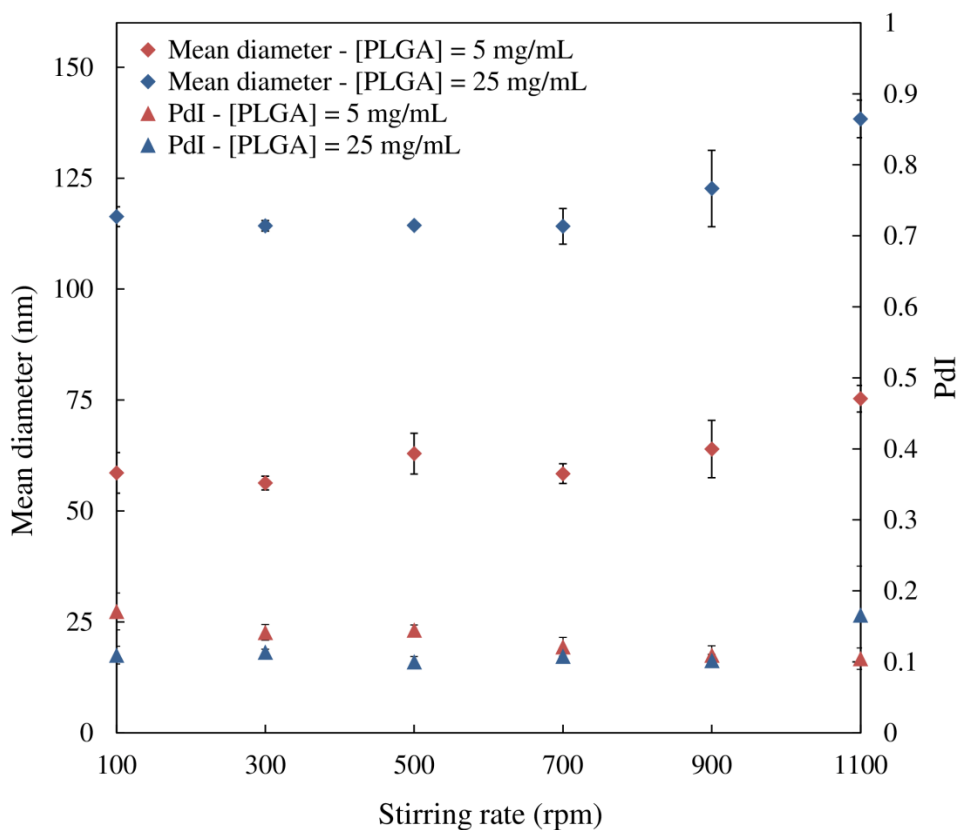


Figure 2.4: Influence of the stirring rate on the size and polydispersity of PLGA 75:25 nanospheres

## 2.4. Incorporation of natamycin in the nanospheres

### 2.4.1. Effect on size and polydispersity

Mean particle diameters and polydispersities of natamycin-loaded PLGA nanospheres are presented in Figure 2.5. Similarly to unloaded formulations, nanoparticles were found monodisperse with narrow distributions and sizes ranging between 60 and 120 nm. Incorporation of natamycin led to a significant decrease in size (10-30 nm) as well as to a visual reduction of aggregates formation in the sample. The effect was observed only up to a limit concentration of preservative above which the diameters leveled. Polydispersity indexes slightly increased while remaining below 0.2, indicating conserved monodispersity of the particles.

Modification of PLGA nanospheres diameter while incorporating the preservative indicates encapsulation and participation of natamycin to the process of nanoparticles formation by nanoprecipitation. An increase in size is however more commonly observed while loading nanospheres with an active ingredient. Several hypotheses can be made to explain this phenomenon.

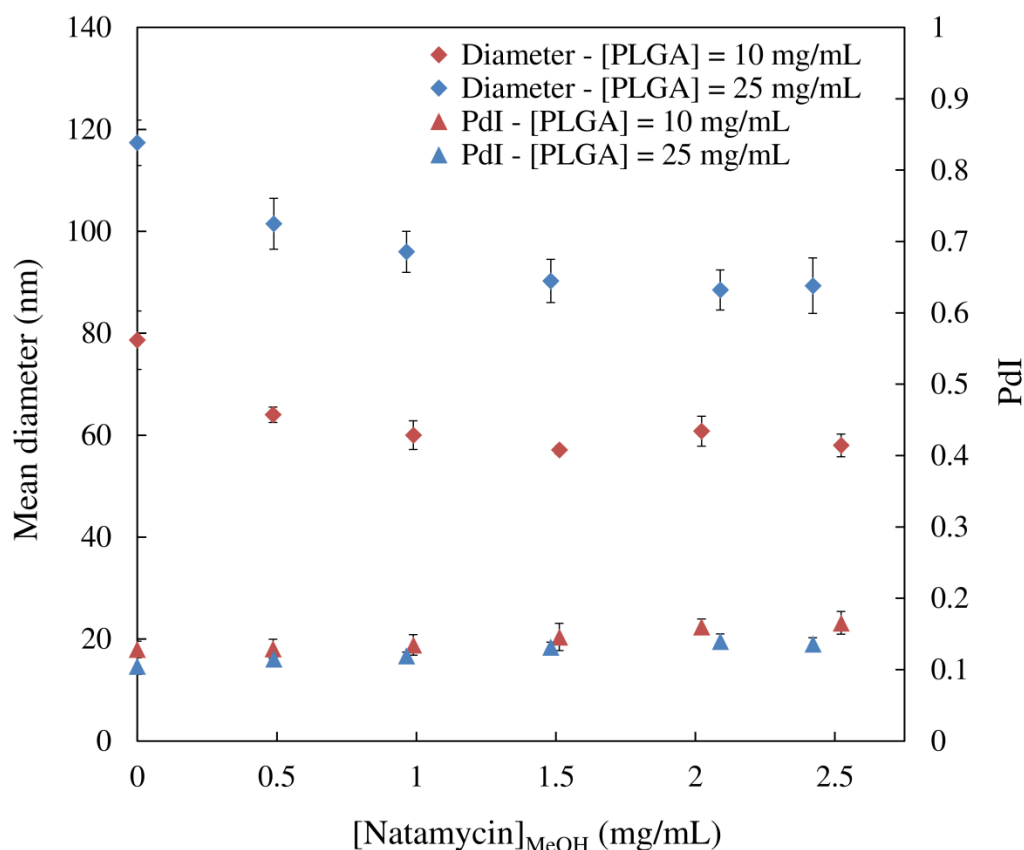


**Figure 2.5: Evolution of mean diameter and polydispersity of nanospheres obtained at variable concentrations of natamycin for two different concentrations of PLGA 75:25**

The first possibility is a stabilizing effect related to the amphiphilic nature of natamycin that could play a role in the kinetics of solvent diffusion as well as interfacial turbulences happening during the nanoparticle formation. To confirm this hypothesis, nanoprecipitation of unloaded PLGA nanospheres was performed in an aqueous phase containing dissolved natamycin at three different concentrations, mimicking concentrations that could be reached by incorporating natamycin at 0.5, 1 and 1.5 mg/mL in methanol. Table 2.1 presents the comparison between nanoparticles prepared by both methods. Presence of natamycin in the aqueous phase does not modify size and polydispersity as significantly as natamycin incorporated in the organic phase, meaning that stabilizing effect is not occurring.

A second option is the presence of water in the organic phase linked to the fact that natamycin is in a trihydrate crystalline form before being dissolved in methanol. Presence of water in the organic phase could have a significant impact on the solvent displacement process by reducing in situ affinity of the polymer for the solvent phase and making the

diffusion faster. Nanoprecipitation of unloaded PLGA nanospheres (25 mg/mL) was performed by adding 2 and 10  $\mu\text{L}$  MilliQ water per mL of methanol in the organic phase (incorporating natamycin at its maximum concentration in methanol would lead to an equivalent of 2.7  $\mu\text{L}$  MQ water/ mL of methanol). Diameters obtained were respectively  $116.4 \pm 0.1$  and  $118.1 \pm 0.5$  nm, indicating no clear influence of water content in the organic phase.

Last hypothesis relates to significant interactions occurring between the antifungal and the polymer in the organic phase, counteracting polymer-polymer, polymer-solvent or polymer-non-solvent interactions. Beck-Broichsitter et al. [22] reported an effect of drug loading in the solvent phase on the Ouzo region, i.e. the region where polymer concentration and S-NS ratio allow formation of nanoparticle suspensions. More specifically, they proved that the incorporation of a small hydrophilic drug allowed a shift of the Ouzo region to higher polymer concentrations due to the formation of a less hydrophobic complex polymer-drug. Supersaturation was as a consequence not reached as fast as in the case of unloaded solvent phase. The authors also highlighted the fact that, to reach size characteristics similar to the unloaded nanoparticles, higher concentrations of polymer must be used. A similar observation can be made with the formulations PLGA/natamycin. For instance, comparison of unloaded PLGA nanoparticles prepared with 10 mg/mL (80.1 nm) were found to have similar diameters than nanosuspensions prepared with 15 mg/mL PLGA and 0.5 mg/mL natamycin (81.3 nm) or with 20 mg/mL PLGA and 1 mg/mL natamycin (80.3 nm). Shift in the Ouzo region to higher polymer concentration via incorporation of natamycin also explains that aggregates are not formed anymore at 25 mg/mL PLGA. This corroborates the idea that natamycin interacts with PLGA within the organic phase and actively participates to the nanoprecipitation process.

**Table 2.1: Effect of presence of natamycin in the organic phase or in the aqueous phase during nanoprecipitation (PLGA 25 mg/mL)**

| [Natamycin] <sub>MeOH</sub><br>(mg/mL) | Natamycin in organic phase |                   | Natamycin in aqueous phase |                   |
|--|----------------------------|-------------------|----------------------------|-------------------|
|  | Mean diameter (nm)         | PdI               | Mean diameter (nm)         | PdI               |
| 0                                      | $117.4 \pm 4.4$            | $0.105 \pm 0.012$ | $117.4 \pm 4.4$            | $0.105 \pm 0.012$ |
| 0.5                                    | $101.5 \pm 5.0$            | $0.115 \pm 0.007$ | $120.7 \pm 0.6$            | $0.112 \pm 0.015$ |
| 1                                      | $96.0 \pm 4.0$             | $0.119 \pm 0.005$ | $117.3 \pm 1.5$            | $0.096 \pm 0.007$ |
| 1.5                                    | $90.3 \pm 4.2$             | $0.131 \pm 0.007$ | $119.1 \pm 0.2$            | $0.112 \pm 0.010$ |

### 2.4.2. Encapsulation and loading efficiencies

Encapsulation and loading efficiencies for natamycin-loaded PLGA nanoparticles are reported in Table 2.2. Variations of encapsulation efficiencies are in accordance with the modifications of size and polydispersities previously described. Higher entrapment levels are observed for low content of natamycin with stabilization above 1.5 mg/mL. Sustained increase of loading efficiency while incorporating higher contents of natamycin confirms the idea of active participation of natamycin to the process of nanoparticle formation.

**Table 2.2: Effect of composition on encapsulation and loading efficiencies of natamycin-loaded PLGA nanospheres**

| [PLGA] <sub>organic phase</sub> (mg/mL) | [Natamycin] <sub>MeOH</sub> (mg/mL) | EE (%)     | LE (%)      |
|---|-------------------------------------|------------|-------------|
| 10                                      | 0.5                                 | 33.3 ± 1.5 | 0.50 ± 0.01 |
|   | 1                                   | 29.4 ± 1.7 | 0.90 ± 0.05 |
|   | 1.5                                 | 25.4 ± 1.7 | 1.22 ± 0.08 |
|   | 2                                   | 18.0 ± 1.8 | 1.15 ± 0.11 |
|   | 2.5                                 | 18.4 ± 1.5 | 1.42 ± 0.11 |
| 25                                      | 0.5                                 | 36.3 ± 1.2 | 0.22 ± 0.01 |
|   | 1                                   | 20.2 ± 1.4 | 0.23 ± 0.02 |
|   | 1.5                                 | 21.6 ± 0.2 | 0.37 ± 0.01 |
|   | 2                                   | 24.8 ± 0.6 | 0.60 ± 0.02 |
|   | 2.5                                 | 25.4 ± 0.6 | 0.71 ± 0.02 |

For both polymer concentrations, encapsulation efficiencies remain in an intermediate limited range, in accordance with previous studies based on the encapsulation of hydrophilic drugs [15-16] that reported a rapid migration and diffusion of this type of molecule together with the solvent during the nanoprecipitation process. Common approaches implemented to improve entrapment of hydrophilic molecules focused on modification of the aqueous phase composition in order to decrease the solubility of the compound to entrap or increase its affinity towards the polymer [23]. Further improvements of the encapsulation of natamycin in the PLGA nano-carriers were attempted by studying the effect of pH modification (MilliQ water replaced by buffers at pH 4 and 9) or addition of NaCl (0.05%-0.1% w/v). Table 2.3 summarizes EE, LE, diameter and PdI obtained for these formulations.

**Table 2.3: Effect of aqueous phase composition on size, polydispersity, EE and LE of natamycin-loaded PLGA nanospheres**

| Aqueous phase  | Mean diameter (nm) | PdI           | EE (%)     | LE (%)      |
|----------------|--------------------|---------------|------------|-------------|
| MilliQ water   | 89.3 ± 5.4         | 0.136 ± 0.009 | 25.4 ± 0.6 | 0.71 ± 0.02 |
| Buffer pH 4    | 158.3 ± 1.6        | 0.101 ± 0.029 | 16.4 ± 0.6 | 0.28 ± 0.01 |
| Buffer pH 9    | 84.2 ± 0.4         | 0.179 ± 0.010 | 22.2 ± 0.8 | 0.38 ± 0.01 |
| NaCl 0.05% w/v | 108.4 ± 0.3        | 0.097 ± 0.007 | 30.7 ± 4.0 | 0.52 ± 0.07 |
| NaCl 0.1% w/v  | 126.6 ± 0.7        | 0.108 ± 0.014 | 24.9 ± 2.2 | 0.42 ± 0.04 |

The pH modification led to significant increase in size or PdI of the nanoparticles, with decrease in the entrapment levels. Change of ionization degree of natamycin via the use of extreme pH could have improved interactions with the polymer. It is however also contributing to higher levels of dissolution in water, which explains that EE% and LE% are not enhanced by the pH modification. Addition of salt in the aqueous phase also had significant effect on the diameter of the nanospheres as well as on the quantities of aggregates visually formed. NaCl has been reported to have a salting-out effect, promoting the fast precipitation of the polymer, and to increase the viscosity of the aqueous phase, reducing the solvent diffusion rate thus being unfavorable to nanoparticle formation [13]. Though a positive effect on natamycin entrapment can be observed for NaCl 0.05% w/v, the reduction of nanoparticle yield is too consequent. Using MilliQ water seems to remain the most favorable option for encapsulation of natamycin.

### 2.4.3. Zeta-potential

Presence of ionized carboxyl PLGA end-groups at the surface of the nanospheres led to negatively charged nanoparticles. Zeta-potential values (Table 2.4) were below -56 mV for all compositions indicating very good stability of the nanosuspensions. Slight variations are observed while incorporating natamycin in the formulation and might be attributed to adsorption of natamycin molecules on the nanospheres via electrostatic interactions between the carboxylic groups of PLGA and the amino group of natamycin. As natamycin is in a slightly positively charged zwitterionic state in MQ water (isoelectric point at pH 6.5 [24]), the resulting partial hiding of the surface charge is compensated by the presence of another carboxylic group on natamycin itself, explaining the limited variation observed.



**Table 2.4: Effect of the presence of natamycin on the zeta-potential of PLGA nanospheres**

| [PLGA] <sub>organic phase</sub> (mg/mL) | [Natamycin] <sub>MeOH</sub> (mg/mL) | Zeta-potential ( $\zeta$ ) (mV) |
|---|-------------------------------------|---------------------------------|
| 10                                      | 0                                   | -59.6 ± 1.4                     |
|   | 0.5                                 | -60.2 ± 1.4                     |
|   | 1.5                                 | -60.3 ± 4.5                     |
|   | 2.5                                 | -61.4 ± 0.7                     |
| 25                                      | 0                                   | -63.7 ± 6.7                     |
|   | 0.5                                 | -62.8 ± 4.0                     |
|   | 1.5                                 | -57.5 ± 6.2                     |
|   | 2.5                                 | -56.3 ± 3.0                     |

#### 2.4.4. Morphology

Nanometric sizes and polydispersity were confirmed by TEM (Figure 2.6) by analysis of the formulation PLGA 25 mg/mL – Natamycin 2.5 mg/mL. Spherical shapes and smooth surface were observed without detection of natamycin crystals.

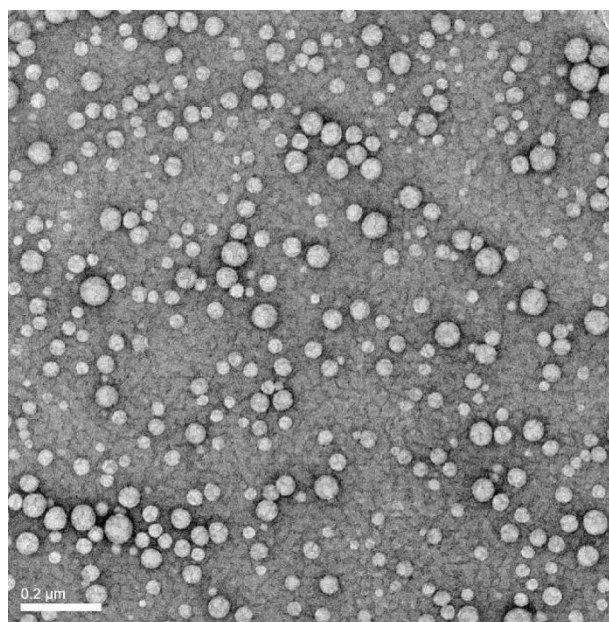


**Figure 2.6: TEM micrographs of natamycin-loaded nanoparticles (scale bar 0.2 μm)**

#### 2.4.5. Physical state of natamycin

Information on the physical state of natamycin molecules encapsulated in the nanospheres and interactions between the antifungal and polymer within the polymeric matrix of the nanoparticles were determined by differential scanning calorimetry, X-ray diffraction and infrared spectroscopy based on the reference formulation PLGA 25 mg/mL - Natamycin 2.5 mg/mL.

DSC thermograms of natamycin, PLGA polymer, loaded/unloaded lyophilized nanoparticles and corresponding physical mixture PLGA-natamycin are shown in Figure 2.7. Natamycin was characterized by three consecutive endothermic transitions around 73°C, 97°C and 134°C, matching the disappearance of the three molecules of water present in the trihydrate crystalline form. The sharp exotherm observed at 227°C is related to its thermal decomposition [24]. The pure PLGA 75:25 exhibits an endothermic event around 54°C, referring to the relaxation peak following the glass transition. Thermal degradation of PLGA starts around 230°C, with an exothermic event at 367°C (not displayed here). No melting point is observed as PLGA is by nature an amorphous copolymer [25]. The physical mixture shows the same endothermic peak related to PLGA glass transition around 54°C. Two of the peaks related to dehydration and the exothermic event for natamycin degradation were also visible but shifted to lower temperatures. These modifications suggest solubilization of natamycin and/or interactions between the preservative and the polymer.

The endothermic event corresponding to the glass transition of PLGA remained visible for both unloaded and loaded nanoparticles but was shifted to lower temperatures with an intensified effect in presence of natamycin, corroborating the idea of interactions occurring between PLGA and the preservative as previously observed by size measurements. No thermal transition related to natamycin was besides observed for loaded nanoparticles indicating that the compound might be amorphous or dispersed in a non-crystalline state in the polymeric matrix.

The physical state of natamycin was further confirmed by the analysis of XRD patterns (Figure 2.8). Pure natamycin powder presents a crystalline pattern comparable to those previously reported for the trihydrate crystalline form [24]. The amorphous nature of PLGA was confirmed by XRD. The physical mixture pattern consists in a simple superposition of both natamycin and PLGA pattern, with the presence of an amorphous zone and several diffraction peaks attributable to the preservative. XRD spectra for both nanoparticles samples were similar to pure PLGA. The complete absence of diffraction peaks corresponding to natamycin reinforces the idea that the compound exists in an amorphous or molecularly-dispersed state within the polymeric matrix.

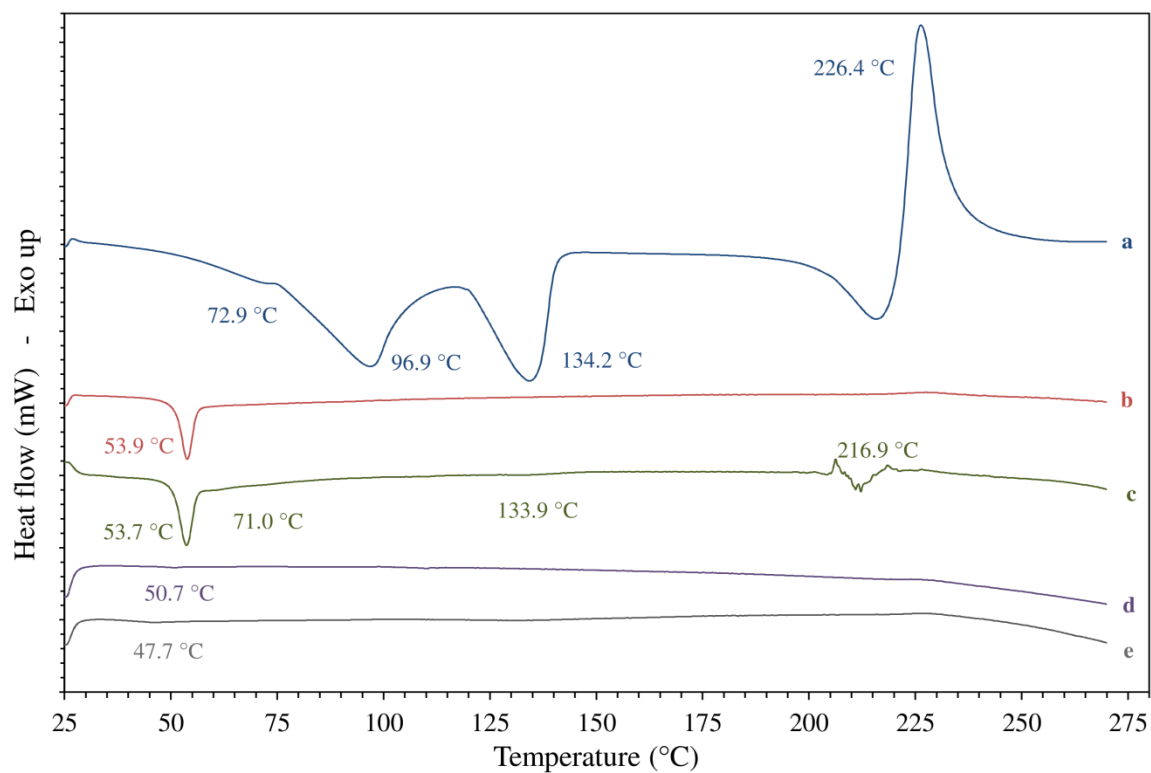


**Figure 2.7:** DSC thermograms of natamycin (a), PLGA (b), physical mixture PLGA/natamycin (c), unloaded (d) and natamycin-loaded PLGA nanospheres (e)

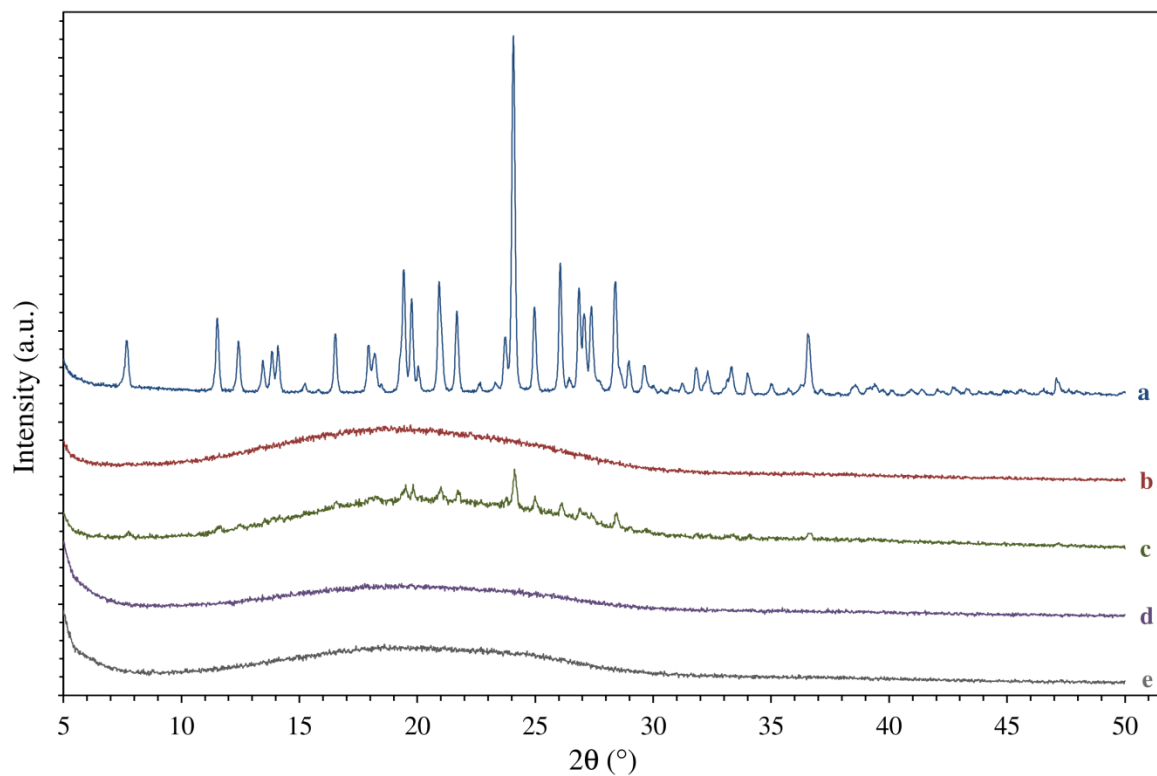


**Figure 2.8:** X-Ray diffractograms of natamycin (a), PLGA (b), physical mixture PLGA/natamycin (c), unloaded (d) and natamycin-loaded PLGA nanospheres (e)

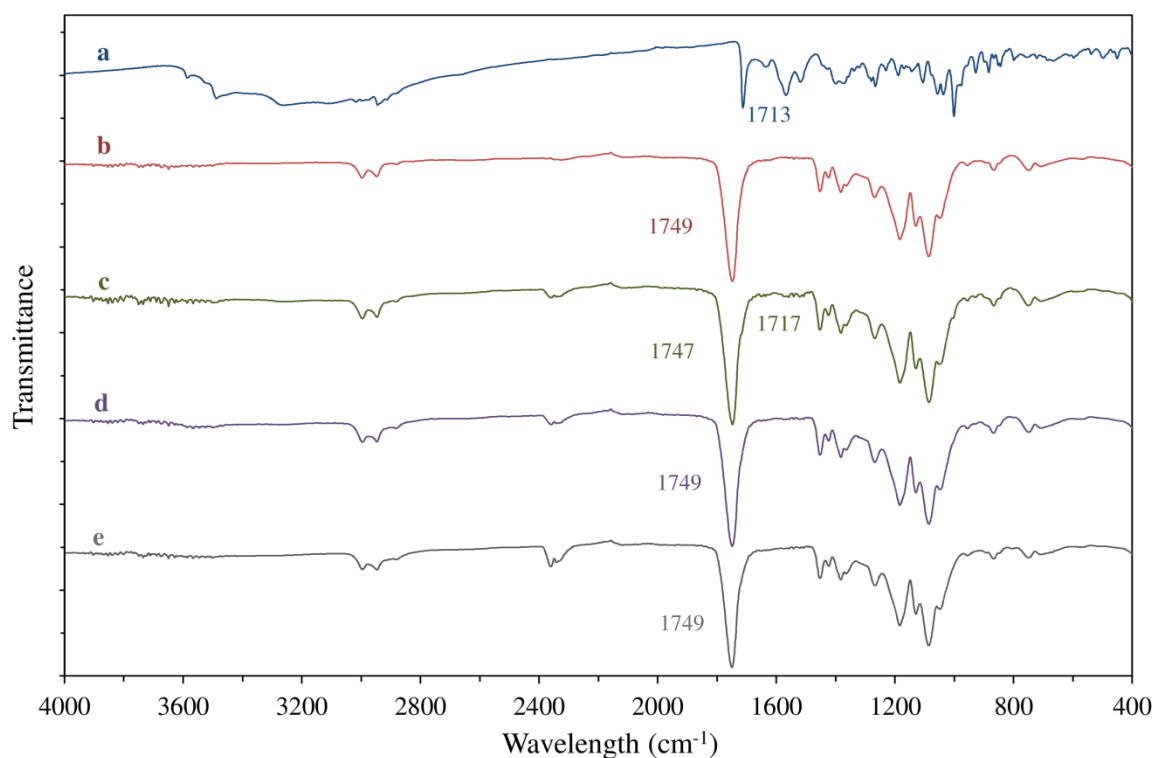


**Figure 2.9:** FT-IR spectra of natamycin (a), PLGA (b), physical mixture PLGA/natamycin (c), unloaded (d) and natamycin-loaded PLGA nanospheres (e)

FT-IR spectra of natamycin, PLGA, physical mixture, unloaded and loaded nanoparticles are displayed in Figure 2.9. PLGA showed characteristic bands of -C-O stretching ( $1050\text{-}1275\text{ cm}^{-1}$ ), -C=O stretching ( $1749\text{ cm}^{-1}$ ) and -CH<sub>2</sub>-CH<sub>3</sub> stretching ( $2850\text{-}3000\text{ cm}^{-1}$ ). For pure natamycin, main peaks contributing from the functional groups of the molecule such as -C-O, -C-N stretching ( $1000\text{-}1270\text{ cm}^{-1}$ ), -CH=CH- stretch (conjugated dienes at  $1570\text{ cm}^{-1}$  and  $\alpha,\beta$ -unsaturated lactone at  $1640\text{ cm}^{-1}$ ), carbonyl -C=O stretching ( $1713\text{ cm}^{-1}$ ), O-H/N-H stretching ( $2500\text{-}3700\text{ cm}^{-1}$ ) and -NH<sub>3</sub><sup>+</sup> stretching at  $3281\text{ cm}^{-1}$  were present. Natamycin was still detected in the physical mixture at very low intensities on the range  $900\text{-}1000\text{ cm}^{-1}$  and  $1500\text{-}1600\text{ cm}^{-1}$  as well as by its C=O stretching, partially superposed with the PLGA carbonyl band. FT-IR recorded at higher ratios natamycin-PLGA (data not shown) indicated a simple superposition of both polymer and antifungal agent spectra. The FT-IR spectra for loaded and unloaded nanoparticles were similar to pure PLGA. Natamycin was not detected in the loaded-nanoparticles which might indicate its dissolution in the polymer matrix and levels too low to be detected by the FT-IR. No significant difference in positions of the absorption peaks of PLGA were observed indicating that the polymer was not involved in significant intermolecular interactions with natamycin in the solid formulations. This is in

accordance with the zeta-potential measurements which suggested rather electrostatic interactions between natamycin and PLGA nanoparticles in suspension.

## 2.5. Performance tests

### 2.5.1. *In vitro* release kinetics

*In vitro* release kinetics profiles of natamycin, physical mixture PLGA-natamycin and loaded nanoparticles (PLGA 25 mg/mL – Natamycin 2.5 mg/mL) are displayed in Figure 2.10.

Pure natamycin showed a slow release pattern with continuous delivery over more than 14 days, in accordance with the progressive dissolution of its crystalline form. A noteworthy difference between pure preservative and physical mixture was observed with a clear acceleration of the release in presence of polymer and a plateau reached after 10 days. This finding could be related either to electrostatic complexation with PLGA or to possible PLGA hydrolysis which could have created a slightly more acidic medium in the dialysis bag, helping in both cases the dissolution of natamycin crystals.

Natamycin-loaded PLGA nanoparticles exhibited a faster release pattern consisting in two phases: an initial burst release of 80% over the first two days, followed by a continuous release at very slow rates up to 7 days. The first phase is attributable to the release of non-encapsulated natamycin either present in solution or adsorbed at the surface of the nanospheres, as evidenced previously by low encapsulation efficiencies and zeta-potential measurements. Higher availability of natamycin in soluble state in the case of nanoparticles is also in accordance with the amorphous state of the compound highlighted by DSC and XRD. The slow following phase is on the other hand related to the progressive release and permeation towards the aqueous medium of natamycin encapsulated within the polymeric matrix [26].

The release data were further fitted with first-order kinetics, Higuchi kinetics and Korsmeyer-Peppas models classically applied to nano-carriers [18-20]. Correlation coefficients  $R^2$  and release rate constants are summarized in Table 2.5. A molecular suspension of natamycin was analysed as a control to determine the effect of the dialysis method itself. Release from this molecular suspension was found to obey a first-order kinetics ( $R^2 = 0.974$ ) with a very fast delivery rate (100% released reached after 2 days), in accordance with the progressive transport of molecular natamycin from the dialysis bag

membrane towards the external medium induced by the sink conditions. Pure natamycin crystals presented a better fitting with the Higuchi model, which is representative from the drug dissolution and diffusion out of a crystalline matrix. Release from the physical mixture was also compatible with the Higuchi model with, as expected, a release rate constant higher than for natamycin alone. In the case of natamycin-loaded nanospheres, the best fitting model and higher correlation coefficient values were found for the first-order kinetics similarly to molecular natamycin, in accordance with the presence of non-encapsulated preservative previously highlighted.

Application of the Korsmeyer-Peppas model gave very good correlations for both natamycin crystals and PLGA nanospheres. Values of  $n$  comprised between 0.43 and 0.85 highlighted an anomalous non-Fickian diffusion mechanism for all samples. High value of  $n$  for polymeric nanospheres indicated a large contribution of swelling/relaxation of the nanoparticles for the release of natamycin rather than a simple Fickian diffusion, in accordance with the complexation PLGA-natamycin identified earlier which is highly likely to slow down the release process.

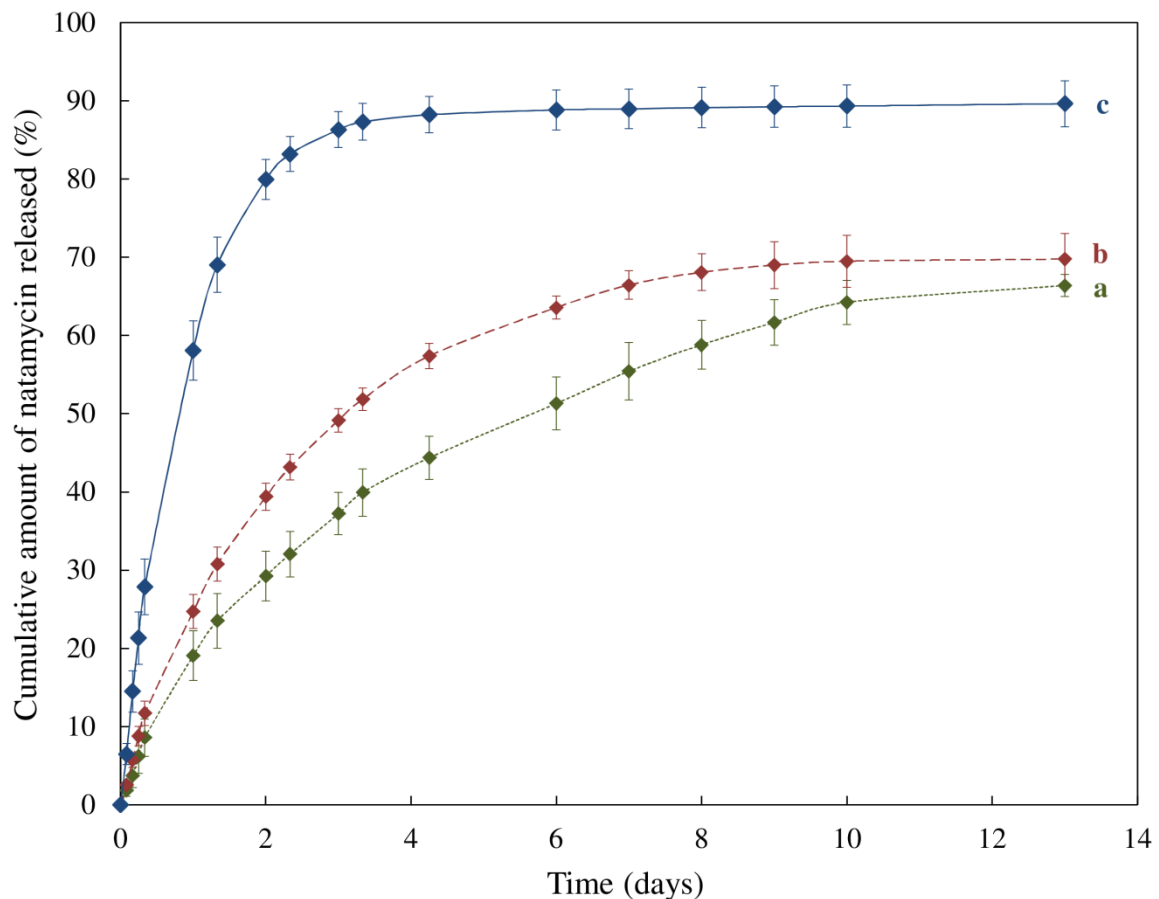


**Figure 2.10:** *In vitro* release profiles of natamycin (a), physical mixture PLGA/natamycin (b) and natamycin-loaded PLGA nanospheres (c)

**Table 2.5: Correlation of release kinetics data using 1<sup>st</sup> order, Higuchi and Korsmeyer-Peppas kinetic models for crystalline natamycin, physical mixture and natamycin-loaded PLGA nanospheres**

| Model                              | First-order    |   | Higuchi        |       | Korsmeyer-Peppas |       |
|------------------------------------|----------------|---|----------------|-------|------------------|-------|
| Sample                             | R <sup>2</sup> | $k$ (10 <sup>-2</sup> h <sup>-1</sup> ) | R <sup>2</sup> | $k$   | R <sup>2</sup>   | $n$   |
| Natamycin crystals                 | 0.940          | 0.48                                    | 0.988          | 4.23  | 0.975            | 0.708 |
| Physical mixture<br>PLGA-natamycin | 0.902          | 0.71                                    | 0.974          | 5.32  | 0.983            | 0.763 |
| PLGA nanospheres                   | 0.975          | 3.1                                     | 0.963          | 10.92 | 0.981            | 0.824 |

### 2.5.2. Antifungal activity against *Saccharomyces cerevisiae*

Figure 2.11 displays the cumulative antifungal activity against *Saccharomyces cerevisiae* observed over 5 days for pure natamycin, physical mixture polymer-preserved and PLGA nanospheres loaded with various amounts of preservative.

Natamycin presented a regular pattern with a similar antifungal activity provided every day over a long period of time (>5 days), in accordance with the slow release kinetics from crystals evidenced via the dialysis bag method and thus sustained release of molecular natamycin available for antifungal activity. As expected from *in vitro* release kinetics results, introduction of PLGA in the physical mixture slightly enhanced the antifungal activity, particularly during the first day, though the sustained pattern over 5 days remain comparable with pure natamycin.

Unloaded nanoparticles did not show activity against the yeast indicating no antifungal effect of PLGA itself. Antimicrobial performance of natamycin-loaded nanospheres differed clearly from the pure preservative, with the major part of the activity occurring during the first 24 h at 2.4 to 3-fold higher levels compared to crystalline natamycin. Absolute cumulative release from formulations containing 0.5, 1.5 and 2.5 mg/mL of natamycin in methanol were respectively 50%, 67% and 77% of the initial content of natamycin, with an absence of antifungal activity detected after 2-3 days. These findings corroborates the biphasic release profile described in 2.5.1, with a clear burst release of preservative molecules over the first two days followed by release at much slower rates, with quantities released too low to be detected by the disk-diffusion assay.

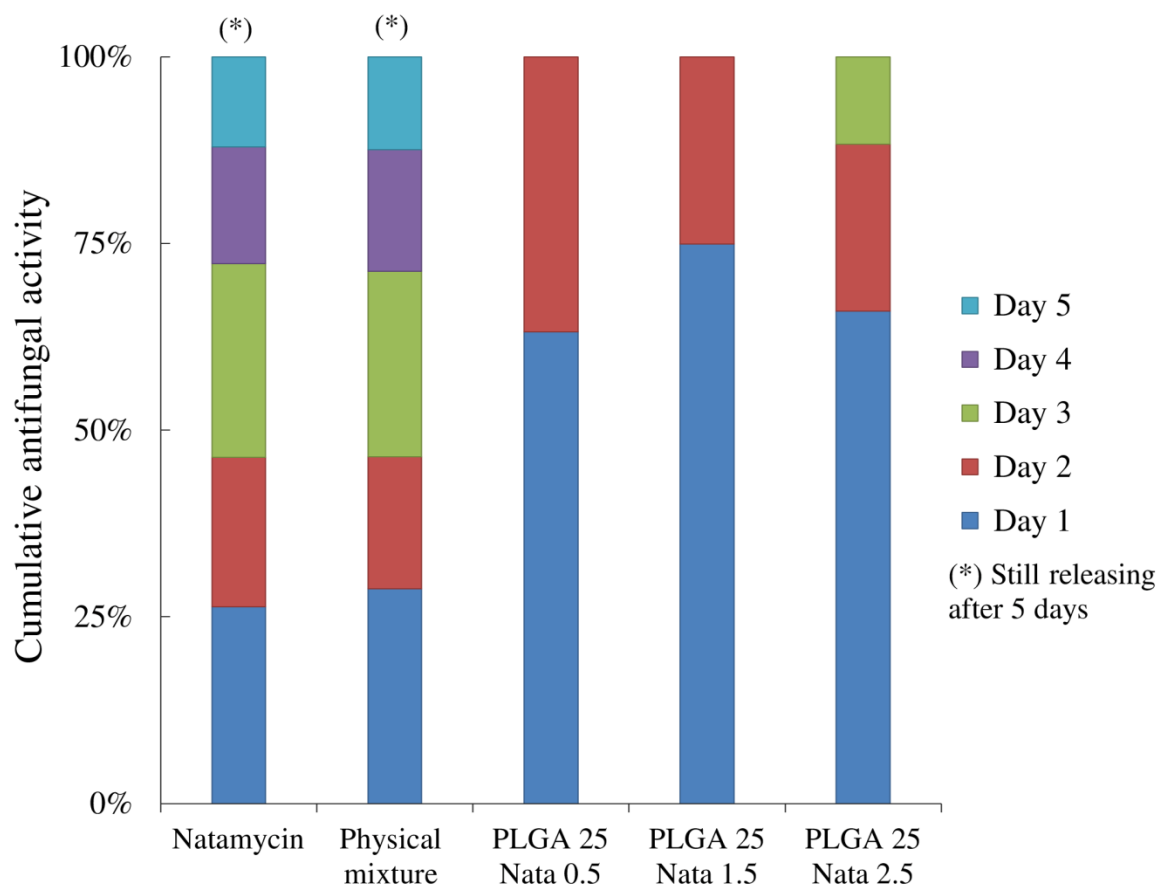


**Figure 2.11: Cumulative antifungal activity observed against *Saccharomyces cerevisiae* for native natamycin, physical mixture PLGA-natamycin and loaded nanoparticles**

## 2.6. Stability tests

Stability tests were performed on unloaded PLGA nanospheres (25 mg/mL), nanospheres containing 2.5 mg/mL of natamycin (around 33 ppm in water) and corresponding suspension of pure natamycin in water (around 35 ppm) under the conditions described in section 2.2.5.

Unloaded nanoparticles did not display significant change in PDI over 10 weeks of storage in the three conditions tested with only slight reduction in size (2-5 nm in average) due to slow erosion and degradation of the polyester. A similar observation was made for natamycin-loaded nanoparticles.

The content of preservative lost upon storage was analyzed by HPLC (Figure 2.12). Natamycin was easily degraded in nano-suspensions stored at room temperature, with a slightly enhanced effect under light exposure in accordance with the known sensitivity of the molecule towards UV. Storage at 4°C enabled to slow down the degradation but loss remained significant compared to the corresponding suspension of pure natamycin in



water where only 19.3% were lost after 10 weeks. Measurement of pH of the nano-suspensions upon storage highlighted an evolution towards a more acidic medium (pH 4.8 initially vs 4.2 after 5 weeks) that would tend to indicate the presence of degradation products of PLGA, likely to catalyze the degradation of natamycin itself.

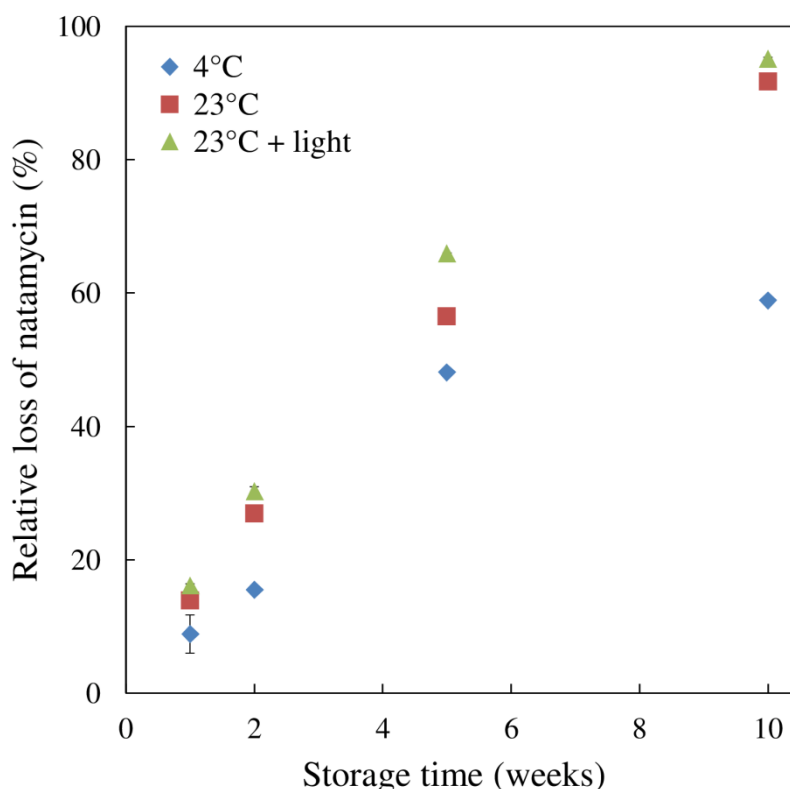


**Figure 2.12: Relative loss of natamycin (%) in PLGA nanospheres prepared by nanoprecipitation under different storage conditions**

## 2.7. Conclusions

Biodegradable polymeric nanospheres were prepared successfully by nanoprecipitation using low molecular weight PLGA (75:25 L:G ratio) dissolved in the mixture acetone/methanol 2:1. A solvent/non-solvent ratio of 4% v/v and an intermediate stirring speed (500 rpm) enabled the formation of monodisperse nanospheres (60-120 nm) with limited formation of large aggregates of polymer. Concentration of PLGA dissolved in the solvent phase was shown to be the most determinant factor to control the size of the nanoparticles.

Incorporation of natamycin, via dissolution in the methanol present in the organic phase, still enabled the formation of nanospheres with limited effect on the polydispersity but clear participation of the preservative compound to the nanoprecipitation process as highlighted by a size reduction of 10-30 nm. In-depth study showed that size reduction is

related to the formation of a PLGA-natamycin complex in the solvent phase that induces a shift in Ouzo region and allows formation of smaller particles. Determination of entrapment levels indicated that up to 25% of the maximum amount of natamycin soluble in methanol could be encapsulated in the selected nanospheres, with the remaining preservative being dissolved in water or adsorbed at the surface of the nanoparticles. Modification of the pH or ionic strength of the aqueous phase did not enhance the encapsulation or led to larger particles or polydisperse nano-suspensions. Analysis of the physical state of natamycin indicated a non-crystalline state and weak interactions, probably electrostatic, towards PLGA. *In vitro* release profiles and antifungal activity assays confirmed that the low encapsulation levels and the modified physical state of natamycin promotes a higher availability of free preservative molecules compared to its classical crystalline form, which could represent a huge advantage for the treatment of food products requiring a high level of antifungal protection at early stages of their preparation.

Stability tests of natamycin polymeric nano-suspensions indicated however a relatively fast degradation of the preservative upon storage, likely to be due to hydrolysis or degradation of the polymer itself. Low levels of encapsulation and inherent low solid content of nano-suspensions prepared by nanoprecipitation also limit the potential use of the developed formulations in real food applications. Both issues should be solved by the preparation of concentrated or dried forms as will be addressed in Chapters 4 and 5 of this thesis.

## Acknowledgments

The authors would like to thank Meng-Yue Wu (National Center for High Resolution Electron Microscopy, Delft University of Technology, The Netherlands) for performing TEM analyses.

## References

- [1] K.S.Soppimath, T.M.Aminabhavi, A.R.Kulkarni, W.E.Rudzinski, Biodegradable polymeric nanoparticles as drug delivery devices, *Controlled Release*, **2001**, 70, 1-20
- [2] A.Kumari, S.K.Yadav, S.C.Yadav, Biodegradable polymeric nanoparticles based drug delivery systems, *Colloids and Surfaces B: Biointerfaces*, **2010**, 75, 1-18
- [3] Y.Ikada, H.Tsuji, Biodegradable polyesters for medical and ecological applications, *Macromol. Rapid Commun.*, **2000**, 21, 117-132
- [4] I.Vroman, L.Tighzert, Biodegradable Polymers, *Materials*, **2009**, 2, 307-344

- [5] C.Vauthier, K.Bouchemal, Methods for the preparation and manufacture of polymeric nanoparticles, *Pharmaceutical Research*, **2009**, 26 (5), 1025-1058
- [6] C.P. Reis, R.J.Neufeld, A.J.Ribeiro, F.Veiga, Nanoencapsulation I. Methods for preparation of drug-loaded polymeric nanoparticles, *Nanomedicine: Nanotechnology, Biology and Medicine*, **2006**, 2, 8-21
- [7] J.P. Rao, K.E.Geckeler, Polymer nanoparticles: Preparation techniques and size-control parameters, *Progress in Polymer Science*, **2011**, 36, 887-913
- [8]H. Fessi, F. Puisieux, J.-P. Devissaguet, N. Ammoury, S. Benita, Nanocapsule formation by interfacial deposition following solvent displacement, *Int. J. Pharm.*, **1989**, 55, R1-R4
- [9] T.Niwa, H.Takeuchi, T.Hino, N.Kunou, Y.Kawashima, Preparations of biodegradable nanospheres of water-soluble and insoluble drugs with D,L-lactide/glycolide copolymer by a novel spontaneous emulsification solvent diffusion method, and the drug release behavior, *Journal of Controlled Release*, **1993**, 25, 89-98
- [10] D.Quintanar-Guerrero, E. Allémann, H. Fessi, E. Doelker, Preparation techniques and mechanisms of formation of biodegradable nanoparticles from preformed polymers, *Drug Dev. Ind. Pharm*, **1998**, 24, 1113–1128
- [11] S.Galindo-Rodriguez, E.Allemand, H.Fessi, E.Doelker, Physicochemical parameters associated with nanoparticle formation in the salting-out, emulsification-diffusion, and nanoprecipitation methods, *Pharmaceutical Research*, **2004**, 21, 1428-1439
- [12] F.Ganachaud, J. L. Katz, Nanoparticles and nanocapsules created using the ouzo effect: spontaneous emulsification as an alternative to ultrasonic and high-shear devices, *ChemPhys Chem* , **2005**, 6, 209–216
- [13] C.E.Mora-Huertas, H.Fessi, A.Elaissari, Influence of process and formulation parameters on the formation of submicron particles by solvent displacement and emulsification-diffusion methods. Critical comparison, *Advances in Colloid and Interface Science*, **2011**, 163, 90-122
- [14] S.Stainmesse, A.-M.Orecchioni, E.Nakache, F.Puisieux, H.Fessi, Formation and stabilization of a biodegradable polymeric colloidal suspension of nanoparticles, *Colloid Polym. Sci.*, **1995**, 273, 505-511
- [15] U. Bilati, E.Allémann, E.Doelker, Development of a nanoprecipitation method intended for the entrapment of hydrophilic drugs into nanoparticles, *Eur. J. Pharm. Sci.*, **2005**, 24, 67-75
- [16] J. Barichello, M. Morishita, K. Takayama, T. Nagai, Encapsulation of hydrophilic and lipophilic drugs in PLGA nanoparticles by the nanoprecipitation method, *Drug Dev. Ind. Pharm.*, **1999**, 25, 471-476
- [17] S.S.D'Souza, P.P.DeLuca, Methods to assess in vitro drug release from injectable polymeric particulate systems, *Pharmaceutical Research*, **2006**, 23(3), 460-474
- [18] P.Costa, J.M. Sousa Lobo, Modeling and comparison of dissolution profiles, *Eur.J.Pharm.Sci.*, **2001**, 13, 123-133
- [19] R.W. Korsmeyer, R.Gurny, E.Doelker, P.Buri, N.A. Peppas, Mechanisms of solute release from porous hydrophilic polymers, *Int.J.Pharm.*, **1983**, 15, 25-35
- [20] P.L. Riger, N.A. Peppas, A simple equation for description of solute release II. Fickian and anomalous release from swellable devices, *J.Control.Rel.*, **1987**, 5, 37-42

- [21] P.Legrand, S.Lesieur, A.Bochot, R.Gref, W.Raatjes, G.Barratt, C.Vauthier, Influence of polymer behavior in organic solution on the production of polylactide nanoparticles by nanoprecipitation, *Int.J.Pharm.*, **2007**, *344*, 33-43
- [22] M.Beck-Broichsitter, E.Rytting, T.Lebhardt, X.Wang, T.Kissel, Preparation of nanoparticles by solvent displacement for drug delivery: A shift in the “ouzo” region upon drug loading, *European Journal of Pharmaceutical Sciences*, **2010**, *41*, 244-253
- [23] T. Govender, S. Stolnik, M.C. Garnett, L. Illum, S.S. Davis, PLGA nanoparticles prepared by nanoprecipitation: drug loading and release studies of a water soluble drug, *J. Control. Release*, **1999**, *57*, 171-185
- [24] H.Brik, Natamycin, *Analytical Profiles of Drug Substances*, Academic Press Inc. (London), **1981**, *10*, 514-557
- [25] A.Lendlein, A.Sisson, *Handbook of Biodegradable Polymers: Isolation, Synthesis, Characterization and Applications*, Chapter 1 - Polyesters, **2011**, Wiley-VCH
- [26] S.Fredenberg, M.Wahlgren, M.Reslow, A.Axelsson, The mechanisms of drug release in poly(lactic-co-glycolic acid)-based drug delivery systems – A review, *Int.J.Pharm.*, **2011**, *415*, 34-52



# Chapter 3

## *Liposomal formulations of natamycin: the benefits of sterol enrichment*

---

Food-grade soybean liposomal suspensions are prepared by the solvent injection method and evaluated as potential nano-delivery systems for natamycin. Unloaded and natamycin-loaded formulations are successfully obtained using methanol as a solvent phase and Epikuron 145V or 200 soybean lecithins as carrier material. Small unilamellar vesicles (< 130 nm) are formed with polydispersities in the range 0.22-0.25 and are able to encapsulate natamycin without significant modification of their size characteristics. Presence of charged phospholipids and reduced content of phosphatidylcholine in the lecithin mixture are found to be beneficial for natamycin encapsulation, indicating electrostatic interactions of the preservative with the polar head of the phospholipids. The chemical instability of natamycin upon storage in these formulations is however significant and proves that uncontrolled leakage out of the liposomes occurs. Performing the solvent injection in acidic aqueous medium enables to enhance the encapsulation of the preservative and reduces the chemical instability at some extent. More efficient prevention of natamycin degradation is obtained by incorporation of sterols (cholesterol, ergosterol) in the lipid mixture and is linked to higher entrapment levels and reduced permeability of the phospholipid membrane provided by the ordering effect of sterols. Comparable action of ergosterol is observed at concentrations 2.5-fold lower than cholesterol and attributed to a preferential interaction natamycin-ergosterol as well as a higher control of membrane permeability. Fine-tuning of sterol concentration allows preparation of liposomal suspensions presenting modulated *in vitro* release kinetics rates and enhanced antifungal activity against the model yeast *Saccharomyces cerevisiae*.

---

Part of this chapter has been submitted as : C. Bouaoud, J.G.J.L. Lebouille, H.E.A. De Braal, E. Mendes, G.M.H. Meesters, Formulation and antifungal performance of natamycin-loaded liposomal suspensions: the benefits of sterol-enrichment, *Journal of Liposome Research*, **2016**, 26 (2), 103-112

### 3.1. Introduction

Liposomal formulations have been extensively developed over the last fifty years for encapsulation and delivery of food active ingredients or drugs [1-3]. Liposomes are commonly defined as closed spherical-shaped vesicles consisting of an internal aqueous core surrounded by one or more lipid bilayers, in a structure similar to biological membranes [4-5]. The lipid bilayer contains polar amphiphilic molecules such as phospholipids [6-7], which possess a hydrophobic double fatty acid tail (acyl chains), with variable composition and length related to their original source, as well as a hydrophilic head, made of a phosphate group connected to a small molecule, conferring a charge or neutral/zwitterionic aspect to the molecule. Classical phospholipids structures are represented in Figure 3.1. For food-grade applications, phospholipids are generally extracted from egg yolk or natural oils (sunflower, soya) in complex mixtures of phospholipids, called lecithins.

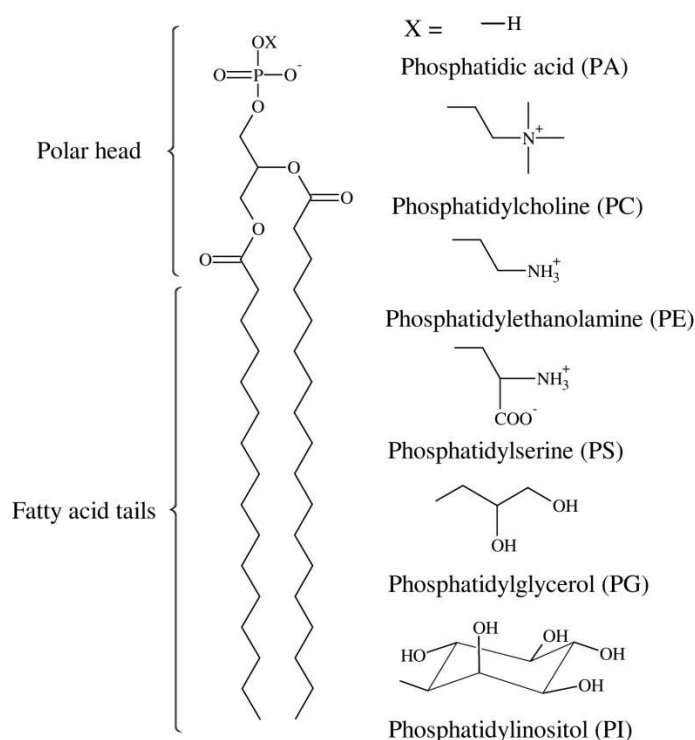


**Figure 3.1: Chemical structure of phospholipids**

Formation of liposomes is based on the non-spontaneous assembly of phospholipids related to unfavorable interactions occurring between these amphiphilic molecules and water [4,8-9]. Under the right conditions, hydrophobic tails are forced to face each other, creating the bilayer, while polar heads are oriented towards the external inner or outer

aqueous medium. During the process, hydrophilic molecules can be encapsulated in the aqueous core and lipophilic molecules in the core of the lipid bilayer while amphiphilic compounds would position themselves preferentially between the phospholipids molecules closed to the inner or outer aqueous phase. Depending on the manufacturing process, liposomes can range from tens of nanometers to a few micrometers and show a variety of structures such as unilamellar (single bilayer), multilamellar (multiple bilayer membranes arranged in a concentric structure) or multivesicular when liposomes contains other random-sized vesicles [4]. Nano-liposomes are known as small unilamellar vesicles (SUVs) with diameters ranging from 20-100 nm. SUVs can be obtained by a simple one-step method, called solvent injection [4,10-11], that could promisingly be applied for natamycin.

The solvent injection technique involves the preparation of a “solvent phase” (namely phospholipids and active ingredient dissolved in an organic solvent miscible in all proportions with water and allowing acceptable dissolution of both components), followed by a fast injection into an aqueous solution (“non-solvent phase”). The commonly accepted mechanism explaining the formation of liposomes through solvent injection is the two-steps non-equilibrium model of vesicles formation proposed by Lasic [9] and illustrated in Figure 3.2. In brief, phospholipid molecules, initially well dissolved in the solvent phase, are exposed to an increasingly polar environment due to the solvent diffusion in water. This gradual exposure to more polar medium decreases the lipid solvation and triggers precipitation at the interface solvent/water with formation of bilayered phospholipids fragments (BPFs). The intermediate structures present open edges that induce thermodynamic instabilities due to the exposure of phospholipid hydrophobic tails to the aqueous environment. As a consequence, BPFs grow (fusion by coalescence/aggregation or integration of solubilized lipid molecules) and bend to reduce exposure. Upon growth and bending, intermediate structures finally close upon themselves, creating the liposomes. Final size of the liposomes can be related to the balance of bending energy and opposite curvature forces involved.

All parameters acting on the microfluidic environment (i.e. the polarity change) and the BPF growth can influence the size and polydispersity of the liposomal suspension [11-12]. Parameters influencing the microfluidic environment are for instance the solvent type, the solvent/non-solvent S/NS ratio, the stirring rate or the temperature. Parameters influencing the growth are for instance the lecithin composition and concentration, the composition of aqueous phase (pH, ionic strength, presence of additives).



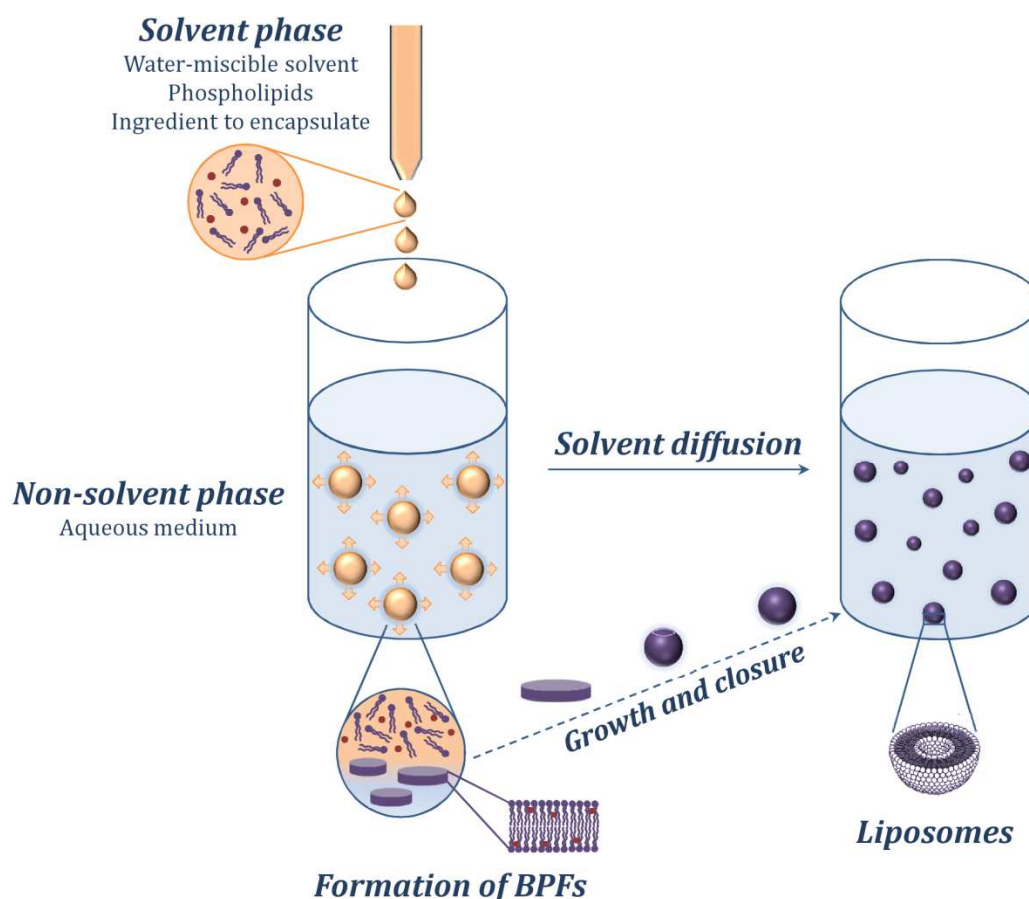


**Figure 3.2: Schematic representation of liposomes formation by the solvent injection method**

Liposomes are recognized as highly versatile carriers, which composition can be fine-tuned to obtain formulations with desired encapsulation and delivery properties. It must however be highlighted that liposomal formulations are frequently encountered to suffer major limitations such as physical instability (fusion, rearrangement) and chemical instability (hydrolysis, oxidation) [13], leading to degradation and/or rapid uncontrolled leakage of the encapsulated compound outside of the vesicles.

Incorporation of sterols in the phospholipid mixture is one of the approaches widely use to counteract these limitations and particularly uncontrolled leakage, mainly by influencing the membrane organization. The lipid bilayer can exist in different physical states [14-15] depending on the lateral organization of phospholipids, their mobility and the molecular order. Two phases are commonly encountered: the gel (solid-ordered) phase and the fluid (liquid-disordered) phase. In the gel phase, phospholipids are packed in a compact way due to maximum elongation of the acyl chains and strong attractive Van der Waals forces. Increase of temperature up to a limit phase transition temperature ( $T_m$ ) leads to more loosely associated phospholipids and lateral expansion of acyl chains. This results in more fluid and permeable membranes with superior mobility of the

phospholipid molecules. Incorporation of sterols such as cholesterol or ergosterol (Figure 3.3) enables the formation of an intermediate phase known as liquid-ordered phase [14,16-17], which presents characteristics of both gel and fluid state. Incorporation of sterol in the gel state disturbs the forces between acyl chains and loosens the packing, leading to more fluid and permeable arrangement. In the fluid state, the rigid hydrophobic moiety of the cholesterol intercalates between mobile acyl chains and modifies their movement, leading to more ordered and less permeable arrangement. Reduced leakage of encapsulated materials, longer term protection and delayed releases have been classically reported as a result of reduced bilayer permeability linked to the presence of sterols [18-20]. In addition, presence of sterols and particularly ergosterol could be a huge advantage to the encapsulation and controlled release of natamycin. Antimycotics are indeed known to interact with sterols present in fungi membrane as part of their antimicrobial action mechanism [21]. Natamycin activity was for instance proven to be linked to strong binding with ergosterol and disturbance of its functional properties in the fungi membrane [22].

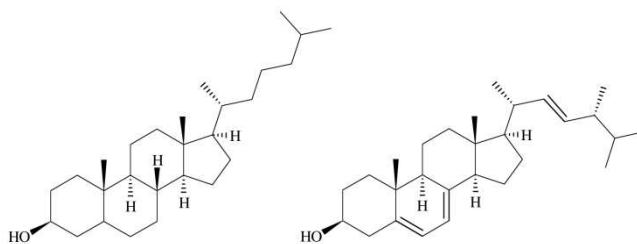


**Figure 3.3: Chemical structure of cholesterol (left) and ergosterol (right)**

The primary objective of this chapter is to assess if natamycin can be efficiently encapsulated in food-grade liposomal formulations prepared by the solvent-injection method and to determine if incorporation of sterols brings an interesting benefit to stability, encapsulation and delivery of the compound. First part of this chapter focuses on the preparation of unloaded and natamycin-loaded sterol-free liposomes obtained from two different soybean lecithins. Formulation parameters influencing the formation of liposomes are investigated in order to form stable and low polydisperse nano-sized unilamellar liposomes. Encapsulation and stability of natamycin in these liposomal formulations are evaluated. Second step describes the enrichment of the phospholipid mixtures with cholesterol and ergosterol and the influence on size, encapsulation and stability of natamycin. Selected formulations were finally submitted to performance tests, namely release kinetics tests and antifungal activity against the model yeast *Saccharomyces cerevisiae*.

## 3.2. Materials and methods

### 3.2.1. Materials

Natamycin (90.6% purity, trihydrate crystalline form, 665.7 g/mol) was kindly supplied by DSM Food Specialties (Delft, The Netherlands) and used without further purification. Deoiled phosphatidylcholine-enriched soybean lecithins Epikuron 145V (50.5% PC, 14.3% PE, < 3% PA, < 1% PL) and Epikuron 200 (93.5% PC) were supplied by Cargill (Hamburg, Germany). Cholesterol (CHOL,  $\geq 99\%$ ) and ergosterol (ERG,  $\geq 95\%$ ) were purchased from Sigma-Aldrich. Methanol EMSURE® ACS from Merck was used for the liposome preparation. Potassium dihydrogen phosphate, methanol and acetonitrile Lichrosolv® were obtained from Merck and used for HPLC analyses. High quality water purified in a MilliQ system was used in all experiments.

### 3.2.2. Preparation of liposomes

Liposomal formulations were prepared using the solvent injection technique. Briefly, Epikuron 145V or Epikuron 200 were dissolved at room temperature in methanol together with natamycin (0.5-2.75 mg/mL) and, when required, with cholesterol (1-5 mg/mL) or ergosterol (0.5-1.5 mg/mL). This organic phase was injected by one-shot addition under moderate stirring (200 rpm) into MilliQ water at a ratio of 4% v/v. The resulting suspension was kept under slow stirring overnight for complete evaporation of organic solvent, before analysis. Formulations are further described in this chapter by the natamycin-to-lecithin (N/L) and sterol-to-lecithin S/L (CHOL/L or ERG/L) weight ratios.

### 3.2.3. Physicochemical characterization of liposomal suspensions

#### 3.2.3.1. Particle size and zeta-potential

The mean particle diameter and polydispersity index (PDI) of the liposomes were determined by Dynamic Light Scattering (DLS) (Zetasizer Nano ZS, Malvern Instruments Ltd., UK). Three consecutive measurements were performed on each suspension at 25 °C at a scattering angle of 173 °, after an equilibration time of 180 seconds. The zeta-potential of the nanoparticles ( $\zeta$ ), was assessed on undiluted nano-suspensions with the same equipment by three consecutive measurements of 50 runs at 25 °C after an equilibration time of 180 seconds. All measurements were performed in triplicate and results are presented as mean  $\pm$  standard deviation (SD).

3.2.3.2. *Morphology*

Morphology of liposomes was investigated using cryogenic transmission electron microscopy (cryo-TEM). Vitrification of aqueous liposomal suspensions was carried out in an automated vitrification robot (FEI Vitrobot™ Mark III). A 3 µL drop was applied to a R2/2 Quantifoil Jena grid (Quantifoil Micro Tools GmbH, Germany) in the environmental chamber of the Vitrobot (25 °C, 99% humidity) and the grid was blotted with two filter papers to remove the excess liquid. Subsequently, the grid was plunged into liquid ethane which was maintained at approximately –183 °C. CryoTEM samples were imaged with the TU/e CryoTitan (FEI, FEG, 300 kV, Gatan Energy Filter, 2k x 2k Gatan CCD camera). Images were acquired using low dose mode, with an exposure time of 1 s at a dose rate of 70 e-/Å<sup>2</sup> per second.

3.2.3.3. *Encapsulation (EE) and loading (LE) efficiencies*

5 mL of liposomal suspension were transferred in Amicon Ultra-15 centrifugal filter units (10 kDa, Millipore, USA) and centrifuged for 50 min at 4500 rpm (Eppendorf centrifuge 5804C, 20 °C). Filtrate and original sample were collected and diluted in methanol before analysis by HPLC. Natamycin content was determined by reverse-phase high-performance liquid chromatography (HPLC). A high pressure liquid chromatograph Ultimate 3000 Dionex equipped with a variable wavelength detector was used. Separation was achieved by injecting 20 µL of sample on a reverse phase column Licrospher® RP18 (Merck, 125 nm x 4 mm, pore size 100 Å) with a mobile phase consisting of 35:65 v/v acetonitrile: potassium dihydrogenphosphate buffer (pH 3.05) at a flow rate of 1.0 mL/min. Natamycin was detected by UV at 303 nm and quantified using a calibration curve designed over the range 0.05-50 ppm ( $R^2 = 0.9996$ ). All HPLC samples were analyzed in triplicate. EE and LE were calculated according to Equations 1 and 2. Determination of EE and LE was performed on three samples for each composition. Results are presented as mean ± SD.

$$EE (\%) = \frac{\text{Total amount of natamycin} - \text{amount of natamycin in the filtrate}}{\text{Total amount of natamycin}} * 100 \quad (\text{Eq. 1})$$

$$LE (\%) = \frac{\text{Total amount of natamycin} - \text{amount of natamycin in the filtrate}}{\text{Amount of phospholipids} + \text{sterols}} * 100 \quad (\text{Eq. 2})$$

### 3.2.4. Stability

Stability tests were performed after 1, 2, 5 and 10 weeks by determining size evolution by DLS and natamycin content evolution by the HPLC method for liposomal formulations stored at 4 °C and room temperature RT (23 ± 2 °C) under light protection or light exposure.

### 3.2.5. Performance tests

#### 3.2.5.1. *In vitro* release kinetics

*In vitro* release studies were carried out using the dialysis bag technique. Liposomal suspensions were used as such, after solvent evaporation. A reference sample was prepared by dispersing natamycin powder in MilliQ water to reach an initial concentration similar to the liposomal formulations. 1 mL of these suspensions was placed in a dialysis bag (Float-A-Lyzer® G2, Biotech Grade Cellulose Ester, MWCO 8-10 kDa, Spectrumlabs) and incubated in 35 mL of MilliQ water at 25 °C in a shaking bath. Total volume was collected at predetermined intervals and replaced with equal volume of fresh release medium to maintain sink conditions. Amount of natamycin in the aliquots was assayed by HPLC. The cumulative percentage of natamycin released was calculated for triplicates and plotted versus time.

To further characterize the rate and mechanism of release of natamycin out of the liposomes, the release data were fitted to classical mathematical models [23] including first-order kinetics (Eq.3), Higuchi kinetics (Eq.4) and Korsmeyer-Peppas model (Eq.5).

$$M_t/M_\infty = 1 - e^{-kt} \quad (\text{Eq. 3})$$

$$M_t/M_\infty = k \cdot t^{1/2} \quad (\text{Eq. 4})$$

$$M_t/M_\infty = k \cdot t^n \quad (\text{Eq. 5})$$

Where  $M_t/M_\infty$  represents the cumulative fraction of drug released at the time  $t$  over the total amount released,  $k$  is the release rate constant and  $n$  is the diffusion exponent indicative of the mechanism of drug release. Fittings were obtained by plotting respectively  $\log(100\% \text{ released})$  vs time (first-order) and  $\% \text{ released}$  vs square root of time (Higuchi). The initial 60% of preservative released were fitted in the Korsmeyer-Peppas model by plot of  $\log(\% \text{ released})$  vs  $\log(\text{time})$  and the value of “ $n$ ” determined from the slope. For swellable nanocarriers [24-25],  $n = 0.43$  represents a release mechanism based only on Fickian diffusion while  $n = 0.85$  corresponds to a case-II transport based on relaxation/swelling of the nano-carriers. Intermediate values indicate an anomalous transport and combination of both diffusion and relaxation phenomenon.

3.2.5.2. *In vitro* antifungal activity

Antifungal activity of natamycin and liposomal suspensions against the model yeast *Saccharomyces cerevisiae* (ATCC 9763) was assessed by agar disk diffusion assay. Briefly, a layer of nutrient OGYE agar inoculated with *Saccharomyces cerevisiae* was allowed to solidify in a Petri dish. Sterile blank disks were placed in a stainless steel cylinder and impregnated with 50  $\mu$ L of nano-suspension. A similar procedure was applied to standard solutions of natamycin to establish a calibration curve on the range 30-300 ppm. The disks impregnated with standards or nano-suspensions were then placed on the solidified agar layer and Petri dishes were kept at 4 °C overnight to allow the diffusion of natamycin. After removal of the disks, plates were incubated at 30 °C for 24h. The diameter of the zone of inhibition was measured and compared to a calibration curve established with the standard samples to determine the quantity of natamycin released. Disks impregnated with the suspensions were transferred to a fresh Petri dish and the procedure was repeated over 5 days to follow the release of natamycin. Results are presented as cumulative activity ( $\mu$ g of natamycin released per day/ total  $\mu$ g of natamycin released over 5 days) calculated from triplicate measurements.

### 3.3. Formulation of sterol-free soybean liposomes

#### 3.3.1. Preparation of unloaded liposomal formulations

Unloaded liposomal formulations were prepared using two deoiled food-grade soybean lecithins, Epikuron 145V and Epikuron 200, to study the effect of lipid composition on formation of liposomes by the solvent injection technique. Epikuron 200 possesses the highest level of neutral PC content while Epikuron 145V presents lower levels of purity and contains also charged phospholipids. Methanol was selected to prepare the organic phase as it enables both natamycin dissolution at acceptable levels (up to 2.75 mg/mL experimentally) [26] and solubilization of the lecithins.

Preliminary work on the formation of unloaded liposomes made of both lecithins (data not shown) indicated that the S/NS ratio must be fixed at 4% v/v for optimal formation of liposomes. This ratio allows an acceptable amount of liposomes in suspension and good reproducibility of the process. Higher content of solvent phase injected either limits the solvent diffusion, creating precipitates and heterogeneous suspensions [11], or leads to a mixture solvent/water sufficient to solubilize all the phospholipids. Regarding stirring rate, it was determined that, for the specific low S/NS

ratio used in this study and the concentration of phospholipids involved, no clear effect was observed on the range 100-600 rpm, while higher speeds leading to fast micromixing and formation of large BPFs thus larger liposomes [26]. Stirring rate was fixed at 200 rpm for further experiments.

Figure 3.4 represents the evolution of size and size distribution of liposomes obtained for both lecithins using the conditions described above. It was evidenced that SUVs can be obtained with a monomodal distribution and the lowest polydispersity for concentrations of Epikuron 145V ranging between 30.0 and 67.5 mg/mL. On this range, size of the liposomes varies nearly linearly between 60 and 130 nm with a polydispersity stable around 0.22-0.25. A similar behavior was observed for Epikuron 200 on the concentration range 5.0-32.5 mg/mL with diameters of 30-130 nm and polydispersity averaging 0.15-0.20. Linear variation as a function of lipid concentration in the organic phase is in accordance with observations of previous authors [11-12, 27-28] and has been explained by the predominant effect of lipid concentration on the formation, growth and closure of intermediate BPFs involved in the solvent injection mechanism. Out of these ranges, tremendous increases in polydispersity and diameters were observed. Low concentrations of phospholipids, particularly in the case of Epikuron 145V, are believed to simply cause the dissolution of the molecules in water helped by the presence of solvent or to cause mixed creation of small micelles and liposomes. At higher concentrations, formation of phospholipid aggregates or clusters of small liposomes is promoted [11,27] as well as closure of BPFs in large structures such as multilamellar or multivesicular structures, leading to huge size discrepancies. Epikuron 200, due to its higher purity and easier packing of the phospholipids in the BPFs and bilayer, leads to the formation of more monodisperse SUVs at lower concentrations than Epikuron 145V.

### **3.3.2. Incorporation of natamycin in sterol-free liposomes**

Natamycin-loaded SUVs were prepared using lecithin concentration ranges determined in 3.3.1 and characterized in terms of size, polydispersity and entrapment efficiencies. Table 3.1 displays results obtained by either varying the concentration of natamycin at fixed concentration of lecithin or varying the concentration of lecithin (Epikuron 145V) at the maximum concentration of preservative soluble in methanol.

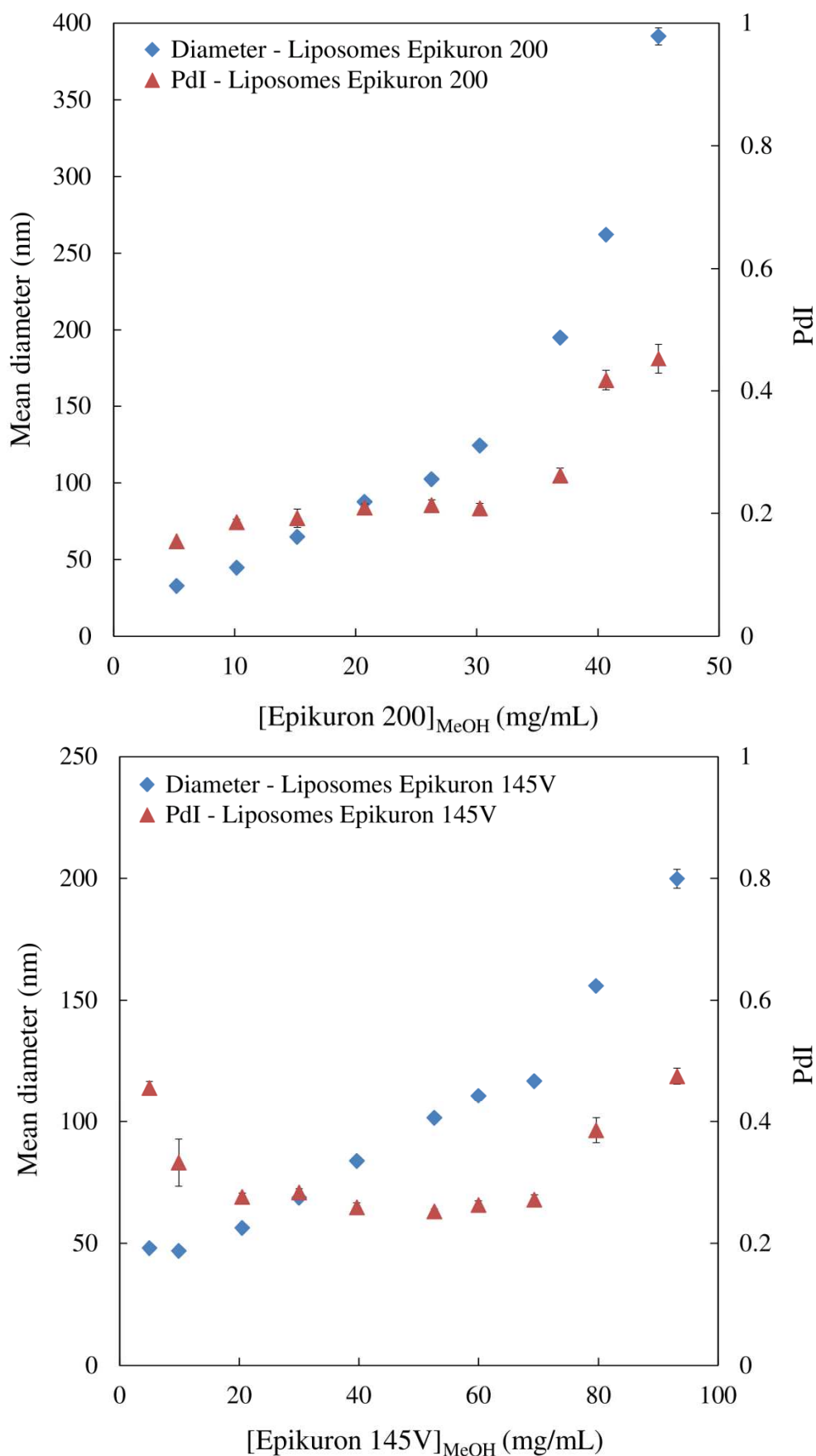


Figure 3.4: Influence of lecithin composition on the size and polydispersity of liposomes obtained by the solvent injection method (top: Epikuron 200 / bottom: Epikuron 145V)



**Table 3.1: Size, PdI, EE and LE as a function of lecithin composition, concentration and N/L ratio**

| Lecithin         | [Lecithin] <sub>methanol</sub><br>(mg/mL) | Ratio<br>N/L | Diameter (nm)<br>± SD | PdI<br>± SD   | EE (%)<br>± SD | LE (%)<br>± SD |
|------------------|---|--------------|-----------------------|---------------|----------------|----------------|
| Epikuron<br>145V | 37.5                                      | 1:15         | 86.9 ± 1.1            | 0.246 ± 0.013 | 62.7 ± 1.2     | 4.3 ± 0.1      |
|                  | 45  | 1:18         | 93.6 ± 0.6            | 0.238 ± 0.005 | 67.8 ± 0.9     | 3.8 ± 0.1      |
|                  | 50  | 1:20         | 115.2 ± 1.0           | 0.217 ± 0.008 | 72.1 ± 1.2     | 3.4 ± 0.1      |
|                  | 62.5                                      | 1:25         | 122.3 ± 1.9           | 0.213 ± 0.011 | 77.3 ± 0.8     | 3.2 ± 0.1      |
|                  | 45  | 1:18         | 93.6 ± 0.6            | 0.238 ± 0.005 | 67.8 ± 0.9     | 3.8 ± 0.1      |
|                  |   | 1:23         | 94.5 ± 0.7            | 0.246 ± 0.006 | 70.7 ± 1.4     | 3.3 ± 0.1      |
|                  |   | 1:30         | 93.8 ± 1.0            | 0.232 ± 0.006 | 81.3 ± 2.0     | 3.1 ± 0.1      |
|                  |   | 1:45         | 92.8 ± 0.9            | 0.240 ± 0.003 | 89.2 ± 3.3     | 2.2 ± 0.1      |
|                  |   | 1:90         | 94.2 ± 0.7            | 0.241 ± 0.011 | 98.6 ± 0.5     | 1.1 ± 0.1      |
|                  | Epikuron<br>200                           | 30           | 1:12                  | 107.5 ± 0.4   | 0.264 ± 0.008  | 52.1 ± 2.9     |
| 1:16             |   |              | 105.5 ± 1.2           | 0.221 ± 0.010 | 49.0 ± 1.6     | 3.0 ± 0.1      |
| 1:23             |   |              | 110.9 ± 0.7           | 0.259 ± 0.009 | 70.7 ± 0.8     | 2.9 ± 0.1      |
| 1:50             |   |              | 106.0 ± 0.8           | 0.195 ± 0.012 | 79.4 ± 4.4     | 1.6 ± 0.1      |

Incorporation of natamycin did not significantly disturb the process of liposomes formation via the solvent injection method whatever N/L ratio was used, with sizes and polydispersity staying in the same range at fixed concentration of lecithin. While varying the concentration of Epikuron 145V, linear variation of size and stable polydispersity were obtained and comparable to unloaded liposomes, indicating no significant effect of the preservative on the liposome formation.

For a fixed concentration of Epikuron 145V (45 mg/mL), encapsulation efficiencies reached a maximum for high ratio N/L. Increasing the concentration of natamycin reduces this level with a plateau reached around the ratio 1:23. Corresponding increased values of loading efficiencies indicate that further incorporation in the membrane occurs but does not compensate for the larger amount of free natamycin molecules, which could lead to the formation of crystals and is not a desired feature. Increase of phospholipid content enables to circumvent this phenomenon but, for the maximum concentration of natamycin achievable in methanol, only up to 77.3% encapsulation efficiency could be obtained on the concentration range enabling formation of SUVs in a controlled way. An analogous saturation phenomenon was observed for Epikuron 200 liposomes. Comparison of both lecithins for similar N/L ratio highlights better affinity of natamycin for Epikuron 145V, i.e. for lower amounts of phosphatidylcholine and higher content of charged phospholipids. This observation is consistent with the slightly positively charged

zwitterionic nature of natamycin at the pH of MilliQ water (5.5-6) and possibly electrostatic interactions with charged phospholipid heads. This also corroborates observations of previous authors regarding the very limited affinity of the preservative for pure phosphatidylcholine bilayers such as Epikuron 200 [22,29].

Zeta-potential measurements confirmed incorporation of natamycin in the liposomes as displayed in Figure 3.5. Presence of charged phospholipids in Epikuron 145V confers to the liposomes a negatively-charged surface (-76.4 mV) whereas Epikuron 200 liposomes were closer from neutral zeta-potentials (-14.3 mV). Incorporation of partially positively charged zwitterionic natamycin in Epikuron 145V SUVs slightly reduced the zeta-potential up to 73.1 mV until reaching the ratio N/L 1:30 where the effect stabilized. This confirms the idea of an incorporation of natamycin by interactions with the polar heads of the phospholipids, either by insertion in the outer part of the bilayer or by complexation at the surface, up to a certain saturation level. This however does not significantly affect the physical stability of the suspensions, contrarily to Epikuron 200 formulations where surface charge reduction reached -3.3 mV for the highest concentration of natamycin.

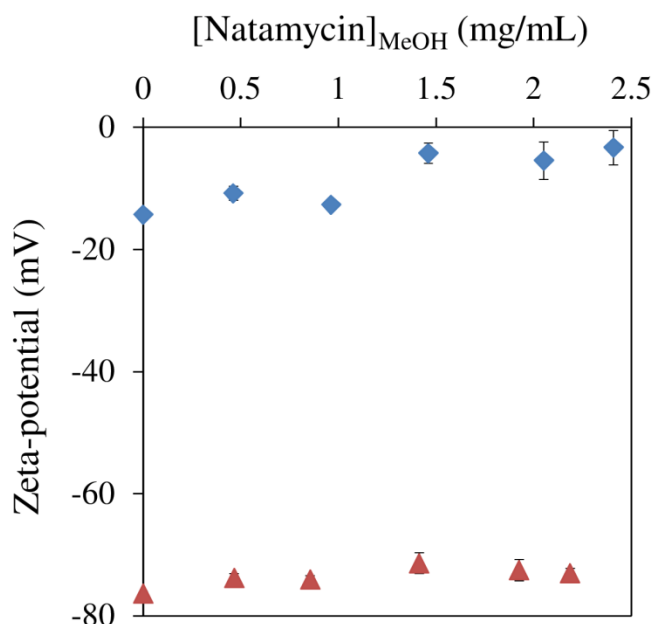


**Figure 3.5:** Influence of natamycin incorporation on the zeta-potential of Epikuron 145V (45 mg/mL – red triangles) and Epikuron 200 (30 mg/mL – blue diamonds) liposomes

Further improvements of encapsulation in Epikuron 145V liposomes were attempted by modification of the pH of the aqueous phase (Table 3.2). Variations of size and PdI can be attributed to the phospholipids themselves as no difference was observed for unloaded liposomes prepared under the same conditions (data not shown). Maximum diameter and polydispersity were observed at pH of the MilliQ water and correspond to the  $pK_B$  of the main components of Epikuron 145V ( $pK_B$  PC = 5.69,  $pK_B$  PE (5.98)) [30-31]. More extreme pHs enhance electrostatic repulsions between polar heads of the phospholipids and lead to smaller and less packed BPFs and liposomes [22]. Determination of encapsulation efficiencies showed little influence on the range 5-7 which can be related to the solubility of natamycin on its own. pH 9 clearly enhances the solubility of natamycin but not its entrapment. Encapsulation at low pH enables higher content of natamycin to be encapsulated due to the balance of natamycin positive charge increase and the still negatively charged liposomes ( $pK_a$  for PC and PE average pH 2.5 [30-31]), that counteract the increase of solubility. pH 4 could thus be an option to increase natamycin entrapment. It is however necessary to determine if natamycin is still protected from degradation under these conditions.

**Table 3.2: Size, PdI, EE and LE as a function of pH for Epikuron 145V liposomes (45 mg/mL – ratio N/L 1:18)**

| pH | Diameter (nm) $\pm$ SD | PdI $\pm$ SD      | EE (%) $\pm$ SD | LE (%) $\pm$ SD |
|----|------------------------|-------------------|-----------------|-----------------|
| 4  | 63.2 $\pm$ 0.3         | 0.200 $\pm$ 0.008 | 95.8 $\pm$ 0.4  | 5.3 $\pm$ 0.1   |
| 5  | 74.7 $\pm$ 0.7         | 0.260 $\pm$ 0.006 | 71.2 $\pm$ 1.9  | 4.0 $\pm$ 0.1   |
| 6  | 93.6 $\pm$ 0.6         | 0.238 $\pm$ 0.005 | 67.8 $\pm$ 0.9  | 3.8 $\pm$ 0.1   |
| 7  | 84.0 $\pm$ 0.8         | 0.230 $\pm$ 0.008 | 67.3 $\pm$ 2.7  | 3.8 $\pm$ 0.2   |
| 9  | 64.9 $\pm$ 0.5         | 0.218 $\pm$ 0.012 | 59.2 $\pm$ 1.6  | 3.3 $\pm$ 0.1   |

### 3.3.3. Morphology of the liposomes

Nano-liposomes made of Epikuron 145V (45 mg/mL - N/L 1:18) were kept as the reference formulation and their morphology further characterized. Cryo-TEM analysis (Figure 3.6) confirmed that solvent injection led to the predominant formation of small unilamellar vesicles. The polydispersity observed by DLS is reflected here by the occasional presence of multilamellar nano-vesicles, though all liposomes remain in the nano-size range. No natamycin crystals were observed in the sample, confirming its encapsulation within the vesicles.

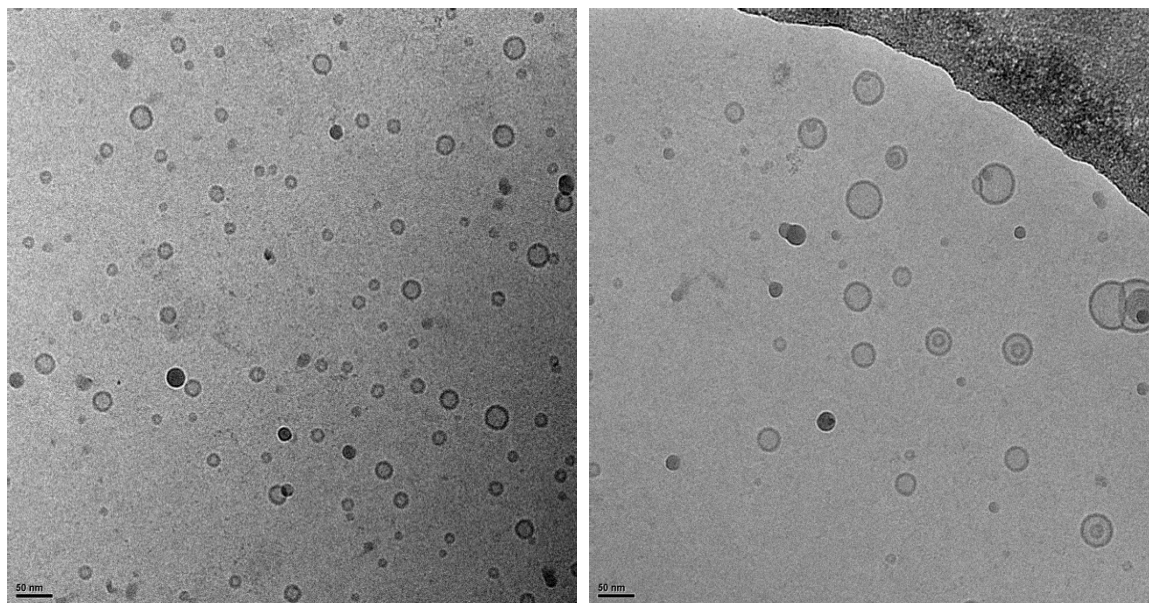


**Figure 3.6: Cryo-TEM micrographs of natamycin-loaded Epikuron 145V liposomes obtained by solvent injection (scale bar 50 nm)**

### 3.3.4. Stability of sterol-free liposomal formulations

Stability of Epikuron 145V liposomes (45 mg/mL – N/L 1:18) prepared in MilliQ water or modified pH aqueous phase was studied by DLS and natamycin content analysis. Under all storage conditions, no significant variations of size and PDI could be noticed (95-105% of original values). As shown in Table 3.3, soybean liposomes however did not enable the efficient protection of natamycin over storage at room temperature with fast degradation of the preservative after 10 weeks. Storage at 4 °C slowed significantly the process but the amount of preservative lost remains significant. Such instability is believed to be linked to the limited encapsulation of natamycin and to the degradation of the phospholipids themselves that might locally create pH changes or trigger oxidation towards which natamycin is sensitive. Epikuron 145V is also a complex mixture of soybean phospholipids, the major part of them displaying phase transition below 0°C (soybean PC: -25 °C / soybean PE: -11 °C) [26-27]. Though DSC analysis (data not shown) on the range -70 to 0 °C did not allow detection of a clear transition, it is highly likely that the bilayer membranes in this study are present in the liquid disordered state, prone to allow consequent leakage of the preservative in the outer aqueous medium and further exposure to degradation at the storage temperatures studied. Acidic pH reduced slightly the degradation, particularly at room temperature, which can be related to higher

levels of encapsulated natamycin and to the higher packing of the phospholipids mentioned previously.

Stability of Epikuron 200 (30 mg/mL – N/L 1:12) liposomes was also investigated but precipitation occurred after one week at room temperature, as expected from the zeta-potential values close to zero.

**Table 3.3: Relative loss of natamycin (%) in loaded-liposomal formulations under different storage conditions**

| Aqueous phase | Storage conditions | After 1 week | After 2 weeks | After 5 weeks | After 10 weeks |
|---------------|--------------------|--------------|---------------|---------------|----------------|
| MQ water      | 4°C                | 2.3 ± 0.2 %  | 6.3 ± 0.2 %   | 21.2 ± 0.1 %  | 31.8 ± 0.1 %   |
|               | RT                 | 21.2 ± 1.4 % | 32.1 ± 0.1 %  | 55.3 ± 0.4 %  | 99.9 ± 0.1 %   |
|               | RT + light         | 19.6 ± 0.1 % | 36.6 ± 2.7%   | 66.3 ± 0.1 %  | 100 ± 0.1 %    |
| pH 4          | 4°C                | 1.8 ± 0.3 %  | 4.7 ± 0.1 %   | 18.3 ± 0.1 %  | 20.4 ± 0.1 %   |
|               | RT                 | 6.8 ± 0.2 %  | 13.1 ± 0.2 %  | 44.5 ± 0.1 %  | 82.1 ± 0.1 %   |
|               | RT + light         | 7.2 ± 0.1 %  | 14.9 ± 0.1%   | 56.0 ± 0.1 %  | 100 ± 0.1 %    |

### 3.4. Sterol-enriched liposomal formulations

#### 3.4.1. Effect on size and encapsulation efficiencies

To further improve entrapment of natamycin in the reference formulation Epikuron 145V (45 mg/mL – N/L 1:18) previously prepared, cholesterol and ergosterol were incorporated in the organic phase, respectively at sterol-to-lipid ratios ranging from 1:9 to 1:45 and 1:30 to 1:90. Analysis of the sizes and encapsulation efficiencies for sterol-enriched formulations are reported in Table 3.4.

Limited influence on diameter and polydispersity was observed while incorporating sterol in the lipid bilayer, as previously reported for lecithin-based liposomes prepared by solvent injection containing amounts of sterol below 20% w/w compared to the amount of phospholipids [11], which is also the case in this study (maximum 11.1 and 3.3% w/w of cholesterol and ergosterol respectively).

An apparent enhancement of encapsulation efficiencies accompanied by an increase in the loading efficiencies confirmed further incorporation of natamycin within the liposomes and can be explained by a higher partitioning of natamycin in the membrane as a result of complexation with the sterols. Comparing both additives, a predominant affinity for ergosterol was noticed, with for instance 15% more encapsulated for the same S/L ratio 1:45. These results confirm observations made by Te Welscher et al. [22] who

showed by binding studies and ITC measurements a 4-7 fold higher affinity of natamycin for ergosterol-enriched DOPC large unilamellar vesicles compared to cholesterol-enriched DOPC vesicles prepared at the same ratio S/L. Conversion of mass ratio of natamycin, ergosterol and cholesterol into molar quantities for the maximum encapsulation observed here showed that natamycin interacts with ergosterol to a ratio close to 1:1 and 1:3.5 in the case of cholesterol, confirming lower affinity for this compound. As ergosterol is present in both inner and outer part of the lipid bilayer, the ratio 1:1 indicates that natamycin is also interacting with ergosterol located in the inner leaflet of the bilayer and confirms the encapsulation within the aqueous core of the liposomes.

**Table 3.4: Effect of the presence of sterol on the size, PdI, encapsulation and loading efficiencies of natamycin in Epikuron 145V liposomes (ratio N/L 1:18)**

| Sterol      | Ratio S/L | Diameter (nm) $\pm$ SD | PdI $\pm$ SD      | EE (%) $\pm$ SD | LE (%) $\pm$ SD |
|-------------|-----------|------------------------|-------------------|-----------------|-----------------|
| None        | -         | 93.6 $\pm$ 0.6         | 0.238 $\pm$ 0.005 | 67.8 $\pm$ 0.9  | 3.8 $\pm$ 0.1   |
|             | 1:45      | 92.2 $\pm$ 0.7         | 0.241 $\pm$ 0.006 | 67.2 $\pm$ 0.2  | 4.1 $\pm$ 0.1   |
|             | 1:18      | 95.6 $\pm$ 0.3         | 0.243 $\pm$ 0.007 | 83.9 $\pm$ 0.9  | 4.9 $\pm$ 0.1   |
| Cholesterol | 1:9       | 94.1 $\pm$ 0.7         | 0.252 $\pm$ 0.007 | 96.2 $\pm$ 0.7  | 5.8 $\pm$ 0.1   |
|             | 1:90      | 93.0 $\pm$ 0.8         | 0.250 $\pm$ 0.008 | 73.4 $\pm$ 1.6  | 4.4 $\pm$ 0.1   |
|             | 1:45      | 93.3 $\pm$ 0.6         | 0.237 $\pm$ 0.005 | 82.5 $\pm$ 1.1  | 5.1 $\pm$ 0.1   |
| Ergosterol  | 1:30      | 96.3 $\pm$ 0.6         | 0.240 $\pm$ 0.006 | 90.1 $\pm$ 1.1  | 5.6 $\pm$ 0.1   |

Another explanation for the enhanced encapsulation could also be linked to the intrinsic ordering effect of sterols and reduction of the membrane fluidity during liposome preparation. Fan et al. [34] reported for instance an increase in encapsulation efficiency of the hydrophilic molecule salidroside within egg PC nano-liposomes prepared by solvent injection while incorporating cholesterol up to 25% w/w. The authors explained this variation by an increase in liposome size, allowing larger amounts of drug to be entrapped within the aqueous core, and the formation of a less permeable liposomal membrane allowing increased amount of salidroside to remain encapsulated after closure of the bilayers. Ramana et al. [35] described a similar behaviour for nevirapine-loaded egg yolk liposomes while incorporation cholesterol at a ratio 9:1 (11.1% w/w). Though no significant effect on size characteristics is visible in our case, formation of a less permeable membrane and retention of natamycin present in the core could explain higher encapsulation levels. As mentioned previously, liposomes formed in this study are indeed

presenting bilayer membranes in the liquid disordered state and incorporation of sterols would logically result in condensing effect and lower fluidity. Due to structural differences resulting in a higher molecular rigidity, ergosterol has been reported to have a greater effect on membrane ordering than cholesterol [16,36-37], which implies a more efficient reduction of membrane permeability at lower sterol concentration. Additionally, binding of natamycin with ergosterol in DOPC model membranes has been shown to not induce disturbance of the ergosterol effect nor increase permeability [22]. In the case of cholesterol on the other hand, Arima et al. [29] demonstrated that the incorporation of natamycin in cholesterol/dipalmitoylPC membranes disturbs the organization of cholesterol molecules and reduces its condensing effect. Lower intrinsic condensing effect of cholesterol and disturbance if natamycin is present could explain a higher permeability and reduced entrapment within the core of the liposomes compared to ergosterol.

### **3.4.2. Stability of sterol-enriched liposomal formulations**

Stability of natamycin in sterol-enriched liposomal formulations (CHOL/L 1:18 and ERG/L 1:45, similar EE% levels as shown in Table 3.3) was studied under different storage conditions over a period of 10 weeks and compared to sterol-free Epikuron 145V liposomes (Figure 3.7). Incorporation of sterols in the bilayer undoubtedly helps maintaining higher levels of intact natamycin upon storage, at a higher extent than modification to acidic pH. A superior effect is once again observed for ergosterol over cholesterol, whatever temperature or light conditions were used.

As both formulations present similar encapsulation efficiency, relative improvements of stability can be directly linked to the higher reduction of membrane permeability mentioned previously in the case of ergosterol, that would promote a limited leakage of preservative out of the liposomes and consequently improved stability of natamycin entrapped in the aqueous core. Specific complexation with sterol is also believed to confer higher protection towards degradation for natamycin incorporated in the bilayer.

## **3.5. Performance tests**

### **3.5.1. *In vitro* release kinetics**

*In vitro* release kinetics were studied to compare the behaviour of the pure preservative, Epikuron 145V liposomes and cholesterol- or ergosterol-enriched liposomes (Figures 3.8 a and b).

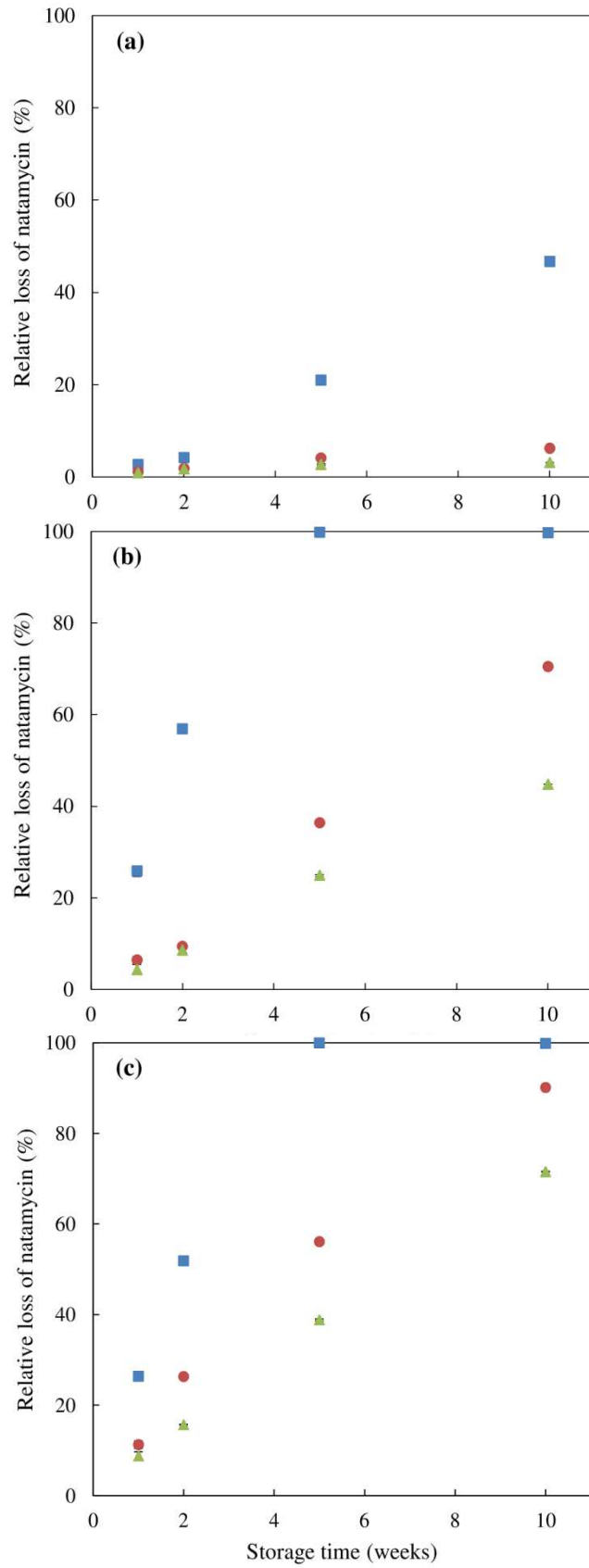


**Figure 3.7: Relative loss of natamycin in liposomal formulations under different storage conditions (a: 4°C / b: RT/ c: RT + light exposure) for sterol-free (blue squares), CHOL/L 1:18 (red dots) and ERG/L 1:45 (green triangles) liposomes**



Pure natamycin showed a slow release pattern with continuous delivery over more than 10 days, in accordance with the progressive dissolution of its crystalline form. Much faster delivery was obtained while incorporating natamycin into sterol-free liposomes with an initial burst release of 50% over the first 36 hours, followed by a slower sustained release phase up to 8 days. The initial burst may be attributed to the presence of natamycin molecules non-encapsulated, present in the outer leaflet of the bilayer or adsorbed at their surface, readily available to be released during the initial stages of the assay. The slow following phase is on the other hand related to progressive release of natamycin encapsulated within the core of the liposomes or in the inner leaflet of the bilayer, which would slowly permeate to the external medium.

Incorporation of cholesterol and ergosterol in the bilayer led to biphasic release profiles similar to sterol-free liposomes but obviously depicting, in a concentration-dependent way, a significant delay and higher levels of retention. These variations are in accordance with the limited availability of free preservative molecules in suspension linked to higher initial encapsulation efficiencies and correspond also to the reduced permeability of the membrane in presence of sterols that will consequently slow down the diffusion of entrapped natamycin towards the external medium. It has to be noticed though that maximum cumulative release of natamycin is also related to the quantity of sterol incorporated with for instance up to 30% of natamycin retained for the highest concentration of ergosterol used. This seems to indicate that the interaction with the sterols might be irreversible binding at some extent, resulting in decreased number of natamycin molecules free in water and detected during the release.

To further understand the release profiles and evaluate the effect of sterols, three major mathematical models (first-order kinetics, Higuchi kinetics and Korsmeyer-Peppas model) classically employed for nano-carriers were fitted with the release kinetics data [23]. Correlation coefficient  $R^2$  and release rate constants for liposomal suspensions and pure natamycin are reported in Table 3.4. A molecular suspension of natamycin was analysed as a control to determine the effect of the dialysis method itself. Release from this molecular suspension was found to obey a first-order kinetics ( $R^2 = 0.974$ ) with a very fast delivery rate (100% released reached after 2 days), in accordance with the progressive transport of molecular natamycin from the dialysis bag membrane towards the external medium induced by the sink conditions. Pure natamycin crystals presented a better fitting with the Higuchi model, which is representative from the drug dissolution

and diffusion out of a crystalline matrix. In the case of liposomal suspensions, the best fitting model and higher correlation coefficient values were found for the first-order kinetics similarly to molecular natamycin. Comparison of release rate constants corroborates the significant slowing down of the process while incorporating high concentrations of sterol as well as the superior effect of ergosterol. Interestingly, formulations with similar encapsulation levels (CHOL/L 1:18 and ERG/L 1:45) display also similar release rates, confirming that initial amount of free natamycin molecules and progressive permeation through the membrane are the limiting factors for release. Application of the Korsmeyer-Peppas model gave very good correlations for both natamycin crystals and liposomal suspensions and values of  $n$  comprised between 0.43 and 0.85 highlighted an anomalous non-Fickian diffusion mechanism. Release out of the crystalline form was found to be rather based on Fickian diffusion while the relatively high value of  $n$  in the case of sterol-free liposomes indicated a release mechanism based on swelling/relaxation in accordance to the high permeability and fluidity of the membrane. Increasing concentration of sterols reduced the diffusion exponent, highlighting a higher contribution of Fickian diffusion to the overall release mechanism. This confirms that the passage of natamycin molecules towards the external medium is hindered by the formation of a more rigid bilayer that acts as an efficient barrier against leakage.

**Table 3.4: Correlation of release kinetics data of natamycin from different liposomes using first-order, Higuchi and Korsmeyer-Peppas kinetic models**

| Model                 | First-order    |   | Higuchi        |      | Korsmeyer-Peppas |       |
|-----------------------|----------------|---|----------------|------|------------------|-------|
| Sample                | R <sup>2</sup> | $k$ (10 <sup>-2</sup> h <sup>-1</sup> ) | R <sup>2</sup> | $k$  | R <sup>2</sup>   | $n$   |
| Natamycin crystals    | 0.940          | 0.48                                    | 0.988          | 4.23 | 0.975            | 0.708 |
| Sterol free liposomes | 0.996          | 1.91                                    | 0.970          | 8.28 | 0.975            | 0.824 |
| CHOL/L 1:45           | 0.984          | 1.68                                    | 0.977          | 8.07 | 0.998            | 0.849 |
| CHOL/L 1:18           | 0.991          | 1.10                                    | 0.955          | 6.43 | 0.992            | 0.720 |
| ERG/L 1:90            | 0.991          | 1.36                                    | 0.959          | 7.14 | 0.992            | 0.855 |
| ERG/L 1:45            | 0.995          | 1.08                                    | 0.942          | 6.17 | 0.998            | 0.800 |
| ERG/L 1:30            | 0.989          | 0.94                                    | 0.953          | 5.80 | 0.998            | 0.745 |

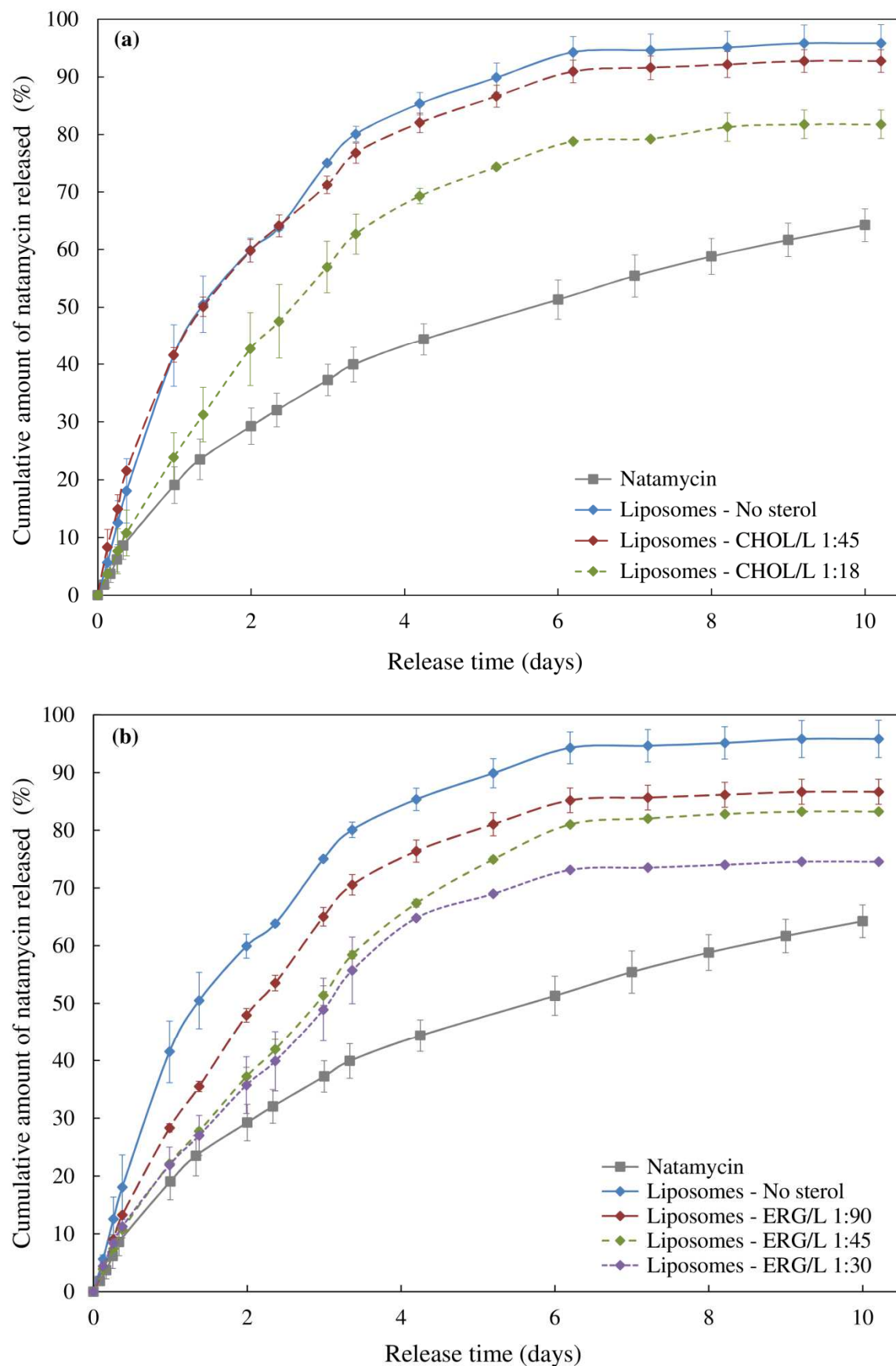
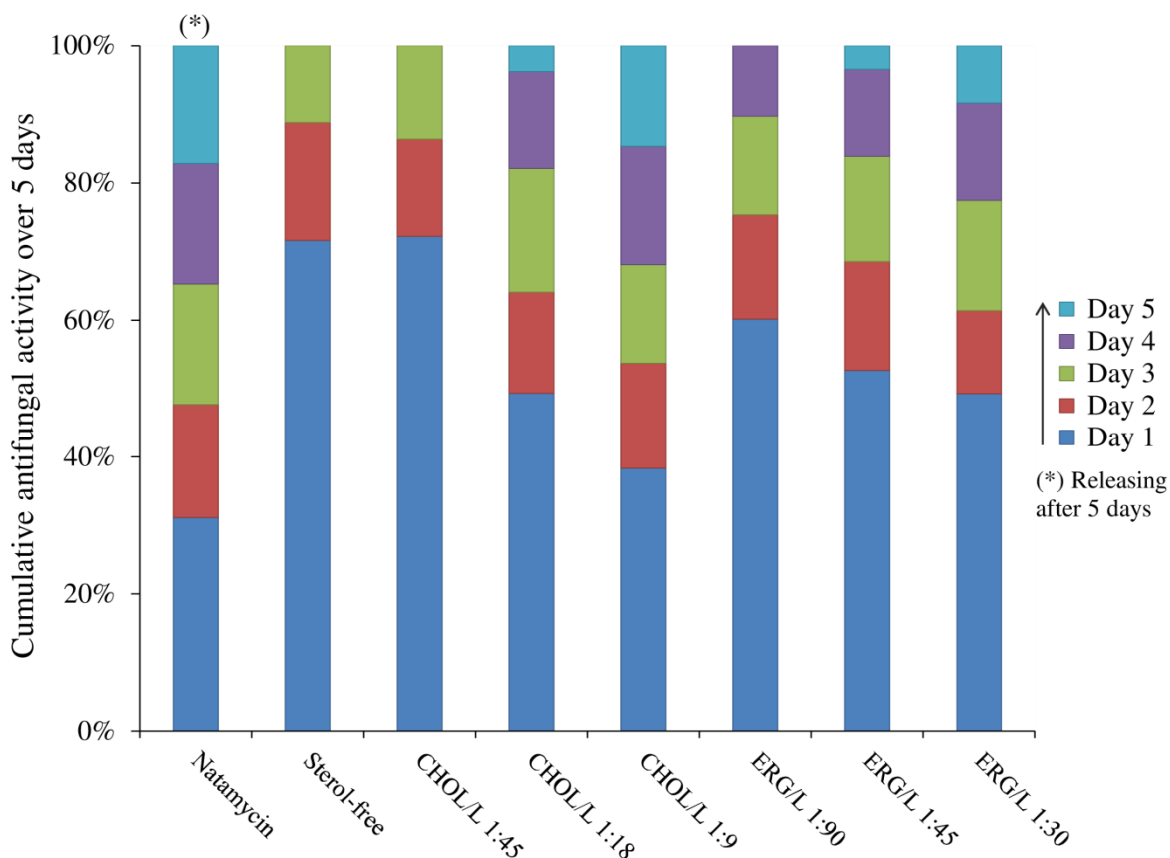


Figure 3.8: In vitro release profiles of natamycin as a function of sterol concentration incorporated in liposomal formulations (a: cholesterol-enriched / b: ergosterol-enriched)

### 3.5.2. Antifungal performance of sterol-enriched loaded liposomes

Figure 3.9 displays the cumulative antifungal activity against *Saccharomyces cerevisiae* observed over 5 days for native natamycin, sterol-free and sterol-enriched loaded liposomes. Unloaded liposomes did not present any activity against the yeast indicating no antifungal effect of soybean lecithins themselves.



**Figure 3.9: Cumulative antifungal activity observed against *Saccharomyces cerevisiae* for native natamycin, sterol-free and sterol-enriched loaded liposomes.**

Natamycin displayed a regular pattern with a similar antifungal activity provided every day over a long period of time (> 5 days). This is in accordance with the slow release kinetics from crystals evidenced in 3.5.1 and sustained release of molecular natamycin available to bind to the ergosterol present in the micro-organisms and thus to participate to the antimicrobial action.

Natamycin-loaded liposomes, with or without sterol enrichment, were characterized by an antimicrobial performance over 3 to 5 days with the major part of the activity occurring in the first 24 hours and a clear enhancement compared to crystalline natamycin. In accordance with *in vitro* release kinetics, concentration and nature of the sterol

incorporated in the bilayers had an effect on the antifungal activity, with the highest sustainability obtained for the highest concentration of sterol. As mentioned already, ratios CHOL/L 1:18 and ERG/L 1:45, which shows similar release rates, display also similar antifungal activity confirming a direct link with the availability of free natamycin molecules in suspension. It has to be mentioned that, as for the release kinetics, the initial content of natamycin is not fully detected due to irreversible binding to the sterol. In the case of ergosterol-enriched liposomes for instance, ratio 1:90, 1:45 and 1:30 led respectively to the detection of only 69%, 54% and 42% of the initial content of natamycin.

### **3.6. Conclusions**

Liposomal formulations were successfully prepared from Epikuron 145V and Epikuron 200 deoiled food-grade soybean lecithins. Nanosized liposomes were formed by the solvent injection method using methanol as a solvent and S/NS ratio of 4% v/v. Phospholipid composition and concentration in the solvent phase were found to be the most determinant parameters controlling the size and polydispersity of liposomal suspensions. SUVs were obtained with a monomodal distribution and lowest polydispersity for Epikuron 145V concentrations of 30.0-67.5 mg/mL with sizes ranging from 60 to 130 nm. Higher purity of Epikuron 200 led to 30-130 nm liposomes on the range 5.0-32.5 mg/mL. Natamycin was successfully entrapped in both lecithins liposomal formulations, without significant modification of sizes and polydispersity. Presence of charged phospholipids and reduced content of phosphatidylcholine in Epikuron 145V enabled the highest encapsulation levels of natamycin, while zeta-potential analysis showed electrostatic interactions of natamycin with the polar heads of the phospholipid indicating partial incorporation in the outer leaflet of the bilayer or adsorption at the surface of the liposomes. Maximum encapsulation was however limited and stability tests highlighted a fast degradation of the preservative over 5 weeks linked to uncontrolled leakage out of the liposomes. Modification of the aqueous phase pH showed possibility of entrapment maximization for acidic pH and slight improvement of the chemical stability due to higher packing and reduced permeability of the membrane.

Incorporation of sterols in the phospholipid mixture proved to be a valuable alternative to pH modification to maximize the entrapment of natamycin within the liposomes, with a comparable action of ergosterol observed at concentrations 2.5-fold

lower than cholesterol indicating a superior affinity towards the preservative. Presence of sterols was found beneficial for the long-term stability of natamycin in the liposomal formulations due to reduced permeability of the bilayer and protective complexation with the antifungal. Release of natamycin out of the liposomes was found to follow first-order kinetics with a significant impact of the concentration and type of sterol involved, in direct relationship with changes in membrane permeability. Higher availability of free natamycin molecules within liposomal formulations compared to its crystalline form allowed enhanced antifungal activity towards the model yeast *Saccharomyces cerevisiae*, with once again dependence towards the concentration and type of sterol involved.

Modulated release rates and enhanced antifungal activity provided by sterol-enriched liposomal formulations provide an interesting approach to overcome challenges linked to the low availability of natamycin and needs of tunability. Stability of the preservative remains however unsatisfying for long-term storage and will be further addressed in Chapters 4 and 5 of this thesis.

## Acknowledgments

The authors would like to thank Paul H.H. Bomans (Soft Matter CryoTEM Research Unit, Eindhoven University of Technology) and Camille Carcouët (DSM Ahead) for performing the cryo-TEM analyses.

## References

- [1] M.Fathi, M.R.Mozafari, M.Mohebbi, Nanoencapsulation of food ingredients using lipid based delivery systems, *Trends in Food Science & Technology*, **2012**, *23*, 13-27
- [2] M.R.Mozafari, K.Khorasvi-Daradni, G.G.Borazan, J.Cui, A.PArdakht, S.Yurdugul, Encapsulation of food ingredients using nanoliposome technology, *International Journal of Food Properties*, **2008**, *11(4)*, 833-844
- [3] A.Sharma, U.S.Sharma, Liposomes in drug delivery: progress and limitations, *Int.J.Pharm.*, **1997**, *154*, 123-140
- [4] A.Laouini, C.Jaafar-Maalej, I.Limayem-Blouza, S.sfar, C.Charcosset, H.Fessi, Preparation, characterization and applications of liposomes: state of the art, *Journal of Colloid Science and Biotechnology*, **2012**, *1*, 147-168
- [5] A.Akbarzadeh, R.Rezaei-Sadabady, S.Davaran, S.W.Joo, N.Zarghami, Y.Hanifehpour, M.Samiei, M.Kouhi, K.Nejati-Koshki, Liposome: classification, preparation and applications, *Nanoscale Research Letters*, **2013**, *8 (102)*
- [6] D.J.Hanahan, A guide to phospholipid chemistry, Oxford University Press, **1997**
- [7] G.Cevc, Phospholipids Handbook, *CRC Press*, **1993**

- [8] M.Antonietti, S.Förster, Vesicles and liposomes: a self-assembly principle beyond lipids, *Advanced Materials*, **2003**, *15*, 1323-1333
- [9] D.Lasic, The mechanism of vesicle formation, *Biochem. J.*, **1988**, *256*, 1-11
- [10] S. Batzri, E.D. Korn, Single bilayer liposomes prepared without sonication, *Biochimica et Biophysica Acta*, **1973**, *298*, 1015-1019
- [11] C. Jaafar-Maalej, R.Diab, V.Andrieu, A.Elaissari, H. Fessi, Ethanol injection method for hydrophilic and lipophilic drug-loaded liposome preparation, *Journal of Liposome Research*, **2010**, *20*, 228-243
- [12] K.Yang, J.T.Delaney, U.S.Schubert,A.Fahr, Fast high-throughput screening of temoporfin-loaded liposomal formulations prepared by ethanol injection method, *J. Liposome Res.*, **2012**, *22*,31-41
- [13] M.Grit, D.J.A.Crommelin, Chemical stability of liposomes: implications for their physical stability, *Chemistry and Physics of Lipids*, **1993**, *64*, 3-18
- [14] M.Eeeman, M.Deleu, From biological membranes to biomimetic model membranes, *Biotechnol.Agron.Soc.Environ.*, **2010**, *14*(4), 719-736
- [15] R.L.Biltonen, D.Lichtenberg, The use of differential scanning calorimetry as a tool to characterize liposome preparations, *Chemistry and Physics of Lipids*, **1993**, *64*, 129-142
- [16] T.Róg, M.Pasenkiewicz-Gierula, I.Vattulainen, M.Karttunen, Ordering effects of cholesterol and its analogues, *Biochimica et Biophysica Acta*, **2009**, *1788*, 97-121
- [17] P.F.F.Almeida, Thermodynamics of lipid interactions in complex bilayers, *Biochimica et Biophysica Acta*, **2009**, *1788*, 72-85
- [18] J.De Gier, J.G. Mandersloot, L.L.M Van Deenen, Lipid composition and permeability of liposomes, *Biochim. Biophys. Acta*, **1986**, *150*, 666-675
- [19] E.A. Disalvo, S.A. Simon, Permeability and stability of lipid bilayers, *CRC Press*, **1995**
- [20] C.Kirby, J.Clarke, G.Gregoriadis, Effect of cholesterol content of small unilamellar liposomes on their stability in vivo and in vitro, *Biochem. J.*, **1980**, *186*, 591-598
- [21] J.M.T. Hamilton-Miller, Chemistry and Biology of the Polyene Macrolide Antibiotics, *Bacteriological Reviews*, **1973**, *37*(2), 166-196
- [22] Y.M. te Welscher, H.H. ten Napel, M. Masià Balagué, C.M. Souza, H. Riezman, B. de Kruijff, E. Breukink, Natamycin blocks fungal growth by binding specifically to ergosterol without permeabilizing the membrane, *J. Biol. Chem.*, **2008**, *283*(10), 6393-6401
- [23] P.Costa, J.M. Sousa Lobo, Modeling and comparison of dissolution profiles, *Eur.J.Pharm.Sci.*, **2001**, *13*, 123-133
- [24] R.W. Korsmeyer, R.Gurny, E.Doelker, P.Buri, N.A. Peppas, Mechanisms of solute release from porous hydrophilic polymers, *Int.J.Pharm.*, **1983**, *15*, 25-35
- [25] P.L. Riger, N.A. Peppas, A simple equation for description of solute release II. Fickian and anomalous release from swellable devices, *J.Control.Rel.*, **1987**, *5*, 37-42
- [26] H. Brik, Natamycin, Analytical Profiles Drug Substances, Academic Press Inc. (London), **1981**, *10*, 513-561
- [27] A.S.Domazou, P.L.Luisi, Size distribution of spontaneously formed liposomes by the alcohol injection method, *Journal of Liposome Research*, **2002**, *12*, 205-220

- [28] M.Pons, M.Foradada, J.Estelrich, Liposomes obtained by the ethanol injection method, *International Journal of Pharmaceutics*, **1993**, 95, 51-56
- [29] A.A.Arima, F.J.Pavinatto, O.N.Oliveira Jr., E.R.P.Gonzales, The negligible effects of the antifungal natamycin on cholesterol-dipalmitoyl phosphatidylcholine monolayers may explain its low oral and topical toxicity for mammals, *Colloids and Surfaces B: Biointerfaces*, **2014**, 122, 202-208
- [30] A.D.Petelska, Z.A.Figaszewski, Effect of pH on the interfacial tension of lipid bilayer membrane, *Biophysical Journal*, **2000**, 78, 812-817
- [31] A.D.Petelska, Z.A.Figaszewski, Interfacial tension of bilayer lipid membrane formed from phosphatidylethanolamine, *Biochimica et Biophysica Acta*, **2002**, 1567, 79-86
- [32] S.D.O'Neill, A.C.Leopold, An assessment of phase transitions in soybean membranes, *Plant Physiol.*, **1982**, 70, 1405-1409
- [33] R.Koynova, M.Caffrey, Phase and phase transitions of the phosphatidylcholines, *Biochimica and Biophysica Acta*, **1998**, 1376, 91-145
- [34] M. Fan, S. Xu, S. Xia, X. Zhang, Preparation of salidroside nano-liposomes by ethanol injection method and in vitro release study, *Eur. Food Res. Technol.*, **2008**, 227, 167-174
- [35] L.N. Ramana, S. Sethuraman, U. Ranga, U.M. Krishnan, Development of a liposomal nanodelivery system for nevirapine, *J. Biomed. Sci.*, **2010**, 17, 57-66
- [36] C.Bernsdorff, R.Winter, Differential properties of the sterols cholesterol, ergosterol, b-sitosterol, trans-7-dehydrocholesterol, stigmasterol and lanosterol on DPPC bilayer order, *J.Phys.Chem.B*, **2003**, 107, 10658-10664
- [37] D.A.Mannock, R.N.A.H. Lewis, T.P.W.McMullen, R.N.McElhaney, The effect of variations in phospholipid and sterol structure on the nature of lipid-sterol interactions in lipid bilayer model membranes, *Chemistry and Physics of Lipids*, **2010**, 163, 403-448





# *Part II*

## *Post-processing of nano-encapsulation systems*



### **Chapter 4**

*Purification and concentration  
by Tangential Flow Filtration*



### **Chapter 5**

*Transformation into powders  
by lyophilization*

*To be yourself in a world that is constantly trying  
to make you something else is the greatest accomplishment.*

Ralph Waldo Emerson



# *Chapter 4*

## *Purification and concentration of nano-suspensions by tangential flow filtration*

---

In this chapter, Tangential Flow Filtration based on polysulfone hollow-fiber membranes is evaluated in concentration or diafiltration modes as a post-processing method to increase the solid particle content, to remove non-encapsulated natamycin and to improve the overall stability of the preservative upon storage in the nano-suspensions.

Application of concentration mode to PLGA nanospheres allows overcoming the low solid content obtained via the nanoprecipitation method with limited modification of size characteristics and good physical stability of the nanoparticles. Increase in solid content and reduction of aqueous volume proved to be beneficial for the chemical stability of the preservative upon storage, with losses 1.6 to 3.7-fold lower than for the original suspension. Use of continuous diafiltration mode is found efficient for removal of untrapped natamycin and unassociated polymer but results in consequent loss of polymeric nanoparticles and extremely low content of preservative left in the nano-carriers, unlikely to provide sufficient antifungal activity.

Application of concentration mode to liposomal formulations offers easier process control and reduced membrane fouling compared to PLGA nanospheres. Limited variations of size are detected but formation of multivesicular structures and rearrangements due to exposure of liposomes to shear stresses are evidenced. Removal of non-encapsulated natamycin does not translate into a better chemical stability of the preservative upon storage, with even 1.3 to 2.8-fold higher levels of loss compared to the original liposomal suspension. Incorporation of sterols allows only minor improvements of mechanical stability of the bilayer and chemical stability of the preservative. Continuous diafiltration is found successful for the removal of free preservative with reduced levels of mechanical stresses applied to the liposomes compared to the concentration mode. Benefits on chemical stability of the preservative or integrity of the liposomes themselves, with or without incorporation of sterol, are however still not clearly evidenced.

---

## **4.1. Introduction**

While development of nano-encapsulation systems is well described and characterized for a large variety of molecules, limited research integrates simultaneously the preparation of the nanoparticles and post-treatments necessary for their use in real consumer applications. Such post-preparation treatments include for instance the purification from large aggregates, unassociated carrier material, non-encapsulated active ingredient or residual solvents involved in the formulation process in order to comply with regulatory requirements or to simply improve the stability of the formulation upon storage. Another relevant aspect is the concentration of nano-suspensions that are obtained in certain cases at low solid content, hampering their use in commercial applications and leading to high costs of transport and storage.

More specifically, main challenges highlighted for natamycin-loaded nano-suspensions prepared in Chapters 2 and 3 relate to a limited chemical stability of the preservative in both PLGA and liposomal suspensions, believed to be due to the presence of untrapped natamycin or unassociated carrier material (PLGA oligomers or single phospholipids molecules). Low solid content, particularly in the case of PLGA nanoparticles prepared by nanoprecipitation, is also considered as a significant drawback and factor of chemical instability.

Various methods were proposed in the literature [1-2] to tackle simultaneously concentration and purification issues regarding nano-suspensions, such as evaporation under reduced pressure [2-3], dialysis [1,4-5], ultracentrifugation [6-7] and tangential flow filtration [8-10]. The first three options are widely used at laboratory scale and provide acceptable answers for the removal of solvent and untrapped molecules. These techniques however are known to trigger premature release of the encapsulated active ingredient or to modify nanoparticles properties (irreversible aggregation, disruption of fragile structures such as liposomes, etc...) and cannot be economically viable at larger scale.

Tangential Flow Filtration (TFF), also known as cross-flow filtration [11-13], is the most recently studied scalable technique and, in our opinion, the most promising approach to purify and concentrate both PLGA nanospheres and liposomes without loss of nanoparticle integrity or premature release of the encapsulated preservative. As illustrated in Figure 4.1, TFF is a pressure-driven filtration process consisting in circulation of a feed suspension tangentially to the surface of a porous membrane and

permeation of liquid in the transversal direction. As for classical filtration (i.e. where the feed flow is perpendicular to the membrane), deposition of particles at the surface of the filter medium or in the pores and formation of a cake layer occur and slow the filtration process via membrane fouling. Application of the cross-flow however allows a constant flush away of adsorbed particles and drastically reduce the membrane fouling phenomena which can be prohibitive while working with nanoparticles (long processing times, pressure build-up, necessity to use filtration aids, high cleaning costs, etc...). As a consequence, steady-state equilibrium is progressively reached between the forces creating deposition of solids on the membrane surface and hydrodynamic forces allowing resuspension of the solids, creating eventually a cake with a defined thickness and defined resistance to filtration. Further theoretical considerations for TFF, mechanisms of fouling and cake properties are given in section 2 of this chapter.

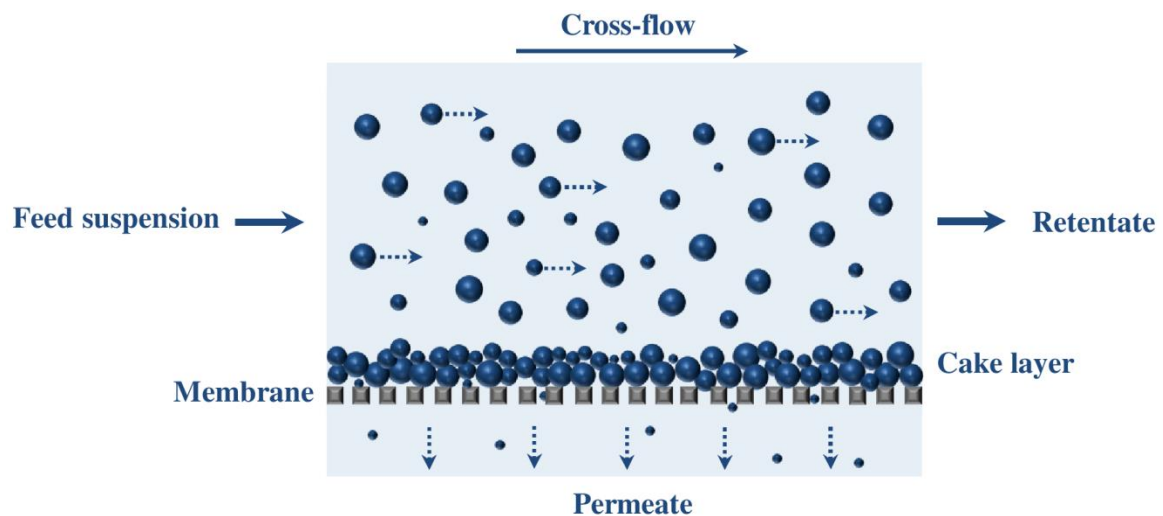
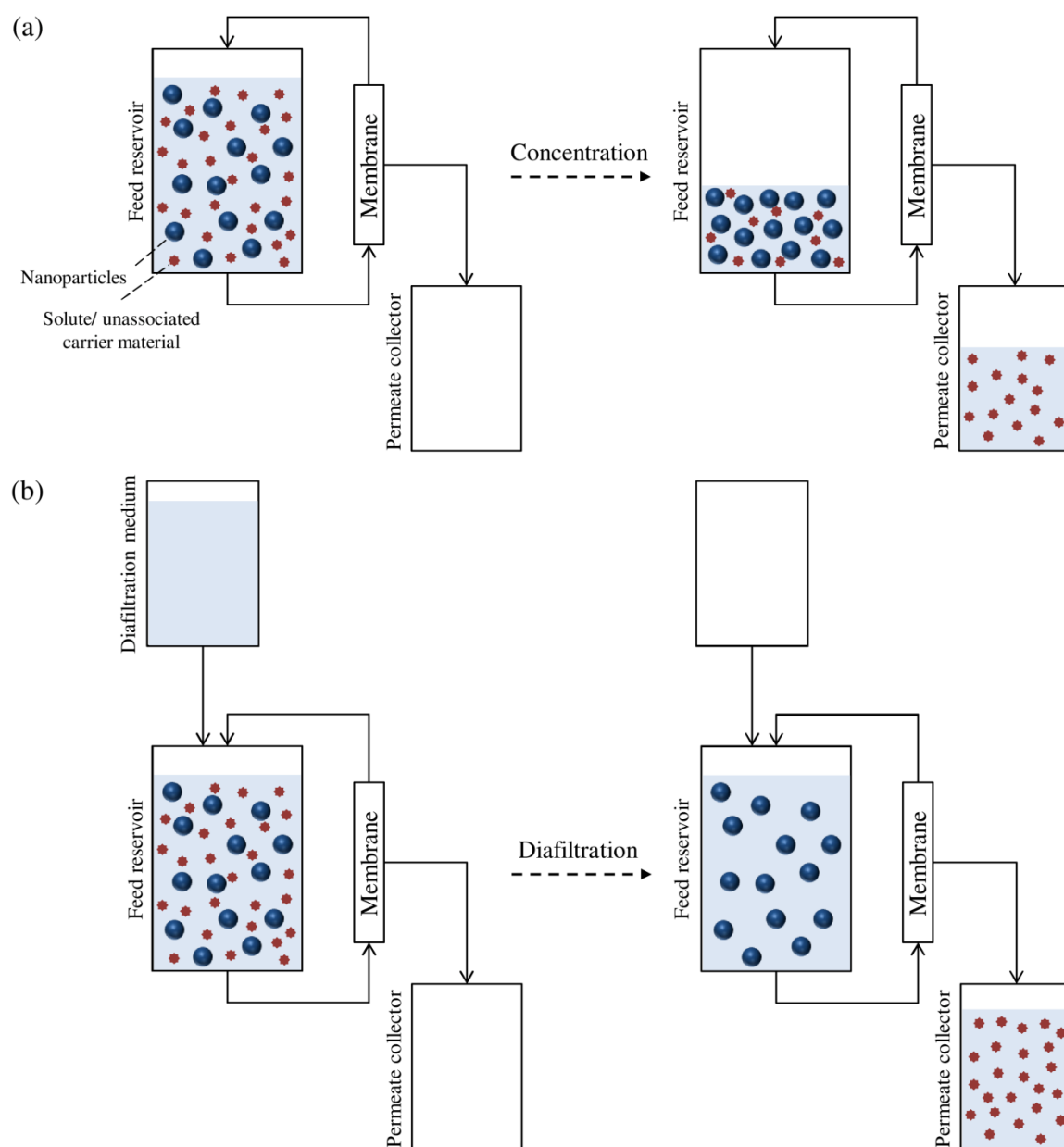


Figure 4.1: Schematic representation of tangential flow filtration for colloidal suspensions

TFF is commonly used in two modes: concentration and diafiltration [12-13]. In concentration mode (Figure 4.2a), the feed/retentate is circulated over the membrane until a certain volume of permeate has been removed and the desired concentration factor is reached. This mode allows the increase of solid content and removal of part of the unassociated compounds. In diafiltration mode (Figure 4.2b), the volume of permeate recovered is replaced by an equivalent volume of diafiltration medium (water in most cases). This mode allows the reduction of residual solvent content to acceptable levels as well as the removal of non-entrapped compounds or carrier material. Addition of fresh water can be performed in two modes: continuous diafiltration, where the diafiltration

medium is added in the feed reservoir at the same rate as the permeate to keep the feed volume constant over the whole filtration process; or discontinuous diafiltration where the sample is first diluted with the diafiltration medium and then concentrated back to the initial volume, similarly to the concentration mode. Continuous mode requires lower volumes of diafiltration medium to achieve the same level of purification. Another possibility to further reduce the diafiltration volume needed is to perform a concentration step beforehand to reduce the initial feed volume, followed by one or several diafiltration steps.



**Figure 4.2: Schematic representation of concentration (a) and diafiltration (b) modes for tangential flow filtration**

Applied to colloidal suspensions and more particularly biodegradable polymeric nanoparticles [1,8-9,14], tangential flow filtration has already proven to be an efficient tool for the removal of surfactants (classically polyvinyl alcohol) and solvents (acetone, THF, ethylacetate) with the aim to meet regulatory demands for pharmaceutical applications. Insignificant effects on size characteristics and loading efficiency of active ingredient in the nanoparticles are usually reported but influence of process parameters and cake formation is, as a general feature, not studied. Limited literature is available for TFF applied to liposomal formulations. Wagner et al. [15] reported for instance the preparation by ethanol injection of dipalmitoylPC/cholesterol liposomes entrapping proteins and the removal of unentrapped protein by TFF using a 100 kDa polysulfone membrane. Authors highlighted a limited change of size and size distribution of the liposomes over the filtration (285 to 290 nm) with appropriate removal of the protein but influence of process parameters was not described. A more in-depth study of lecithin-based liposomes concentration by cross-flow microfiltration was reported by Hwang et al. [10], with the objective of separating liposomes (around 400 nm) from unassociated phospholipids molecules. Authors reported there the influence of filtration pressure and cross-flow rate on the efficiency of the separation as well as the formation of cake layer. One specific element to keep in mind for the liposome filtration is their mechanical fragility [16] and the possibility, while applying excessive filtration pressures, of the liposomes being extruded through the membrane pores causing a significant loss of lipid materials in the permeate.

In this chapter, polysulfone hollow fibers [11-12,17-18] have been chosen as the model filtration membrane due to their extensive use in industrial processes and their established use for nanoparticle processing and diafiltration. Hollow fibers consist in a bundle of membrane fibers, allowing a large filtration area and limited shear stress generation linked to feed flow, which could be beneficial in the case of liposomes.

The objective is here to evaluate the possibility of purification and concentration of the reference natamycin-loaded PLGA nanospheres and liposomal suspensions developed in Chapters 2 and 3. More particularly, an assessment of benefits in terms of natamycin stability, solid content increase and purification as well as possible limitations for scaling-up will be performed.



Effect of various process parameters (filtration pressure, pore size (described as molecular weight cut-off MWCO), mode, continuous/discontinuous) on the final properties of the nano-suspensions (nanoparticle loss, natamycin loss, evolution of size characteristics, encapsulation efficiency, morphology and stability upon storage in terms of size and natamycin content) will be evaluated. Preliminary interpretation in terms of cake properties will also be provided.

## 4.2. Basic principles of Tangential Flow Filtration

Tangential Flow Filtration consists in the application of a feed flow parallel to a porous membrane (“cross-flow”) and permeation of liquid in the transversal direction. Particles in suspension are submitted to various external forces (Figure 4.3) that influence their deposition on the surface of the membrane (drag forces due to the tangential and permeate flows, gravity) and forces that influence their resuspension (Brownian motion, hydrodynamic lift, adhesion on the membrane, interparticular forces) [13,19-21]. Over a certain period of time, forces reach steady-state equilibrium, resulting in a stationary membrane fouling level. Equilibration of the system is reflected by a typical flux decline over time, showing a transient state followed by a plateau.

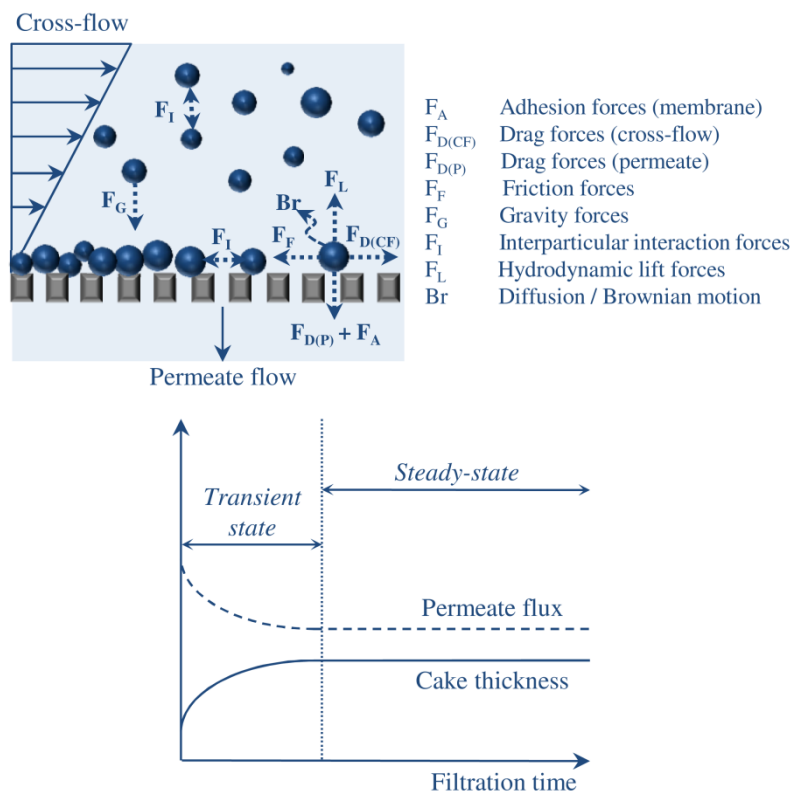


Figure 4.3: Forces and flux decline in Tangential Flow Filtration

Transient state relates directly to the membrane fouling [12,19-22] and is commonly acknowledged to occur in several steps. At the very early stages of the filtration, deposition of solutes by adsorption on the membrane is classically detected. As suspended particles approach the membrane surface and permeate starts flowing through, pore blocking and concentration polarization occur. Pore blocking can happen at complete, intermediate or standard levels depending on the size of the particles. When the particle size is larger than the membrane pore, complete blocking of the pore entrance is observed. For similar ranges of particle and pore size, intermediate blocking happens due to a mixture of complete blocking of the entrance or deposition inside the pore channels. When particles are smaller than the pores, a standard blocking occurs with a combination of deposition inside the pore channels or at the surface of the membrane, while some particles go through the permeate. Concentration polarization corresponds to the formation of a concentrated layer of particles in the vicinity of the membrane, leading to local high particle concentration compared to the bulk. As filtration proceeds further and concentration of particle is sufficiently high to allow bridging over the pores, formation of the cake layer takes place. Over time, the cake becomes multilayered and denser by further deposition and sweeping away until reaching the steady-state.

Rapidity and extent of membrane fouling depends on several parameters [20,23-24] linked to the particles (size, polydispersity, shape/deformability, concentration in suspension, affinity for the membrane), to the solutes present (concentration, molecular weight, affinity for the membrane), to the filtration parameters (filtration pressure, flow rate) and to the membrane itself (material, pore size and geometry, MWCO). In the case of ultrafiltration, membranes are characterized not by their pore size but by their MWCO, i.e. the molecular weight of a globular-shape protein that is at 90% retained by the membrane. It is common practice to select a MWCO 3-6 times smaller than the compound/particles to be retained.

Tangential Flow Filtration processes are mathematically described in terms of transmembrane pressure (TMP or  $\Delta P$ ), flux decline and resistance to filtration [19-20]. TMP describes the average pressure applied over the membrane during the filtration and is calculated as the difference of pressure measured at the feed, retentate or permeate end of the membrane (Eq.4.1). Pressure is usually not applied at the permeate end. Experimentally, the TMP is preferentially kept constant during the whole process.

$$\Delta P = \frac{1}{2} (P_{feed} + P_{retentate}) - P_{permeate} \quad (4.1)$$

Flux decline is described by the classical filtration rate equation in presence of cake (Eq.4.2) developed from the Darcy's law [13,19,22,24]. The permeate flux  $Q_p$  is linked to the filtration pressure  $\Delta P$  by considering the resistance to fluid flow through a porous medium (membrane and/or cake layer).  $V_p$  represents the permeate volume,  $t$  the filtration time,  $A$  the filtration area,  $\mu$  the viscosity of the fluid and  $R_t$  the overall filtration resistance opposed to the fluid.

$$Q_p(t) = \frac{1}{A} \frac{V_p(t)}{t} = \frac{\Delta P}{\mu R_t} \quad (4.2)$$

$R_t$  is represented by a resistance-in-series model [12,20,22] (Eq.4.3) summing the contribution of filtration resistance due to the membrane itself ( $R_m$ ), the cake formation ( $R_c$ ) and the pore blocking ( $R_p$ ).

$$R_t = R_m + R_c + R_p \quad (4.3)$$

$R_m$  corresponds to the intrinsic resistance of the membrane [25-26] and is usually determined prior to filtration (Eq.4.4) by the measurement of steady-state clean water flux  $Q_w$  at the desired filtration pressure.

$$Q_w = \frac{\Delta P}{\mu R_m} \quad (4.4)$$

$R_p$  corresponds to the contribution of the pore blocking and is usually neglected or integrated as part of the cake resistance, as it happens during the transient stage of the filtration process. Experimentally,  $R_p$  can be determined after filtration by circulating fresh water until the whole cake is swept away and measuring again the steady-state clean water flux. Difference between the initial  $R_m$  measured before filtration and the one obtained afterwards gives directly the value of  $R_p$ .

$R_c$  can be linked to specific properties of both cake and particles and is described by the equation 4.5 where  $\alpha_c$  represents the specific filtration resistance of the cake,  $m_c$  the cake mass,  $\rho_p$  the particle density,  $\varepsilon$  the porosity of the cake and  $h_c$  the cake layer thickness.

$$R_c = \alpha_c \frac{m_c}{A} = \alpha_c \rho_p (1 - \varepsilon) h_c \quad (4.5)$$

The Kozeny-Carman equation [19,27] (Eq.4.6) is the most popular model used to describe  $\alpha_c$  as a function of particle diameter  $d_p$  and cake porosity  $\varepsilon$ , provided that the particles are spherical, monodisperse and non-deformable/compressible.

$$\alpha_c = \frac{180 (1-\varepsilon)}{\rho_p d_p^2 \varepsilon^3} \quad (4.6)$$

Table 4.1 summarizes the influence of some parameters related to the filtration and the particle properties on the cake resistance and flux decline. Parameters are usually not independent from each other and final flux decline and cake resistance depend as mentioned earlier on the equilibrium achieved.

**Table 4.1: Effect of filtration parameters and particle characteristics on the flux decline and cake resistance**

| Parameter                          | Influence on flux decline and cake resistance if the parameter is increased  |
|------------------------------------|--|
| Cross-flow velocity<br>[23-24]     | Faster initial flux decline due to higher deposition rate of particles<br>Higher cross-flow drag forces<br>Higher cake porosity due to faster deposition<br>Higher shear rate (important in the case of shear-sensitive particles)   |
| TMP<br>[23-24,28]                  | Higher permeate drag flow forces<br>Faster initial flux decline due to higher deposition rate of particles<br>Higher compression of the cake<br>Increase or decrease in porosity dependent on the particle deformability   |
| Particle concentration<br>[23-24]  | Higher deposition rate, linked usually to an increase in porosity<br>Faster initial flux decline<br>Higher shear rate<br>Increased cake mass   |
| Mean diameter<br>[23-24,27-28]     | Diminution in cake resistance / final flux decline<br>Possible increase in resistance due to complete pore blocking<br>Faster deposition rate on the membrane and reduced sensitivity to resuspension  |
| Polydispersity<br>[27-28]          | Reduction of specific filtration resistance<br>Porosity increased by the presence of larger particles<br>Porosity decreased by the presence of smaller particles which can deposit in the depth of the cake  |
| Shape /deformability<br>[27]       | Increase in cake resistance if deviation from spherical shape<br>Reduction of porosity   |
| Interactions<br>[20-21, 24, 29-30] | Strong interparticular affinity <ul style="list-style-type: none"> <li>• If aggregation before deposition, faster initial flux decline and increased porosity</li> <li>• Stronger resistance to cross-flow drag forces (consequently increased cake mass)</li> <li>• Porosity reduction</li> <li>• Higher cake resistance</li> </ul><br>Strong affinity for the membrane <ul style="list-style-type: none"> <li>• Faster flux decline</li> </ul> |

### 4.3. Materials and methods

#### 4.3.1. Materials

Natamycin (90.6% purity, trihydrate crystalline form) was kindly supplied by DSM Food Specialties (Delft, The Netherlands) and used without further purification. Deoiled phosphatidylcholine-enriched soybean lecithin Epikuron 145V was supplied by Cargill (Hamburg, Germany). Cholesterol (CHOL,  $\geq 99\%$ ), ergosterol (ERG,  $\geq 95\%$ ) and PLGA polymer Resomer<sup>®</sup> RG752H (L:G ratio 75:25, MW 4-15 kDa) were purchased from Sigma-Aldrich. Methanol EMSURE<sup>®</sup> ACS and dried acetone Seccosolv<sup>®</sup> were purchased from Merck and used for the preparation of the nanosuspensions or cleaning of membranes. Potassium dihydrogen phosphate, methanol and acetonitrile Lichrosolv<sup>®</sup> were obtained from Merck and used for HPLC analyses. High quality water purified in a MilliQ system was used in all experiments.

#### 4.3.2. Preparation of nano-suspensions

PLGA nanospheres were prepared by the nanoprecipitation technique described in Chapter 2, for a concentration of PLGA of 37.5 mg/mL in acetone, 2.5 mg/mL of natamycin in methanol and a ratio acetone/methanol 2:1 v/v. 100 mL batches of nano-suspensions were obtained by 10 successive one-shot injections of 0.4 mL of organic phase in MilliQ water under moderate magnetic stirring. The resulting nanosuspension was kept overnight under slow stirring for complete evaporation of organic solvent.

Liposomal suspensions were prepared using the solvent injection technique as described in Chapter 3, for a concentration of Epikuron 145V and natamycin of respectively 45 mg/mL and 2.5 mg/mL in methanol. If necessary, cholesterol and ergosterol were also added to the organic phase at respectively 1-2.5 mg/mL (ratios CHOL/L 1:45 and 1:18) and 0.5-1 mg/mL (ratios ERG/L 1:90 and 1:45). Batches of 110 mL of liposomes were obtained by 11 successive one-shot injections of 0.4 mL of organic phase in MilliQ water under moderate magnetic stirring. The resulting suspension was kept under slow stirring overnight for complete evaporation of the methanol.

#### 4.3.3. Experimental set-up

A TFF system (Figure 4.4) was set-up manually using a 500-mL Pellicon XL Labscale reservoir (Merck Millipore, Germany) equipped with a stirbase, a valve to adjust the retentate flow and two pressure gauges to measure feed and retentate pressure. A diaphragm pump Liquipor<sup>®</sup> 1300 KT.18 RC (KNF Neuberger, Germany) was used for

the circulation of the suspension. A peristaltic pump P-1 equipped with a 1 mm diameter silicone tubing (GE Healthcare Life Sciences, UK) was used for the addition of pure water in the case of diafiltration.

Single-use MicroKros<sup>®</sup> polysulfone hollow fiber membranes (Spectrum Laboratories Inc., USA) were used for the filtration and available in two MWCO (10 kDa (~1-2.5 nm pore size) and 50 kDa (~ 4-5 nm pore size)) for an effective filtration area of 11 cm<sup>2</sup>. Before use, membranes were flushed manually with successively 30 mL of methanol and 60 mL of MilliQ water to remove any remaining traces of glycerol use for their dry storage. They were then mounted in the TFF device and flushed with 1L of pure water before starting any experiments. Membranes are incompatible with acetone and have a limited resistance to exposure to high contents of methanol.

Filtrations were performed at room temperature under a stirring speed of 100 rpm to ensure homogeneity of the feed. Time, volume of feed ( $V$ ), volume of permeate ( $V_p$ ), volume of diafiltrate ( $V_d$ ) and volumes sampled from the feed for analysis were recorded by weight measurement. Filtrations were performed at constant TMP by adjusting the retentate valve and the pump speed. TMP were fixed at 5, 7.5 and 12.5 psi (corresponding respectively to pressures of 10 /10 /15 psi on the inlet gauge ( $P_{\text{feed}}$ ) and 0/5/10 psi on the outlet gauge ( $P_{\text{retentate}}$ ). All cross-flow were laminar under the chosen conditions. Before filtration of the nano-suspension, transmembrane pressures were adjusted by recirculation of MilliQ water and measurement of clean water flux  $Q_w$  was performed to further calculate the filtration resistance of the membrane  $R_m$ .

#### **4.3.4. Concentration step**

The concentration process was performed with 100-mL feed volume of nano-suspensions. The retentate was directed back to the feed reservoir while 4-mL permeate fractions were collected in pre-weighed containers. Collection times were recorded to monitor the permeate flux  $Q_p$ . 2mL-aliquots were taken out of the feed reservoir after collection of 4 permeate fractions. Concentration was performed until the retentate volume approached the hold-up volume of the system (approximately 20-25 mL), which corresponds to a concentration factor of 1/4-1/5. Analyses performed on permeate and retentate fractions are described in part 4.3.6.

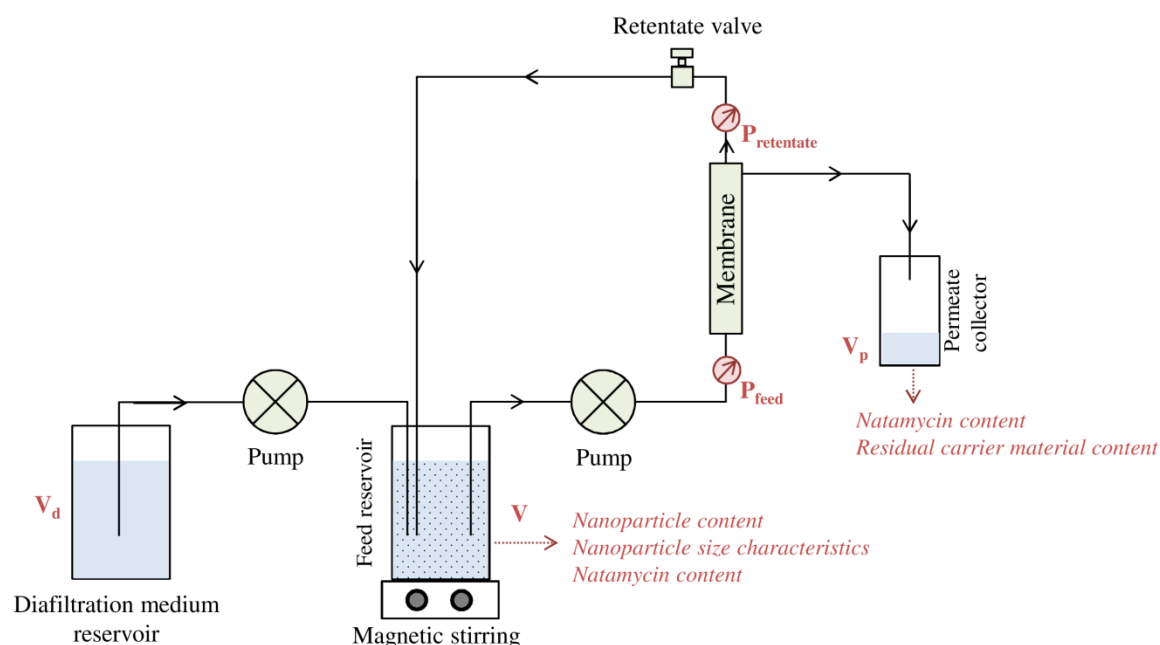


Figure 4.4: TFF experimental set-up

### 4.3.5. Diafiltration step

Discontinuous diafiltration was performed by addition of a 100-mL diafiltration volume of pure water to the feed followed by concentration of this mixture using the conditions described in 4.3.4. Permeate fractions of 14 mL were in this case collected and aliquots of 2 mL of retentate taken simultaneously. Continuous diafiltration was performed by addition of pure water at the same rate as the permeate removal, while keeping the recirculation of retentate back to the reservoir. Permeate fractions of 14 mL were in this case collected and aliquots of 2 mL of feed sample taken at the same time. Volumes of diafiltrate added were continuously recorded and adjusted to ensure balance with the permeate flow. Analyses performed on permeate and retentate fractions are described in part 4.3.6.

### 4.3.6. Fraction analyses

#### 4.3.6.1. Particle size characteristics

The mean particle diameter and size distribution width of the nanoparticles before and after filtration were determined by Dynamic Light Scattering (DLS) (Zetasizer Nano ZS, Malvern Instruments Ltd.,UK). Three consecutive measurements were performed on each suspension at 25 °C at a scattering angle of 173 °, after an equilibration time of 180 seconds. All measurements were performed in triplicate and results are presented as mean particle diameter  $\pm$  mean distribution width. Variation of size between native suspension and final retentates are presented as  $\Delta$  mean diameter /  $\Delta$  distribution width.

#### 4.3.6.2. Natamycin content

Natamycin content in native suspension, permeate and retentate fractions was determined by reverse-phase high-performance liquid chromatography (HPLC), after dilution in methanol for liposomes or acetonitrile/methanol 50:50 for PLGA nanospheres to allow disruption of the nano-carriers. A high pressure liquid chromatograph Ultimate 3000 Dionex equipped with a variable wavelength detector was used. Separation was achieved by injecting 20  $\mu\text{L}$  of sample on a reverse phase column Licrospher<sup>®</sup> RP18 (Merck, 125 nm x 4 mm, pore size 100 Å) with a mobile phase consisting of 35:65 v/v acetonitrile: potassium dihydrogenphosphate buffer (pH 3.05) at a flow rate of 1.0 mL/min. Natamycin was detected by UV at 303 nm and quantified using a calibration curve designed over the range 0.05-50 ppm ( $R^2 = 0.9996$ ). All HPLC samples were analyzed in triplicate. Final concentration factor (CF) of natamycin is calculated as the ratio of natamycin concentration in the final retentate over the initial concentration.

#### 4.3.6.3. Nanoparticle content

Nanoparticle content in retentate fractions was determined by count rate analysis measurement by DLS. For this purpose, retentate fractions were first diluted back approximately to the initial solid content. Three DLS consecutive measurements were performed as described in 4.3.6.1 with an attenuation factor set at 5. Determination of relative concentration of particles left in the retentate was performed by comparison to count rates measured with a calibration curve previously established with dilutions of the native suspension (0.05-0.9 mg/mL for both types of nano-suspensions). The final concentration factor of nanoparticles is calculated as the ratio of nanoparticle concentration in the final retentate over the initial concentration.

To determine loss of polymer or lipid materials in the permeate, a filtration was performed under the same membrane/pressure conditions with an unloaded nano-suspension and permeate fractions were analyzed by UV-Vis spectrophotometry (UNICAM UV300, ThermoSpectronic, UK) on the range 200-600 nm (bandwidth 2 nm, scan speed Intelliscan) using a 1-cm quartz cuvette. Similarly to count rate analysis, a calibration curve was pre-established based on dilutions of the native suspension (0.05-0.9 mg/mL) and absorbance at 375 nm for PLGA nanoparticles and 275 nm for liposomes.



#### 4.3.6.4. Viscosity

Viscosities of native suspension or retentate fractions were determined at room temperature using a viscometer Brookfield DVII+Pro Extra (Brookfield Engineering Laboratories Inc., USA) equipped with a ULA spindle. Analysis was performed at a spinning rate of 100 rpm with measurement of 15 consecutive points.

#### 4.3.6.5. Liposome morphology

Morphology of liposomes was investigated using cryogenic transmission electron microscopy (cryo-TEM). Vitrification of aqueous liposomal suspensions was carried out in an automated vitrification robot (FEI Vitrobot™ Mark III). A 3 µL drop was applied to a R2/2 Quantifoil Jena grid (Quantifoil Micro Tools GmbH, Germany) in the environmental chamber of the Vitrobot (25 °C, 99% humidity) and the grid was blotted with two filter papers to remove the excess liquid. Subsequently, the grid was plunged into liquid ethane which was maintained at approximately –183 °C. Cryo-TEM samples were imaged with the TU/e CryoTitan (FEI, FEG, 300 kV, Gatan Energy Filter, 2k x 2k Gatan CCD camera). Images were acquired using low dose mode, with an exposure time of 1s at a dose rate of 70 e-/Å<sup>2</sup> per second.

#### 4.3.6.6. Encapsulation efficiency in liposomes

Encapsulation efficiency (EE) of natamycin within liposomes was evaluated on the native suspension and final retentate obtained at the end of the filtration. 5 mL of liposomal suspension were transferred in Amicon Ultra-15 centrifugal filter units (10 kDa, Millipore, USA) and centrifuged for 50 min at 4500 rpm (Eppendorf centrifuge 5804C, 20 °C). Filtrate obtained by centrifugation and initial sample were collected and diluted in methanol before analysis by HPLC, as described in 4.3.6.2. EE were calculated according to Equation 4.7. EE determination was performed in duplicate and results are presented as mean ± standard deviation.

$$EE (\%) = \frac{\text{Total amount of natamycin} - \text{amount of natamycin in the filtrate}}{\text{Total amount of natamycin}} * 100 \quad (4.7)$$

#### 4.3.6.7. Stability

Stability tests were performed over 1, 5 and 10 weeks for native and concentrated formulations stored at 4 °C (no light) and room temperature RT (23 ± 2 °C) under light exposure. Evolution of the samples was followed by size analysis as described in 4.3.6.1 and determination of natamycin content evolution by the HPLC method described in 4.3.6.2.

## 4.4. Tangential Flow Filtration applied to PLGA nanospheres

### 4.4.1. Concentration of PLGA nanospheres

Concentration of PLGA nanospheres was performed as described in section 4.3.4 with the evaluation of the 50 kDa MWCO membrane under three different transmembrane pressures (5, 7.5 and 12.5 psi). Experimental observations showed that concentration could be successfully achieved in all cases though filtration pressure required significant manual adjustments over the process to be maintained constant, particularly for the highest TMP. Rinsing the membrane with water after filtration of PLGA nanoparticles flushed out aggregates of polymer, confirming that formation of a cake occurred. Final retentates showed an intensified bluish color, indicating that increase in solid content was achieved, without the formation of aggregates or natamycin crystals visible in suspension. Viscosities were not significantly modified during the process.

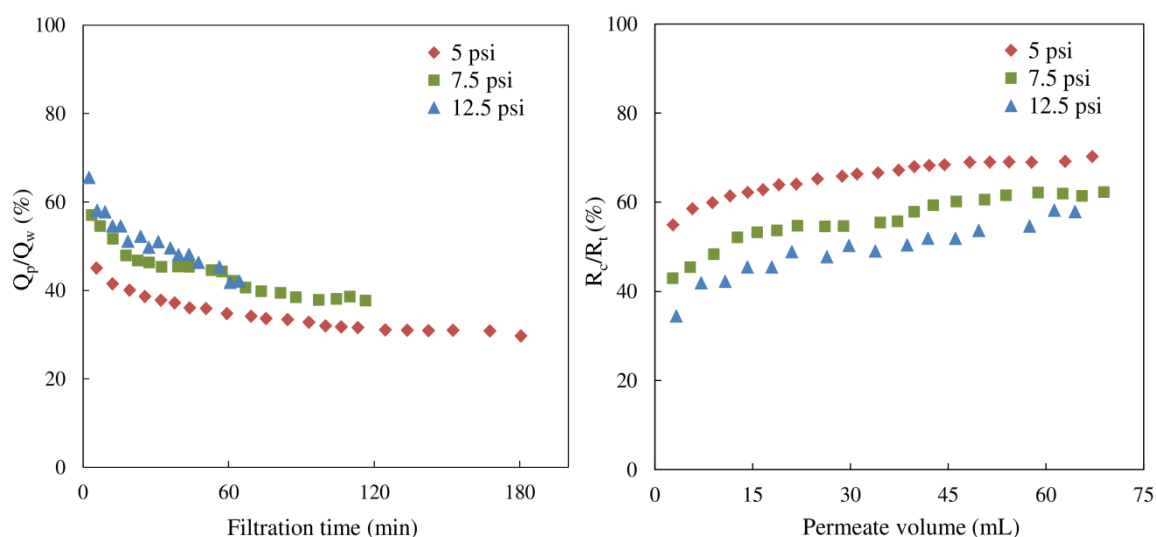
#### 4.4.1.1. Fouling and flux decline

Figure 4.5 presents the evolution of relative permeate flux over time and variation of the relative contribution of the cake to the overall resistance as a function of permeate volume.

Flux decline is observed under all conditions with an intensified effect compared to pure water for lower filtration pressures. For the two lowest filtration pressures, flux decline stabilized over time, indicating that the fouling and cake formation approached the pseudo-steady state. Flux decline keeps however occurring for the highest filtration pressure, in accordance with the pressure build-up and need for readjustment observed experimentally. These findings are in agreement with the theory of cake formation described in section 4.2, considering that for a high TMP, a fast deposition of particles and cake building is expected but is counteracted by a fast sweeping-away of the particles by the cross-flow. As a result, equilibration to steady-state can require longer filtration times.

Analysis of the relative cake contribution to the overall filtration resistance confirms an influence of the transmembrane pressure in accordance with the flux decline. Higher contributions are observed for 5 psi with around 69% of the total filtration resistance due to the fouling of PLGA nanoparticles on the membrane, while 62% are reached for 7.5 psi. Absence of steady-state for 12.5 psi is confirmed by the constant increase of resistance

over time, with a contribution inferior to 7.5 psi. According to Equation 4.5, decrease in filtration resistance can hypothetically be linked to a decrease in cake thickness or specific cake resistance, itself linked to an increase in porosity. Deposition of PLGA nanoparticles on the membrane was confirmed by determination of particle concentration in the feed via count rate measurement (Figure 4.6). A final relative loss of polymeric material of approximately respectively 18.6%, 37.0% and 22.2% was observed for filtration pressures of 5, 7.5 and 12.5 psi. The limited loss of polymer for the lowest TMP pressure, combined with the relatively high contribution of the cake to the filtration resistance, indicates that, rather than a thicker layer deposited, the cake is more compact and less porous than for 7.5 psi. The limited loss for 12.5 psi is in accordance with the idea that the cake formation is disturbed by the cross-flow forces and that particles get resuspended continuously. In this case, cake thickness is thus reduced. Porosity is also expected to be higher due to higher deposition rates that do not let time to the particles to arrange themselves in preferential positions. Calculation of concentration factors reveals respectively 2.84, 2.52 and 2.60-fold higher nanoparticle concentration for the filtration pressures of 5, 7.5 and 12.5 psi, indicating that under any conditions an increase in solid content in suspension can be achieved.



**Figure 4.5: Relative permeate flux decline (left) and cake resistance variation (right) during concentration of PLGA nanospheres by TFF under various transmembrane pressures**

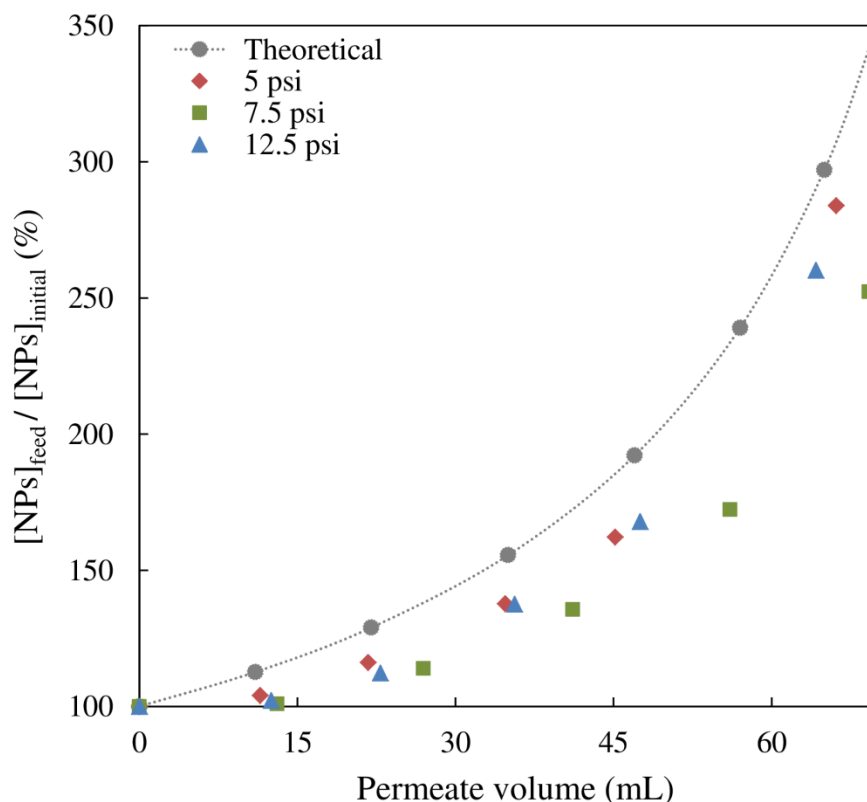


**Figure 4.6: Relative concentration of PLGA nanoparticles in the feed as a function of permeate volume during concentration by TFF under various transmembrane pressures**

DLS analyses did not allow the detection of nanoparticles in permeate fractions, either due to their absence in the permeate or from their low concentration in suspension, making them undetectable by dynamic light scattering. The same observation can be made for UV scans of the permeate fractions that did not allow detection of PLGA in the calibration range pre-established, indicating negligible amounts lost in permeate.

Analyses of retentate fractions showed limited variations of mean diameter and distribution width over the filtration process (Table 4.2). The slight increase in mean diameter for 5 and 12.5 psi indicates a preferential loss of the smallest nanoparticles during the filtration, either by loss to the permeate or by stronger adsorption on the membrane/cake. The slight increase in size distribution for 12.5 psi highlights the presence of aggregates that might be formed during the process of constant fouling/defouling mentioned. Upon storage, mean diameter and size distribution returned to their original value indicating separation of the aggregates formed during the fouling. No significant destabilization of the nano-suspensions was overall visible compared to the native suspensions.

**Table 4.2: Evolution of mean diameter (nm) and size distribution width (nm) of PLGA nanoparticles upon concentration by TFF and storage at 4°C (14 days)**

| TMP (psi) | Concentration step |                 | Upon storage      |                 |
|-----------|--------------------|-----------------|-------------------|-----------------|
|           | Native suspension  | Final retentate | Native suspension | Final retentate |
| 5         | 81.7 ± 31.0        | 84.0 ± 31.6     | 79.7 ± 29.1       | 79.8 ± 29.6     |
| 7.5       | 81.1 ± 28.8        | 79.5 ± 29.0     | 76.6 ± 27.3       | 78.0 ± 28.6     |
| 12.5      | 80.2 ± 30.6        | 83.6 ± 37.0     | 77.0 ± 31.2       | 78.7 ± 28.9     |

#### 4.4.1.2. Removal and stability of natamycin

Figure 4.7 presents the relative variation of concentration of natamycin in permeate and retentate fractions as a function of filtration time. The decline of natamycin content during the filtration as calculated from permeate analysis presents a linear variation proportionally to the permeate volume, which is consistent with mass balance predictions (Appendix A). The decline of natamycin content as calculated from retentate fractions analysis showed a large deviation from linear behavior due to additional loss of natamycin via either adsorption on the membrane and deposition of nanoparticles encapsulating a part of the preservative, as described in Equation 4.14 (Appendix A). The deviation is particularly intense at the early stages with around 10-12% removed before sampling of the first retentate fraction. The final deviations indicate respectively 1, 5.2 and 3.5% of additional loss due to absorption of nanoparticles and/or natamycin on the membrane for 5, 7.5 and 12.5 psi. These results are in accordance with the relative loss of polymeric materials mentioned previously. The absorption of free natamycin could also have an influence as the recirculation of a natamycin-saturated solution performed for 7.5 psi showed for instance an average loss of 11% after 1 hour. This contribution is however likely to be limited compared to cake formation.

Calculation of concentration factors for natamycin gave for 5, 7.5 and 12.5 psi respectively 1.06, 0.99 and 1.22. This indicates that the enrichment of natamycin via the concentration process is rather limited, as expected from limited initial encapsulation efficiency of natamycin and loss of nanoparticles in cake.

Comparison of stability between the native suspension and the three final retentates obtained at different TMP (Figure 4.8) showed however a clear benefit of filtration upon storage at 4°C. Enhancement of stability is remarkably improved for 5 psi with a 3.7-fold loss reduction after 10 weeks, which could be linked to the limited loss of polymeric nanoparticles and gentler processing mentioned earlier.

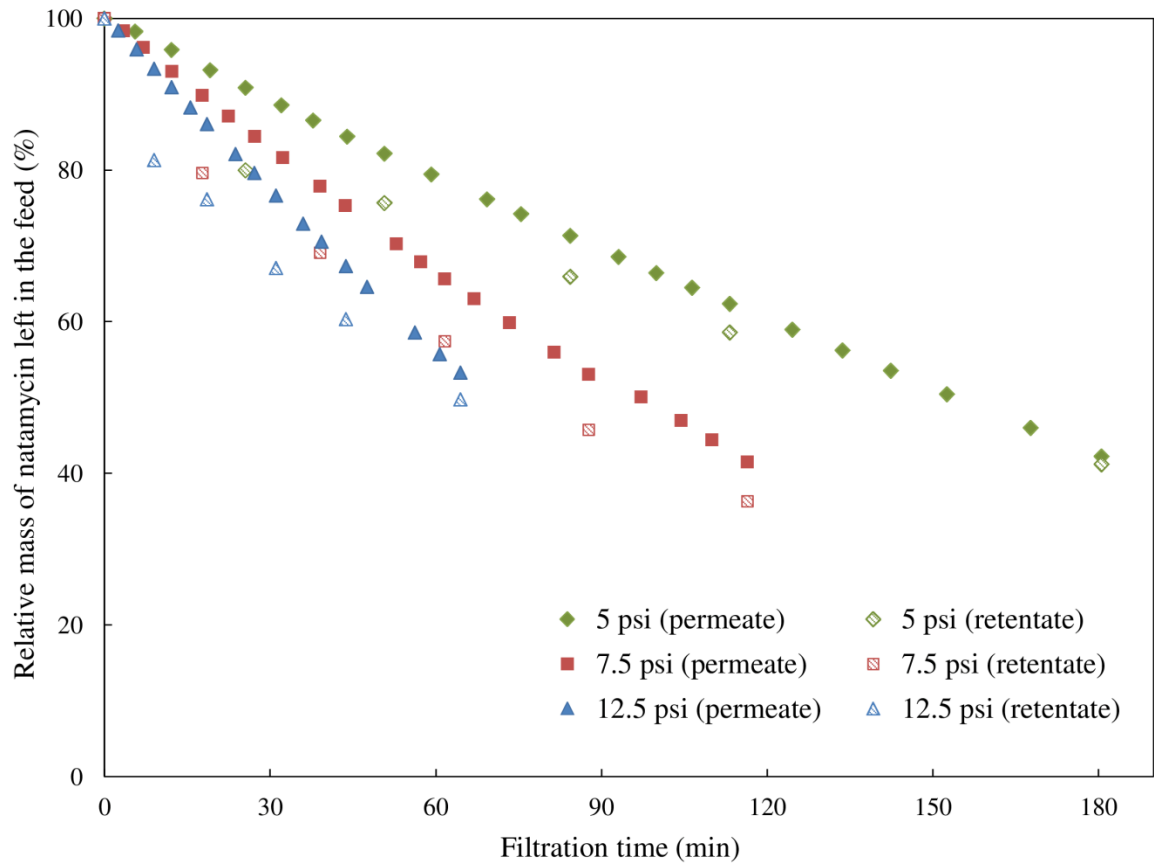


Figure 4.7: Cumulative mass of natamycin left in the feed as calculated from permeate (filled symbols) and retentate (striped symbols) analysis during TFF under various transmembrane pressures

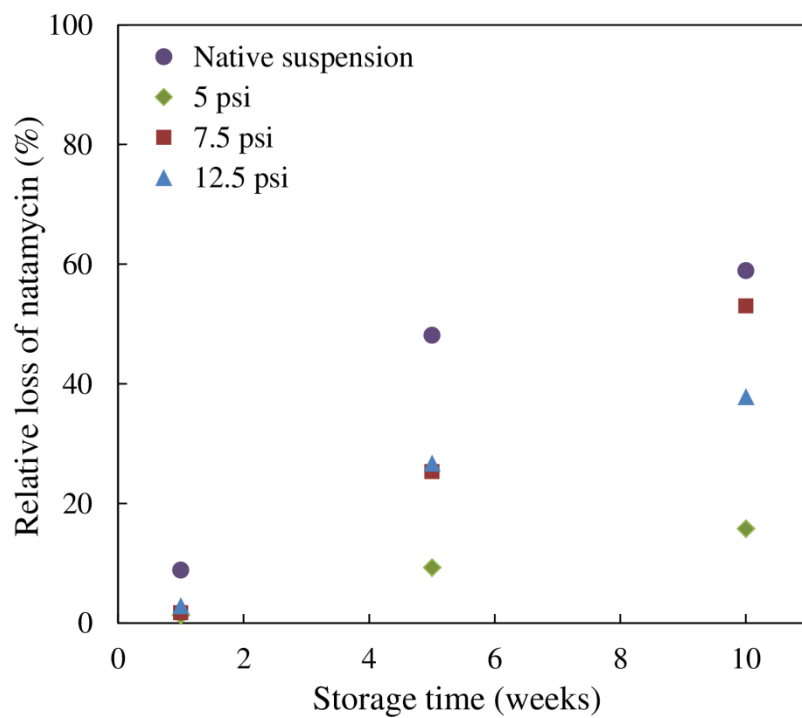
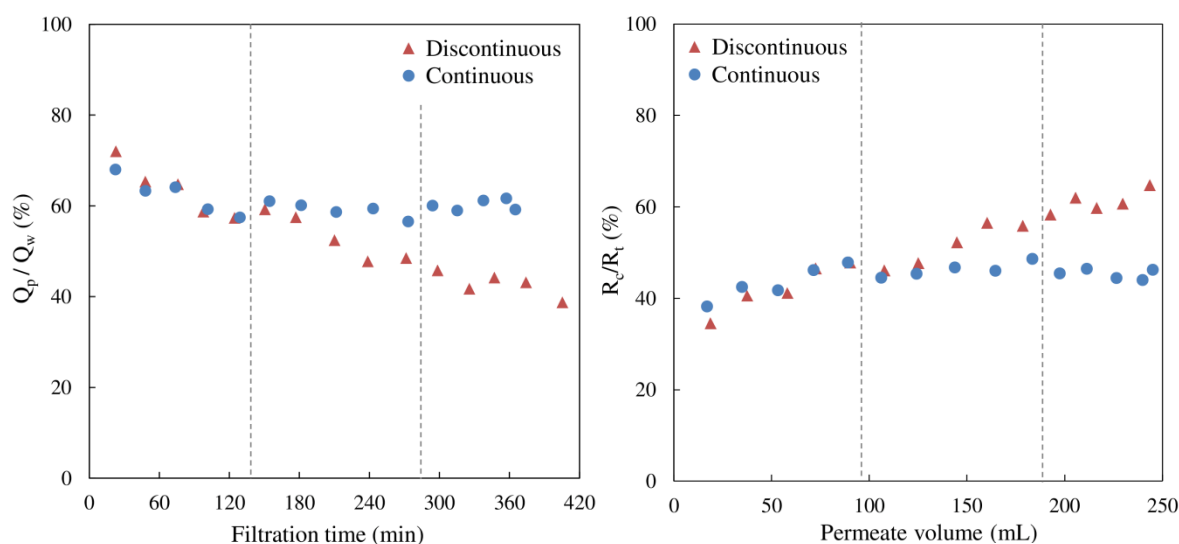


Figure 4.8: Relative loss of natamycin upon storage at 4°C for native suspension and TFF-processed retentates

#### 4.4.2. Diafiltration of PLGA nanospheres

Further removal of non-entrapped natamycin was attempted using discontinuous and continuous diafiltration modes as described in section 4.3.5. In both cases, two diafiltration steps were performed (100 mL diafiltrate volumes) followed by concentration. Steps are represented by dashed lines in the following graphs. TMP was fixed at 7.5 psi to allow processing of the various steps on the same day.

Figure 4.9 displays the evolution of relative permeate fluxes over time and relative resistance due to the cake during the diafiltration in discontinuous and continuous mode.



**Figure 4.9: Relative permeate flux and cake resistance variations during diafiltration of PLGA nanoparticles in discontinuous (red triangles) and continuous (blue dots) modes**

Both modes presented similar resistance and flux decline during the first step, indicating fouling of the membrane and cake formation as previously observed. For further steps however, flux kept declining in the case of discontinuous mode without reaching a steady-state, even after the final concentration step. The slow fouling is likely to be related to the very low initial solid content in the feed (half of the initial concentration due to the addition of 100-mL diafiltrate volume) and consequently to a low deposition rate of particles at the surface of the membrane. On the contrary, continuous diafiltration allowed stabilization and steady-state, with a final 45% of cake contribution to filtration resistance.

Fouling evolution was confirmed by the variation of PLGA concentration evaluated by count rate analysis as illustrated in Figure 4.10. Discontinuous mode showed a limited loss of polymer during the diafiltration steps (respectively 8.3% and 18.0% of cumulative loss at the end of each step) confirming slow cake formation. Fouling was more intense

during the concentration step with a final loss of 32.8%. Comparatively, loss of polymeric material was significant for the first continuous diafiltration step (around 22.8%) in accordance with the rapid flux decline and cake formation. Achievement of steady-state led to limited additional loss during the two latter steps of the process (respectively 34.5% and 45.7% cumulative loss). Opposite variation of cake resistance and relative loss of nanoparticles during the first step of diafiltration clearly indicates a much reduced porosity in the case of discontinuous mode. This is consistent with the slower cake formation and larger amount of time available for a specific arrangement of the particles towards each other in a more compact layer.

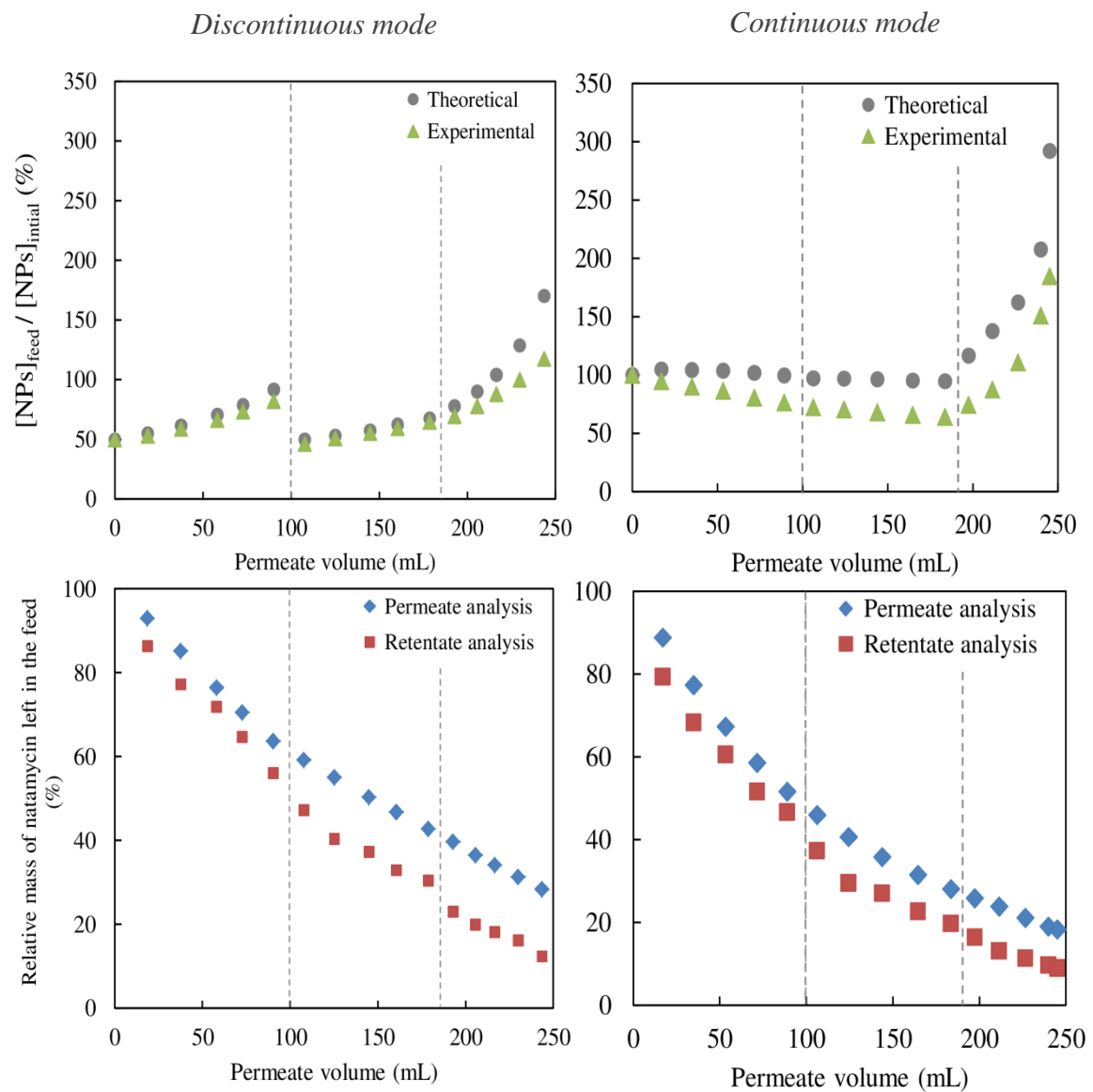


**Figure 4.10: Relative concentration of PLGA nanoparticles and natamycin in the feed during diafiltration as determined by permeate and retentate analyses in discontinuous (left) and continuous (right) mode**



Figure 4.10 also highlighted an overall faster loss of natamycin in permeate in the case of continuous diafiltration mode with an approximate additional 12% removed at each step of the process compared to discontinuous mode. Variation for each mode is in accordance with the mass balance described in Appendix B that predicts a linear decline in the case of discontinuous mode, while continuous mode leads to an exponential decrease. The evolution of natamycin concentrations measured in retentate and permeate fractions exhibited, as previously observed for the concentration step, a deviation between the two values due to absorption of natamycin and PLGA nanoparticles. The deviation was clearly higher for the discontinuous mode with respectively 7.6, 12.2 and 16.0% adsorbed for each step, compared to 5.0, 8.4 and 9.3% for the continuous mode. The main explanation for this higher absorption level and the fact that the absorption keeps increasing significantly during the process can once again be linked with the flux decline observation and the limited cake formation during the first steps of discontinuous filtration that allowed higher absorption of free natamycin molecules compared to a surface already pre-covered with nanoparticles.

**Table 4.3: Overall performance of TFF diafiltration modes applied to PLGA nanospheres and effect on stability**

|   | Discontinuous mode                          | Continuous mode                             |
|---|---|---|
| Processing time (h)   | 6.8   | 6.1   |
| Total loss of PLGA (%)  | 32.8 ± 0.1                                  | 45.7 ± 0.1                                  |
| Mean diameter ± distribution width (nm)                                 | 81.1 ± 29.9 (native)<br>75.5 ± 28.9 (final) | 79.4 ± 29.5 (native)<br>73.3 ± 30.2 (final) |
| Mean diameter ± distribution width (nm) after<br>14 days storage at 4°C | 77.7 ± 26.8 (native)<br>75.5 ± 27.3 (final) | 76.5 ± 27.3 (native)<br>72.0 ± 25.8 (final) |
| Total loss of natamycin (%)   | 87.7 ± 0.1                                  | 91.1 ± 0.1                                  |
| Total loss of natamycin on the membrane (%)                             | 16.0 ± 0.1                                  | 9.3 ± 0.1                                   |
| Concentration factor  | 0.25  | 0.24  |
| Relative loss upon storage at 4°C (%)                                   | 72.7 ± 0.2 (1 week)<br>78.1 ± 0.1 (5 weeks) | 68.0 ± 0.2 (1 week)<br>77.5 ± 0.1 (5 weeks) |

The overall performance of both diafiltration modes is summarized in Table 4.3. Additionally to previous considerations regarding relative loss and absorption of both PLGA and natamycin, it is worth mentioning that both modes led to a reduction of mean diameter, though size distribution remained in the same range. Final retentate particles were however remarkably more stable in size upon storage than what was observed in the

concentration step, which goes in the sense of a removal of unassociated oligomers that could catalyze the degradation. In both cases however, stability of the remaining natamycin was not improved and even further degraded. Concentration factors far below 1 indicated consequent removal of natamycin via the diafiltration process which led to concentrations below the solubility limits and subsequently to enhanced degradation.

#### **4.4.3. Conclusions for PLGA nano-suspensions**

Tangential Flow Filtration and hollow fibers can be used to concentrate natamycin-PLGA nano-suspensions at lab scale. Low filtration rates induced by low transmembrane pressure offer the best possibility for stable cake formation and reduced losses of polymeric nanoparticles by fouling. This however also implies longer filtration times that might not necessarily be relevant for large scale applications. As desired, increase in solid content in suspensions is achieved with limited modification of size characteristics and stability of the nanospheres. Though obtained nanosuspensions are not significantly enriched in natamycin, reduced levels of chemical instability upon storage are observed and bring a benefit to the formulation.

Evaluation of continuous and discontinuous diafiltration for further removal of untrapped natamycin demonstrated a superiority of continuous mode in terms of processing times and controlled fluxes that could facilitate implementation at large scale. Fouling and loss of polymeric material are however consequent in both cases for the hollow-fibers membranes studied here, though a clear benefit for nanoparticle stability is observed due to reduction in unassociated polymer left in suspension. Removal of untrapped natamycin is also achieved via diafiltration leading to extremely low concentrations of preservative in the formulation and consequently to enhanced degradation upon storage, which is not beneficial for the formulation.

## 4.5. Tangential Flow Filtration applied to liposomal suspensions

### 4.5.1. Concentration of liposomes

#### 4.5.1.1. Influence of TMP and MWCO

Concentration of sterol-free natamycin-loaded liposomal suspensions was performed as described in section 3.4 with the evaluation of two MWCO (10 and 50 kDa) combined with three transmembrane pressures (5, 7.5 and 12.5 psi). Experimental observations showed that concentration could be successfully achieved in all cases. Final retentates presented an intensified yellowish aspect compared to the native suspension and formation of natamycin crystals was not visible though final concentration in suspension (140-180 ppm) is far above the solubility limit (20-50 ppm). In terms of processing, sharp declines in permeate flux were observed in the first few minutes of the filtration, after which TMP and permeate flux stayed stable without necessity of pressure adjustment.

Figure 4.11 presents the time courses of relative permeate flux as a function of various MWCO and TMP combinations as well as corresponding variation of cake resistance in relationship with the permeate volume. Filtration pressure did not have a significant impact for the 10 kDa membrane, which shows similar time to steady-state and only slight modification of cake resistance (respectively 59.3% and 60.5% for 7.5 and 12.5 psi). Comparison between various TMP for the 50 kDa membrane on the other hand highlighted a clear effect of the filtration pressure on the time required to reach steady-state and on the cake resistance (respectively 53.4%, 49.2% and 45.9% for 5, 7.5 and 12.5 psi). As a general feature, longer processing times seem to lead to higher cake resistance which might be explained by either a higher mass of cake or the formation of a more compact cake due to slower deposition rates. As displayed in Table 4.4, lipid losses calculated from count rate analyses of the feed indicate higher levels of phospholipid removal with higher TMP and intensified or similar effect while considering the same TMP for higher MWCO. Direct relationship between the lipid loss, the TMP and the cake resistance obtained in Figure 4.11 is however not straightforward. Comparing for instance 10 and 50 kDa at 12.5 psi for which similar lipid losses are observed but cake resistance is clearly different, possible hypotheses could be: 1) a loss of phospholipids preferentially from the feed to the permeate instead of deposition on the cake which would lead to reduced cake resistance for the same total lipid loss; or 2) a higher cake mass deposited coupled with higher levels of porosity while working with the higher MWCO which would also lead to reduced cake resistance.

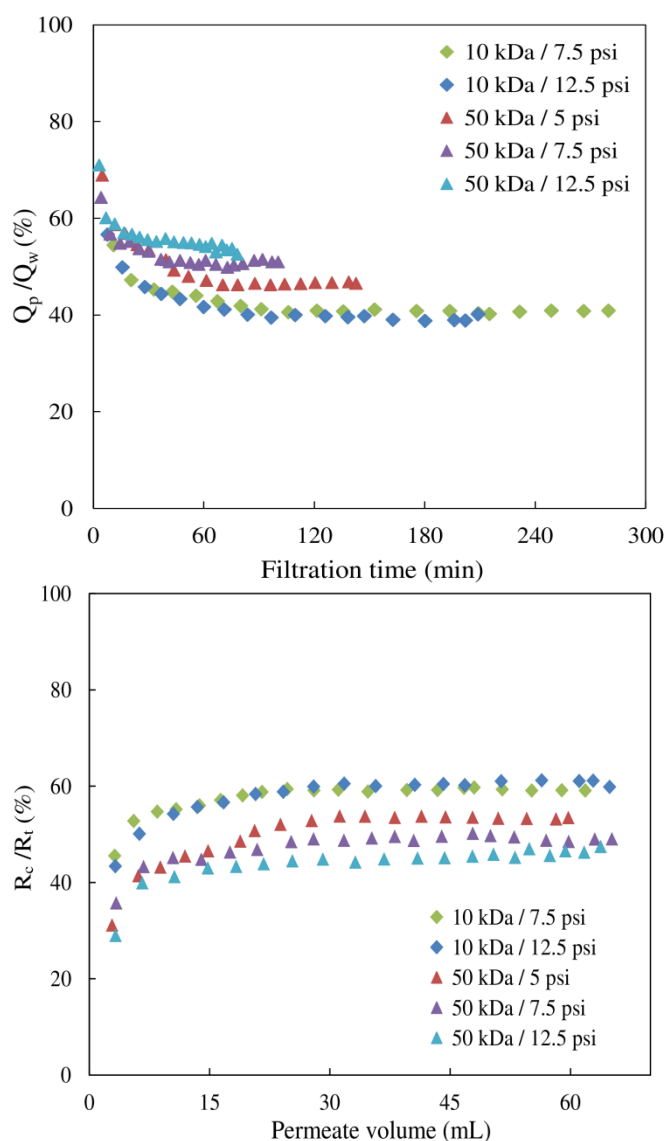


**Figure 4.11: Relative permeate flux decline and cake contribution to overall filtration resistance during sterol-free liposomes filtration as a function of MWCO and TMP**

**Table 4.4: Influence of TMP and MWCO parameters on lipid and natamycin losses, size characteristics and encapsulation in sterol-free loaded-liposomes**

| MWCO (kDa) | TMP (psi) | Lipid loss (%) | $\Delta$ mean diameter / $\Delta$ distribution (nm) | Natamycin loss (permeate analysis) (%) | Natamycin loss (retentate analysis) (%) | $CF_{\text{natamycin}}$ (-) | $\Delta$ EE (%) |
|------------|-----------|----------------|---|--|---|-----------------------------|-----------------|
| 10         | 7.5       | 24.9 ± 0.2     | 2.9 / 2.1   | 28.9 ± 0.1                             | 32.7 ± 1.5                              | 1.74 ± 0.02                 | 14.0 ± 0.7      |
|            | 12.5      | 33.2 ± 0.8     | 1.8 / 0.3   | 30.4 ± 0.1                             | 42.7 ± 0.8                              | 1.63 ± 0.06                 | 13.2 ± 1.4      |
| 50         | 5         | 26.7 ± 0.8     | 2.6 / 1.1   | 31.0 ± 0.4                             | 31.9 ± 0.8                              | 1.73 ± 0.04                 | 12.8 ± 1.8      |
|            | 7.5       | 34.6 ± 1.2     | 3.7 / 1.5   | 30.7 ± 0.1                             | 38.6 ± 2.0                              | 1.79 ± 0.09                 | 15.0 ± 0.8      |
|            | 12.5      | 33.3 ± 0.8     | 4.3 / 2.9   | 30.5 ± 0.1                             | 41.9 ± 0.7                              | 1.65 ± 0.01                 | 16.4 ± 1.6      |

To validate the first hypothesis, unloaded liposomal suspensions were processed under the same TMP/MWCO conditions as natamycin-loaded liposomes and permeate fractions were analyzed by UV to determine amounts of phospholipid lost. Variation of free phospholipid concentration in the permeate fractions showed a linear increase as a function of permeate volume collected, indicating that, after steady-state is achieved, phospholipid removal keeps occurring by direct transfer of monomers to the permeate. Rate of lipid removal was found dependent on the TMP/MWCO, with final cumulative loss in permeate as disclosed below:

- ✓ 10 kDa: 5.4% for 7.5 psi; 8.0% for 12.5 psi
- ✓ 50 kDa: 5.5% for 5 psi; 3.1% for 7.5 psi; 3.7% for 12.5 psi

Lipid losses in permeate were less important for the 50 kDa membrane comparatively to 10 kDa for the same filtration pressure. Combined with the higher or similar total lipid losses for the highest MWCO, these results tend to indicate that 50 kDa lead to higher cake masses deposited, which would go rather in the direction of the second hypothesis. Higher mass of cake deposited in the case of 50 kDa can explain the higher retention of phospholipid monomers as free phospholipids are likely to remain trapped in the cake or to be flushed away back to the feed instead of being transported to the permeate [10]. Comparing the various TMP for 50 kDa and taking into account the relative losses to permeate, it is possible to conclude that a higher mass of cake is deposited onto the membrane with a higher porosity while raising the filtration pressure. Similarly, for 10 kDa, increase of TMP leads to higher mass of cake but similar resistance which corroborates again the idea of higher porosity for 12.5 psi.

Mean diameter and size distribution of the liposomes rose during the filtration process with a pronounced effect for the 50 kDa membrane and higher TMP. Observation of size characteristics during the filtration indicated an initial shrinkage of mean diameter that slowly re-equilibrated to values larger than the initial size after collection of the second retentate fraction. The preservation of liposomal morphology was confirmed by cryo-TEM analysis of the final retentate fraction (Figure 4.12) for the MWCO 50 kDa and TMP 7.5 psi. Compared to the native suspension, presence of larger vesicles and multilamellar arrangement is however visible, pointing out that some rearrangements and fusion of liposomes occurred during the TFF process as a result of shear stresses and loss of phospholipids molecules.

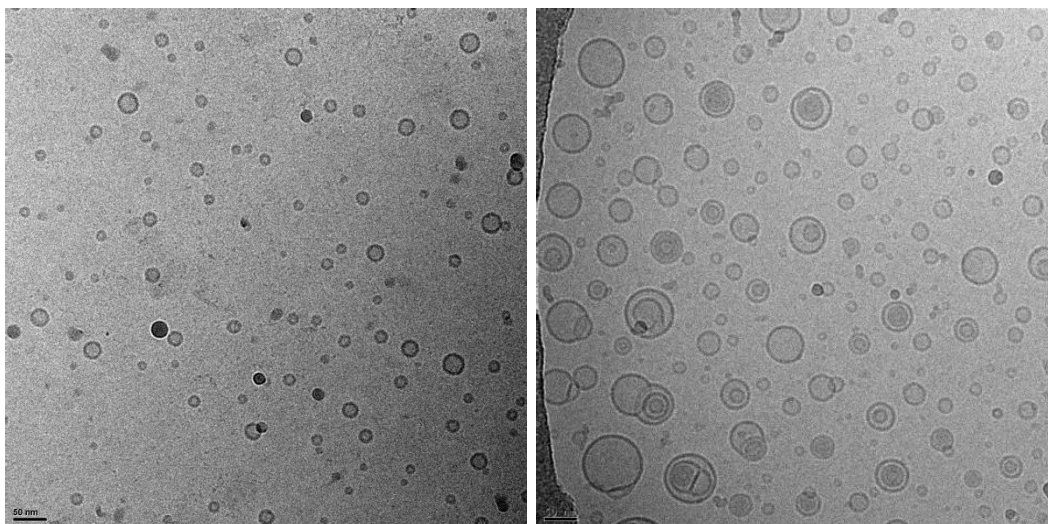


**Figure 4.12: Cryo-TEM micrograph of the native liposomal suspension (left) and final retentate (right) obtained after concentration by TFF (scale bar - 50 nm)**

Final losses of natamycin in permeate (Table 4.4) were found to be comparable for all MWCO/TMP conditions and rate of removal showed the expected linear dependence to the permeate volume collected (Appendix A), suggesting that rearrangement of the liposomes and loss of phospholipid monomers did not lead to a more important leakage of natamycin. Comparison of permeate and retentate fractions indicated increased removal of natamycin by adsorption on the membrane while increasing the TMP for both MWCO membranes. This deviation is consistent with the deposition of loaded liposomes in the cake layer, which as previously mentioned also increased with higher transmembrane pressure. Variations of encapsulation levels averaging 13-16% and concentration factors superior to 1 confirmed preferential removal of non-entrapped natamycin and efficiency of the TFF process to reach higher concentrations of preservative in suspension.

Stability of natamycin in the liposomal suspension was nonetheless negatively and considerably impacted by the concentration process for both storage at 4 °C without light and room temperature upon light exposure (Figure 4.13). A direct effect of both MWCO and filtration pressure was visible, with a significant benefit for the combination 50 kDa/12.5 psi. Preferred explanation for this phenomena is the lowest processing time required for the concentration that avoided extensive recirculation of the permeate and longer exposure times to shear forces, detrimental to the fragility and permeability of the lipid bilayer. Lowest relative variation of size and size distribution for 50 kDa/12.5 psi compared to other combinations after 5 weeks storage at 4 °C corroborated this idea of reduced impact on the liposomes while limiting processing times.

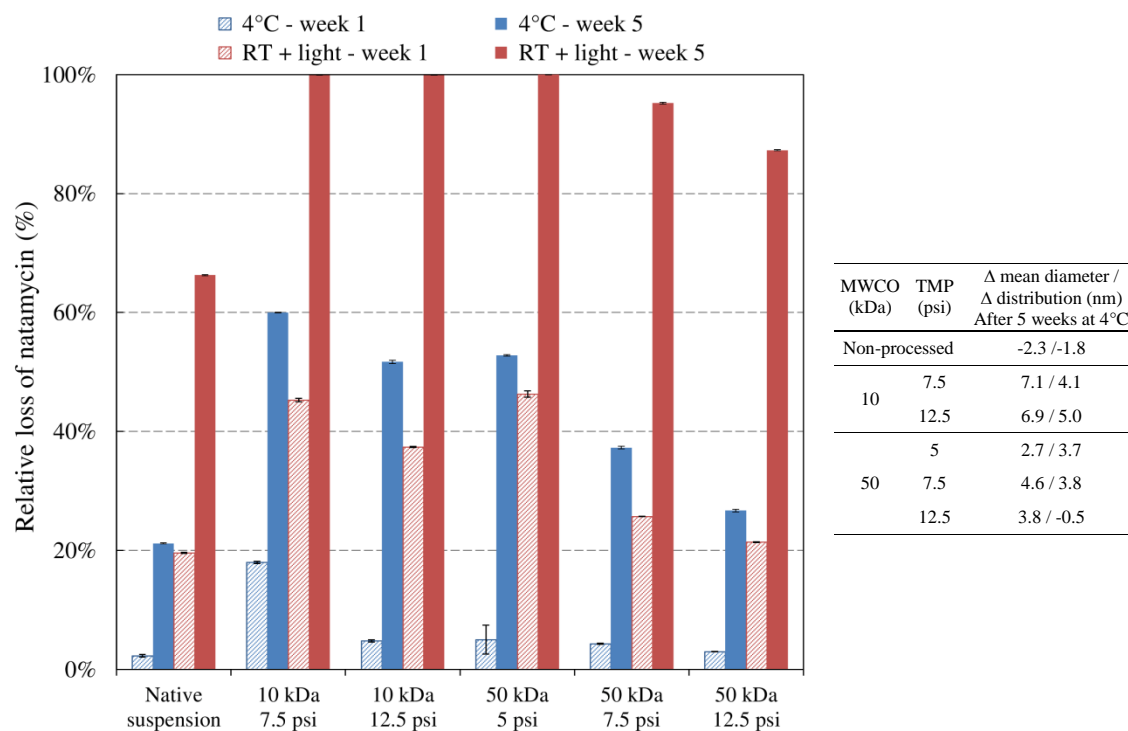


**Figure 4.13: Relative loss of natamycin upon storage for sterol-free liposomal suspensions concentrated by TFF under various MWCO and TMP conditions and effect on size characteristics**

#### 4.5.1.2. Influence of sterol incorporation

Influence of cholesterol and ergosterol incorporation on the filtration process was studied at 7.5 psi for the 50 kDa membrane to determine if mechanical strength brought by these compounds [31] could help overcome the instability previously evidenced. Reference formulations developed in Chapter 3 are used here based on CHOL/L ratios 1:45 and 1:18 and ERG/L ratios 1:90 and 1:45. As previously observed for sterol-free formulations, samples could be processed with stabilization of the flux decline and conservation of liposomes in suspension (yellow-bluish translucent aspect). No crystals or visible precipitation of natamycin and/or sterol occurred during the process. Table 4.5 summarizes results regarding losses of liposomes and natamycin, final encapsulation efficiency and effect on size characteristics for various sterol contents. Figure 4.14 represents the corresponding evolution of cake contribution to the overall filtration resistance as a function of permeate volume.

Final flux declines obtained at steady state were in a comparable range (around 50%) for sterol-free and cholesterol-enriched liposomes. Contribution of the cake to the overall resistance was also similar (around 49%) and stabilized after collection of 15 mL of permeate. Count rate analysis however indicated a benefit of incorporating cholesterol in low amounts for a slight reduction in total lipid losses. Unloaded sterol-free and

cholesterol enriched formulations were submitted to TFF concentration and UV analyses performed to determine the fraction of phospholipid monomers lost in the permeate. While the sterol-free sample was characterized by a linear progressive loss up to a final 3.1%, CHOL/L 1:145 and CHOL/L 1:18 samples showed the highest loss of phospholipid in the first permeate fraction followed by stabilization over time up to respectively 5.3 and 5.6%. This behaviour tends to indicate a destabilization of cholesterol-enriched samples at the beginning of the concentration process and could explain the slightly higher variation of size and size distribution observed by DLS for these samples.

Presence of ergosterol remarkably delayed the flux stabilization phase with respectively 21 and 32 mL of permeate volume required to reach steady-state for ratios ERG/L 1:90 and 1:45. Final cake resistance was also reduced respectively to 45% and 44%, which cannot be directly related to the loss of lipid measured in the retentate (Table 4.5). Determination of phospholipid losses in permeate for the corresponding unloaded ergosterol-enriched suspensions showed a linear pattern similar to the sterol-free sample and lower amounts of lipid material removed with respectively 2.0 and 1.6% losses achieved for ERG/L1:90 and ERG/L 1:45. This behaviour, combined with a limited variation in size characteristics, indicates that ergosterol-enriched samples were less disturbed by the TFF process than cholesterol-enriched formulations, which could be linked to the higher mechanical stability of lipid bilayers in presence of ergosterol previously mentioned in Chapter 3 [31-33]. Presence of ergosterol improving packing and interactions between phospholipids might also have for consequence a reduced initial amount of unassociated lipid monomers compared to sterol-free and cholesterol-enriched formulations, which could explain the reduced losses detected in the permeate. Delayed flux declines in the case of ergosterol suggested in any case that the mechanism of fouling occurred first via deposition of unassociated phospholipid molecules. Steady-state lower cake resistance for ergosterol compared to cholesterol at the same ratio S/L 1:45, though the estimated deposited mass is higher, highlighted a lower specific filtration resistance of the cake probably linked to a larger porosity. Preferred explanations for this latter are the superior rigidity of ergosterol-enriched liposomes, bringing lower deformability and reducing the packing of the liposomes, as well as the previously mentioned reduced amount of unassociated lipid monomers, which could have deposited during circulation in the cake and locally decreased the porosity.



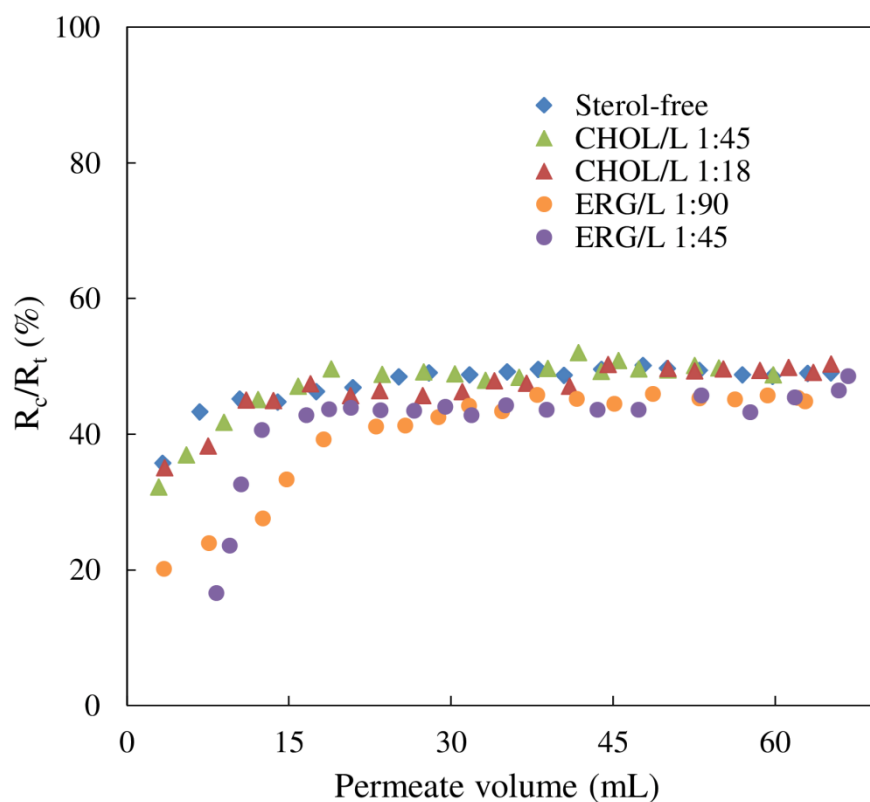


**Figure 4.14:** Cake contribution to overall filtration resistance during sterol-enriched liposomes concentration by TFF as a function of MWCO and TMP parameters

**Table 4.5:** Influence of sterol type and concentration on lipid and natamycin losses, size characteristics and encapsulation in sterol-enriched liposomes

| Sterol content | Lipid loss (%) | $\Delta$ mean diameter / $\Delta$ distribution (nm) | Natamycin loss (permeate analysis) (%) | Natamycin loss (retentate analysis) (%) | $CF_{\text{natamycin}}$ (-) | $\Delta$ EE (%) |
|----------------|----------------|---|--|---|-----------------------------|-----------------|
| No sterol      | $34.6 \pm 1.2$ | 3.7 / 1.5   | $30.7 \pm 0.1$                         | $38.6 \pm 2.0$                          | $1.79 \pm 0.01$             | $15.0 \pm 0.8$  |
| CHOL/L 1:45    | $30.2 \pm 0.7$ | 5.1 / 3.9   | $26.8 \pm 0.1$                         | $30.7 \pm 1.3$                          | $1.80 \pm 0.02$             | $13.0 \pm 1.9$  |
| CHOL/L 1:18    | $37.7 \pm 0.3$ | 2.9 / 2.3   | $19.9 \pm 0.1$                         | $21.9 \pm 0.8$                          | $2.20 \pm 0.01$             | $5.7 \pm 1.6$   |
| ERG/L 1:90     | $28.8 \pm 0.4$ | 2.9 / -0.7  | $25.5 \pm 0.1$                         | $32.9 \pm 1.6$                          | $1.81 \pm 0.02$             | $11.6 \pm 2.8$  |
| ERG/L 1:45     | $36.6 \pm 0.2$ | 2.0 / 0.8   | $19.4 \pm 0.1$                         | $21.9 \pm 0.6$                          | $2.43 \pm 0.01$             | $4.7 \pm 1.4$   |

Determination of natamycin content confirmed, as previously observed for sterol-free liposomes, that untrapped natamycin was mainly removed during the process, allowing the obtention of concentration factors superior to 1 with a clear superiority while using ergosterol and increased amount of sterol involved in the formulation. Improvement of entrapment levels was also visible for all samples with limited variation for the most sterol-enriched compositions due to initial higher levels of entrapment as described in Chapter 3. Initial lower levels of non-encapsulated natamycin in suspension also explained the variation of relative preservative loss in permeate fraction. Smaller deviation between natamycin losses in permeate and retentate for highest content of sterols involved, though liposome deposition on the membrane as well as the loading of natamycin in these formulations are more important than sterol-free, goes in the sense of a large removal of free natamycin molecules by adsorption on the membrane.

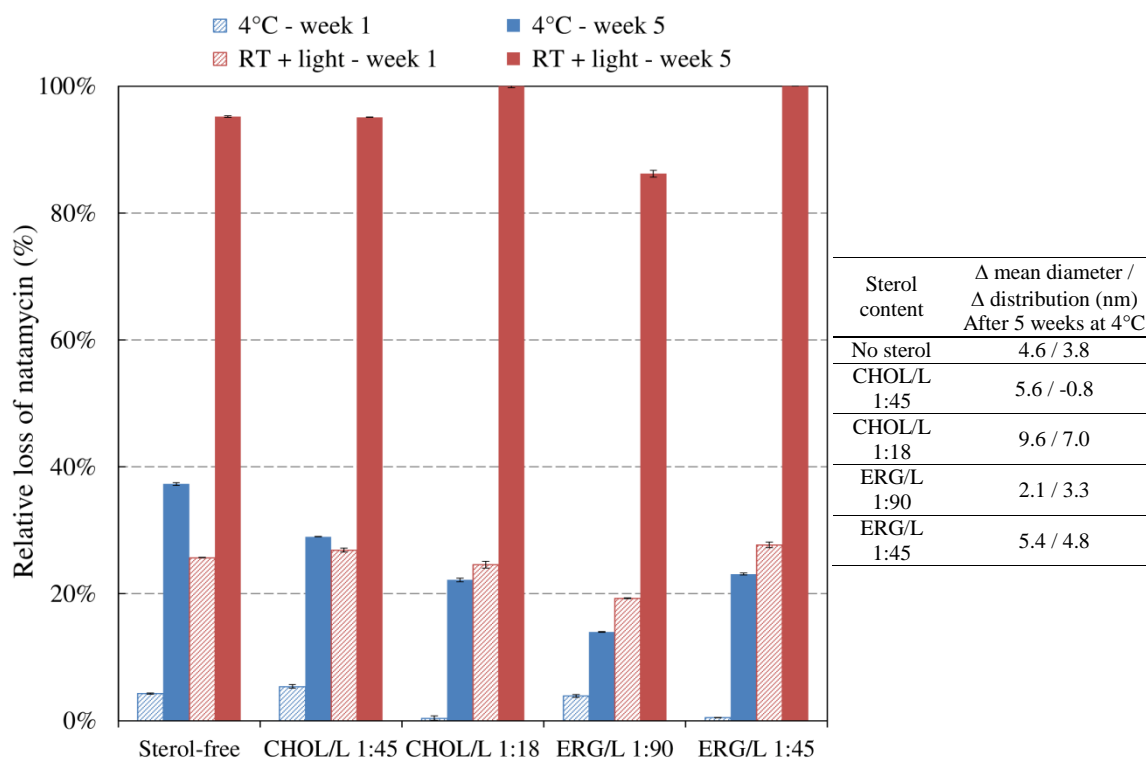


**Figure 4.15: Relative loss of natamycin upon storage for concentrated sterol-enriched liposomal suspensions and effect on size characteristics**

Stability of natamycin in the formulation was slightly enhanced over 5 weeks at 4°C for all compositions and at room temperature with light exposure for the lowest amount of sterols (Figure 4.15). The benefit of sterol incorporation was however not significant contrary to what was demonstrated in Chapter 3 for native suspensions. This means that the presence of sterol does not allow maintaining acceptable integrity and physical

stability of the liposomes by counteracting shear stresses and rearrangements due to the increase of solid content during the concentration step.

#### **4.5.2. Diafiltration of liposomes**

Removal of untrapped natamycin was efficiently achieved using the TFF concentration mode. Negative consequences on the preservative chemical stability upon storage are however observed, linked either to the high final content of phospholipid in the suspension, in favor of enhanced hydrolysis, and/or to the reduced physical integrity of the liposome bilayer due to the TFF process. In this purpose, diafiltration was attempted to determine if removal of free natamycin without modification of lipid solid content in suspension could bring further benefits to the preservative stability. Continuous mode was here preferred as extreme dilutions while adding a whole diafiltrate volume and repetition of concentration steps happening in the discontinuous mode were expected to be detrimental to the physical integrity of the liposomes.

Continuous diafiltration was performed as described in section 4.3.5 using 4 diafiltrate volumes (75 mL) for the 50 kDa membrane at 12.5 psi. Both sterol-free and cholesterol-enriched (CHOL 1:18) natamycin-loaded formulations were studied to determine if the presence of sterol could be advantageous for the stability. Table 4.6 summarizes the parameters and characteristics of the liposomal suspensions before and after diafiltration as well as the effect on stability upon storage. Flux stabilized very quickly and remained stable over the whole filtration, without influence of the presence of cholesterol. Relative contribution of cake to the overall filtration resistance was found to be lower than for concentration mode (around 40% compared to 45% for the same combination MWCO/TMP) due to the unvariable solid content in the feed and to the negligible loss of lipid material determined by count rate analysis which indicates very limited cake formation. While calculating lipid losses over the process, it can be seen that in the case of the sterol-free formulation, up to 5.2% of phospholipids were removed from the feed before recovery of the first permeate fraction due to absorption on the membrane. Cross-flow drag forces however allowed resuspension to the feed over time which explains the limited total lipid loss observed. In the case of the sterol-enriched formulation, loss remained below 1% along the whole filtration.

Observations of mean diameter and size distribution indicated minor reduction of both parameters compared to the native suspension, contrary to what was observed in

concentration mode, which can be linked to the slight losses of phospholipids monomers. Improvement of encapsulation efficiency was expectedly less significant for the cholesterol-enriched formulations due to initial lower content of free natamycin. Both formulations however reached a final encapsulation efficiency of 99.4% indicating that removal of non-entrapped natamycin occurred as desired. Limited loss of natamycin via adsorption on the membrane can be directly linked to the limited deposition of loaded liposomes on the membrane surface.

**Table 4.6: Comparison of sterol-free and cholesterol-enriched liposomal suspensions processed by continuous diafiltration**

|  | Sterol-free   | CHOL 1:18   |
|--|---|---|
| $R_c/R_t$ (%)  | $40.5 \pm 0.7$                                      | $40.2 \pm 0.7$  |
| Total lipid loss (%)   | $0.5 \pm 0.8$                                       | $0.8 \pm 1.0$   |
| Mean diameter $\pm$ distribution width (nm)                              | $98.7 \pm 46.7$ (native)<br>$96.1 \pm 45.4$ (final) | $106.9 \pm 50.7$ (native)<br>$102.1 \pm 49.4$ (final) |
| Mean diameter $\pm$ distribution width (nm) after 5 weeks storage at 4°C | $99.8 \pm 48.1$ (native)<br>$94.8 \pm 46.1$ (final) | $108.0 \pm 51.1$ (native)<br>$96.7 \pm 47.1$ (final)  |
| Total loss of natamycin (%)  | $64.9 \pm 0.1$                                      | $43.8 \pm 0.1$  |
| Total loss of natamycin on the membrane (%)                              | $10.7 \pm 0.1$                                      | $3.3 \pm 0.1$   |
| Concentration factor   | 0.36  | 0.59  |
| $\Delta$ EE (%)  | $31.9 \pm 0.6$                                      | $9.1 \pm 0.5$   |

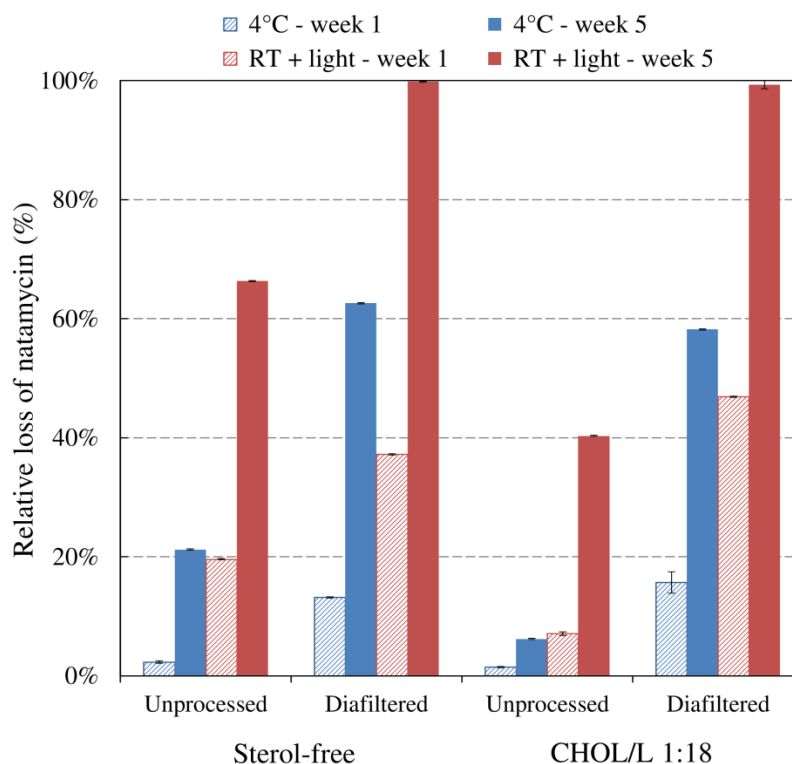


**Figure 4.16: Relative loss of natamycin upon storage for unprocessed or diafiltered liposomal suspensions**

No clear benefit could however be highlighted for the preservative stability compared to unprocessed suspensions (Figure 4.16), whether or not sterol was incorporated. Reduced amount of natamycin left in suspension and further decrease in size and size distribution of the liposomes, proving rearrangement over time and consequently leakage of natamycin out of the nano-carriers, are the most likely hypotheses for the absence of improvement of stability via diafiltration.

### **4.5.3. Conclusions for liposomal suspensions**

Use of Tangential Flow Filtration for the concentration of liposomal suspensions proved to be efficient for the improvement of natamycin encapsulation efficiency by removal of non-entrapped preservative and increase in solid content. Flux decline and cake resistance were found to be dependent on both transmembrane pressure and molecular weight cut-off, with variable effects on lipid removal by adsorption on the membrane or by loss of phospholipids monomers in the permeate. Limited variation of size characteristics were observed but cryo-TEM highlighted the formation of multivesicular structures and the existence of some rearrangements during the filtration process. Though concentration of liposomes was in all cases increased and the content of free natamycin reduced, stability of the preservative upon storage was not improved and even negatively impacted, with even 1.3 to 2.8-fold higher levels of loss compared to the original suspension. Best process conditions to ensure the long-term stability were obtained for 50 kDa and 12.5 psi, probably linked to the shorter processing time and thus reduced exposure of the liposomes to shear stresses and contact with the membrane. Incorporation of sterols, known to improve the initial encapsulation of natamycin inside the liposomes as well as the mechanical stability of the liposomes, allowed only minor improvement of natamycin stability upon storage and no clear improvement of the resistance of liposomes to the filtration process. High content of phospholipids in suspension at the end of the filtration, likely to catalyze hydrolysis and oxidation, and disturbance/rearrangements of the bilayer, which would have triggered release during the process, could be the reasons for the enhanced degradation of natamycin.

Continuous diafiltration attempts performed to reduce the content of untrapped natamycin without the disadvantage of higher phospholipid content, proved to be achievable without significant loss of phospholipids. Upon storage, enhanced variation in size characteristics and absence of improvement of the preservative stability were

however obtained even while incorporating sterol in the formulation, confirming that the enhanced mechanical fragility of liposomes after the filtration process is the key to the instability.

## **4.6. Conclusions**

In this chapter, Tangential Flow Filtration based on polysulfone hollow-fiber membranes was evaluated for the concentration and purification of natamycin-loaded PLGA and liposomal nano-suspensions with main focus on increasing the solid particle content, removing untrapped natamycin and improving the preservative stability upon storage.

The concentration step was successful for both types of nanoparticles with loss of natamycin and nano-carriers dependent on the filtration pressure and MWCO membrane chosen. PLGA nanoparticles were found to be relatively sensitive to fouling and pressure build-up, with reduced losses of both nano-carrier and preservative materials obtained for the lowest filtration rates. Though the concentration step allowed increase in solid content as desired, enrichment of natamycin was not significant but removal of part of the free natamycin proved to be beneficial for storage stability, with losses 1.6 to 3.7-fold lower than for the original suspension. Concentration of liposomal suspensions on the other hand allowed easier process control and more stable fluxes over time. Removal of untrapped natamycin was confirmed by improvement in the encapsulation efficiencies and concentration factors. Increase in relative phospholipid concentration, exposure of liposomes to shear stresses and rearrangement into multivesicular structures during the process proved however to have a detrimental effect on the chemical stability of the preservative upon storage. Concentration of sterol-enriched liposomes did not allow significant reduction of natamycin degradation upon storage or further protection of the integrity of the phospholipid bilayer during the TFF process, compared to the benefits highlighted in Chapter 3.

Application of diafiltration steps proved to be efficient for more intense removal of untrapped natamycin in suspension for both types of nano-carriers. Continuous diafiltration appeared to be the most processable method for the handling of PLGA nanospheres compared to discontinuous diafiltration, though losses of polymeric material remained significant in both cases (32-45%). Very low initial encapsulation efficiency of natamycin and removal of non-encapsulated natamycin led however to extremely low

concentrations of preservative and to a disadvantageous decrease in chemical stability with 78% of loss observed after only 5 weeks. Application of continuous diafiltration to liposomal suspension was performed successfully for sterol-free or sterol-enriched formulations with negligible cake formation and loss of phospholipids during the process. Once again, increase in encapsulation efficiency of natamycin within the nano-carriers and presence of sterol did not translate into an improvement upon storage of the chemical stability of the preservative or integrity of the liposomes themselves.

In a nutshell, Tangential Flow Filtration based on polysulfone hollow fiber membranes and the lab scale system implemented in this study is slightly beneficial in the case of PLGA nanospheres for the enhancement of natamycin stability upon storage, providing that the nano-suspensions are processed under low filtration pressures to avoid excessive fouling of the membrane. Further studies of the effect of membrane characteristics (pore size, material, configuration) and in-depth understanding of the cake formation would be profitable for further reduction of the fouling and the development of a scalable process with hollow-fibers. Other methods such as freeze-drying should also be considered (see Chapter 5) and could provide higher advantages for the formulations without causing the extensive losses of polymeric material observed here. Regarding liposomal suspensions, performing TFF in both concentration and continuous diafiltration modes with our lab scale system did not bring an obvious advantage compared to formulations developed in Chapter 3. Further work on both concentration and diafiltration processes for natamycin-loaded liposomal suspensions would require a more in-depth understanding of the physical stability of the liposome bilayer. Particularly, effect of the shear stress forces involved in the filtration, effect of sterol incorporation on the bilayer integrity and compressibility and mechanism of deposition/disruption of the liposomes on the membrane surface would be elements to consider. Use of hydrophilic or lipophilic markers loaded in the liposomes could for instance help following the evolution of bilayer permeability during the filtration and upon storage. Atomic Force Microscopy is another interesting option to test the integrity of the bilayer before and after filtration and to obtain direct information on the sterol influence [34]. The lab-scale system implemented in this study should also be reconsidered to offer a better monitoring of the process, particularly in terms of temperature control, likely to have a strong influence on the rearrangement of the bilayers too.

## 4.7. Nomenclature

|               |  |
|---------------|--|
| A             | Filtration area ( $m^2$ )  |
| C             | Concentration of natamycin in feed ( $\mu g/mL$ )                    |
| $C_0$         | Initial concentration of natamycin ( $\mu g/mL$ )                    |
| $C_p$         | Concentration of natamycin in permeate ( $\mu g/mL$ )                |
| CF            | Concentration factor (%)   |
| d             | Mean particle diameter   |
| $h_C$         | Cake thickness (m)   |
| $m_C$         | Cake mass (kg)   |
| m             | Mass of natamycin in feed ( $\mu g$ )                                |
| $m_0$         | Initial mass of natamycin ( $\mu g$ )                                |
| $m_{ads}$     | Mass of natamycin adsorbed on the membrane ( $\mu g$ )               |
| $m_{loss}$    | Mass of natamycin lost via nanoparticle loss ( $\mu g$ )             |
| $m_p$         | Mass of natamycin in permeate ( $\mu g$ )                            |
| $M_{NP}$      | Mass of nanoparticles in feed (mg)                                   |
| $Q_p$         | Permeate flux ( $m^3 \cdot m^{-2} \cdot s^{-1}$ )                    |
| $Q_w$         | Clean water permeate flux ( $m^3 \cdot m^{-2} \cdot s^{-1}$ )        |
| $R_c$         | Filtration resistance due to the cake ( $m^{-1}$ )                   |
| $R_m$         | Filtration resistance due to the membrane ( $m^{-1}$ )               |
| $R_p$         | Filtration resistance due to pore blocking ( $m^{-1}$ )              |
| $R_t$         | Overall filtration resistance ( $m^{-1}$ )                           |
| t             | Filtration time (min)  |
| $\Delta P$    | Transmembrane pressure /pressure drop (psi)                          |
| V             | Feed volume (mL)   |
| $V_d$         | Diafiltration volume (mL)  |
| $V_0$         | Initial feed volume (mL)   |
| $V_p$         | Permeate volume (mL)   |
| $\alpha_c$    | Average specific filtration resistance of cake ( $m \cdot kg^{-1}$ ) |
| $\varepsilon$ | Cake porosity (-)  |
| $\mu$         | Fluid viscosity ( $kg \cdot m^{-1} \cdot s^{-1}$ )                   |
| $\rho_p$      | Particle density ( $kg \cdot m^{-3}$ )                               |
| $\theta_{EE}$ | Fraction of encapsulated natamycin                                   |

## 4.8. Appendices

The simplified following models predict the variation of amount of natamycin eliminated from the feed during either concentration or diafiltration step. It is important to highlight here that a fraction of the compound is in a “solute” state (in solution or deposited at the nanoparticle surface) while the rest is encapsulated within the nanoparticles.  $\theta_{EE}$  symbolizes the fraction of encapsulated natamycin and can be calculated directly from encapsulation efficiency measurements.



#### 4.8.1. Appendix A: Mass balance for concentration step

The amount of natamycin left in the feed reservoir is equal to the initial mass minus the mass of solute eliminated in the permeate fractions or adsorbed on the membrane and the mass of encapsulated natamycin lost via adsorption of nanoparticles, as summarized in Equation 4.8.

$$m(t) = m_0 - m_p(t) - m_{ads}(t) - m_{loss}(t) \quad (4.8)$$

Where  $m_0 = C_0 V_0$  (4.9)

And  $m_p(t) = C_p(t) V_p(t)$  (4.10)

Assuming negligible adsorption of the solute on the membrane during filtration ( $m_{ads}(t) \sim 0$ ), concentration of dissolved material on both permeate and feed sides of the membrane is deemed to be equal and to represent the concentration of non-encapsulated solute in the nano-suspension, assuming that the filtration does not trigger leakage from the nano-carrier. This can be represented by the relation 4.11:

$$C_p(t) = \text{constant} = C_0 (1 - \theta_{EE}) \quad (4.11)$$

Leading to  $m_p(t) = (1 - \theta_{EE}) C_0 V_p(t)$  (4.12)

Loss of encapsulated natamycin linked to the loss of nanoparticles can on the other hand be directly related to the mass of nanoparticles lost during the filtration by the following expression:

$$m_{loss}(t) = \theta_{EE} m_0 \frac{M_{NP}(t)}{M_{NP}(t=0)} \quad (4.13)$$

Equation 4.8 can then be transformed into:

$$\frac{m(t)}{m_0} = 1 - (1 - \theta_{EE}) \frac{V_p(t)}{V_0} - \theta_{EE} \frac{M_{NP}(t)}{M_{NP}(t=0)} \quad (4.14)$$

NB: As  $M_{NP}$  is related to the mass of cake, the contribution of natamycin loss through adsorption of nanoparticles at the membrane surface is expected to become constant as steady-state is reached, leading to a simple linear dependence of  $m(t)$  to  $V_p(t)$ .

#### 4.8.2. Appendix B: Mass balance for diafiltration step

##### *Discontinuous diafiltration*

Discontinuous diafiltration can be considered as a concentration step for which  $V_0$  has to be replaced by  $V_0 + V_d$  in equation 4.14, leading to:

$$\frac{m(t)}{m_0} = \left( \frac{V_0 + V_d}{V_0} \right) - (1 - \theta_{EE}) \frac{V_p(t)}{V_0 + V_d} - \theta_{EE} \frac{M_{NP}(t)}{M_{NP}(t=0)} \quad (4.15)$$

### Continuous diafiltration

Considering at a first glance the absence of loss through direct natamycin or nanoparticles absorption, loss of solute in the feed during continuous diafiltration can be described by the simple mass balance:

$$\frac{d m(t)}{dt} = - \frac{dV_p(t)}{dt} C_p(t) \quad (4.16)$$

Assuming that the volume of feed is kept constant by the addition of diafiltrate medium ( $dV(t)/dt = 0$ ) and that both concentrations of solute in feed and permeate are equal on both sides of the membrane, equation 4.16 can be transformed into:

$$\frac{d m(t)}{m(t)} = \frac{d C(t)}{C(t)} = - \frac{dV_p(t)}{V(t)} (1 - \theta_{EE}) \quad (4.17)$$

Further integration of equation 4.17 and incorporation of the term described by the equation 4.13 to take into account loss due to the adsorption of nanoparticles, the following relationship is obtained to describe the continuous diafiltration.

$$\frac{m(t)}{m_0} = \exp \left( - (1 - \theta_{EE}) \frac{V_p(t)}{V_0 - V_p(t) + V_d(t)} \right) - \theta_{EE} \frac{M_{NP}(t)}{M_{NP}(t=0)} \quad (4.18)$$

## References

- [1] C.Vauthier, K.Bouchemal, Methods for the preparation and manufacture of polymeric nanoparticles, *Pharmaceutical Research*, **2008**, 26(5), 1025-1058
- [2] C.Vauthier, B.Cabane, D.Labarre, How to concentrate nanoparticles and avoid aggregation ?, *Eur.J.Pharm.Biopharm.*, **2008**, 69, 466-475
- [3] Patent US2009/0294357, Method for concentrating nanosuspensions
- [4] E.Leo, C.Contado, F.Bortolotti, B.Pavan, A.Scatturin, G.Tosi, S.Manfredini, A.Angusti, A.Dalpia, Nanoparticle formulation may affect the stabilization of an antiischemic prodrug, *Pharmaceutical Nanotechnology*, **2006**, 307, 103-113
- [5] H.-Y.Kwon, J.-Y.Lee, S.-W.Choi, Y.Jang, J.-H.Kim, Preparation of PLGA nanoparticles containing estrogen by emulsification-diffusion method, *Colloids Surf.A*, **2007**, 182,123-130

- [6] T.Govender, S.Stolnik, M.C.Garnett, L.Illum, S.S.Davis, PLGA nanoparticles prepared by nanoprecipitation: drug loading and release studies of a water soluble drug, *J.Control.Release*, **1999**, 57, 171-185
- [7] V.Torchilin, V.Weissig, *Liposomes: A Practical Approach*, OUP Oxford, **2003**
- [8] G.Dalwadi, H.E.A.Benson, Y.Chen, Comparison of diafiltration and tangential flow filtration for purification of nanoparticle suspensions, *Pharmaceutical Research*, **2005**, 22, 2152-2162
- [9] I.Limayen, C.Charcosset, H.Fessi, Purification of nanoparticle suspensions by a concentration/diafiltration process, *Separation and Purification Technology*, **2004**, 38, 1-9
- [10] K.-J.Hwang, Y.-C.Chang, The use of cross-flow microfiltration in purification of liposomes, *Separation and Purification Technology*, **2004**, 39, 2557-2576
- [11] K.Scott, R.Hughes, *Industrial Membrane Separation Technology*, Chapman & Hall, Ireland, **1996**
- [12] M.Cheryan, *Ultrafiltration and Microfiltration Handbook 2<sup>nd</sup> Edition*, CRC Press LLC, USA, **1998**
- [13] C.Tien, *Introduction to cake filtration: Analyses, Experiments and Applications*, Elsevier B.V., Amsterdam, **2006**
- [14] G.Dalwadi, V.B.Sunderland, Purification of PEGylated nanoparticles using tangential flow filtration (TFF), *Drug Development and Industrial Pharmacy*, **2007**, 33, 1030-1039
- [15] A.Wagner, K.Vorauer-Uhl, H.Kattinger, Liposomes produced in a pilot scale: production, purification and efficiency aspects, *European Journal of Pharmaceutics and Biopharmaceutics*, **2002**, 54, 213-219
- [16] J.-J.Foo, V.Chan, K.-K.Liu, Coupling bending and shear effects on liposome deformation, *Journal of Biomechanics*, **2006**, 39, 2338-2343
- [17] K.S.Sutherland, G.Chase, *Filters and Filtration Handbook*, Elsevier Ltd, Burlington USA, **2011**
- [18] C.Y.Feng, K.C.Khulbe, T.Matsuura, A.F.Ismail, Recent progresses in polymeric hollow fiber membrane preparation, characterization and applications, *Separation and Purification Technology*, **2013**, 111, 43-71
- [19] S.Ripperger, W.Gösele, C.Alt, *Filtration 1.Fundamentals*, Ulmann's Encyclopedia of Industrial Chemistry, Wiley-VCH Verlag, Germany, **2012**
- [20] W.R.Bowen, F.Jenner, Theoretical descriptions of membrane filtration of colloids and fine particles: an assessment and review, *Advances in Colloid and Interface Science*, **1995**, 56, 141-200
- [21] G.Belfort, R.H.Davis, A.L.Zydney, The behavior of suspensions and macromolecular solutions in cross-flow microfiltration, *Journal of Membrane Science*, **1994**, 96, 1-58
- [22] G.B.Van der Berg, C.A.Smolders, Flux decline in ultrafiltration processes, *Desalination*, **1990**, 77, 101-133
- [23] M.Zhang, L.Song, Mechanisms and parameters affecting flux decline in cross-flow microfiltration and ultrafiltration of colloids, *Environmental Science & Technology*, **2000**, 34, 3767-3773

- [24] S.Hong, R.S.Faibish, M.Elimelech, Kinetics of permeate flux decline in crossflow membrane filtration of colloidal suspensions, *Journal of Colloid and Interface Science*, **1997**, *196*, 267-277
- [25] K.-J.Hwang, T.-T.Lin, Effect of morphology of polymeric membrane on the performance of cross-flow microfiltration, *Journal of Membrane Science*, **2002**, *199*, 41-52
- [26] N.Dizge, G.Soydemir, A.Karagunduz, B.Keskinler, Influence of type and pore size of membranes on cross flow microfiltration of biological suspension, *Journal of Membrane Science*, **2011**, *366*, 278-285
- [27] Y.Endo, M.Alonso, Physical meaning of specific cake resistance and effects of cake properties in compressible cake filtration, *Filtration & Separation*, **2001**, *38*, 43-46
- [28] K.-J.Hwang, Y.-L.Hsu, K.-L.Tung, Effect of particle size on the performance of cross-flow microfiltration, *Advanced Powder Technology*, **2006**, *17*, 189-206
- [29] S.Kim, M.Marion, B.-H.Jeong, E.M.V.Hoek, Crossflow membrane filtration of interacting nanoparticle suspensions, *Journal of Membrane Science*, **2006**, *284*, 361-372
- [30] M.-S.Chun, G.-Y.Chung, J.-J.Kim, On the behavior of the electrostatic colloidal interaction in the membrane filtration of latex suspensions, *Journal of Membrane Science*, **2001**, *193*, 97-109
- [31] T.Róg, M.Pasenkiewicz-Gierula, I.Vattulainen, M.Karttunen, Ordering effects of cholesterol and its analogues, *Biochim.Biophys.Acta*, **2009**, *1788*, 97-121
- [32] C.Bernsdorff, R.Winter, Differential properties of the sterols cholesterol, ergosterol, b-sitosterol, trans-7-dehydrocholesterol, stigmasterol and lanosterol on DPPC bilayer order, *J.Phys.Chem.B*, **2003**, *107*, 10658-10664
- [33] D.A.Mannock, R.N.A.H. Lewis, T.P.W.McMullen, R.N.McElhaney, The effect of variations in phospholipid and sterol structure on the nature of lipid-sterol interactions in lipid bilayer model membranes, *Chemistry and Physics of Lipids*, **2010**, *163*, 403-448
- [34] E.Spyratou, E.A.Mourelatou, M.Makropoulou, C.Demetzos, Atomic force microscopy: a tool to study the structure, dynamics and stability of liposomal drug delivery systems, *Expert Opinion on Drug Delivery*, **2009**, *6*, 305-317



# *Chapter 5*

## *Lyophilization of polymeric and liposomal nano-suspensions*

---

In this chapter, natamycin-loaded PLGA nanospheres and liposomal suspensions are submitted to lyophilization to establish if this method can bring substantial enhancement to their physical and chemical stability compared to aqueous suspensions and/or concentrates obtained by Tangential Flow Filtration. The influence of various protective excipients (glucose, sucrose, trehalose, lactose, mannitol and sorbitol) at different concentrations is investigated in each step of the lyophilization process to establish conditions maintaining the integrity of the nanoparticles and resulting in easily redispersible powders able to protect efficiently both natamycin and nano-carriers towards degradation over time.

Trehalose above 2.5% w/v turns out to be the most appropriate protectant at every step of the lyophilization process for both PLGA nanospheres and liposomal suspensions with or without sterol enrichment. Easily redispersible amorphous cakes are formed and allow conservation of integrity and size characteristics of the nano-carriers just after preparation and upon a 10-week storage period. Natamycin stability is clearly enhanced compared to aqueous suspensions and concentrates obtained by TFF for both nano-carrier systems.

The other saccharides glucose, sucrose and lactose are found inferior to trehalose in terms of cryoprotection, lyoprotection or efficient stabilization upon storage linked to various reasons such as collapsed structures, recrystallization, high residual moisture content and chemical reactivity towards natamycin.

Mannitol and sorbitol are identified as efficient stabilizers and protectants against degradation and leakage of natamycin from PLGA nanoparticles, but do not allow on their own the formation of acceptable cakes or protection of the nanoparticle integrity.

---

## 5.1. Introduction

Aqueous nano-suspensions of polymeric nanoparticles and liposomes prepared in Chapters 2 and 3 were both found unsuitable for long-term storage due to chemical instability of natamycin. In the case of PLGA nanospheres, low solid content intrinsic to the nanoprecipitation method and limited initial encapsulation efficiency of natamycin within the particles result in a large exposure of dissolved natamycin to aqueous medium and thus to degradation. The polymeric nano-carriers themselves are known to endure autocatalytic hydrolysis while stored in liquid form for an extensive period [1-2], which is likely to trigger further release of the preservative but also to increase the acidity of the medium and cause further degradation of natamycin. Similarly, in the case of liposomal suspensions, hydrolysis and oxidation of phospholipids are classically happening [3] and could catalyze chemical reactions with the antifungal. Reorganization of liposomes over time by aggregation or fusion [4-5] and permeability of the bilayer are also factors that result in leakage of entrapped material in the aqueous medium and are detrimental for the stability.

Improvement of physical and chemical stability of the formulation could be achieved by transforming the nano-suspensions into dry powders to reduce exposure to water and degradation phenomena such as hydrolysis and oxidation. In addition to the possible benefits for the shelf-life of the product, powders are also easier to handle by customers and require reduced costs of storage and transport compared to aqueous suspensions and/or concentrates. Lyophilization, also known as freeze-drying, is one of the approaches commonly used at industrial scale for the preparation of food or pharmaceutical powders [6-8] and has also been reported suitable for the drying of polymeric nanospheres [9] and liposomes [10].

Lyophilization is a well-established dehydration method consisting in freezing the sample and removing water by sublimation to form easily redispersible porous cakes. Freezing is the first step of the process and can be performed experimentally by fast cooling (liquid nitrogen, dry ice bath) or slower cooling by using temperature ramps. Freezing of the sample allows the progressive formation of ice crystals while gradually leading to an increase in concentration of particles or other solutes present in the medium. Concentration and ice crystal formation continues up to a certain point where the viscosity of the medium becomes too high. At this point, the sample contains the maximum amount of ice crystals, the minimum of unfrozen water and the

solutes/particles. This so-called maximally freeze-concentrated suspension is characterized by a defined glass transition temperature  $T'_g$  [7-9]. Freezing temperature is usually set-up at least 10°C below the  $T'_g$  to ensure complete formation of ice crystals and facilitate further steps of the process.

Once the sample is frozen, a primary drying step is implemented and consists in transferring some heat to the system under reduced pressure to allow sublimation of ice crystals into vapor. This step is usually the longest phase of the freeze-drying process and has to be carried out 5 to 10°C below the collapse temperature  $T_c$  of the freeze-concentrated suspension [9-10] (1-2°C higher than the  $T'_g$  classically), which corresponds to the temperature where the material softens up to the point of not being able to maintain its own structure, resulting in collapsed and usually high water-containing cakes.

A shorter second drying step is finally performed to remove unfrozen water that could not be sublimated during the primary drying. Reduced pressure and much higher temperatures than for primary drying are involved (typically 20-50°C) to ensure maximized removal of water molecules and limit the presence of residual moisture in the final cake [9-10] that could be highly detrimental for the stability upon storage. Temperature at this stage must be kept below the  $T_g$  of the anhydrous dry product to maintain the powder in an amorphous state.

Though this technique involves relatively mild conditions, various stresses can be induced at each phase of the process and can have a detrimental effect on the nanoparticles. Freezing is usually considered as the most aggressive step due to mechanical stresses linked to the formation of ice crystals [11] that can be critical while considering fragile and deformable particles such as liposomes [12]. Progressive increase in particle concentration during ice formation and thus closer contact can also induce destabilization by aggregation of PLGA nanoparticles or fusion of liposomal arrangements. For this latter, the cooling procedure also reduces interaction with water molecules, which is detrimental for the conservation of the bilayer structure, and can also trigger transition from fluid to gel phase if the phase transition temperature  $T_m$  is reached, which has consequences on the permeability of the membrane as described in Chapter 3. During the drying steps, physical destabilization linked to a more concentrate state of particles is also likely to occur leading to further aggregation or fusion. In the case of liposomes, dehydration and removal of water favor rearrangement of the phospholipids in a tighter conformation, leading to a much higher  $T_m$  and dry phospholipids in a gel state



at temperatures where fully-hydrated liposomes will still be in fluid state [10,13], which has consequences on the permeability and the reconstitution into vesicles after drying. Additionally, if liposomes are prepared with a mixture of phospholipids with different  $T_m$  or in presence of other components such as sterols, phase separation and rearrangement can occur and have significant consequences on the integrity of the vesicular structures and retention of encapsulated compounds.

Loss of integrity of the nanoparticles due to the various stresses induced by the lyophilization can be overcome by addition of excipients aiming at cryo-/lyoprotection respectively during the freezing step and the drying steps. Sugars are commonly employed for this purpose in food or pharmaceutical applications [7-10] due to their innocuous nature and their ability to act as bulking agents, stabilizers and tonicity adjusters. The protective action of these compounds is directly linked to their vitrification during freezing that result in the formation of a glassy sugar matrix where the density and ordering of ice crystals is reduced [9,14]. As a consequence, mechanical stresses as well as possible contact between nanoparticles are hindered. This physical barrier is maintained during the drying step and restricts mobility of the nanoparticles, avoiding further aggregation as well as diffusion or leakage of the encapsulated compounds. In the case of liposomes, sugars have also proven to be able via hydrogen bonding to replace efficiently water molecules interacting with the phospholipid heads [10,14-15]. This “water replacement” allows maintaining the bilayer in a “hydrated” state and contributes to the conservation of  $T_m$  in dry state close or inferior to the ones of fully-hydrated liposomes, reducing chances of disruption and leakage. Relative protective effectiveness of cryo-/lyo-protectants depends on their specific interactions with the nanoparticles, on the relative ratio protectant/nanoparticles involved and the process parameters chosen.

The objective of this chapter is to evaluate the possibility of lyophilization of the reference natamycin-loaded PLGA nanospheres and liposomal suspensions obtained in Chapters 2 and 3, aiming at developing formulations with the following desired properties:

- ✓ Sustained initial characteristics of the nanoparticles (size, polydispersity, zeta-potential) upon reconstitution just after lyophilization and after storage.
- ✓ Acceptable aspect of the lyophilizates (non-collapsed cake, limited residual moisture, easy and fast reconstitution in water).
- ✓ Enhanced chemical stability of natamycin upon storage.

To this purpose, several classical cryoprotectants compatible with food applications (saccharides (glucose, sucrose, lactose and trehalose) and polyols (mannitol, sorbitol)) and their optimal concentration to maintain the integrity of the nanoparticles in each step of the freeze-drying process were investigated for both nano-systems. The effectiveness of each protective excipient for the stabilization of natamycin and nano-carriers upon storage was characterized under different temperatures on a 10-week period. In the case of liposomes, effect of the bilayer composition and incorporation of sterol, which has already proven to be determinant for the stability in aqueous suspensions, have also been studied to establish if they could bring benefits for the dry-state storage.

## 5.2. Materials and methods

### 5.2.1. Materials

Natamycin (90.6% purity, trihydrate crystalline form) was kindly supplied by DSM Food Specialties (Delft, The Netherlands) and used without further purification. Deoiled phosphatidylcholine-enriched soybean lecithin Epikuron 145V was supplied by Cargill (Hamburg, Germany). Cholesterol (CHOL,  $\geq 99\%$ ), ergosterol (ERG,  $\geq 95\%$ ) and PLGA polymer Resomer<sup>®</sup> RG752H (L:G ratio 75:25, MW 4-15 kDa) were purchased from Sigma-Aldrich. Methanol EMSURE<sup>®</sup> ACS and dried acetone Seccosolv<sup>®</sup> were purchased from Merck and used for the preparation of the nano-suspensions. Potassium dihydrogen phosphate, methanol and acetonitrile Lichrosolv<sup>®</sup> were obtained from Merck and used for HPLC analyses. High quality water purified in a MilliQ system was used in all experiments.

Cryo-/lyo-protectants were chosen among monosaccharide (glucose), disaccharides (sucrose, trehalose, lactose) and polyols (mannitol, sorbitol). *D*-(+)-glucose (BioXtra,  $\geq 99.5\%$ , 180.2 g/mol), anhydrous  $\beta$ -lactose ( $\geq 99\%$ , 342.3 g/mol) and *D*-sorbitol (BioUltra,  $\geq 99.5\%$ , 180.2 g/mol) were purchased from Sigma-Aldrich. *D*-(+)-trehalose dihydrate ( $\geq 99\%$ , 378.3 g/mol) was obtained from VWR and *D*-(+)-sucrose (342.3 g/mol) from Merck. Mannitol (Pearlitol<sup>®</sup> 200SD, 180.2 g/mol) was provided by Roquette Pharma. Glucose and lactose are both reducing sugars. Chemical structure and typical range of glass transitions for freeze concentrate ( $T'_g$ ) and anhydrous dry forms ( $T_g$ ) of these excipients [10,16-19] are presented in Figure 5.1.

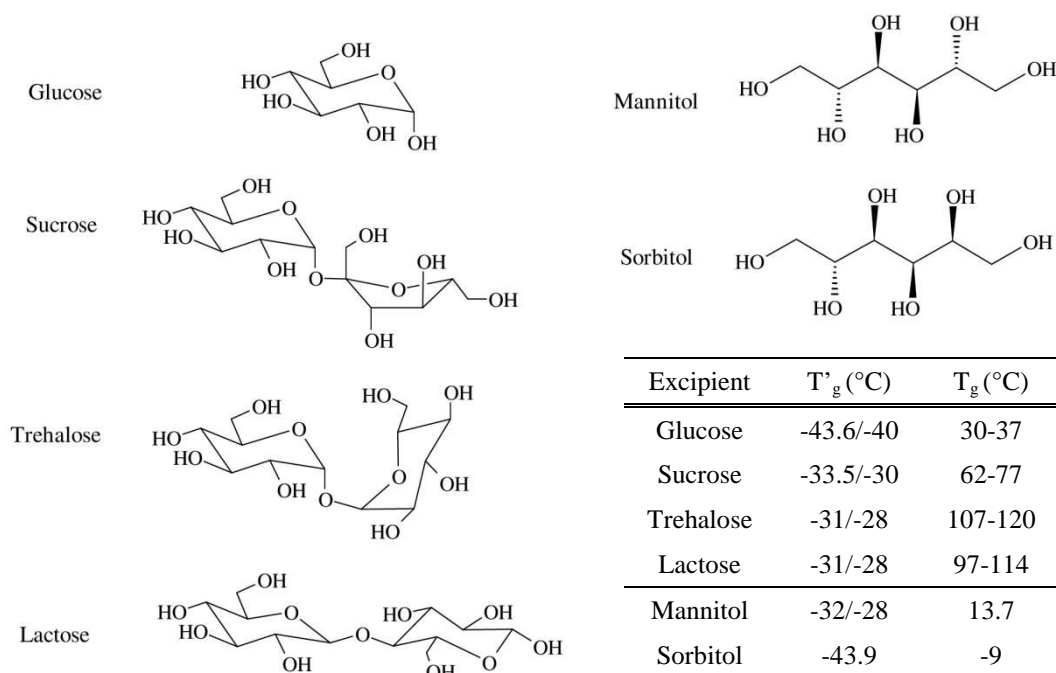


Figure 5.1: Chemical structure and glass transitions of sugar excipients for lyophilization

### 5.2.2. Preparation of nano-suspensions

PLGA nanospheres were prepared by the nanoprecipitation technique described in Chapter 2, for a concentration of PLGA of 37.5 mg/mL in acetone, 2.5 mg/mL of natamycin in methanol and a ratio acetone/methanol 2:1 v/v. 100 mL batches of nano-suspensions were obtained by 10 successive one-shot injections of 0.4 mL of organic phase in MilliQ water under moderate magnetic stirring. The resulting nano-suspensions were kept under slow stirring overnight for complete evaporation of organic solvent. Final samples contain nanoparticles at a solid content of 1 mg/mL (0.1% w/v).

Liposomal suspensions were prepared using the solvent injection technique described in Chapter 3, for a concentration of Epikuron 145V and natamycin of respectively 45 mg/mL and 2.5 mg/mL in methanol. If necessary, cholesterol and ergosterol were also added to the organic phase at respectively 1-2.5 mg/mL (ratios CHOL/L 1:45 and 1:18) and 0.5-1 mg/mL (ratios ERG/L 1:90 and 1:45). Batches of 100 mL of liposomes were obtained by 10 successive one-shot injections of 0.4 mL of organic phase in MilliQ water under moderate magnetic stirring. The resulting suspensions were kept under slow stirring overnight for complete evaporation of the methanol. Final samples contain liposomes at a solid content of 1.8 mg/mL (0.18% w/v).

### 5.2.3. Lyophilization

The protective agents were added as powder to the nano-suspensions at 1, 2.5 and 5% w/v. Mixtures were submitted to moderate magnetic stirring for 15 min to allow full dissolution of the sugars. 2mL-aliquots of the formulations obtained were dispensed in glass cryo-vials. 2 mL of protectant-free samples were used as a control. Mean particle diameter, polydispersity and zeta-potential of each sample were assessed by DLS before and after addition of the protective agent as described in section 5.2.5.1.

Lyophilization was performed with an industrial Advantage 2.0 Bench Top freeze-dryer Model XL (VirTis, SP Scientific, New York, USA) equipped with a temperature-controlled shelf and coupled with a XDS-10 dry-vacuum pump (BOC Edwards, Crawley, UK). The freeze-drying cycle was performed in three steps: 1) ramp freezing from room temperature to -60°C (rate 1.5°C/min) with an additional 180 min hold at -60°C; 2) primary drying at a shelf temperature of -50°C and a pressure of 60 µbar for 2000 min; 3) secondary drying at a shelf temperature of 20°C and a pressure of 50 µbar for 480 min. After reestablishment of ambient pressure, cryo-vials were sealed and stored at 4°C until further use. Freeze-drying was performed in duplicate and the cake aspect at the end of the lyophilization recorded.

To assess the integrity of the nanoparticles after lyophilization, cakes were reconstituted to the initial volume of suspension by slow injection of 2 mL MilliQ water along the wall of the vial to avoid foaming. Samples were allowed to sit for 15 min to ensure proper cake wetting. Mean particle diameter, PdI and zeta-potential of each sample were measure by DLS as described in section 5.2.5.1.

### 5.2.4. Freeze-thawing

In order to evaluate the resistance of the nanoparticles during the freezing step, a freeze-thawing cycle [20] was performed with a 2mL-aliquot of the protectant-enriched formulations described in section 5.2.3. Samples were placed in the freeze-dryer, cooled from room temperature ( $23 \pm 2^\circ\text{C}$ ) to -60°C with a cooling rate of 1.5°C/min and held at this temperature for an additional 180 min hold. After this period, the freeze-dryer was stopped and thawing was performed by letting the samples go back to room temperature. Mean particle diameter and PdI of each sample were measure by DLS before and after freeze-thawing as described in section 5.2.5.1.

## 5.2.5. Physicochemical characterization

### 5.2.5.1. Particle size and zeta-potential

The mean particle diameter ( $d$ ) and polydispersity index (PdI) of the nanospheres were determined by Dynamic Light Scattering (DLS) (Zetasizer Nano ZS, Malvern Instruments Ltd, UK). Three consecutive measurements were performed on each nano-suspension at 25°C at a scattering angle of 173°, after an equilibration time of 180 seconds. The zeta-potential of the nanoparticles ( $\zeta$ ), was assessed on undiluted nano-suspensions with the same equipment by three consecutive measurements of 200 sub-runs at 25°C after an equilibration time of 180 seconds. For both size and zeta-potential, the concentration of protective excipient present in water was used in the Zetasizer software to take into account induced modifications of viscosity and refractive index. All measurements were performed in triplicate. Influence of the different steps of the process (1: addition of protective excipient; 2: freeze-thawing; 3: freeze-drying; 4: storage) were evaluated by calculation of the ratio of mean size/PdI/ $\zeta$  obtained at each step on the initial characteristics of the suspension (ratio expressed as  $d_f/d_i$ ,  $PdI_f/PdI_i$  and  $\zeta_f/\zeta_i$ ). It is important to highlight here that, for steps 2-4, initial characteristics correspond to values obtained for the protectant-enriched suspensions (step 1).

### 5.2.5.2. Natamycin content

Natamycin content in native suspensions and freeze-dried cakes was determined by reverse-phase high-performance liquid chromatography (HPLC) after dilution or resuspension in methanol. A high pressure liquid chromatograph Ultimate 3000 Dionex equipped with a variable wavelength detector was used. Separation was achieved by injecting 20  $\mu$ L of sample on a reverse phase column Licrospher<sup>®</sup> RP18 (Merck, 125 nm x 4 mm, pore size 100 Å) with a mobile phase consisting of 35:65 v/v acetonitrile: potassium dihydrogenphosphate buffer (pH 3.05) at a flow rate of 1.0 mL/min. Natamycin was detected by UV at 303 nm and quantified using a calibration curve designed over the range 0.05-50 ppm ( $R^2 = 0.9996$ ). All HPLC samples were analyzed in triplicate.

### 5.2.5.3. Differential scanning calorimetry (DSC)

Thermograms of pure and lyophilized excipients as well as freeze-dried samples containing nanoparticles were recorded on a differential scanning calorimeter DSC7

(Software Pyris Series, Perkin-Elmer, USA). Accurately weighed samples (2-10 mg) were analyzed at a scan rate of 10°C/min covering the temperature range 25-275°C.

#### 5.2.5.4. Determination of residual moisture content

Residual moisture content in the freeze-dried formulations was determined by Karl-Fisher titration using a Metrohm 736GP Titrino (Mettler-Toledo, Switzerland). Lyophilized samples were analyzed after preparation and upon 10 weeks of storage, using methanol as solvent for dissolution of the powders.

#### 5.2.6. Stability tests

To evaluate the stability of the lyophilized systems, cryo-vials sealed directly at the end of the freeze-drying procedure were stored at -20°C, 4°C and room temperature (23 ± 2°C) under light protection and ambient relative humidity. After 10 weeks, natamycin content left in the samples was analyzed by HPLC as described in section 5.2.5.2, and resuspension was also performed to evaluate changes in mean diameter, PDI or zeta-potential as described in section 5.2.5.1.

### 5.3. Lyophilization of PLGA nanospheres

Cryo-/lyo-protectants were chosen among monosaccharide (glucose), disaccharides (sucrose, trehalose, lactose) and polyols (mannitol, sorbitol). Powders of these excipients were directly added in the nano-suspensions at concentrations ranging from 1 to 5% w/v (ratios PLGA/protectant 1:10 to 1:50). The freeze-drying was pre-optimized (data not shown) to select parameters that would allow successful lyophilization for all sugars involved. Freezing temperature was fixed at -60°C to ensure a temperature below the  $T_g$  of all protective excipients studied (see Figure 5.1) and consequently maximized ice crystal formation. Protectant-enriched suspensions were submitted to a freeze-thawing cycle [20] at this temperature to get a preliminary idea of the effect of the cooling procedure on the integrity of the nanospheres. Primary drying was performed at -50°C to be at least 5°C below the collapse temperature of glucose and sorbitol, which present the lowest  $T_g$  used in this study. Secondary drying was performed at 20°C to remain below the transition temperature  $T_g$  of the anhydrous sugars.

### 5.3.1. Addition of cryoprotectants and freeze-thawing

As illustrated in Table 5.1, addition of cryoprotectants in the formulations did not significantly disturb size characteristics of the PLGA nanospheres. Slight reduction of mean diameters occurred and progressively increased with the concentration of sugar involved, which is attributed to the osmotic pressure induced by the excipients and possible efflux towards the outer medium of residual water entrapped within the PLGA nanoparticles during the nanoprecipitation process. A more pronounced shrinkage effect was observed for lactose, mannitol and sorbitol and might be linked to higher interactions with the particle surface due to a relative planar structure in the case of lactose compared to other disaccharides and to the flexible linear conformation of polyols [21]. Limited variations while introducing higher contents of these three protectants suggest a saturation effect and already significant coverage of the surface at 1% w/v. Polydispersity values were overall slightly reduced compared to the native suspension. For saccharides, polydispersity was found the closest to the original values while using the highest concentration of excipient. The opposite variation was observed for mannitol and sorbitol and pointed out that the osmotic dehydration induced by the polyols is accompanied by a homogenization of particle size.

Observation of zeta-potentials indicated a relatively unchanged surface charge while using glucose, sucrose and trehalose. A more pronounced effect and less negative zeta-potential was noticed while incorporating lactose, mannitol and sorbitol, which indicates partial hiding of the charge and confirms higher interactions of cryoprotectant molecules with the particle surface previously highlighted by diameter changes. A slightly enhanced effect is visible for sorbitol compared to its isomer mannitol. This can be explained by the difference in molecular conformation of both compounds in water which has been reported to be a rigid planar zig-zag conformation for mannitol while sorbitol was able to bend and create more hydrogen bondings [22], which would favor interactions with the particle surface.

Freeze-thawing in absence of cryoprotectant did not affect significantly the nano-suspension, with mean diameters and polydispersities remaining close to their original values. Tyndall effect and bluish aspect of the suspensions were also conserved without formation of macroscopic aggregates visible. Absence of physical destabilization during the freezing step can be explained by the low solid content of the suspension and thus reduced probability of contact between the nanoparticles.

**Table 5.1: Evolution of size characteristics of PLGA nanospheres upon addition of cryoprotectants and after freeze-thawing**

| Cryoprotectant | Concentration<br>(% w/v) | After addition of cryoprotectant |               |                   | After freeze-thawing |               |
|----------------|--------------------------|----------------------------------|---------------|-------------------|----------------------|---------------|
|                |                          | $d_f/d_i$                        | $PdI_f/PdI_i$ | $\zeta_f/\zeta_i$ | $d_f/d_i$            | $PdI_f/PdI_i$ |
| None           | -                        | -                                | -             | -                 | 1.012                | 0.956         |
| Glucose        | 1                        | 1.002                            | 0.932         | 0.953             | 1.001                | 1.092         |
|                | 2.5                      | 0.982                            | 0.978         | 1.034             | 1.001                | 0.835         |
|                | 5                        | 0.952                            | 1.024         | 1.034             | 0.987                | 0.942         |
| Sucrose        | 1                        | 0.997                            | 0.960         | 1.050             | 1.001                | 0.864         |
|                | 2.5                      | 0.984                            | 0.992         | 1.003             | 0.990                | 0.974         |
|                | 5                        | 0.957                            | 0.995         | 1.023             | 1.003                | 0.852         |
| Trehalose      | 1                        | 0.996                            | 0.951         | 1.057             | 1.006                | 1.016         |
|                | 2.5                      | 0.969                            | 0.981         | 0.965             | 0.994                | 0.946         |
|                | 5                        | 0.941                            | 0.981         | 1.002             | 1.003                | 0.977         |
| Lactose        | 1                        | 0.966                            | 0.943         | 0.983             | 1.394                | 1.624         |
|                | 2.5                      | 0.959                            | 0.982         | 0.900             | 0.990                | 1.081         |
|                | 5                        | 0.946                            | 1.011         | 0.878             | 1.007                | 1.062         |
| Mannitol       | 1                        | 0.979                            | 0.957         | 0.952             | 1.482                | 2.187         |
|                | 2.5                      | 0.982                            | 0.953         | 0.988             | 2.168                | 3.285         |
|                | 5                        | 0.972                            | 0.938         | 0.963             | 3.829                | 3.852         |
| Sorbitol       | 1                        | 0.984                            | 0.981         | 0.988             | 0.981                | 0.989         |
|                | 2.5                      | 0.973                            | 0.965         | 0.923             | 0.981                | 0.864         |
|                | 5                        | 0.968                            | 0.933         | 0.915             | 0.984                | 0.934         |

Glucose, sucrose and trehalose were found effective for the cryoprotection of PLGA nanospheres, whatever concentration involved, and allowed conservation of the bluish translucent aspect of the suspensions. Limited changes in mean diameters occurred compared to the original cryoprotectant-enriched suspension. Chemical nature of the saccharides did not seem to have a significant influence on the cryoprotection intensity as previously observed in the literature for other polymeric nano-systems [18,23-24], which might also be linked to the fact that the native nano-suspension was itself resistant to the freeze-thawing. In the case of lactose however, a minimum of 2.5% w/v was necessary to maintain the integrity of the nanoparticles upon freezing without significant modification of mean diameter and polydispersity. A less effective cryo-protection towards PLGA nanoparticles while employing lactose compared to other saccharides was also observed by Saez et al. [18].

Nano-suspensions containing mannitol were clearly destabilized during the freeze-thawing process and showed large modifications in both size and polydispersity for all concentrations used. Analysis of the DLS profile highlighted the appearance of a large population around 900-1000 nm, attributed to the presence of mannitol crystals. This



polyol is known to recrystallize in suspension at low temperature (-15°C to -25°C) during the thawing part of the cycle [25-26]. Such crystallization has been reported at several occasions to compromise the integrity of nanoparticles [18,23,27] by exerting further mechanical stresses or by inducing phase separation and aggregation of the particles. Though the lyophilization process does not involve a real thawing stage in aqueous suspension and thus mannitol could still be able to provide efficient protection, it is however very likely that a similar recrystallization phenomenon will also take place during the primary drying stage. Sorbitol, on the other hand, did not disturb the nano-suspension significantly and displayed further decrease in the mean diameter in relationship with further osmotic effect during the freezing step. Influence of sorbitol concentration was negligible in accordance with the surface saturation existing above 1% w/v suggested after addition of the cryoprotectant.

### 5.3.2. Lyophilization and stability of the nano-carriers upon storage

Though the cryoprotectant-free nano-suspension was resistant to the freeze-thawing process, macroscopic and irreversible aggregation occurred during freeze-drying leading to a powder that could not be resuspended appropriately. Dramatic changes in size and polydispersities were observed by DLS analysis with ratios  $d_w/d_i$  and  $PdI_w/PdI_i$  averaging respectively 21.8 and 5.2, confirming that protective excipients must be added to the formulation. While incorporating lyoprotectants, visual aspect of the lyophilizates and resuspension properties were found strongly dependent on the nature of the sugar involved. Figure 5.2a summarizes the variations of mean diameter, PdI and zeta-potential variations for resuspended lyoprotected cakes just after lyophilization, while Figure 5.2b displays the variation for the same samples after storage of the cakes at 4°C for 10 weeks. Table 5.2 presents a summary of corresponding residual moisture content and aggregation scale observed after resuspension and storage.

Glucose led to the formation of a collapsed gel-like structure whatever concentration was used. Though attention was paid to maintain the primary temperature drying below the collapse temperature of this carbohydrate, the vitreous matrix was logically not as stable as other carbohydrates with higher  $T'_g$  and thus more likely to lose its porous structure by collapsing. Another explanation could be a reduction of the  $T'_g$  linked to the incorporation of PLGA nanoparticles in the carbohydrate matrix. Absence of such disturbance has however been reported for similar polymeric nanoparticles [18,23], with in general even slightly higher  $T'_g$  observed which should rather be in favor of

stabilization of the glassy matrix. Despite this poor cake aspect and stickiness, resuspension could be achieved very easily and PLGA particles retained their nanometric size without significant aggregation. A similar phenomenon was described by Hirsjärvi et al. [28] and indicates that, though glucose cannot form appropriate cake structures under the lyophilization conditions implemented in this study, it was still able to provide a stabilizer effect for the nanoparticles. Resuspension after 10 weeks of storage was however not satisfying with clear aggregation further occurring, except for the lowest concentration of glucose, as a result of the limited bulking effect of the collapsed cakes.

**Table 5.2: Residual moisture content and aggregation scale observed after resuspension of lyophilized cakes just after freeze-drying and after 10 weeks storage at 4°C ((√) No aggregation / (+) Scarce aggregation /some large particles detected by DLS / (++) Significant aggregation/multimodal population detected by DLS / ND: not determined)**

| Cryoprotectant | Concentration (% w/v) | After freeze-drying |                       | After storage (10 weeks, 4°C) |                       |
|----------------|-----------------------|---------------------|-----------------------|-------------------------------|-----------------------|
|                |                       | Aggregation scale   | Residual moisture (%) | Aggregation scale             | Residual moisture (%) |
| None           | -                     | ++                  | ND                    | ND                            | ND                    |
| Glucose        | 1                     | √                   | ND                    | √                             | ND                    |
|                | 2.5                   | √                   | 1.6                   | ++                            | 2.1                   |
|                | 5                     | √                   | 5.5                   | ++                            | 3.8                   |
| Sucrose        | 1                     | +                   | 3.4                   | ++                            | 0.1                   |
|                | 2.5                   | ++                  | 0.6                   | ++                            | 0.1                   |
|                | 5                     | ++                  | 0.4                   | ++                            | 0.1                   |
| Trehalose      | 1                     | +                   | 3.6                   | √                             | 3.1                   |
|                | 2.5                   | √                   | 3.0                   | √/+                           | 2.9                   |
|                | 5                     | √                   | 2.3                   | √/+                           | 2.1                   |
| Lactose        | 1                     | +                   | 4.3                   | +                             | 2.9                   |
|                | 2.5                   | √                   | 1.9                   | +                             | 3.2                   |
|                | 5                     | √                   | 2.3                   | ++                            | 1.9                   |
| Mannitol       | 1                     | ++                  | 1.6                   | ++                            | 1.0                   |
|                | 2.5                   | ++                  | 1.4                   | ++                            | 1.2                   |
|                | 5                     | ++                  | 1.1                   | ++                            | 1.0                   |
| Sorbitol       | 1                     | ++                  | 3.2                   | ++                            | 1.0                   |
|                | 2.5                   | ++                  | 1.6                   | ++                            | 2.2                   |
|                | 5                     | ++                  | 1.2                   | ++                            | 1.3                   |

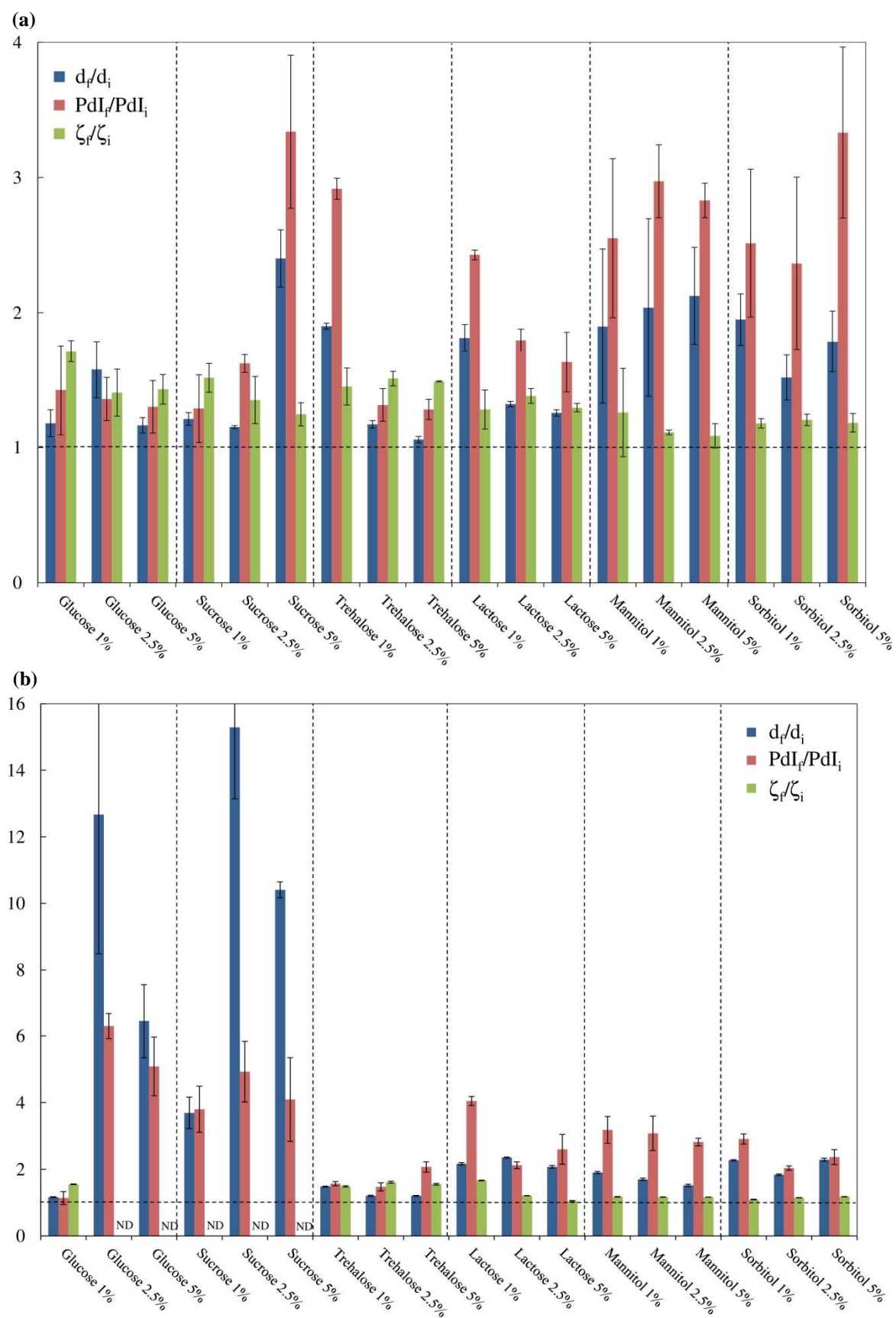


**Figure 5.2: Evolution of mean diameter, polydispersity and zeta-potential of PLGA nanospheres in lyophilized cakes resuspended just after lyophilization (a) or after 10 weeks storage at 4°C (b) (ND: not determined)**

Among disaccharides, trehalose and lactose both allowed formation of white fibrous cakes with a uniform aspect and a dry volume identical to the original colloidal suspension. All cakes were easily reconstitutable with the translucent and bluish aspect of the original suspensions. Moisture content averaged 2-4% for both lyoprotectants and did not significantly evolve over time. Presence of some large aggregates and significant modification of size and polydispersity was detected for both compounds at 1% w/v, suggesting that a minimum concentration is required to ensure both cryo and lyo-protection. Further increase in trehalose concentration resulted in reduced modifications of mean diameter and polydispersity and better conservation of the integrity of the particles just after lyophilization as well as upon storage. In the case of lactose, 2.5 and 5% w/v were characterized by acceptable nano-sizes though polydispersity remains relatively high compared to trehalose. Variations upon storage were also found more intense, with appearance of aggregates and visual reduction of the homogeneity of the suspensions.

Sucrose also allowed formation of cakes but a tendency to collapse while brought back to room temperature and heterogeneity between replicates were observed (sticky layer at the bottom, dry crust on the top, etc.). Presence of large aggregates and turbid aspect were obtained after reconstitution of the suspensions. Just after lyophilization, Karl-Fisher analysis showed extremely low residual moisture content except for the lowest concentration of sucrose. Further reduction of moisture content occurred upon storage for all samples with a significant loss for 1%w/v. The preferred explanation for this behavior is a partial collapse of the cake structure due to high residual moisture and the recrystallization of sucrose. Sucrose displays a lower glass transition in the dry state than lactose and trehalose (62-77°C) which could have been further reduced due to the plasticizer effect of residual water and would explain the collapse at room temperature. At temperatures causing the collapse of the cake, sucrose crystallization has been evidenced to occur rapidly [17,29] and to be accompanied by a sudden loss of moisture content, which is consistent with our observations. Low moisture contents for 2.5 and 5 % w/v indicate that crystallization has already occurred. Though mean diameter and polydispersity of resuspended nanoparticles remained in acceptable ranges for 1 and 2.5% w/v, crystallization visually further occurred during the storage period and did not allow maintaining integrity of the nanoparticles.

For the same concentration, trehalose was overall found to provide the highest level of protection just after freeze-drying and upon 10 weeks of storage compared to the other

saccharides. Superiority of trehalose for lyoprotection has been proven at many occasions [19,30] and linked to the absence of internal hydrogen bonding that allow a flexible molecular structure and higher possibility of interactions with the particle surface during drying. High transition temperature in the dry state and low hygroscopicity are also recognized properties [31] that explain the superior stabilization of the nano-carriers upon storage.

Mannitol- and sorbitol-enriched suspensions resulted in acceptable cakes with similar initial volume and lower residual moisture than trehalose and lactose. Cakes were however non-porous and brittle and led to poorly redispersed suspensions with high levels of aggregation and large modifications in terms of size and polydispersity. No significant difference was noticed between both polyols, contrary to what was observed after the freeze-thawing. It is also interesting to mention that no significant modification of size characteristics occurred upon storage, highlighting that mannitol and sorbitol are still effective for the stabilization of the nanoparticles upon storage.

Comparison of zeta-potential values just after freeze-drying for the different lyoprotectants and concentrations involved in this study confirmed the superiority of polyols already observed in section 5.3.1. For all compounds, nanoparticle surfaces were found more negatively charged than the original and protectant-enriched suspensions (ratio  $\zeta_f/\zeta_i > 1.1$ ), with negligible evolution upon storage. As described in Chapter 2, incorporation of natamycin in PLGA formulations led to slightly less negatively charged nanospheres due to partial absorption of natamycin, in a positively charged state in MilliQ water. Reduced zeta-potentials indicate in our case desorption of natamycin from the surface of the PLGA nanoparticles during the lyophilization process, occurring at a larger extent when saccharides are used. Polyols on the other hand ensured good conservation of the original surface properties of the particles which is consistent with the higher surface protection already observed upon addition and freeze-thawing.

### **5.3.3. Thermal analysis of lyophilized PLGA cakes**

Freeze-dried PLGA cakes prepared from suspensions containing 2.5% w/v of lyoprotectant were analyzed after lyophilization for further understanding of their physical state. Figure 5.3 presents thermograms obtained for the pure excipient (native or after lyophilization) and for lyophilized protectant-enriched PLGA suspension.

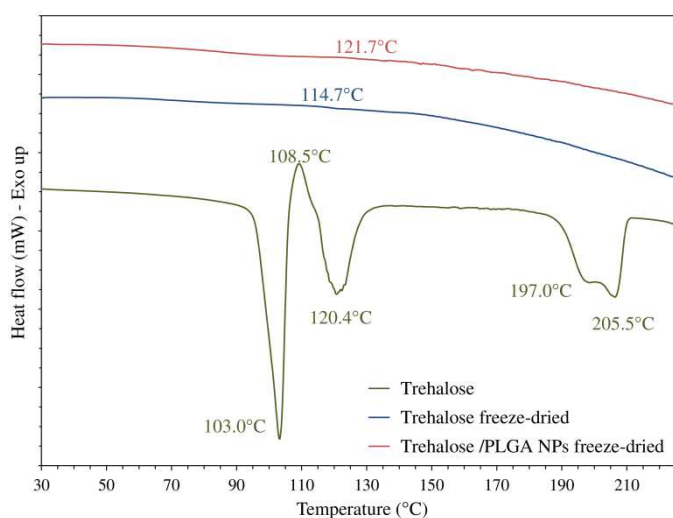
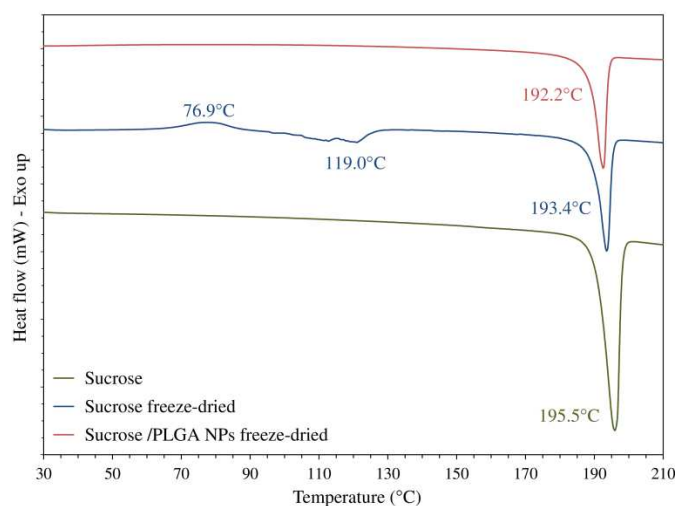
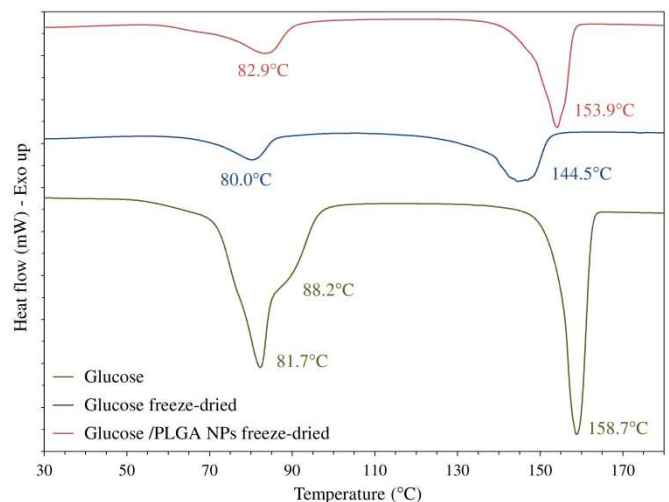
Analysis of glucose thermograms confirmed the presence of adsorbed water with broad endotherms corresponding to the loss of water molecules around 80-83°C for both lyophilized samples. Melting points, observed at 158.7°C for native glucose [16], were slightly shifted respectively to 144.5°C and 153.9°C in presence or absence of PLGA nanoparticles, confirming a plasticizer effect due to residual moisture. Glass transitions were not detected in the range 30-37°C in accordance with the already sticky and viscous aspect of the samples that indicates a glass transition below room temperature.

Native crystalline sucrose was characterized by a sharp endotherm peak at 195.5°C attributed to melting [16-17]. Freeze-dried sucrose presented a different pattern with the presence of an exotherm peak at 76.9°C followed by a broad endotherm, in accordance with the transition of amorphous to crystalline sucrose and subsequent loss of water [17,29]. In presence of PLGA nanoparticles, absence of crystalline transition and water removal confirmed the recrystallization of the cake and the low moisture content determined by Karl-Fisher titration. The melting point was in this case shifted to lower values (192.2°C) which could indicate a slight plasticizer effect of the nanoparticles themselves.

Dihydrate trehalose displayed a complex DSC thermogram [32-33] with a first endotherm at 103.0°C attributed to the loss of one molecule of water, followed by an exotherm at 108.5°C attributed to the partial transformation into another crystalline polymorph and a less defined endotherm at 120.4°C allocated to the loss of the second molecule of water. The two endotherms at 197°C and 205.5°C correspond to the melting of both anhydrous crystalline polymorphs forms of trehalose. Observations of lyophilized samples in presence or absence of PLGA nanoparticles confirmed the amorphous nature of cakes with glass transition visible respectively at 114.7°C and 121.7°C, preceded by low intensity endotherms relative to loss of residual water centered at 86.4°C and 95.4°C.

DSC profile of anhydrous  $\beta$ -lactose presented a glass transition at 118.5°C followed by a relaxation endotherm and a melting point at 240.2°C [34]. Freeze-dried sample was characterized by a typical amorphous profile [35] with a glass transition at much lower temperature (98.7°C). Presence of a melting point at 217.5°C and a broad endotherm between 65-85°C indicates however partial formation of crystalline monohydrate  $\alpha$ -lactose. In presence of PLGA nanospheres, the DSC thermogram revealed the presence of both  $\alpha$ -monohydrate and anhydrous  $\beta$  polymorph, with for this latter glass transition, melting point and degradation shifted to lower values, indicating plasticization effect due

to the nanoparticles themselves. Partial transformation to  $\alpha$ -lactose monohydrate in the cakes, known to be less soluble in water than the  $\beta$ -polymorph and possible further evolution upon time [36] could explain difficulties to redisperse lactose samples after storage and high levels of polydispersities identified in section 5.3.2.



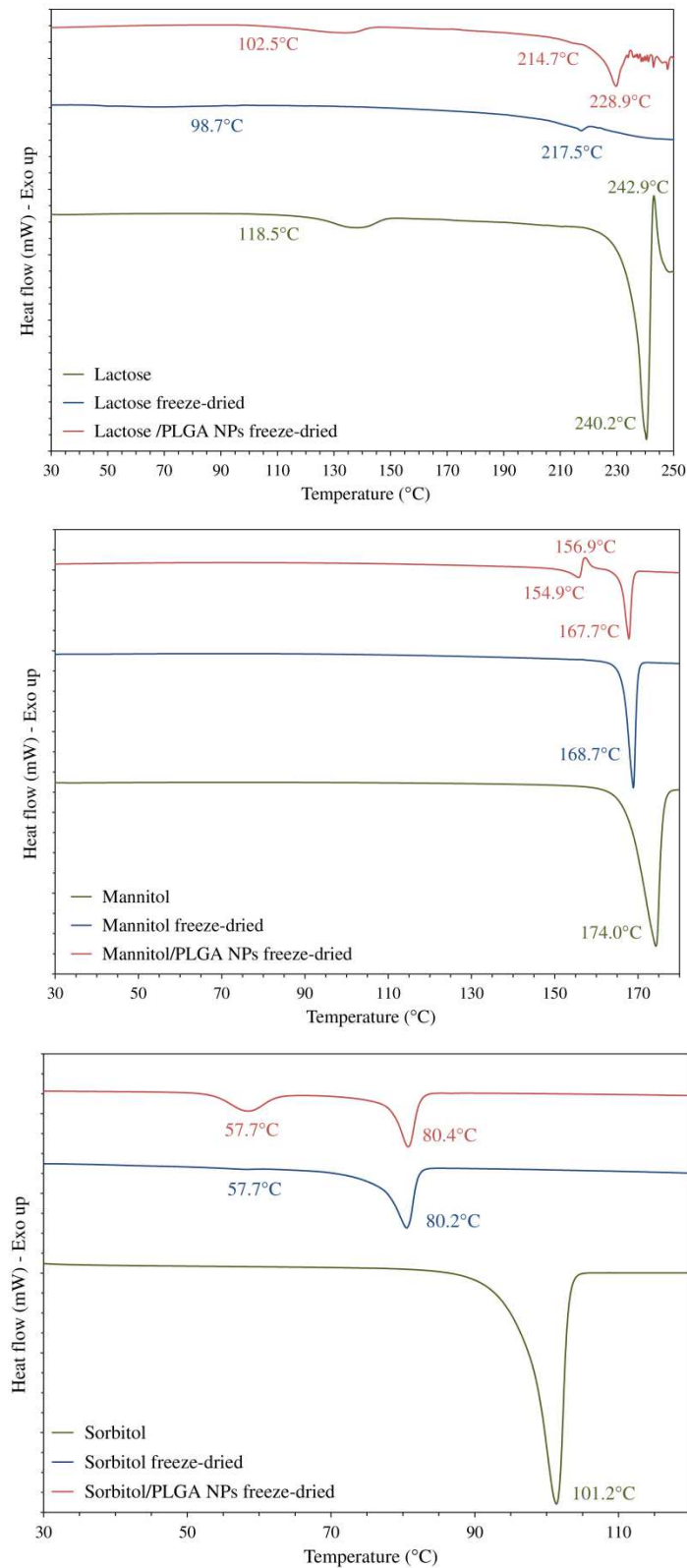


**Figure 5.3: DSC thermograms of lyoprotectants (green), freeze-dried lyoprotectants (blue) and freeze-dried samples containing PLGA nanospheres (red)**



Native mannitol presented a typical anhydrous crystalline melting point at 174.0°C. Mannitol was obtained in crystalline form after freeze-drying with a slightly shifted melting point at 168.7°C, probably due to the presence of residual moisture. Incorporation of PLGA nanospheres further decreased the melting point to 167.7°C and was accompanied by other endotherm/exotherm events at 154.9°C and 156.9°C which might be linked to the transition and degradation of another polymorphic form [26]. Crystalline physical state of mannitol after freeze-drying explains the brittle aspect of the cake and high levels of aggregation observed.

Similarly to mannitol, sorbitol was characterized by a crystalline profile both in its native form and after freeze-drying, which explains the brittle aspect of the cakes. Pure sorbitol was defined by a melting point at 101.2°C, representative from its anhydrous  $\gamma$ -polymorph. Freeze-dried samples displayed two endotherms around 57.7°C and 80.4°C specific from dehydration and melting of the monohydrate  $\alpha$ -form of sorbitol [37], evidencing a change of conformation of sorbitol during recrystallization.

#### **5.3.4. Natamycin stability upon storage**

Stability of natamycin in lyophilized formulations stored at -20°C, 4°C and 25°C in vials sealed at ambient relative humidity at the end of the freeze-drying process was studied over 10 weeks. Results obtained in presence of the different lyoprotectants and concentrations are presented in Figure 5.4.

Trehalose was once again found to be the most efficient saccharide with losses of preservative remaining below 8% at both -20°C and 4°C. Storage at 25°C was found a bit less favorable, which might be due to higher molecular mobility of natamycin within the cake linked to the temperature approaching the glass transition temperature of the PLGA nanospheres (before 47.7°C as determined in Chapter 2). No significant differences were observed between the three different concentrations present in the sample, though 1% w/v proved earlier to not be able to maintain nanoparticles integrity after freeze-drying.

Sucrose gave slightly higher levels of degradation with again no large difference for the three concentrations at -20°C and 4°C. Losses were enhanced at 25°C and far superior to trehalose due to previously reported recrystallization of sucrose at ambient temperature and absence of protection towards leakage of the preservative from the nanoparticles.

Lactose on the other hand showed a clear destabilization of natamycin compared to trehalose whatever concentration was used, with an enhanced effect for storage above 4°C. A similar but intensified behavior was visualized for samples containing glucose. Observations of HPLC profiles indicated a clear decrease of the signal attributed to natamycin compared to other impurities detected at 303 nm (classically around 94-97% of relative area in native natamycin, while glucose and lactose samples stored at 25°C reached respectively 70-78% and 86-92%). The analysis of the profiles (Figure 5.5) highlighted the presence of two impurities for glucose- and lactose-containing samples, identified as molecules similar to natamycin where the amino group has been replaced by a hydroxyl group or where the first double bond in the tetraene evolved from conformation trans to cis [38]. Glucose and lactose are both reducing carbohydrates, i.e. that they are able to react with amines in presence of water [39] which could explain the transformation in hydroxyl group for the first impurity. Higher residual moisture left in glucose lyophilized cakes and non-glassy state due to the collapsed structure are likely to enhanced mobility of natamycin and reactions with the sugar, which explains superior losses observed while using glucose. For this sugar, the determination of natamycin content just at the end of the lyophilization also showed the presence of this impurity at higher level than for other samples (85-91% of relative area), which highlighted already some degradation in the original suspension or during the freeze-drying process. Changes in conformation of the tetraene in the case of the second impurity might be explained by a more favorable interaction with the sugar compared to the native form of natamycin.

Mannitol and sorbitol were both suitable for the long-term protection of natamycin in lyophilized samples, though temperature of storage seemed to have a larger importance than for carbohydrates. Limited losses in these matrices despite a more brittle cake and limited protection of the nanoparticle size might be linked to previous observations regarding low levels of desorption of natamycin from the surface of the particles noticed by zeta-potential and better surface coverage likely to provide a much better barrier towards leakage of natamycin in the outer cake during storage. Slightly higher losses for sorbitol might be linked to a higher hygroscopicity of this molecule compared to mannitol, as revealed by the presence of a hydrate form in DSC.

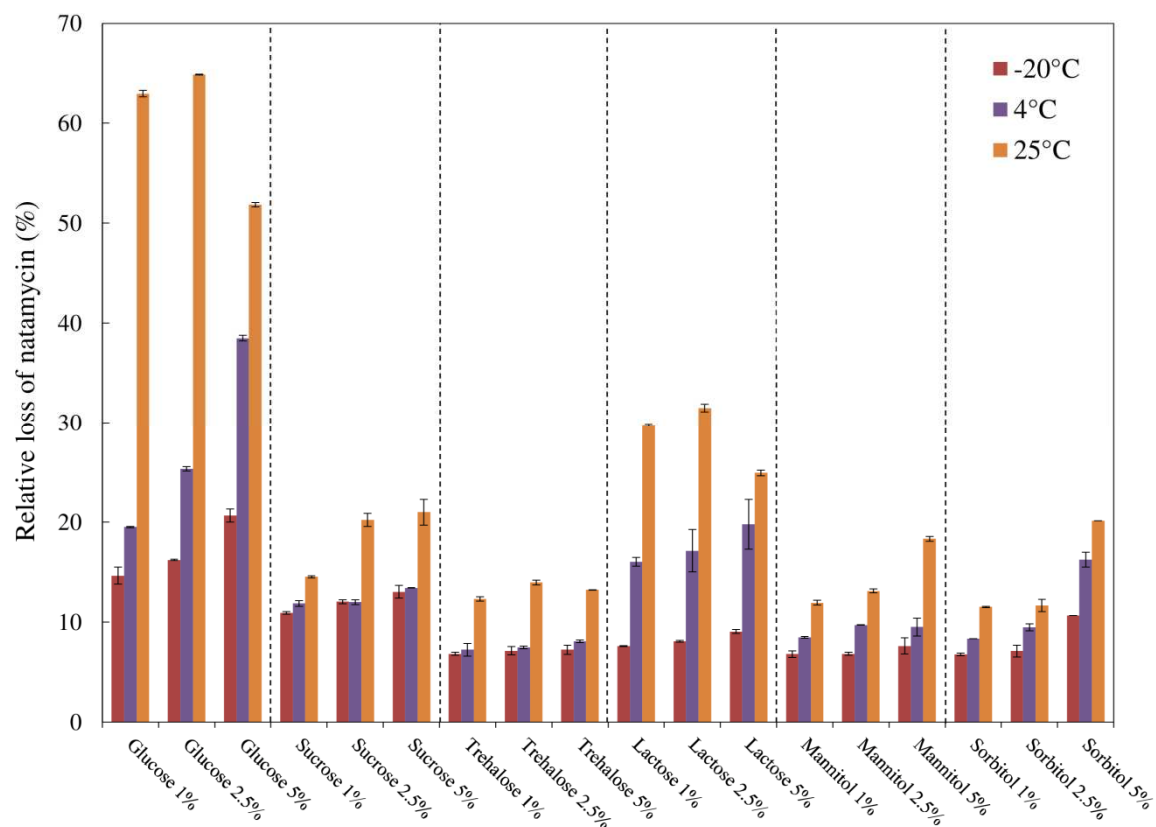


Figure 5.4: Natamycin losses in lyophilized PLGA nanospheres after 10 weeks storage at -20°C, 4°C or 25°C as a function of lyoprotectant type and concentration

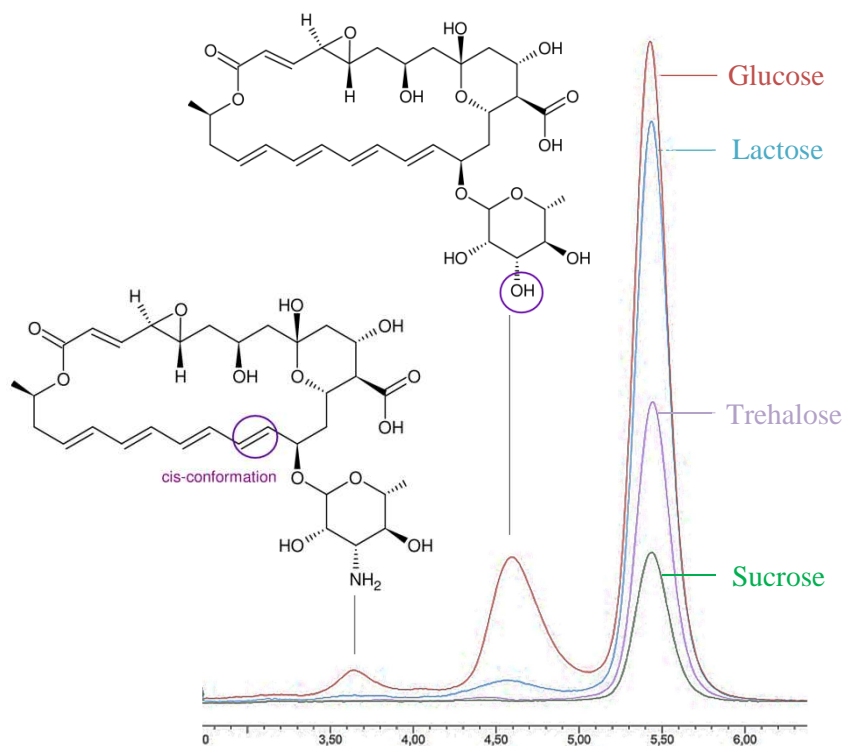


Figure 5.5: HPLC profiles of natamycin and impurities in lyophilized PLGA nanoparticles (cryoprotectant 1%w/v) after 10 weeks storage at 25°C

### 5.3.5. Conclusions for PLGA nanospheres

Glucose, sucrose, trehalose, lactose, mannitol and sorbitol added at 1, 2.5 and 5% w/v were evaluated for the cryo/lyo-protection of natamycin-loaded PLGA nano-suspensions. Addition of these protective excipients was found to have limited effect on the initial size characteristics of the suspension with only a slight osmotic dehydration observed. Efficient cryoprotection was observed during freeze-thawing studies for all samples, except mannitol which showed crystallization upon re-heating. The original nano-suspension without cryoprotectant was however also found quite resistant to the freezing process without noticeable aggregation of the nanoparticles.

While going to the drying stages however, presence of lyo-protectants was found essential for the preservation of nanoparticles integrity and good resuspension. Saccharides offered overall better conservation of the size characteristics than polyols. Among the carbohydrates, trehalose and lactose above 2.5% w/v displayed the best lyophilized cake aspect, resuspension properties and conservation of nanoparticle integrity. Polymorphic changes of lactose during freeze-drying led however to the formation of large aggregates and non redispersible fractions upon storage. Though glucose was able to sustain the integrity of the nanoparticles, the samples displayed a collapsed aspect and a high residual moisture content which did not enable stabilization on the long-term nor easy processing. Sucrose also did not allow formation of cakes with acceptable properties due to a high sensitivity to crystallization that limited the conservation of nanoparticle properties upon storage. Evaluation of natamycin stability in the formulations confirmed the superiority of trehalose over other saccharides, while the reducing sugars glucose and lactose were found reactive towards natamycin, inducing structural changes detrimental for the antifungal activity.

Polyols resulted in the formation of brittle crystalline cakes unable to maintain nanoparticle integrity during the lyophilization process. Upon storage however, size characteristics and zeta-potential did not vary significantly which indicates limited subsequent aggregation of PLGA nanospheres and reduced desorption/leakage of natamycin out of the particles compared to saccharides, confirmed by an acceptable stability of the preservative upon storage.

Overall, best compromise in terms of acceptable cake aspect, sustained initial characteristics and stability upon storage of both natamycin and nano-carriers was obtained for trehalose above 2.5% w/v.

## 5.4. Lyophilization of liposomal suspensions

The preliminary screening of the six protective excipients used for PLGA nanospheres highlighted a clear destabilization of the liposomes in presence of sorbitol and mannitol, which might be linked to their crystallization and the known mechanical fragility of liposomes. Glucose, sucrose, trehalose and lactose were selected for further use in this study at concentrations ranging from 1 to 5% w/v (ratios liposome/protectant 1:5.5 to 1:28). Liposomes with or without inclusion of cholesterol and ergosterol were investigated and the effect of nature and concentration of sterol on the final lyophilized powder was assessed. Liposomes were evaluated after addition of the cryoprotectants, freeze-thawing, freeze-drying and storage for 10 weeks at 4°C, as previously performed for PLGA nanospheres.

### 5.4.1. Lyophilization of sterol-free liposomes

#### 5.4.1.1. Addition of cryoprotectants and freeze-thawing

Table 5.3 illustrates the effect of cryoprotectant addition on the size characteristics and zeta-potential of the liposomal suspensions. A reduction of mean diameter of liposomes in direct relationship with an increase in cryoprotectant concentration was observed for all carbohydrates involved in the formulations. For similar concentrations, higher disturbances were observed in the following order: lactose > sucrose > trehalose > glucose. Polydispersities were remarkably unchanged for glucose, sucrose and trehalose, indicating that the change of mean diameters is only linked to shrinkage of the liposomes in relationship with the osmotic pressure effect of the carbohydrates present in the medium. Reduction of the zeta-potential was overall observed for the three saccharides and confirmed interactions with the phospholipid heads. In the case of lactose however, large variations of size, polydispersity and in particular zeta-potential were observed. Such a behavior has been previously reported by Wessman et al. [40] and attributed to the osmotic chock created while adding lactose as a powder in a liposomal suspension originally prepared in water, which is also the approach chosen in this study. The authors highlighted a reduction in mean diameter, disappearance of spherical unilamellar vesicles and formation of either collapsed or multi-lamellar structures. Incorporation of lactose within the bilayer due to destabilization of the structure might explained the zeta-potential variations.

Relatively good resistance of the native liposomal suspension upon application of the freeze-thawing cycle was observed, with only a slight reduction of mean diameter linked to the presence of smaller population detected by DLS around 15 nm. Several authors reported clear instability of liposomes during freeze-thawing cycles [13,41] while crossing the gel-liquid transition temperature  $T_m$  of the bilayer during the cooling and reheating processes. As mentioned in Chapter 3, Epikuron 145V is a complex mixture of soybean phospholipids all having individual transition temperatures far below 0°C. DSC analysis of Epikuron 145V liposomes did not enable to detect any transition temperature on the range -70°C/0°C. It is thus highly likely that our liposomal suspensions did not experience transition and rearrangement under the freeze-thawing conditions studied here, which explains the physical stability observed.

**Table 5.3: Evolution of size characteristics of liposomes upon addition of cryoprotectants and freeze-thawing**

| Cryoprotectant | Concentration<br>(% w/v) | After addition of cryoprotectant |               |                   | After freeze-thawing |               |
|----------------|--------------------------|----------------------------------|---------------|-------------------|----------------------|---------------|
|                |                          | $d_f/d_i$                        | $PdI_f/PdI_i$ | $\zeta_f/\zeta_i$ | $d_f/d_i$            | $PdI_f/PdI_i$ |
| None           | -                        | -                                | -             | -                 | 0.912                | 1.085         |
| Glucose        | 1                        | 1.017                            | 1.025         | 0.916             | 0.860                | 0.962         |
|                | 2.5                      | 0.982                            | 1.007         | 0.921             | 0.867                | 0.948         |
|                | 5                        | 0.923                            | 1.000         | 0.937             | 0.869                | 0.920         |
| Sucrose        | 1                        | 0.944                            | 1.012         | 1.335             | 0.915                | 1.003         |
|                | 2.5                      | 0.868                            | 1.048         | 0.770             | 0.914                | 0.890         |
|                | 5                        | 0.852                            | 1.074         | 0.911             | 0.893                | 0.841         |
| Trehalose      | 1                        | 0.966                            | 1.022         | 1.107             | 0.890                | 0.974         |
|                | 2.5                      | 0.918                            | 1.085         | 0.930             | 0.905                | 0.872         |
|                | 5                        | 0.860                            | 1.034         | 1.014             | 0.893                | 0.880         |
| Lactose        | 1                        | 0.864                            | 0.974         | 1.064             | 0.922                | 0.819         |
|                | 2.5                      | 0.783                            | 0.898         | 0.600             | 0.968                | 0.797         |
|                | 5                        | 0.752                            | 0.863         | 0.533             | 0.961                | 0.858         |

Freeze-thawing in presence of carbohydrates resulted in further reduction of mean diameter and polydispersities compared to the protectant-enriched suspensions. Relative effect of saccharides on size reduction was found more intense for glucose > trehalose > sucrose > lactose and is in direct relationship with the respective ability of each sugar to form hydrogen bonding with phospholipid heads and to act as an efficient water replacer. Monosaccharides like glucose are indeed known to interact more tightly with phospholipids compared to disaccharides due to their reduced molecular weight and their higher molecular flexibility [42], which explains the superior shrinkage of liposomes

observed. Within disaccharides, trehalose is generally recognized as the most efficient cryo-protectant compared to sucrose and lactose due to a higher flexibility of the glycosidic bond [43] as well as the absence of intramolecular hydrogen bonding [19,30-31,42] that favors intermolecular interactions with phospholipids. Limited modifications for lactose-containing samples tend to indicate that further collapsing and rearrangement of the vesicular structures do not occur significantly during the freezing step. Overall reduced polydispersities for all carbohydrates after freeze-thawing suggested homogenization of the formulations due to further osmotic dehydration and displacement of water molecules linked to higher levels of interactions between sugar and phospholipid heads.

#### 5.4.1.2. Lyophilization and stability of liposomes upon storage

The native liposomal suspension was as expected not resistant to the drying process and led to the formation of yellow sticky deposits similar to raw lecithins on the wall of the cryo-vials. Resuspension could not be achieved appropriately and DLS analyses confirmed the loss of liposomal structure and formation of several populations of particles. Figure 5.6 presents the evolution of size characteristics and zeta-potential after freeze-drying and after storage at 4°C for 10 weeks for the four carbohydrates studied.

As previously reported for PLGA nanospheres, process conditions used in the primary drying led to the formation of collapsed glucose structures in which yellow coloration was additionally observed and pointed out partial phase separation of the lecithins. After redispersion, DLS analyses highlighted the presence of a small population (15 nm) and an overall reduction of the mean diameter, though polydispersity and zeta-potential remain very stable compared to the original lyoprotectant-enriched suspension. Stability upon storage was however not conserved with a clear increase in mean diameter and polydispersity upon storage, which might be linked to further phase separation or even degradation of the phospholipids themselves due to high residual moisture.

Sucrose was also not found satisfying for the lyoprotection of Epikuron 145V liposomes. As previously noticed for PLGA nanospheres and also reported in the literature for other liposomal systems [44], cakes evolved rapidly after lyophilization due to recrystallization of the sucrose close to room temperature. Resuspension was however possible and allowed conservation of liposomal structure accompanied with a small micellar population around 15 nm for all compositions. Mean diameters and polydispersities were reduced compared to the original suspension. Upon storage,

crystallization further occurred for the 5% w/v sample and appearance of a yellow coloration indicated phase separation of the lecithins. Destabilization and poor reconstitutability after storage were reflected in a high polydispersity and large increase in mean diameter for this sample. Concentrations of 1 and 2.5% w/v allowed better conservation of size characteristics. However, more negative zeta-potentials, despite the surface coverage by sucrose, would tend to indicate hydrolysis of the phospholipids into negatively charged phosphatidic acid [3].

Trehalose and lactose gave the best cake aspect as previously reported for PLGA nanospheres. As for cryoprotection, lyoprotective effect of trehalose was more intense than sucrose and lactose and led to further reduction of the size characteristics of the liposomes though remaining in an acceptable nano-range, confirming the ability of trehalose to stabilize small unilamellar vesicles previously reported in the literature [45-47]. Lower modifications were obtained for the highest concentration of trehalose involved. Zeta-potential was relatively well conserved compared to the native suspensions, which indicates that strong interactions were already established at the surface of the liposomes right after the addition of lyoprotectant and that they could be maintained over the whole freeze-drying process. Upon storage, 5% w/v gave the best stabilization properties and adequate reconstitution of the nano-liposomes without significant evolution of size characteristics. For all concentrations, zeta-potential evolved to slightly less negatively charged surface which corresponds to further interactions with the trehalose.

Lactose-containing lyophilized samples displayed the most limited impact on the size and polydispersities of liposomes compared to the corresponding protectant-enriched suspensions, with ratios  $d_f/d_i$  close to 1 for concentrations superior to 2.5% w/v. For these samples, zeta-potential was however significantly more negative than before freeze-drying, which indicates partial desorption of lactose and equilibration of surface charge towards the values obtained for liposomes alone in water. Upon storage, slight augmentations of size and polydispersity were visible, with 1% w/v giving overall the best stabilization. Concentrations 2.5 and 5% w/v led to large variations, which might be attributed by the desorption of lactose previously mentioned, and were also accompanied by the formation of a fraction not redispersible in water, believed to be the polymorphic monohydrate  $\alpha$ -form observed for PLGA nanospheres.



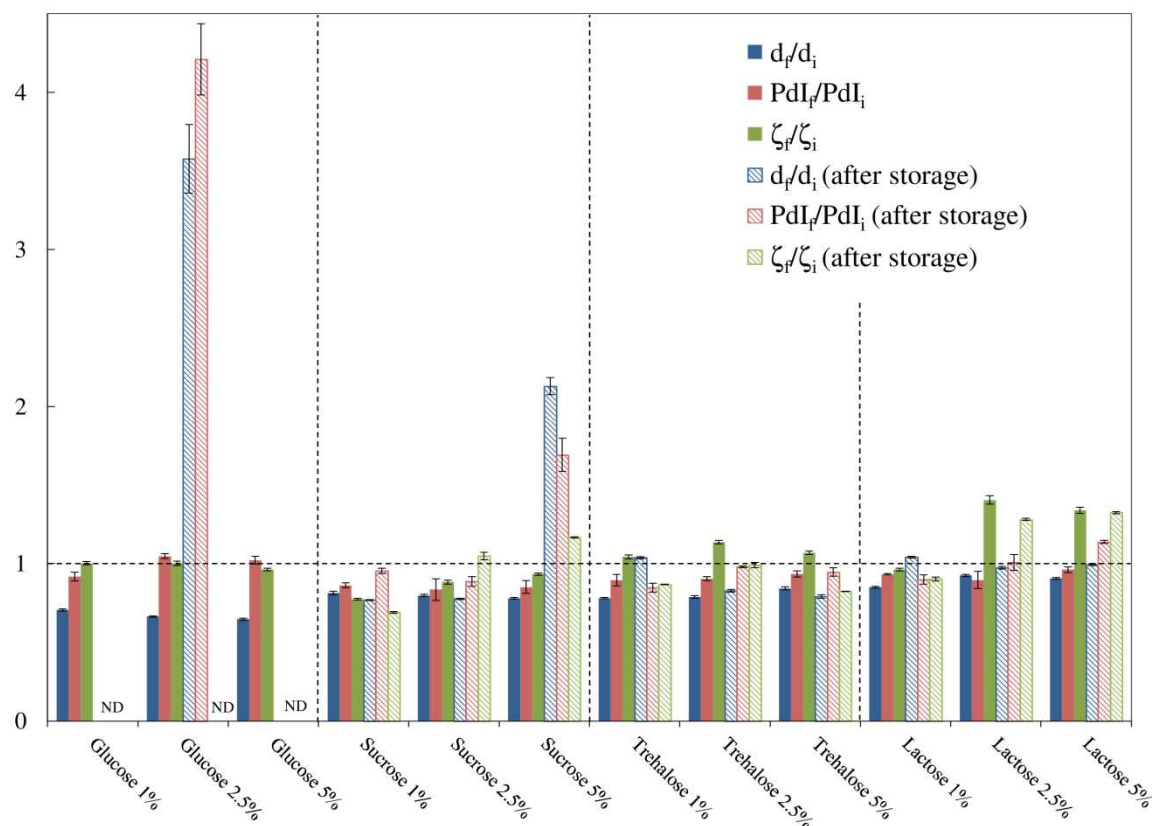


**Figure 5.6: Evolution of mean diameter, polydispersity and zeta-potential of liposomes in lyophilized cakes resuspended just after lyophilization or after 10 weeks storage at 4°C (ND: not determined)**

## 5.4.2. Lyophilization of sterol-enriched liposomes

### 5.4.2.1. Addition of cryoprotectants and freeze-thawing

Further studies on sterol-enriched liposomes were performed with sucrose, trehalose and lactose to determine if the presence of sterols had an influence on the lyophilization process, particularly on the effectiveness of the protective excipient. Table 5.4 illustrates the effect of cryoprotectant addition (5% w/v) and freeze-thawing cycle on the size characteristics and zeta-potential of the liposomal suspensions.

Slight modifications of mean diameter and polydispersities were observed after addition of cryoprotectants in sterol-enriched formulation compared to the sterol-free sample. In the case of sucrose and trehalose, mean diameters were inferior to the sterol-free samples though polydispersity remained stable. Reduced values of  $\zeta_f/\zeta_i$  indicated additionally a higher level of interaction between the carbohydrate and the bilayer due to the presence of sterols. While increasing the relative concentration of cholesterol and ergosterol incorporated in the bilayer, opposite variations were observed due to possible competition between the sterol and the sugar. Presence of cholesterol has been reported to

help interactions of the phospholipid molecules with carbohydrates by intercalation in the bilayer and disruption of lipid-lipid intermolecular interactions [48-49], which explains reduction of diameters and more positive zeta-potential while increasing the concentration. Effect of ergosterol was found superior to the one of cholesterol while considering the same concentration, though increase in ergosterol content seemed detrimental for the interaction with the sugar. Known higher ordering effect of ergosterol in phospholipid bilayer [50-51] could explain its superiority over cholesterol at the same concentration in relationship with more intense disruption of lipid-lipid interactions. Ergosterol brings however a higher level of rigidity which could - above a certain concentration - make hydrogen bonding more difficult to achieve and could explain the variation of size and zeta-potential.

**Table 5.4: Evolution of size characteristics of sterol-free and sterol-enriched liposomes upon addition of cryoprotectants (5% w/v) and freeze-thawing**

| Cryoprotectant<br>(5% w/v) | Sterol<br>composition | After addition of cryoprotectant |               |                   | After freeze-thawing |               |
|----------------------------|-----------------------|----------------------------------|---------------|-------------------|----------------------|---------------|
|                            |                       | $d_f/d_i$                        | $PdI_f/PdI_i$ | $\zeta_f/\zeta_i$ | $d_f/d_i$            | $PdI_f/PdI_i$ |
| Sucrose                    | No sterol             | 0.852                            | 1.074         | 0.911             | 0.893                | 0.841         |
|                            | CHOL/L 1:45           | 0.833                            | 1.027         | 0.823             | 0.899                | 0.837         |
|                            | CHOL/L 1:18           | 0.825                            | 1.053         | 0.624             | 0.939                | 0.815         |
|                            | ERG 1:90              | 0.818                            | 1.000         | 0.597             | 0.906                | 0.821         |
|                            | ERG 1:45              | 0.827                            | 1.015         | 0.643             | 0.891                | 0.851         |
| Trehalose                  | No sterol             | 0.860                            | 1.034         | 1.014             | 0.893                | 0.880         |
|                            | CHOL/L 1:45           | 0.837                            | 1.012         | 0.884             | 0.889                | 0.865         |
|                            | CHOL/L 1:18           | 0.823                            | 1.022         | 0.651             | 0.939                | 0.892         |
|                            | ERG 1:90              | 0.830                            | 1.013         | 0.614             | 0.901                | 0.891         |
|                            | ERG 1:45              | 0.824                            | 1.044         | 0.696             | 0.896                | 0.876         |
| Lactose                    | No sterol             | 0.752                            | 0.863         | 0.533             | 0.961                | 0.858         |
|                            | CHOL/L 1:45           | 0.791                            | 0.939         | 0.749             | 1.027                | 0.917         |
|                            | CHOL/L 1:18           | 0.832                            | 0.850         | 0.390             | 1.090                | 0.797         |
|                            | ERG 1:90              | 0.782                            | 0.913         | 0.370             | 1.032                | 0.883         |
|                            | ERG 1:45              | 0.817                            | 0.848         | 0.403             | 1.041                | 0.818         |

A different evolution of mean diameters and polydispersities was obtained in the case of lactose with higher concentration of sterols being favorable to size conservation and higher homogeneity. The variations in zeta-potential were however still significant, confirming that destabilization due to the osmotic shock created by the addition of lactose was not counteracted by the presence of sterol. In the case of ergosterol, smaller and larger populations even appeared in the DLS profile and might indicate some

recrystallization of the poorly water-soluble ergosterol due to its phase separation from the bilayer.

Upon freeze-thawing, further reduction in size and polydispersity were observed for sucrose- and trehalose-containing samples, as previously described for sterol-free liposomes, without possibility to highlight significant benefits of the presence of sterols. Superiority of lactose during the freeze-thawing was once again observed with very limited evolution of mean diameters, though polydispersity further decreased compared to the cryoprotectant-enriched formulations confirming further osmotic dehydration particularly for the highest concentration of sterol.

#### 5.4.2.2. Lyophilization and stability of sterol-enriched liposomes upon storage

Figure 5.7 displays size characteristics and zeta-potentials obtained after freeze-drying and storage of the lyophilizates for 10 weeks at 4°C.

Crystalline and yellow aspect of lyophilized sucrose-containing samples previously reported for sterol-free liposomes was encountered again while working with sterol-enriched samples. Resuspension just after freeze-drying still allowed recovery of liposomes with a size much closer to the original sample than in the case of sterol-free liposomes, confirming that the sterol played a role on the mechanical stabilization of the membrane during drying. Crystallization upon storage however led to completely collapsed liposomes and did not allow efficient stabilization whatever sterol and concentration involved.

Lactose-containing cakes were difficult to redisperse and presence of large undissolved particles in the suspension was obvious, due either to recrystallization of the sterol or formation of the monohydrate  $\alpha$ -lactose. Resuspension after lyophilization showed a higher increase in size for the cholesterol-enriched samples, while ergosterol-enriched formulations remained close to the original values. Larger disturbances compared to sterol-free were observed upon 10-week storage with low contents of cholesterol and high content of ergosterol clearly leading to destabilization. This confirms that relative concentration sterol/lyoprotectant has an influence on the drying process and that an optimum has to be found.

Samples containing trehalose gave satisfying stabilization just after freeze-drying and upon storage. Reduced disturbances of the liposomes during drying compared to sterol-free suspensions were reflected in ratios  $d_f/d_i$  closer to 1, confirming a benefit of the

presence of sterol. Limited modifications in size, PdI and zeta-potential after 10-week storage confirmed good stabilization properties of trehalose. Absence of significant effect of content of sterol incorporated in the membrane proved that the lyoprotection is mainly provided by the trehalose and that presence of sterol did not disturb interactions between sugar and phospholipid heads. These results are in accordance with previous studies that reported that trehalose was still efficient even in presence of high amount of cholesterol [46,49,52] and that interactions with phospholipids were not competitive, trehalose binding preferentially to P=O group of the phospholipids while cholesterol interacts with C=O groups at a deeper level in the membrane.

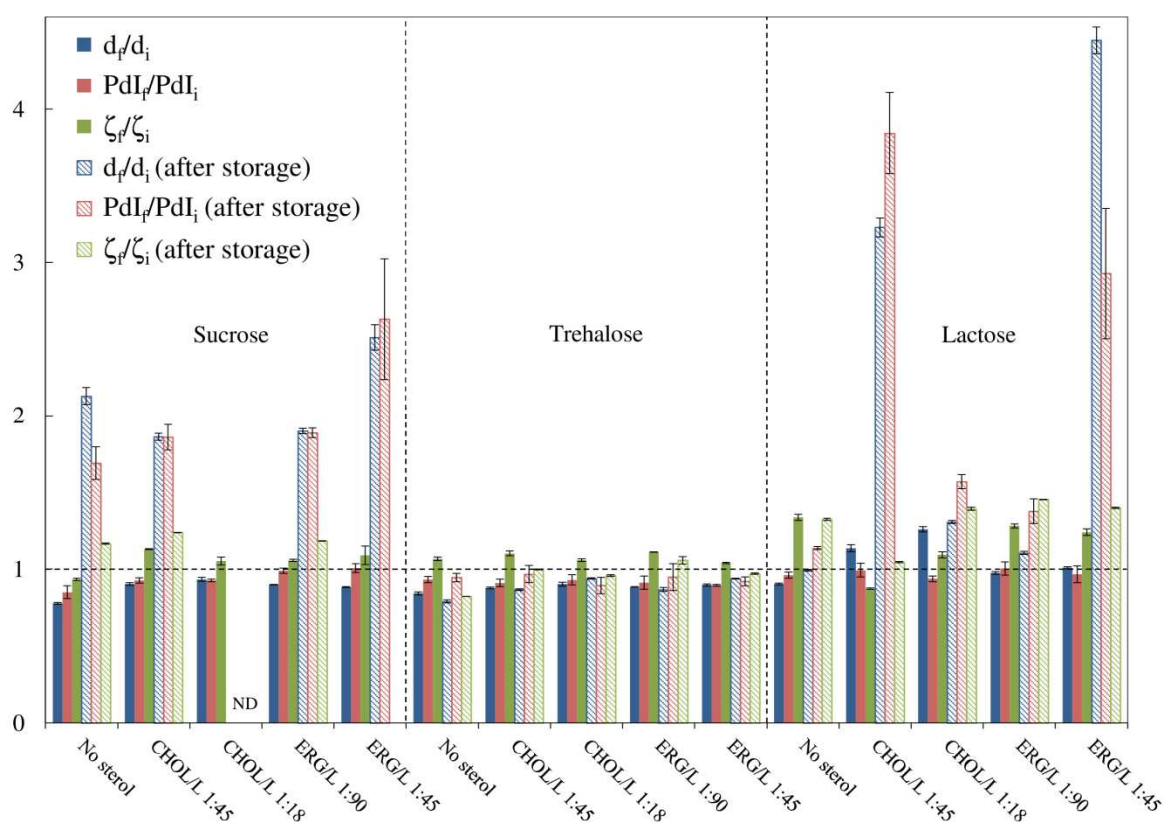


**Figure 5.7: Evolution of mean diameter, polydispersity and zeta-potential of sterol-enriched liposomes in lyophilized cakes resuspended just after lyophilization or after 10 weeks storage at 4°C (ND: not determined)**

### 5.4.3. Thermal analysis of liposomal lyophilized cakes

Freeze-dried liposomal cakes were analyzed by DSC just after lyophilization for further understanding of their physical state. Figure 5.8 displays thermograms obtained for sucrose- and lactose-protected liposomes.

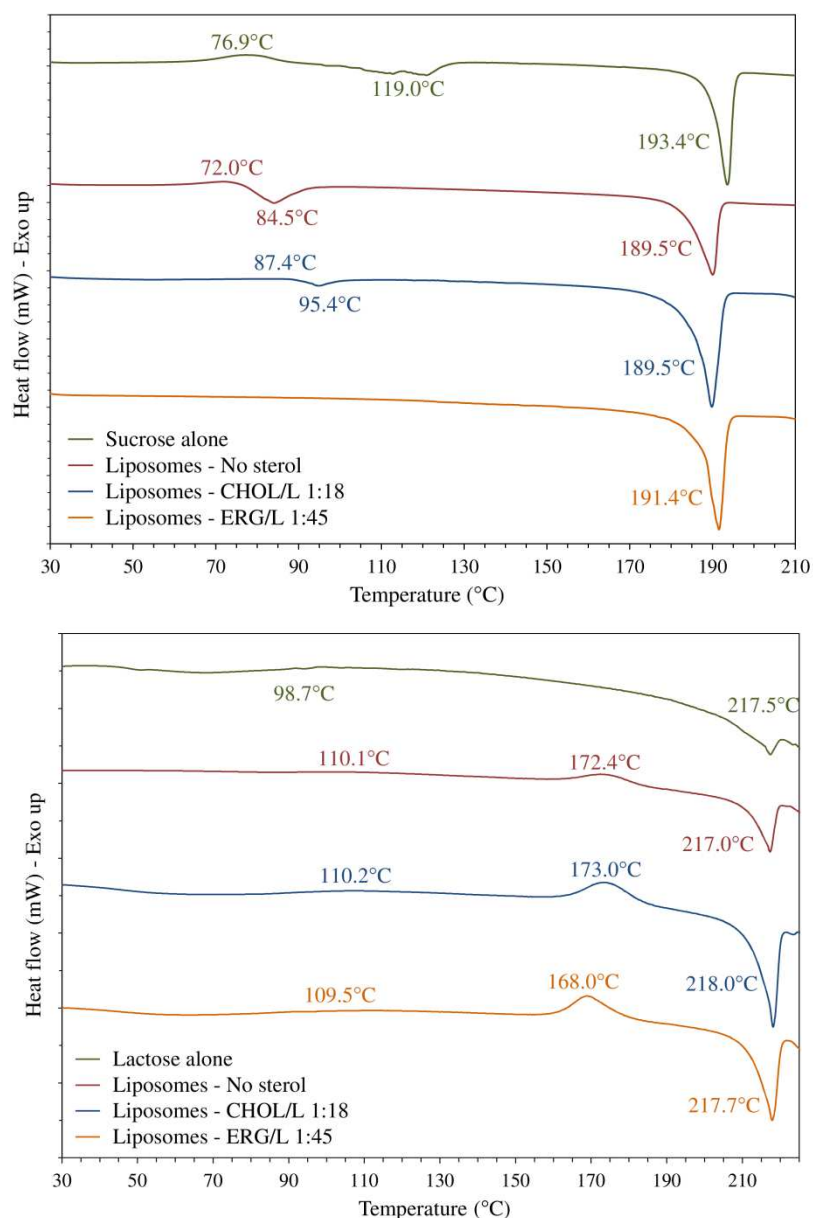


**Figure 5.8: DSC thermograms of sterol-free and sterol-enriched liposomes freeze-dried in presence of sucrose (top) and lactose (bottom)**

As mentioned in section 5.3.3, freeze-dried sucrose was found in an amorphous state with the presence of an exotherm corresponding to the transition amorphous to crystalline followed by an endotherm indicating loss of water. These two events were detected in sterol-free and cholesterol-enriched samples, accompanied by a melting point shifted to 189.5°C. The intensity of the crystalline transition and the loss of water were found lower than for sucrose alone and more intense in the case of sterol-free samples, which indicate that the presence of phospholipids and cholesterol favors the recrystallization of sucrose from amorphous state after lyophilization. No crystalline transition was observed in the case of ergosterol-enriched samples, highlighting that recrystallization was already completed while using this sterol.

DSC thermograms of sterol-free and sterol-enriched liposomes confirmed the formation of  $\alpha$ -monohydrate lactose, in accordance with aggregates and non-immediate redispersion experienced after resuspension mentioned earlier. Appearance of an exotherm at respectively 172.4, 173.0 and 168.0°C for sterol-free, CHOL/L 1:18 and ERG/L 1:45 highlighted the recrystallization of lactose and confirmed the amorphous nature of the cake after lyophilization. Shift to lower temperatures in the case of ergosterol corroborated the lower stability observed upon storage for ERG/L 1:45 compared to CHOL/L 1:18. No other crystallization peaks were visualized in the thermogram which indicate that sterols remained non crystalline.

Trehalose samples presented once again completely amorphous profiles for all liposomal compositions. Glass transition present at 114.7°C for pure lyophilized trehalose was shifted respectively to 103.7°C, 100.4°C and 100.2°C for sterol-free, CHOL/L 1:18 and ERG/L 1:45, indicating some plasticization effect due to the presence of sterols in the lipid bilayer.

#### **5.4.4. Natamycin stability in sterol-free and sterol-enriched lyophilized formulations**

Figure 5.9 presents the relative losses of natamycin for liposomes freeze-dried in presence of glucose, sucrose, trehalose and lactose at different concentrations. All formulations were relatively stable at -20°C with a slight superiority of trehalose and a limited impact of the concentration of lyoprotectant used.

At 4°C and 25°C, instability was evidenced for glucose as expected from the collapsed cake aspect. Higher concentrations of glucose provided slightly better protection levels but degradation via reaction with the amino group of natamycin previously mentioned for PLGA nanospheres was clearly visible on the HPLC profiles. For all concentrations of glucose, the corresponding impurity was present in larger quantities than observed for polymeric nanospheres and reached intensities comparable to natamycin (relative area for natamycin signal ranging between 40-46% compared to 70-78% in the case of PLGA). Enhanced degradation for liposomes compared to polymeric nanoparticles, though initial encapsulation efficiencies are much higher, corroborates the idea of phase separation of lecithins and exposure of natamycin to residual moisture and reactions with the sugar. It is also highly likely that amino groups present in phospholipids, particularly in the case of PE molecules, would have reacted with glucose

too [39] leading to further instability of the bilayer and leakage of the preservative. Modifications of the HPLC profile were evidenced as well for lactose, with a relative area of natamycin signal ranging for 90-92% at 25°C (86-93% for PLGA nanospheres) and main presence of the impurity linked to a change of conformation trans – cis (see Figure 5.5). This would tend to indicate rather rearrangement of natamycin rather than degradation and a more efficient protection than glucose due to the formation of an amorphous cake with lower residual moisture content. Sucrose-containing samples were as expected also unstable, particularly at 25°C, due to recrystallization and phase separation of phospholipids, leading to further exposure of natamycin. The highest level of degradation was observed for 5% w/v in accordance with the highest variation of size characteristics upon storage described for this sample in section 5.4.1.2. Degradation levels remain in all cases much lower while using trehalose, confirming good stabilization of the liposomal structure and formation of an efficient barrier towards leakage of the preservative. Larger variations of size characteristics upon storage evidenced previously for 1% w/v trehalose were reflected in slightly more important losses of natamycin and confirmed that a minimum of 2.5% w/v should be used.

Further studies of the stability in presence of trehalose and lactose were performed for sterol-enriched formulations as displayed in Figure 5.10. It can be seen that whatever temperature of storage was used, trehalose-protected formulations kept offering the best protection. Only minor differences due to the presence of sterols were detected at 25°C with reduced losses for larger content of sterol and a slight superiority of ergosterol for the same concentration, in accordance with similar conservation of size characteristics by trehalose but higher initial encapsulation efficiency in the case of ergosterol.

A similar but more tangible effect of sterol nature and content in the bilayer was observed for lactose-protected samples, though degradation levels remain comparable to sterol-free samples. Comparison of relative area occupied by natamycin signal in the HPLC spectra (respectively around 91.3% and 93.0% for CHOL/L 1:45 and 1:18 and 91.5% and 93.5% for ERG/L 1:90 and 1:45 compared to 91.1% for sterol-free sample), indicated a direct relationship between intensity of the impurities and sterol content, thus initial encapsulation efficiencies. Huge variations of sizes observed during resuspension after storage did not have direct consequences on the stability which corroborates the idea of recrystallization of lactose itself, evidenced by DSC, rather than crystallization of sterols or enhanced permeability of the phospholipid bilayer.

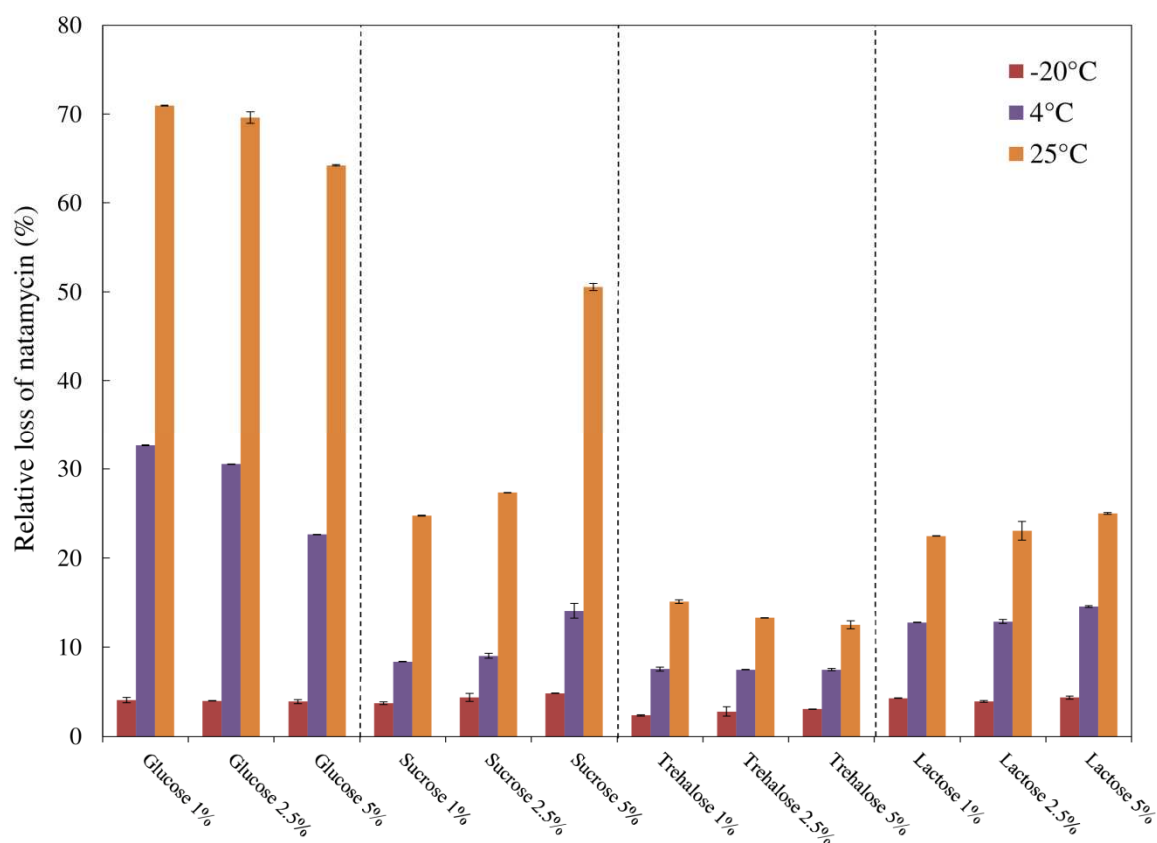


Figure 5.9: Natamycin losses in lyophilized sterol-free liposomes after 10 weeks storage at -20°C, 4°C or 25°C as a function of lyoprotectant nature and concentration

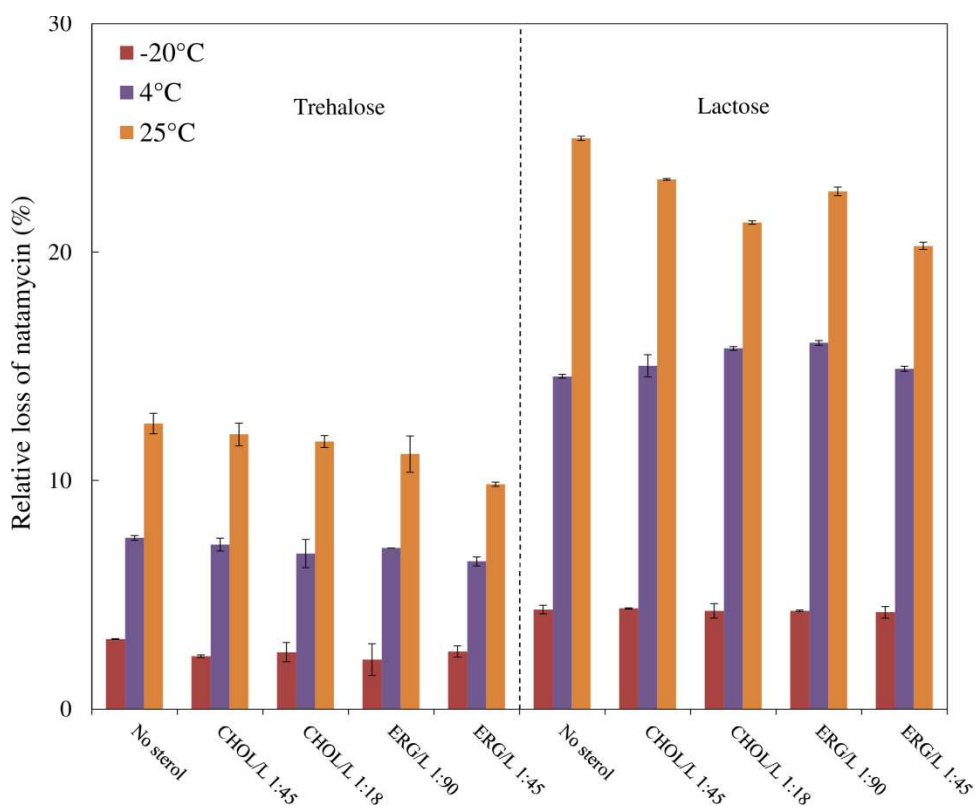


Figure 5.10: Natamycin losses in lyophilized sterol-enriched liposomes after 10 weeks storage at -20°C, 4°C or 25°C in presence of trehalose and lactose



#### 5.4.5. Conclusions for liposomal suspensions

Glucose, sucrose, trehalose and lactose added at 1, 2.5 and 5% w/v were evaluated for the cryo- and lyo-protection of natamycin-loaded liposomal suspensions in presence or absence of cholesterol and ergosterol in the lipid bilayer.

Addition of these protective agents was found to have a larger impact on the initial size characteristics and zeta-potential than in the case of PLGA nanospheres. Respective interactions between the liposomes and the saccharides were clearly dependent on the flexibility and ability for each compound to establish hydrogen bonding with the phospholipid heads. Higher levels of interactions after addition in the liposomal suspension were found in the order glucose < trehalose < sucrose < lactose with lactose-containing samples showing signs of rearrangement due to the osmotic shock created by the addition of sugar. Upon freeze-thawing, the variation was opposite with no further rearrangement for lactose-enriched samples while trehalose and glucose provided tighter interactions with the phospholipid heads and reduced diameters.

Glucose and sucrose were found inappropriate for the freeze-drying of liposomes under the process conditions used in this study. The first one led to collapsed cakes, phase separation over storage, disruption of the liposomes and high levels of degradation of natamycin due to reaction with the amino group of the preservative and phospholipids. Sucrose also led to partially collapsed cakes which recrystallized upon storage and did not allow conservation of the integrity of the liposomes nor efficient protection of natamycin.

Trehalose used above 2.5% w/v allowed a good stabilization at each stage of the freeze-drying process and provided appropriate protection for both liposomal structure and natamycin upon storage. Acceptable cakes were also obtained with lactose but could not be redispersed fully due to the formation of the monohydrate  $\alpha$ -lactose polymorph during the process. Though lactose led to the least disturbed size characteristics during the drying stage compared to the initial protectant-enriched suspension, large variations in the zeta-potential were visualized and sizes could not be maintained over storage, suggesting disruption of the bilayer structure. Levels of natamycin degradation compared to trehalose were also clearly more intense.

The incorporation of cholesterol and ergosterol in the formulations overall enhanced the cryoprotective effect of sucrose, trehalose and lactose during freeze-thawing cycle. The impact on drying was less visible, with only slight improvements of the lyoprotective properties of trehalose and destabilization in the case of lactose. Benefits for natamycin

stability were observed, in direct relationship with the nature and concentration of sterol involved, but were overall negligible compared to the effect of the protectant itself.

Overall, the best compromise in terms of acceptable cake aspect, sustained initial characteristics and stability upon storage of natamycin was obtained with trehalose above 2.5 % w/v, in presence or absence of sterols.

## **5.5. Conclusions**

In this chapter, lyophilization of PLGA nanospheres and liposomal suspensions was evaluated in presence of monosaccharides (glucose), disaccharides (sucrose, trehalose, lactose) and polyols (mannitol, sorbitol) known for their cryo-/lyo-protective properties.

Trehalose was overall found superior to other excipients for both PLGA nanospheres and liposomes with or without sterol. Amorphous and easily redispersible cakes were obtained in a reproducible way and allowed conservation of nanoparticle size characteristics during freezing, drying and upon storage. Both nano-carriers as well as natamycin were also favorably physically and chemically stabilized.

Other saccharides were less efficient in terms of cryo- or lyo-protection. Glucose and sucrose for instance, despite their good stabilizer properties, led to collapsed or crystallized cakes that did not prevent aggregation of polymeric nanospheres or resulted in phase separation of phospholipids upon storage. Natamycin was consequently exposed to degradation and residual moisture at a larger extent than for trehalose and also interacted negatively with reducing sugars such as glucose. Good bulking properties of lactose allowed formation of acceptable cakes but partial formation of a less soluble crystalline lactose polymorph and strong osmotic shock while added in suspension were not found suitable for maintaining the physical integrity of nanospheres and liposomes. Adding to that the reducing properties of lactose, natamycin could not efficiently be stabilized compared to trehalose.

Polyols turned out to not be compatible with liposomal formulations but were found efficient stabilizers and protectants against degradation and leakage of natamycin from PLGA nanoparticles. Though interactions with the nanospheres and coverage of the surface was strong compared to saccharides, mannitol and sorbitol were obtained in crystalline form during lyophilization and could not provide an efficient bulking effect during the drying step leading to high levels of aggregation.

Lyophilization appears overall to be a more promising technique than Tangential Flow Filtration for the enhancement of the stability of natamycin and nano-carriers upon storage. Combinations of protective excipients remain to be evaluated, particularly trehalose/polyol mixtures, to determine if further benefits in terms of stability and reduced leakage of natamycin could be obtained. Stability also needs to be further investigated on the long term, particularly with a focus on residual humidity, to determine the optimum storage conditions. In the case of liposomes, cryo-TEM analyses and release behavior experiments should also be implemented to confirm whether or not structural modification during lyophilization had consequences on the bilayer permeability.

## References

- [1] D.Lemoine, C.François, F.Kedzierewicz, V.Preat, M.Hoffman, P.Maincent, Stability studies of nanoparticles of poly(epsilon-caprolactone), poly(D,L-lactide) and poly(D,L-lactide-co-glycolide), *Biomaterials*, **1996**, 22, 2191-2197
- [2] A.Bellabella, C.Vauthier, H.Fessi, J.-P. Devissaguet, F.Puisieux, In vitro degradation of nanospheres from poly(D,L-lactides) of different molecular weights and polydispersities, *International Journal of Pharmaceutics*, **1996**, 129, 95-102
- [3] M.Grit, D.J.A.Crommelin, Chemical stability of liposomes: implications for their physical stability, *Chemistry and Physics of Lipids*, **1993**, 64, 3-18
- [4] B.Heurtault, P.Saulnier, B.Pech, J.-E. Proust, J.-P.Benoît, Physico-chemical stability of colloidal lipid particles, *Biomaterials*, **2003**, 24, 4283-4300
- [5] V.Torchilin, V.Weissig, Liposomes: A Practical Approach, *OUP Oxford*, **2003**
- [6] G.-W. Oetjen, P.Haseley, Freeze-drying, *John Wiley & Sons*, **2008**
- [7] T.-C. Hua, B.-L.Liu, H.Zhang, Freeze-drying of pharmaceuticals and food products, *Elsevier*, **2010**
- [8] F.Franks, T.Auffret, Freeze-drying of pharmaceuticals and biopharmaceuticals, *Royal Society of Chemistry*, **2008**
- [9] W.Abdelwahed, G.Degobert, S.Stainmesse, H.Fessi, Freeze-drying of nanoparticles: Formulation, process and storage considerations, *Advanced Drug Delivery Reviews*, **2006**, 58, 1688-1713
- [10] C.Chen, D.Han, C.Cai, X.Tang, An overview of liposome lyophilization and its future potential, *Journal of Controlled Release*, **2010**, 142, 299-311
- [11] J.C.Kasper, W.Friess, The freezing step in lyophilization: Physico-chemical fundamentals, freezing methods and consequences on process performance and quality attributes of biopharmaceuticals, *European Journal of Pharmaceutics and Biopharmaceutics*, **2011**, 78, 248-263
- [12] G.J.Fransen, P.J.M.Salemink, D.J.A.Crommelin, Critical parameters in freezing of liposomes, *International Journal of Pharmaceutics*, **1986**, 33, 27-35
- [13] J.H.Crowe, L.M.Crowe, J.F.Carpenter, C.A.Wistrom, Stabilization of dry phospholipid bilayers and proteins by sugars, *Biochem. J.*, **1987**, 242, 1-10

- [14] W.Q.Sun, A.C.Leopold, L.M.Crowe, J.H.Crowe, Stability of dry liposomes in sugar glasses, *Biophysical Journal*, **1996**, *70*, 1769-1776
- [15] L.M.Crowe, C.Womersley, J.H.Crowe, D.Reid, L.Appel, A.Rudolph, Prevention of fusion and leakage in freeze-dried liposomes by carbohydrates, *Biochimica et Biophysica Acta*, **1986**, *861*, 131-140
- [16] Y.Roos, Melting and glass transitions of low molecular weight carbohydrates, *Carbohydrate Research*, **1993**, *238*, 39-48
- [17] A.-C. Eliasson, Chapter 2: Mono- and disaccharides: selected physico-chemical and functional aspects in: Carbohydrates in Food, *CRC Press*, **2006**
- [18] A. Saez, M. Gúzman, J. Molpeceres, M.R. Aberturas, Freeze-drying of polycaprolactone and poly(D,L-lactic-glycolic) nanoparticles induces minor particle size changes affecting the oral pharmacokinetics of loaded drugs, *European Journal of Pharmaceutics and Biopharmaceutics*, **2000**, *50*, 379-387
- [19] L.M.Crowe, D.S.Reid, J.H.Crowe, Is trehalose special for preserving dry biomaterials, *Biophysical Journal*, **1996**, *71*, 2087-2093
- [20] P.V.Date, A.Samad, P.V.Devarajan, Freeze Thaw: A simple approach for prediction of optimal cryoprotectant for freeze-drying, *AAPS PharmSciTech*, **2010**, *11*, 304-313
- [21] A.Lerbret, P.E.Mason, R.M.Venable, A.Cesàro, M.-L.Saboungi, R.W.Pastor, J.W.Brady, Molecular dynamics studies of the conformation of sorbitol, *Carbohydrate Research*, **2009**, *344*, 2229-2235
- [22] J.R.Grigera, Conformation of polyols in water: molecular-dynamics simulation of mannitol and sorbitol, *J.Chem.Soc. Faraday Trans.1*, **1988**, *84*, 2603-2608
- [23] M.Holzer, V.Vogel, W.Mäntele, D.Schwartz, W.Haase, K.Langer, Physico-chemical characterization of PLGA nanoparticles after freeze-drying and storage, *European Journal of Pharmaceutics and Biopharmaceutics*, **2009**, *72*, 428-437
- [24] S.De Chasteigner, H.Fessi, G.Cavé, J.P.Devissaguet, F.Puisieux, Freeze-drying of itraconazole-loaded nanosphere suspensions: a feasibility study, *Drug Dev.Res.*, **1996**, *38*, 116-124
- [25] R.K.Cavatur, N.M.Vemuri, A.Pyne, Z.Chrzan, D.Toledo-Velasquez, R.Suryanarayanan, Crystallization behavior of mannitol in frozen aqueous solutions, *Pharmaceutical Research*, **2002**, *19*, 894-900
- [26] A.I.Kim, M.J.Akers, S.L.Nail, The physical state of mannitol after freeze-drying: effects of mannitol concentration, freezing rate and a noncrystallizing cosolute, *Journal of Pharmaceutical Sciences*, **1998**, *87*, 931-935
- [27] L.Yu, N.Milton, E.G.Groleau, D.S.Mishra, R.E.Vansickle, Existence of a mannitol hydrate during freeze-drying and practical implications, *Journal of Pharmaceutical Sciences*, **1999**, *88*, 196-198
- [28] S.Hirsjärvi, L.Peltonen, J.Hirvonen, Effect of sugars, surfactant and tangential flow filtration on the freeze-drying of poly(lactic acid) nanoparticles, *AAPS PharmSciTech*, **2009**, *10*, 488-494
- [29] B.Makower, W.B.Dye, Sugar crystallization, equilibrium moisture content and crystallization of amorphous sucrose and glucose, *J.Agric.Food Chem.*, **1956**, *4*, 72-77

- [30] S.Ohtake, Y.J.Wang, Trehalose: current use and future applications, *Journal of Pharmaceutical Sciences*, **2011**, *100*, 2020-2053
- [31] J.L.Green, C.A.Angell, Phase relations and vitrification in saccharide-water solutions and the trehalose anomaly, *J.Phys.Chem.*, **1989**, *93*, 2880-2882
- [32] L.S.Taylor, P.York, Characterization of the phase transitions of trehalose dehydrate on heating and subsequent dehydration, *Journal of Pharmaceutical Sciences*, **1998**, *87*, 347-355
- [33] B.T.Raimi-Abraham, J.G.Moffat, P.S.Belton, S.A.Barker, D.Q.M.Craig, Generation and characterization of standardized forms of trehalose dehydrate and their associated solid-state behavior, *Crystal Growth Design*, **2014**, *14*, 4955-4967
- [34] R.Price, P.M.Young, Visualization of the crystallization of lactose from the amorphous state, *Journal of Pharmaceutical Sciences*, **2004**, *93*, 155-164
- [35] L.Wu, X.Miao, Z.Shan, Y.Huang, L.Li, X.Pan, Q.Yao, G.Li, C.Wu, Studies on the spray dried lactose as carrier for dry powder inhalation, *Asian Journal of Pharmaceutical Sciences*, **2014**, *9*, 336-341
- [36] Y.H.Roos, Chapter 2: Solid and liquid states of lactose in: Advanced Dairy Chemistry, Volume 3: lactose, water, salts and minor constituents, *Springer Science + Business Media*, 2009
- [37] S.Quinquet, C.Grabielle-Madellmont, M.Ollivon, Influence of water on pure sorbitol polymorphism, *J.Chem.Soc., Faraday Trans. 1*, **1988**, *84*, 2609-2618
- [38] I.A.L.A.Boogers, Isolation and identification of natamycin impurities, *Internal DSM R&D report*, **2003**
- [39] V.Kumar, G.S.Banker, Maillard reaction and drug stability in: Maillard reactions in chemistry, food and health, *Woodhead Publishing Ltd*, **2005**
- [40] P.Wessman, K.Edwards, D.Mahlin, Structural effects caused by spray- and freeze-drying of liposomes and bilayer disks, *Journal of Pharmaceutical Sciences*, **2010**, *99(4)*, 2032-2048
- [41] B.Stark, G.Pabst, R.Prassl, Long-term stability of sterically stabilized liposomes by freezing and freeze-drying: Effects of cryoprotectants on structure, *European Journal of Pharmaceutical Sciences*, **2010**, *41*, 546-555
- [42] C.S.Pereira, P.H.Hünenberger, Interaction of the sugars trehalose, maltose and glucose with a phospholipid bilayers: A comparative molecular dynamics study, *Journal of Physical Chemistry B*, **2006**, *110*, 15572-15581
- [43] R.Lefort, P.Bordat, A.Cesaro, M.Descamps, Exploring the conformational energy landscape of glassy disaccharides by cross polarization magic angle spinning <sup>13</sup>C nuclear magnetic resonance and numerical simulations. II. Enhanced molecular flexibility in amorphous trehalose, *The Journal of Chemical Physics*, **2007**, *126*, 014511
- [44] E.C.A. van Winden, D.J.A. Crommelin, Long term stability of freeze-dried, lyoprotected doxorubicin liposomes, *European Journal of Pharmaceutics and Biopharmaceutics*, **1997**, *43*, 295-307
- [45] L.M.Crowe, J.H.Crowe, A.Rudolph, C.Womersley, L.Appel, Preservation of freeze-dried liposomes by trehalose, *Archives of Biochemistry and Biophysics*, **1985**, *242*, 240-247

- [46] P.R.Harrigan, T.D.Madden, P.R.Cullis, Protection of liposomes during dehydration or freezing, *Chemistry and Physics of Lipids*, **1990**, 52, 139-149
- [47] T.D.Madden, M.B.Bally, M.J.Hope, P.R.Cullis, H.P.Schieren, A.S.Janoff, Protection of large unilamellar vesicles by trehalose during dehydration: retention of vesicle contents, *Biochimica et Biophysica Acta – Biomembranes*, **1985**, 817, 67-74
- [48] A.V.Popova, D.K.Hincha, Effects of cholesterol on dry bilayers: interactions between phosphatidylcholine unsaturation and glycolipid or free sugar, *Biophysical Journal*, **2007**, 93, 1204-1214
- [49] M.Doxastakis, A.K.Sum, J.J de Pablo, Modulating membrane properties: the effect of trehalose and cholesterol on a phospholipid bilayer, *J.Phys.Chem.B*, **2005**, 109, 24173-24181
- [50] T.Róg, M.Pasenkiewicz-Gierula, I.Vattulainen, M.Karttunen, Ordering effects of cholesterol and its analogues, *Biochimica et Biophysica Acta*, **2009**, 1788, 97-121
- [51] D.A.Mannock, R.N.A.H. Lewis, T.P.W.McMullen, R.N.McElhaney, The effect of variations in phospholipid and sterol structure on the nature of lipid-sterol interactions in lipid bilayer model membranes, *Chemistry and Physics of Lipids*, **2010**, 163, 403-448
- [52] S.Ohtake, C.Schebor, S.P.Palecek, J.J.de Pablo, Phase behavior of freeze-dried phospholipid-cholesterol mixtures stabilized with trehalose, *Biochimica et Biophysica Acta*, **2005**, 1713, 57-64









# *Chapter 6*

## *General conclusion and outlook*

*Now this is not the end.  
It is not even the beginning of the end.  
But it is, perhaps, the end of the beginning.*  
Winston Churchill

Food spoilage has become in the last decades one of the biggest challenges faced by the food industry with a significant amount of raw materials, food, feed and agricultural products thrown away every day at each level of the supply chain. Contamination by micro-organisms resulting in products unacceptable for human consumption is listed as one of the major causes of food spoilage and can be at a large extent prevented by preservation methods among which application of antimicrobial compounds is quite popular. In the past years, a growing demand of customers for more natural antimicrobials and reduced processing treatments, coupled with high research costs and numerous regulatory hurdles set by health authorities while considering development of new preservative molecules, has led the food antimicrobial suppliers to preferentially focus on the reformulation and improvement of already approved ingredients, aiming at maximizing their antimicrobial efficiency and adapting their functionality to new food applications.

Natamycin, a naturally-occurring preservative produced by DSM Food Specialties, is one of the most widely used antifungal molecules for the protection of food surfaces. This compound presents several appealing properties linked to its natural origin, long history of safe use, efficiency at relatively low concentrations and limited impact on organoleptic properties of food products. Current existing formulations based on crystalline natamycin particles face however several challenges to provide appropriate antimicrobial activity. Low aqueous solubility, linked to a complex zwitterionic molecular structure, is the first hurdle encountered and limits significantly the availability of natamycin in dissolved state necessary for antifungal activity and diffusion towards the sites of action, leading in some cases to heterogeneous protection and difficulty to maintain the minimum inhibitory concentration required towards micro-organisms. Natamycin in a dissolved state is in addition very sensitive to unfavorable environmental conditions such as extreme pHs, exposure to UV light or oxidation, which can lead to significant levels of undesired early-stage degradation. Finally, crystalline formulations of natamycin offer limited specificity and tunability, which narrows the possibilities for controlled release and development of new food applications.

In this PhD thesis, incorporation of natamycin within nano-encapsulation systems was explored to evaluate if these new formulations could bring effective answers to the issues of availability, early-stage degradation and limited tunability identified for the native crystalline preservative. A product development approach was implemented with **Part I** focusing on the development and characterization of nano-carriers presenting suitable

properties for the encapsulation, delivery and protection of the preservative, while *Part II* describes further treatment of the obtained nano-suspensions and transformation into purified, concentrated or dried products that could be commercialized.

## **6.1. Conclusions and future work regarding the formulation and characterization of nano-encapsulation systems**

In *Part I* of this thesis, nano-encapsulation systems based on biodegradable polymeric nanospheres and liposomes were evaluated as model nano-carriers for natamycin and compared in terms of relative benefits and limitations for the encapsulation, delivery, antifungal performance towards a model yeast and stability of the preservative. Restricted solubility properties of natamycin in both aqueous medium and organic solvents limited the possible preparation methods of nanoparticles to single-step injection of an organic phase containing the carrier material, the preservative and a solvent (or solvent mixture) fully miscible with water, into an aqueous phase.

In *Chapter 2*, biodegradable polymeric nanospheres were successfully obtained by nanoprecipitation of an organic phase composed of a low molecular weight poly(lactide-co-glycolide) (PLGA) (ratio L:G 75:25) dissolved in an acetone/methanol 2:1 v/v mixture at 10-25 mg/mL. One-shot injection of this organic phase in water led to the formation of nano-sized spherical particles (60-120 nm) with a narrow polydispersity (0.15-0.2). Incorporation of natamycin within the formulation evidenced an active participation of the preservative to the nanoprecipitation process with mean diameters reduced by 10-30 nm, attributed to the formation of a PLGA-natamycin complex via electrostatic interactions, more hydrophilic than PLGA alone. Determination of entrapment levels showed that only up to 25% of the maximum amount of natamycin soluble in methanol could be encapsulated in the nanoparticles (maximum 1.4% of loading efficiency) while zeta-potential proved partial adsorption at the surface via electrostatic interactions with the PLGA carboxylic groups. Modification of the aqueous phase composition by changing pH or ionic strength did not enhance the encapsulation or even destabilized the nanoparticles. Physical state analysis highlighted the presence of natamycin in an amorphous or molecularly-dispersed state within the polymeric matrix and presence of weak interactions with the polyester. Limited levels of encapsulation and presence of non-crystalline natamycin translated into higher availability of free preservative

molecules and into faster release kinetics rates (80% released over the first 48 h compared to 29% for crystalline natamycin). This was also reflected in an enhanced antifungal activity over the first two days of treatment applied to cultures of the model yeast *Saccharomyces cerevisiae*. Stability tests of natamycin-loaded polymeric suspensions indicated however a relatively fast degradation of the preservative upon storage, likely to be due to the chemical instability of the polymer itself, to the presence of non-encapsulated natamycin at a too large extent and to the inherent low solid content of nano-suspensions achievable via the nanoprecipitation technique.

In **Chapter 3**, nano-liposomal suspensions were successfully prepared by the solvent injection method using methanol as a solvent for various food-grade soybean lecithins. Small unilamellar vesicles (< 130 nm) were obtained with monomodal distribution but less controlled polydispersities than PLGA nanospheres (0.21-0.26), and were able to encapsulate natamycin without significant modification of their size characteristics. Presence of charged phospholipids and reduced content of phosphatidylcholine in the lecithin mixture were found to be beneficial for natamycin encapsulation, indicating electrostatic interactions of the preservative with the polar head of the phospholipids and partial incorporation within the bilayer. The chemical instability of natamycin upon storage in these formulations was however significant and suggested uncontrolled leakage out of the liposomes. Performing the solvent injection in acidic aqueous medium enabled to improve the encapsulation of the preservative and reduced the chemical instability at some extent, due to enhanced electrostatic interactions with the phospholipids. More efficient prevention of natamycin degradation was obtained by incorporation of sterols (cholesterol, ergosterol) in the lipid mixture, linked to higher entrapment levels (up to 90-96% of the maximum amount of natamycin soluble in methanol, corresponding to 5.6-5.8% of loading efficiency) and reduced fluidity of the phospholipid membrane due to the ordering effect of sterols. Comparable action of ergosterol was observed at concentrations 2.5-fold lower than cholesterol and attributed to a preferential interaction of natamycin–ergosterol as well as a higher control of membrane permeability. Sterol-free liposomes were characterized by a much faster release rate than crystalline natamycin with a burst release of 50% over the first 36 h (23.5% for pure natamycin), corresponding to an enhanced antifungal activity. Addition of sterols in the bilayer allowed fine-tuning of the permeability of the bilayer, resulting in modulated release rates and durations of antifungal activity against the model yeast *Saccharomyces cerevisiae*.

Liposomal formulations, particularly when enriched with sterols, offer overall several advantages over PLGA nanospheres such as the use of methanol as single solvent that allows incorporation of higher levels of natamycin; the obtention of more concentrated systems in terms of solid content; higher levels of entrapment of natamycin and possibilities of tunable controlled release by playing with the composition of the lipid membrane. It is however worth mentioning that larger variability between batches is observed for liposomal suspensions, with random presence of much larger vesicular structures that can be detrimental for reproducible and homogeneous behaviors once applied on a food product. Incorporation of sterols and complexation with natamycin, though useful for the encapsulation and stability of the preservative, do not allow full availability of the initial amount of antimicrobial molecules due to irreversible retention within the lipid bilayer. Both carriers gave in any case the proof of principle that nano-encapsulation of natamycin can bring an answer to the desired higher availability of preservative molecules in a molecular state, as evidenced by enhanced antifungal activity towards the model yeast. Possible tunability of the formulations was also identified for liposomes but remains to be further optimized for both nano-systems, aiming at more controlled release and at efficient protection on the longer term. Formulations obtained in this study indeed all present significant initial burst release and total delivery achieved over maximum 8 days, which could be interesting only for food products where a high level of protection is required at early stages of the preparation, such as cheese for instance in which a large amount of moisture favorable to microbial growth is present at the beginning and reduces upon storage and drying of the product. More importantly, nano-encapsulation systems did not bring an acceptable answer to chemical instability of the preservative, with losses of natamycin remaining at levels too high to be acceptable for commercialization even for the best formulations identified.

Choice of the carrier material and further tuning of the composition of the nano-systems should be the first elements to reconsider to maximize encapsulation efficiencies and to reduce exposure of natamycin to the external medium due to uncontrolled leakage, which should bring benefits for the stability. Various PLGA polyesters with different ratios L:G and molecular weights as well as polycaprolactone (not reported) were evaluated in Chapter 2 and selected based exclusively on reproducibility of the nanoprecipitation process and acceptable sizes and polydispersities. Further

understanding of the interactions polymer-preservative occurring within the organic phase or in the aqueous medium could be beneficial to prescreen other polymers and to enhance encapsulation efficiencies. Other biodegradable polymers such as polysaccharide derivatives (chitosan, starch), suitable for nanoprecipitation and showing enough polar/ionic properties to be compatible with natamycin, remain to be assessed. Compatibility with the solvent mixture required for solubilization of natamycin at acceptable levels should however be verified beforehand, as the presence of methanol can significantly disturb the solubilization of the polymer itself and prevent formation of nanoparticles. In the case of liposomes, the choice was made to focus on the preparation of vesicles based on soybean lecithins which could realistically be considered while scaling-up and commercializing the liposomal formulations, due to their food-grade nature and availability in large quantities at low prices. These lecithins are however complex mixtures of phospholipids, making it difficult to understand the behaviour of the lipid bilayer and the mechanism of interaction with natamycin. Lecithins also contain residual fatty acids known to accelerate degradative reactions among phospholipids, leading to higher permeability of the membrane and leakage of encapsulated compounds. It would be interesting to study more in depth the affinity of natamycin with simplified systems based on purified phospholipids with well-defined acyl chains and polar heads, in order to confirm the preferential affinity of natamycin for charged compounds compared to phosphatidylcholine, as suggested in Chapter 3, and to help refining the composition of the lecithin mixture to use to maximize encapsulation levels. A similar simplification approach should be applied to build knowledge on the relative effect of cholesterol and ergosterol on the membrane permeability as well as possible contribution or disturbance due to the formation of complexes with natamycin. Particularly, it would be highly relevant to determine the effect of sterols and preservative on phase transition temperature of the bilayer that could not be detected for the lecithins used in this study, but could bring relevant insights on the mechanical resistance of the liposomes for a better choice of storage conditions and development of post-processing treatments.

Surface modification of the nanoparticles by deposition of a protective layer (oppositely charged polymer or surfactant) during or after preparation should also be included in future work. This could not only provide additional benefits for the encapsulation and prevention of leakage of natamycin to the outer medium but also improve the physical stability of the nano-carriers during storage and/or post-processing.

Coating with polyethylene glycol PEG and poly(vinyl alcohol) PVA is the most commonly reported method to provide steric stabilization of both polymeric nanoparticles and liposomes. Positively-charged food-grade polyelectrolytes have also been efficient for surface coverage of polymeric and lipid nanoparticles. Chitosan and poly-lysine for instance could be interesting polyelectrolytes to evaluate as they are also known to have antimicrobial properties towards bacteria, which could provide versatile formulations combining antifungal and antibacterial properties if necessary. Fine-tuning to answer needs for a specific food application could be obtained easily by adapting the thickness of the coating layer to reach the desired release rates or by selecting a coating degrading upon certain conditions (for instance pH or temperature) to provide triggered release when necessary.

Addition of stabilizers would also be a convenient approach to overcome inherent hydrolysis and oxidation phenomenon occurring within the samples. Particularly, pH control agents should be introduced to prevent extreme variations linked for instance to the increased presence of lactic and glycolic oligomers in the medium due to autocatalytic degradation of PLGA, likely to catalyze hydrolysis of natamycin itself. Incorporation of antioxidants and/or UV absorbers should also be considered in both the aqueous phase, to protect natamycin initially not entrapped or released by leakage overtime, and the nanoparticles themselves, especially in the case of liposomal suspensions to prevent oxidative mechanisms within the bilayer and provide further protection of the encapsulated material. In-depth analysis of degradation products obtained after storage for both carrier and preservative materials should help identifying the major degradative reactions and refining the exact type of stabilizer needed.

Finally, other types of nano-carriers could also be considered such as polymeric micelles and polyelectrolyte-based nanoparticles. Polymeric micelles [1] can be prepared by the same nanoprecipitation technique than polymeric nanospheres, based on the use of block copolymers containing hydrophilic and hydrophobic units (classically PEG and PLGA) that lead to a core-shell type of arrangement. Though the disappearance of PLGA charges due to binding with PEG might be detrimental for interactions with natamycin, presence of a shell at the exterior of the particles could provide higher levels of retention and protection of natamycin towards leakage. The possibility to enrich the core of the micelles with pure PLGA has also been reported successful [2] and could provide further electrostatic interactions with the preservative. Polyelectrolyte-based nano-carriers [3],



prepared by ionic gelation in presence of salts or by complexation of two oppositely-charged polymers, could also be an interesting option to explore. Possible advantages of these formulations are the large versatility of natural food-grade polyelectrolytes available, their polar and charged nature that ensure good interaction with natamycin and the absence of solvent required for the preparation of the nanoparticles which would be a huge advantage compared to other nano-systems studied here.

## **6.2. Conclusions and future work regarding the post-processing of nano-encapsulation systems**

In *Part II* of this thesis, post-treatments of the nano-suspensions obtained in Part I were applied to simultaneously develop commercially suitable formulations and tackle stability issues of both nano-carrier and preservative identified previously. The purification from non-encapsulated preservative and unassociated carrier material as well as the preparation of concentrated nanoparticle suspensions have been addressed by Tangential Flow Filtration. Transformation of liquid suspensions into redispersible dry powders - easier to store, transport and handle by the customers - has been explored by lyophilization. Both techniques have been commonly implemented at large scale for industrial purposes and could be considered for scaling-up at a later stage of the research. Focus here was put on the evaluation and comparison of both methods in terms of conservation of the nanoparticle integrity and original size characteristics, undesired premature release of the encapsulated preservative and benefits for the physical stability of the nanoparticles and chemical stability of natamycin upon storage.

In *Chapter 4*, Tangential Flow Filtration, a pressure-driven filtration method already proven to be successful with nanoparticles, was implemented at lab scale based on polysulfone hollow-fiber membranes. TFF was used in concentration and continuous diafiltration modes to evaluate respectively the possibility of increasing the solid content of particles by reducing the volume of aqueous phase and to assess if purification by removal of non-encapsulated natamycin and unassociated carrier material could be achieved.

Application of concentration mode to PLGA nanospheres allowed overcoming the low solid content obtained via the nanoprecipitation method with limited modification of size characteristics and good physical stability of the nanoparticles, though the process

was found relatively sensitive to loss of polymeric material by membrane fouling and required long filtration times. Increase in solid content and reduction of aqueous volume proved to be beneficial for the chemical stability of the preservative upon storage, with losses 1.6 to 3.7-fold lower than for the original suspension. Implementation of continuous diafiltration mode was found efficient for removal of untrapped natamycin and unassociated polymer but resulted in consequent loss of polymeric nanoparticles and extremely low content of preservative left in the nano-carriers, unlikely to provide sufficient antifungal activity.

Application of concentration mode to liposomal formulations offered easier process control and reduced membrane fouling compared to PLGA nanospheres. Removal of free natamycin and increase in encapsulation efficiencies were observed but did not translate into a better chemical stability of the preservative upon storage, with even 1.3 to 2.8-fold higher levels of loss compared to the original liposomal suspension. Though limited variations of size characteristics were detected, formation of multivesicular structures and rearrangements due to exposure of liposomes to shear stresses were evidenced and could have led to leakage of the natamycin, which would explain the reduced stability upon storage. Incorporation of sterols allowed only minor improvements of chemical stability of the preservative, at a much lower extent than benefits highlighted in Chapter 3, and did not contribute efficiently to prevention of rearrangement of the liposomes during the filtration process. Continuous diafiltration was found successful for the removal of free preservative with reduced levels of mechanical stresses applied to the liposomes compared to the concentration mode. Benefits on chemical stability of the preservative or integrity of the liposomes themselves, with or without incorporation of sterol, were however still not clearly evidenced in this case.

In *Chapter 5*, lyophilization was implemented for the preparation of dried products from natamycin-loaded polymeric and liposomal suspensions. This well-established dehydration method consists in the freezing of the sample followed by removal of water by sublimation of ice crystals. Cryo-/lyoprotectants are usually added to preserve the products to be dried from mechanical stresses occurring during the process such as ice crystal formation or increase in product concentration. In this chapter, the influence of various food-grade protective excipients (glucose, sucrose, trehalose, lactose, mannitol and sorbitol) was investigated in each step of the lyophilization process to establish conditions and composition maintaining the integrity of the nanoparticles and resulting in

easily redispersible powders able to increase the shelf-life of both natamycin and nano-carriers.

Trehalose above 2.5% w/v proved to be the most efficient protectant at each step of the lyophilization process for both polymeric and liposomal suspensions, with negligible benefit of sterol enrichment. Easily redispersible amorphous cakes were formed and allowed maintaining integrity and size characteristics of the nano-carriers just after preparation and upon storage, though addition in the liposomal suspensions resulted in slight modifications due to osmotic effects. Natamycin stability was clearly enhanced compared to aqueous suspensions for both nano-carrier systems. Glucose and sucrose proved to be efficient protectants during the freezing stage but did not allow formation of acceptable dry cakes under the process conditions used in this study. Collapsed structure for glucose and fast recrystallization for sucrose triggered aggregation of PLGA nanoparticles and phase separation of liposomes, even in presence of sterols. Insufficient protection of the nano-carriers, high residual moisture content and reducing properties in the case of glucose were found detrimental for the stability of natamycin. Good bulking properties of lactose allowed formation of acceptable cakes but partial formation of a less soluble monohydrate crystalline polymorph and strong osmotic shock while added in suspension were not suitable for maintaining the physical integrity of nanospheres or liposomes. Instability of natamycin due to reducing properties of this sugar was also observed, though at a lower extent than with glucose. Mannitol and sorbitol appeared to be incompatible with liposomal formulations but were found efficient stabilizers and protectants against degradation and leakage of natamycin from PLGA nanoparticles. Due to crystallization during drying, mannitol and sorbitol could however not provide an efficient bulking effect leading to undesired aggregation and poor redispersibility of the nanoparticles.

Regarding PLGA nanospheres, lyophilization in presence of trehalose was found superior to Tangential Flow Filtration with a better conservation of size characteristics, even upon resuspension and storage, limited aggregation and absence of loss due to fouling on the membrane. In the case of liposomes, mechanical stresses occurring in both techniques induced at some extent modifications of size characteristics and rearrangement of the vesicles. Further analysis of liposomal morphology, antimicrobial tests and *in vitro* release kinetics after post-processing treatments are required to identify the method showing fewer consequences on the bilayer integrity and permeability. Nevertheless,

lyophilization was in any case found much superior to filtration for the physical and chemical stability of both natamycin and nano-carriers upon storage, indicating that conservation of the nano-suspensions in a liquid form, even purified and/or concentrated, is not the most promising approach.

Lyophilization remains to be further optimized in terms of cryo-/lyoprotectants involved to maximize benefits at each stage of the process. Using for instance the identified stabilization properties of mannitol and sorbitol against leakage of natamycin in combination with the efficient properties of trehalose for the integrity of the nanoparticles could lead to advantageous dried products. Antimicrobial tests should also be performed to determine if the presence of sugars, usually used by fungi as a nutrient, are not detrimental for the antimicrobial activity of natamycin. The method of incorporation of the protective excipients, carried out here by addition of the protectant powder into nano-suspensions prepared originally in water, should also be reconsidered to evaluate if the osmotic shock, observed especially for liposomal suspensions and lactose, could be reduced. Incorporation in the aqueous phase before nanoprecipitation or solvent injection is a possible option, provided that the increase in viscosity is not unfavourable to diffusion of the solvent in the aqueous phase and do not hinder formation of the nanoparticles. More importantly, the lyophilization process should be performed with larger volumes to confirm efficient protection of the nanoparticle integrity and foresee possible hurdles for scaling-up.

Though lyophilization offers better perspectives, definite conclusions about the performances of Tangential Flow Filtration applied to nanoparticles cannot be drawn at this stage of the research. Results observed in this study were indeed highly dependent on the homemade set-up implemented, which did not offer the possibility to fully monitor the filtration process (temperature, cross-flow velocity, etc...). Variability between batches of nanoparticles, single-use membranes involved and frequent samplings during the process were also identified as possible sources of inaccuracy and disturbance. The recommended action would be to perform a similar study at a much larger scale (minimum 500 mL) which would not only allow gathering more reliable processing parameters for further modelling and understanding of membrane fouling, but also reduce the inaccuracy levels. Employing large-scale equipment would also enable an easier screening of other configuration, material or pore size of ultrafiltration membranes, which might have a totally different behaviour towards fouling of nanoparticles. This would of

course require also the development of a standardized and reproducible method to scale-up the production of the nano-suspensions. Evaluation of industrial systems such as multi-inlet jet mixers, microfluidics or membrane contactors adaptable to solvent injection methods [4-7] could bring an interesting alternative to the manual preparation implemented so far. These systems could also be used in line with the filtration, allowing combined preparation and post-treatment of much larger volumes than lyophilization.

## References

- [1] Z.L. Tyrell, Y.Shen, M. Radosz, Fabrication of micellar nanoparticles for drug delivery through the self-assembly of block copolymers, *Progress in Polymer Science*, **2010**, 35, 1128-1143
- [2] J.G.J.L. Lebouille, L.F.W. Vleugels, A.A. Dias, F.A.M. Leermakers, M.A. Cohen Stuart, R.Tuinier, Controlled block copolymer micelle formation for encapsulation of hydrophobic ingredients, *Eur. Phys. J. E*, **2013**, 36, 107-119
- [3] J.H.Hamman, Chitosan based polyelectrolyte complexes as potential carrier materials in drug delivery systems, *Mar. Drugs*, **2010**, 8, 1305-1322
- [4] Y.Liu, Formulating nanoparticles by flash nanoprecipitation for drug delivery and sustained release, Princeton University, **2007**
- [5] B.Yu, R.J.Lee, L.J.Lee, Microfluidic methods for production of liposomes, *Methods Enzymol.*, **2009**, 465, 129-141
- [6] C.Charcosset, H.Fessi, Preparation of nanoparticles with a membrane contactor, *Journal of Membrane Science*, **2005**, 266, 115-120
- [7] T.T.Pham, C.Jaafar-Maalej, C.Charcosset, H.Fessi, Liposome and niosome preparation using a membrane contactor for scale-up, *Colloids and Surfaces B: Biointerfaces*, **2012**, 94, 15-21

# *Acknowledgments*

Here we are finally, acknowledging all the people who helped and supported at different levels during this long and painful journey. Pressure is high, as, let's admit it, most of you will probably only read this section of the thesis!

My personal acknowledgments shall start with my promotor Prof. Andreas Schmidt-Ott and copromotor Gabriele M.H. Meesters, who offered me the opportunity to take part to this PhD project. Several institutions and companies contributed to the funding and hosting of this project and should also be acknowledged: The Marie Curie 7<sup>th</sup> Framework Program via the Initial Training Network PowTech, DSM Food Specialties and the DSM Biotechnology Center (DownStream Processing department) and the Delft University of Technology (Faculty of Chemical Engineering).

Precious scientific mentoring and contribution to my personal development came from three persons all along these four years and I cannot emphasize more how grateful I am to them.

Henriette de Braal, Senior Scientist at DSM and group lead in the DSP department, thanks for your genuine personality, pragmatism and reactivity which made my work and life so much easier in countless occasions. It was great to have you around bringing some optimism and positive energy, particularly during the last phase of the thesis. My sincere apologies for stealing some of your rainy (and non-rainy) weekends for the intensive proofreading of chapters. Thanks also for all the feedback and in-depth input on personal development that you gave me at several occasions. Your commitment, fair judgment, great sense of responsibilities and ability to put other people's interests before your own are a huge source of inspiration. You might not have a PhD in science but you for sure could get one in engaging people!

Jérôme Lebouille, Senior Application Development specialist at DSM Biomedical, I am glad I found someone who understands so well what it means to be a PhD in an industrial environment and all the sacrifices that it requires. Your always sharp pieces of advice at personal level helped me go through all the difficulties in a much smoother way, particularly during the first year, and gave me better understanding on how to survive in a large company as DSM. Thanks also for your creative tips for the project and publications! Finally, simply thanks for taking the time for me at any occasion despite your very busy agenda!

Eduardo Mendes, Associate Professor at the TU Delft and copromotor of this thesis, thanks for your voluntary contribution to the project, your open-mindedness and your support, which were more than welcomed when the times were tough. I am glad to see that it is possible to evolve in your career but still to treat other people with respect, generosity and genuine interest. Very happy to see also that being a scientist is not incompatible at all with sport, culture and art!

This project could never have been finished on time without the help and hard work (to not say torture) of three amazing students. Sala Xu from the Haagse Hogeschool, thanks for the first formulations of polymeric nanoparticles and all the interrogations and considerations that your work generated. You were my first intern ever and this has been a pleasure to meet you and help developing your skills! Hanan Al-Kutubi from the TU Delft, despite all the troubles that you've got to set up the filtration device, you always kept trying hard and coming with suggestions that really helped. Thanks for the energy that you put in this project! Thanks also for the nice discussions about future and people skills! Your maturity is impressive and you will go far in life, no doubt. We'll see each other at your PhD defence! Michèle Uhring from Chimie Paristech, you were not afraid to start a fully new part of my project and you've been a very serious, reliable and committed person all along these 5 months. I am glad that you enjoyed your stay in the Netherlands and proud to see that you were able to grow in your professional project at various levels.

I gratefully acknowledge the support given by all my colleagues from the DSM Biotechnology Center and the DSP department. Although my topic was not at 100% suitable with the activities of the company, I have always been able to find assistance and solutions when necessary! Special words go to Thomas van Drünen, great deskmate for a couple of months who kept me in the loop of nice activities and things going on within DSM; Andre Groenendaal and Albert-Jon Vis, for letting me squat the fume hood for the past four years, for challenging my Dutch understanding at many occasions and for nice supportive conversations during the last part of this thesis; Esteban Freydehl, for always trying hard to transmit your enthusiasm (and I did not made this task easy!) and checking from time to time if I was still alive or just zombie-walking; Nienke Hylkema for the very important proofreading of my Dutch abstract; Arthur Janse for your help with the interns. I would also like to acknowledge people who were a precious help for setting-up devices and performing analyses: Angelina Dekker for the antimicrobial tests; Silvia Gosiewska for ATR analyses; Man Lai, Jan-Hein Willemsen and Udo Lamers for troubleshooting the HPLC so many times; Ibo Özkan, Hans Jansen and Marcel Jansen for support while setting-up the tangential flow filtration device.

I would like to extend these acknowledgments to my colleagues from the Delft University of Technology and particularly to the technical assistants Ben Norder, Duco Bosma and Pieter Droppert for their availability and precious help with DSC, XRD and SEM analyses.

Many many thanks to all the interns who passed by DSM, especially the “first batch” Nina, Rico, Telmo, Stella, Boyd, Rita and Winnie without forgetting Klaus, the only one who can understand the long Marie Curie journey! Life was much funnier with you! Thanks for all these nice dinners, DSM Next events, Queen’s days, Queen’s nights, parties and all the rest! Nina, I think I would definitely not have survived the first year if you had not been around bringing some positive energy. Hope that we can keep in touch for a couple of years more as we did until now! Klaus, I still remember your relief and happiness the day you told me you had a date for your defense. Well, my turn!

Of course, I would like to thank with all my heart the PowTech fellows for unforgettable memories and travels! Oh dear (Bill©)! What a tremendous but weird feeling to meet you guys for only a couple of weeks but to feel so close and to have much more fun and laughs than on the rest of the year! I will remember for a long time the meetings in Paris, Cork, Zürich, Budapest, Delft, Goteborg and Brussels! Intensive emotionally but so unique! Cannot wait to organize our first unofficial PowTech meeting! A very special thank for Marine! Your enthusiasm and your undisputed craziness are so refreshing and so precious to me! I need more people like you in my life, definitely! Sven, as you can see I stole some of your after-WCS-events-thanks-facebook-message tricks to write these acknowledgments! Good to meet someone with whom I share the same point of view on the relative importance of science and dance in life! Hope to catch up with you for some wild discussions about cinema, dance, musicals, stretching, pole dance, whatever...! Marta, really good to have you here during 6 months, thanks for the nice chats and always curious and open-minded attitude (I mean, seriously, who else than you could go see the Dalai-Lama and do roller disco on the same month)! Thanks also for your support during the final stage of this thesis! Keep up girl! David, thanks for letting me mourning so often, only a few people could have born it as long as you did! It was great to organize the PowTech event with you (and find you a monk lover on the way)! Bill, the sweetest American I know, I will remember you every time a guy shakes my hand! See you during our next breakfast by Skype! Pooja, our very special Spice girl! I’ve fallen in love with your inimitable way of speaking French! Katarina, glad you were crazy enough to try a special dance class with me and Sven! Still impressed by your performance! Emré, every time I hear the words “Challenge accepted”, three things will come to my mind for the rest of my life: Santa Maria / sanitary hat / afro hair-cut!



Let's be honest, doing this PhD did not let any real space for creativity, inspiration, proudness and sense of reward for the hard work performed. I hopefully had the chance to get that from my personal sporty life and from amazing inspirational teachers. A great thanks to all the fitness instructors at the RhythmSports in Den Haag for these funny workouts that helped me to stay fit both mentally and physically! A special thanks to Yue Mee for the intensive boxing training / crazy duo-triple step choreographies and Leonie for the most advanced killer pilates I've been given to do! A great thanks to Chantal Jimenez and the girls (and the guy) at De Vak for the modern dance lessons and fun improvisations! We rocked the show with the sweetest choreography ever (flower power)! Last but not least, my deepest gratitude goes to my pole dance family Sportief Paaldansen. Stepping into your world was a true life revelation and I deeply enjoyed flying around and defying gravity (and muscular pain, bruises, blisters, injuries, etc...) with you all! Experiencing such an open-minded and challenging atmosphere with infinite possibilities has been my bubble of oxygen for the past two years. A huge thanks to my hardcore warrior teachers Apple and Eefje for pushing my mental and flexibility limits week after week! Thanks also to Ezi and Paaldans Zoetermeer for the scary but always full of enthusiasm acrobatics trainings. Never thought I could nail some of these crazy head/elbow/handstands or duo tricks. It was also a pleasure to discover with you the joy of aerial hoop and silks, definitely worth it! Overall, thanks to the very dynamic Dutch aerial community to bring the sparkle of magic and inspiration that was desperately missing!

Very special acknowledging words go finally to Guillaume Rousseau, the person who convinced me to do a PhD 7 years ago (God, that turned out not to be such a great idea at the end!). Thanks for proving me that French nationality and high levels of emotional intelligence can coexist! Your commitment, trust and always fair judgment have been a true inspiration for me years ago and I hope to be able one day to have as much faith in life and people as you do.

Clotilde Bouaoud  
April 2016



# Curriculum Vitae

Clotilde BOUAOUD

cbouaoud@gmail.com

Born in Maubeuge (France), 14<sup>th</sup> July 1986

## Education

**2011-2015** Delft University of Technology /DSM Food Specialties

PhD student and Early-Stage Researcher for the Marie Curie EU FP7 Initial Training Network PowTech (powtech.sik.se)

**2009-2010** École Nationale Supérieure de Chimie de Lille (*Lille- France*)

MSc in Chemistry and Engineering of Formulation – with honors

**2006-2009** École Nationale Supérieure de Chimie de Paris (*Paris - France*)

Master Degree in Chemical Science and Engineering

**2004-2006** Lycée Albert Châtelet Preparatory School (*Douai –France*)

University-level preparation for the nationwide competitive entrance exams of the French Schools of Engineering

## Professional experience

**September 2015- present**

IFF

Hilversum - Netherlands

Applied Development Scientist I

*Development of fragrance-loaded delivery systems for consumer products (laundry care)*

**August 2011 – August 2015**

DSM Food Specialties

Delft - Netherlands

Assistant Scientist within the Downstream Processing department of the DSM Biotechnology Center

*Development of nano-encapsulation systems for the encapsulation of the food antifungal natamycin*

**March- August 2010**

IQAC - CSIC

Barcelona – Spain

MSc project

*Formulation and physico-chemical characterization of fluorescent polymeric nanoparticles from oil-in-water nano-emulsions templates.*

**February-August 2009**

CNRS EA-CMF 4478

Lille - France

Master degree project - Industrial collaboration with IFF

*Development and validation of kinetic and thermodynamic tools for the prediction of the oxidation behaviour of fragrant molecules.*

**March-August 2008**

COLAS

Paris - France

Trainee

*Synthesis of green surfactants and evaluation of their performance in the formulation of bituminous oil-in-water emulsions.*

# *List of publications*

C. Bouaoud, S. Xu, E. Mendes, J.G.J.L. Lebouille, H.E.A. De Braal, G.M.H. Meesters, Development of biodegradable polymeric nanoparticles for encapsulation, delivery and improved antifungal performance of natamycin, *Journal of Applied Polymer Science*, **2016**, 133, 43736

C. Bouaoud, J.G.J.L. Lebouille, H.E.A. De Braal, E. Mendes, G.M.H. Meesters, Formulation and antifungal performance of natamycin-loaded liposomal suspensions: the benefits of sterol-enrichment, *Journal of Liposome Research*, **2016**, 26 (2), 103-112

C. Bouaoud, G.M.H. Meesters, Submicron natamycin particles, Patent WO/2015/044465